STUDIES ON THE INFLUENCE OF ADMIXTURES ON THE PERMEATION AND MECHANICAL CHARACTERISTICS OF FOAM CONCRETE FOR USE IN LIGHT-WEIGHT INTERLOCKING BLOCKS

A Thesis Submitted
in Partial Fulfilment of the Requirements
for the Degree of

DOCTOR OF PHILOSOPHY

by

ABHISHEK KAMISETTY

DEPARTMENT OF CIVIL ENGINEERING
INDIAN INSTITUTE OF TECHNOLOGY GUWAHATI
GUWAHATI-781039, INDIA

September, 2024

Dedicated

To my

Mother: Late Smt. Vijaya Laxmi Kamisetty

Family

And

Daughter: Abhya Sri Magana Kamisetty

STATEMENT

I, hereby declare that the content embodied in this thesis entitled ***"Studies on the Influence of Admixtures on the Permeation and Mechanical Characteristics of Foam Concrete for use in Light-weight Interlocking Blocks"*** is the result of investigations carried out by me at the Department of Civil Engineering, Indian Institute of Technology Guwahati, Guwahati, India.

In keeping with the general practice of reporting scientific observations, due acknowledgements have been made wherever the work described is based on the findings of other investigators.

Abhishek.k

Date:

Place: IIT Guwahati

Abhishek Kamisetty
Roll no: 186104111
Ph. D. Research Scholar
Department of Civil Engineering
Indian Institute of Technology Guwahati
Guwahati-781039, Assam, India

भारतीय प्रौद्योगिकी संस्थान गुवाहाटी
Indian Institute of Technology Guwahati

CERTIFICATE

This is to certify that the thesis entitled ***"Studies on the Influence of Admixtures on the Permeation and Mechanical Characteristics of Foam Concrete for use in Light-weight Interlocking Blocks"*** *by* ***Abhishek Kamisetty*** *(Roll No: 186104111), a student of the Department of Civil Engineering, Indian Institute of Technology Guwahati, submitted for the award of the degree of Doctor of Philosophy, is a record of bonafide research work carried out by him under our joint supervision and that this work has not been submitted elsewhere for a degree. In our opinion, the thesis is up to the standard of fulfilling the requirements of the doctoral degree as prescribed by the regulations of this Institute.*

Date:

Place: IIT Guwahati

Dr. Indu Siva Ranjani Gandhi
Assistant Professor
Department of Civil Engineering
Indian Institute of Technology Guwahati
Guwahati-781039, Assam, India

Dr. Abhishek Kumar
Associate Professor
Department of Civil Engineering
Indian Institute of Technology Guwahati
Guwahati-781039, Assam, India

ACKNOWLEDGEMENT

I would like to take this opportunity to express my gratitude to everyone who helped with this thesis and supported me during my studies. This thesis would not have been possible without them.

I would like to start by expressing my gratitude to my supervisors, Dr. Indu Siva Ranjani Gandhi and Dr. Abhishek Kumar, for their unwavering belief in me and support. Being their Ph.D. student has been an honor. I am incredibly grateful for all of their time, suggestions, and advice in helping to make my Ph.D. experience interesting and productive. Their vast experience in the area of structural and geotechnical engineering and willingness to impart their knowledge has helped in my research work.

Besides my supervisors, I would like to thank my Doctoral committee members: Dr. Anil Kumar Mishra, Dr. Ravi K, Dr. Prabu Vairakannu for their encouragement and fruitful suggestions at various stages of my research work.

I thank the Head of Civil Engineering department (former and present), faculty in-charge of Infrastructure engineering and Management laboratory and Structural Laboratory (former and present) and staff members viz. scientific officer Dr. Arun Ch. Borsaikia, technical superintendent Mr. Pranab Hazarika, Junior Technician Mr. Saurabh Kr. Mudoi and Mr. Mitu Ali for helping me in extensive physical work for providing uninterrupted help accomplishing the Ph.D. work. I also would like to would like to acknowledge the support provided by Central Instruments Facility and Department of Civil Engineering, IIT Guwahati

I thank my lab mates and colleagues and my seniors Dr. Arya Anuj Jee, Dr. Sritam Swapnardashi Sahu, Dr. Khwairakpam Selija, Mr. Sathishraj Mani, Mr. Vijayan C, Mr. Ujjwal Jyoti Dutta, Mr. M Leela Sai Ranga Rao, Mr. Chandrashekhar Wagh, Mr. Uday Boddepalli, Mr. Amit Kumar Sahu, Dr. Jyotish Kumar Das, Dr. Jnyanendra Kumar Prusty, Dr. Joy Kumar Mondal, Mr. Niranjan Borah, Mr. Surender Singh, Mr. Hrik Chaudhury, Ms. Sudeepta Malakar, Ms. Jenny Laura RVS, Mr. Aman Alok, Ms. Nicola Thounaojam, Mr. Arup Kumar Mohapatra, Mr. Akhil Charak, Mr. Divyesh Sharma, Mr. Rahul Das, Mr. Rahul Sonkar, Mr. Aniket, Mr. Nitesh Royal, Mr. Rahul Singh, Ms. Adyasha Priyadarshini for the stimulating discussions and the sleepless nights we were working together before deadlines. A very special thanks to my juniors for their

invaluable advice and feedback on my research and for always being so supportive of my work during my Ph.D. I have no words to thank all my friends who have made the stay at IIT Guwahati a memorable one.

Lastly, and the most importantly, I would like to thank my parents (Ravi Kumar Kamisetty, Vijaya Laxmi Kamisetty), brothers (Avinash Kamisetty, Abhijeeth Kamisetty), wife (Smt. Divya Kamisetty), daughter (Abhya Sri Magana Kamisetty), sister-in-law (Smt. Madhuri Chopparapu) and niece (Bhargavi Kamisetty), for all their love and encouragement. I consider myself nothing without them. They gave me enough moral support, encouragement and motivation to accomplish my goals.

Above all, I believe that everything happens for a good reason, so I thank almighty for giving me exposure to such a life changing experience of Ph.D.

Abhishek.k

Date: Abhishek Kamisetty

Place: IIT Guwahati

ABSTRACT

Foam concrete (FC), generally classified as a cellular light-weight concrete with density ranging from 400 kg/m^3 – 1850 kg/m^3, is produced by the introduction of stable air voids into the cement paste (or mortar). Based on the existing literature, it is evident that besides the conventional filling and thermal insulation applications, FC also has potential for specialized applications such as stabilization of weak soils, seismic isolation medium for underground reactor containments and tunnel linings and subbase layer in case of road pavements. Further, highly permeable material such as FC, has the potential to stabilize unstable slopes, through its application in landfills, horizontal/ vertical drains and retaining walls and providing reliable drainage path in order to dissipate pore water pressure and make slopes drier and stronger. However, the literature review concludes that the quantum of research reported in aforementioned areas is very limited.

Conventional FC is typically proportioned to achieve only low compressive strength (e.g., between 1 and 10 N/mm^2), suitable for its use in void fill and trench reinstatement, and thus the material is largely disregarded for use in structural section. Adding to above, it is surprising to note that very few researchers have used class F FA as potential alternative for sand in FC. Moreover, use of PP fiber in FC showed enhancement in the tensile strength, water absorption capacity and permeability. From the limited literature available on the use of FA, PP fiber and their combination, it is evident that their combined use, helps in the enhancement of mechanical properties and permeation characteristics of FC.

Particularly for concrete structures such as retaining walls, dams, reservoirs, and marine structures, interaction with water is more common rather than gas/ air/ water vapour, hence it is more rational to measure the permeability of FC using the water permeability method. Here it is to be noted that, the existing sample sealing mechanism to measure water permeability of porous concrete such as FC, have limitations such as ingress of molten sealant into sample and applicability to only low-pressure head (3 kg/cm^2). Hence, a novel sealing mechanism using the rubber membrane and iron clamp setup has been developed in the present study to measure the water permeability of FC for higher pressure of up to 7 kg/cm^2.

Another important fact is manual error, construction cost, time and resource consumption can be reduced through the incorporation of interlocking concept in masonry. Hence, it is

evident that, the interlocking block (IB) concept along with highly permeable materials such as FC, can facilitate construction of dry cast segmental retaining walls even in remotely placed locations.

The present study is restricted to FC and foam concrete interlocking block (FCIB) made of preformed foaming method with the identified mix components viz. ordinary Portland cement (OPC) 43 grade, sand (< 300 μm), FA (up to 100% as sand replacement), PP fiber (up to 1%), superplasticizer (PCE based), sodium lauryl sulphate (SLS) (surfactant) and carboxymethyl cellulose (CMC) (additive). A constant cement sand ratio of 1:2 is adopted throughout the study. The first phase of studies comprises of studies on the relative fresh state, hardened state and permeability properties of FC (with design density of 1000 kg/m^3 (FC1), 1500 kg/m^3 (FC2) and 1800 kg/m^3 (FC3) produced using FA (50% as sand replacement) and PP fiber (0.05%) along with variation in foam content. Here it is to be noted that, for use in retaining wall applications, minimum strength of at least 20.7 N/mm^2 is needed as per ASTM C1372-23 guidelines. Further, addition of foam and PP fiber enhance the permeability of FC while decreasing its spreadability and mechanical properties. Based on the preliminary investigations it was found out that the FC2 (density = 1500 kg/m^3), is exhibiting a maximum compressive strength of 14.2 N/mm^2 along with a satisfactory permeability of 10^{-3} cm/s.

Having identified the potential mix composition of FC which could result in desired strength as well as permeability for its intended application, further studies are attempted to improve the strength and permeability of FC2 through variation in FA level and fiber content. The matrix modification of FC2 using both FA and PP fiber have shown a significant increase in compressive strength of FC2 up to 462% and 358% with a maximum of 25 N/mm^2 and 29 N/mm^2 compressive strength for the SFC2F4P2 mix at the age of 28 days and 56 days respectively. Further, the split tensile strength of these combination mixes is exhibiting significant enhancements of up to 573% and 512% at the age of 28 days and 56 days respectively due to combined effect of FA and PP fiber. Based on the experimental outcomes, the SFC2F1P2, SFC2F2P2, SFC2F3P2 and SFC2F4P2 mixes have been selected as most suitable mixes (based on cube strength results) for the intended application in accordance with ASTM C1372-23.

Further, studies on properties of FCIB (blocks and triplets) produced with satisfactory mixes (i.e., SFC2F1P2, SFC2F2P2, SFC2F3P2 and SFC2F4P2) have been conducted in

terms of compressive strength, shear resistance and permeation characteristics. Due to the variation in IB pattern, shape and size, the compressive strength of FCIB is found to be 57% to 74% of FC cubes of size 50 mm which is in line with the literature reported by Jaafar et al., 2006. However, out of all the mixes, only the SFC2F4P2 mix (at 56 days of curing) meets the minimum compressive strength requirement of 20.7 N/mm^2 as recommended by ASTM C1372-23, for its intended use as dry-cast segmental retaining wall units.

As a next step, the mechanical properties i.e. compressive strength and shear resistance of the masonry triplets prepared using the proposed FCIB is examined. It is discovered that the compressive strength of FCIB triplets ranges from 30% to 51% of FCIB, which is in line with research results reported by Jaafar et al., 2006. Further, these FCIB triplets have a shear resistance that ranges from 18% to 36% of their compressive strength when loading is in a direction perpendicular to the header or stretcher face. Additionally, due to the improved ductility behaviour derived from PP fiber, both FCIB and triplets (under compressive or shear forces) exhibit a prolonged load bearing capacity. Furthermore, the water absorption by these FCIB's is in the range of 10% to 17% at various testing ages, which is within the limits recommended by ASTM C1372-23. On the other hand, these FC2 mixes are exhibiting a water permeability in the order of 10^{-5} cm/s which is higher than that of the conventional concrete. Hence, the proposed FCIB produced with SFC2F4P2 mix consisting of cement: FA= 1:2 and PP fiber content of 0.4% at W/S of 0.3 and SP dosage of 1.1% (at 56 days of curing) has the potential to be used in dry cast segmental retaining walls to facilitate dissipation of pore water pressure behind retaining walls. However, further studies are needed to verify the pore water pressure dissipation effect when used in retaining walls.

Keywords: Foam concrete, interlocking block, foam concrete interlocking block, synthetic surfactant, fly ash, polypropylene fiber, superplasticizer, water to solid ratio, density, spreadability, compressive strength, split tensile strength, flexural strength, shear resistance, water absorption, permeability, triplets.

भारतीय प्रौद्योगिकी संस्थान गुवाहाटी
Indian Institute of Technology Guwahati

TABLE OF CONTENTS

भारतीय प्रौद्योगिकी संस्थान गुवाहाटी
Indian Institute of Technology Guwahati

LIST OF FIGURES

LIST OF TABLES

भारतीय प्रौद्योगिकी संस्थान गुवाहाटी
Indian Institute of Technology Guwahati

LIST OF ABBREVIATIONS AND NOTATIONS

AAC	Autoclaved aerated concrete
ACI	American concrete institute
ASTM	American society for testing and materials
C	Base mix (mortar) for foam concrete
CMC	Carboxymethyl cellulose
C-S-H	Calcium silicate hydrate
Ca $(OH)_2$	Calcium hydroxide
CT	Computed tomography
f_c	Compressive strength
f_t	Split tensile strength
f_{mor}	Flexural strength
FA	Fly ash
Fa, F0, F1, F2, F3, F4	Sand replacement level with fly ash
FC	Foam concrete
FC1	Foam concrete with target fresh density = 1000 kg/m^3
FC2	Foam concrete with target fresh density = 1500 kg/m^3
FC3	Foam concrete with target fresh density = 1800 kg/m^3
FCIB	Foam concrete interlocking block
IB	Interlocking block
IS	Indian standard
OPC	Ordinary Portland cement
PCE	Polycarboxylic ether superplasticizers
PP FIBER	Polypropylene fiber
P_s, P0, P1, P2, P3, P4, P5	Total solids replacement level with polypropylene fiber
RILEM	International union of laboratories and experts in construction materials, systems and structures (RILEM, from the name in French)
SLS	Sodium lauryl sulphate
S	Mixes with varying SP dosage (at constant W/S of 0.3)
SP	Superplasticizer
W	Mixes with varying W/S (without SP addition)

W/S	Water-to-solid ratio

CHAPTER 1
INTRODUCTION

1.1 GENERAL

Foam concrete (FC), generally classified as a cellular light-weight concrete with density ranging from 400 kg/m^3 – 1850 kg/m^3, is produced by the introduction of stable air voids into the cement paste (or mortar). Based on the existing literature, it is evident that besides the conventional filling and thermal insulation applications, FC also has potential for specialized applications such as stabilization of weak soils, seismic isolation medium for underground reactor containments and tunnel linings and subbase layer in case of road pavements. Further, highly permeable material such as FC, can stabilize unstable slopes, through its application in landfills, horizontal/ vertical drains and retaining walls and providing reliable drainage path in order to dissipate pore water pressure and make slopes drier and stronger [Tosun, 2014]. On the other hand, any structure's seismic behaviour is primarily influenced by its mass, strength, and stiffness, as well as by all other factors that may have an impact on those characteristics [Kilic et al., 2003]. The main principle for seismic resistant design is to avoid unnecessary mass, and hence the use of light-weight FC can reduce the structure's self-weight and subsequently reduce the intensity of seismic forces [Bertero et al., 1980, Bhattacharya and Agarwal, 2014, Talukdar et al., 2017]. In this line, several researchers have proved that, the energy absorption capacity of FC is higher than the conventional concrete [Batra et al., 2023, Gandhi et al., 2023]. Hence, the provision of sustainability of essential infrastructure such as nuclear reactor, pavements, etc. can be ensured through the usage of innovative material capable of mitigating the aforementioned natural hazards along with satisfactory performance with respect to codal provisions.

1.2 LIGHT-WEIGHT/ CELLULAR CONCRETE

Light-weight/ cellular concrete is commonly manufactured by various methods. Out of these, primarily four different types viz. light-weight aggregate concrete, pervious concrete, autoclaved aerated concrete (AAC) and FC have been shown great interest by several researchers around the globe. Therefore, these methods are briefly introduced in this section.

The conventional concrete is generally prepared using water, cement, sand and coarse aggregate. The aggregate in conventional concrete is replaced with light weight aggregate such as fly ash (FA) pellets, ceramic waste, pumice, coconut shell, etc., to reduce its density [Agarwal et al., 2021]. However, the water permeability of light-weight aggregate concrete is in the order of 10^{-11} cm/s which is very low when compared to FC [Liu et al., 2011].

Alternative method of making concrete lighter is to eliminate sand from the mix constituents, which leaves the voids between coarse aggregate unoccupied making the concrete pervious commonly known as pervious concrete or no fines concrete. However, though the permeability of such concrete is very high (in the order of 1 cm/s), clogging of the aforementioned pores leads to decrease in its permeability in the long run [Sun et al., 2019].

Another commonly used light-weight concrete is AAC, which consists of a mix of lime, sand (or FA), cement, water, and an expansion agent (aluminum powder). The reaction between the aluminum powder (Al), water (H_2O) and calcium hydroxide ($Ca(OH)_2$) causes microscopic hydrogen bubbles to form, expanding the concrete. After evaporation of the hydrogen, the highly closed-cell, aerated concrete is cut to size and steam-cured in a pressurized chamber (an autoclave) [Uddin et al., 2006, Xu et al., 2019]. However, AACs are controlled by the requirements of factory autoclaving and inflexible hardening process, making it tedious manufacturing process and expensive, which restricts it for precast units.

In FC, air bubbles are generally introduced into neat cement paste or mortar by mixing preformed foam or mix-foaming agents in order to produce air voids. As the concrete hardens, these bubbles disintegrate, leaving air voids of similar sizes. The compressive strength and permeability of FC is found to range between 10 N/mm^2 to 70 N/mm^2 and 10^{-8} cm/s to 10 cm/s respectively [Hilal et al., 2014, Amran et al., 2020a, Yuan et al., 2021].

Among the aforementioned light-weight/ cellular concretes, FC seems to be a potential material for the intended use in the retaining wall applications, considering the strength and permeability requirements. Hence, as a next step, a detailed literature review is conducted with respect to FC and summarized in the further sections.

1.3 FOAM CONCRETE

FC is defined as a cellular concrete which can be classified as a light-weight concrete (density of 400–1850 kg/m^3) produced by introduction of stable voids within the hardened cement paste or mortar that creates cellular structure in concrete. FC is recognized for its high flowability, low cement content, low aggregate usage [Valore, 1954], and excellent thermal insulation [Richard et al., 1975, Wagh et al., 2021]. Furthermore, the FC is considered as an economical solution in fabrication of large-scale light-weight construction materials and components such as structural members, partitions, filling grades, and road embankment infills due to its easy production process from manufacturing plants to final position of the applications [Tikalsky et al., 2004, Uddin et al., 2006, Ramamurthy et al., 2009]. It is an economical, environmentally friendly, light-weight semi-structural material that provides seismic isolation, fire resistance, thermal and acoustic insulation and found to be suitable for both in-situ and pre-cast applications [Mohrenholtz et al., 1982, Zhao et al., 2013, Tosun, 2014, Wagh et al., 2021, Kou et al., 2022]. Conventional FC is typically proportioned to achieve only low compressive strength (e.g., between 1 and 10 N/mm^2), suitable for its use in void fill and trench reinstatement, and thus the material is largely disregarded for use in structural section. Although there may be highly innovative solutions, unless strength of atleast 25 N/mm^2 can be achieved, both economically and in an environmentally sustainable manner, most engineers and designers are unlikely to give FC serious attention for structural application. [ACI Committee 523, 1993,1996, 2006, 2009, Narayanan and Ramamurthy, 2000, Kearsley and Wainwright, 2001, Cox and Dijk, 2002, Jones and McCarthy, 2005a, 2005b, Nambiar and Ramamurthy, 2007a, 2007b, 2008, Ramamurthy et al., 2009].

1.4 HISTORY OF FC

The Portland cement-based FC was first patented by Axel Eriksson in 1923, FC has surprisingly a way long history [Valore, 1954]. There is also evidence of this type of technology being used by the Egyptians over 5000 years ago, with similar results. Though these are very early air entrained concretes, they were extremely basic with no control over air content, etc., and they cannot be considered as FC in true sense [Jones and McCarthy, 2005b]. The lack of specialized materials and equipment had limited its use to small-scale projects and its application as an insulation material but over the past 20 years a significant improvement was observed in production equipment and better-quality

surfactants (foaming agents). This has not only enabled the use of FC on a larger scale but also over a wide range of applications.

The estimated yearly market size for FC in the UK is between 250,000 and 300,000 m^3, which includes one very large mine stabilization project. The FC market in Western Canada was estimated to be 50,000 m^3 annually. Moreover, a floor heating system's key component, FC, accounts for about 250,000 m^3 of construction volume in Korea each year. FC 's superior qualities, including its light-weight design and ability to insulate against heat waves, have made it a popular material in the Middle East for mitigating the negative effects of temperature fluctuations and reducing the negative effects of earthquakes. In Holland, FC was used as road sub-base (as the load carrying requirement was low) in the construction of bridge abutments due to its low density and a significant savings in cost was realized due to reduction of the foundation size and the wall thickness. Furthermore, FC applications are economical during the repair and restoration phases [Amran et al., 2015]. In the year 1997, a successful trial was attempted in Delhi, India by G.B. Singh, who had constructed a G + 3 storied building with FC [Singh, 2005]. Recently, researchers have tried various techniques for improvement in strength of FC. Basically, uniform cellular structure is a key factor for producing concrete with good mechanical properties. Hence a significant way to improve concrete strength was witnessed by introducing additive that leads to protection of the bubbles from collapse leading to uniform cellular structure [Siva et al., 2015].

1.5 ADVANTAGES AND APPLICATIONS OF FC

Global experience has shown that the special technological feature of FC allows it to be used for multipurpose applications which include:

- Thermal and soundproofing insulation of floors.
- Thermal insulation of flat, mono-pitch and double-pitch roofs.
- Cavity filling, well backfilling, masonry grouting.
- Setting up pipeline monolithic thermal insulation.
- Production of building blocks and wall panels (of different designations).
- Monolithic low-rise and individual house building.
- Levelling floors.
- Road sub-bases and maintenance.

- Bridge abutments and repairs.
- Ground stabilization.

It has been proved that buildings of FC with a thickness of 150 mm can withstand flames for four hours at a temperature of up to 12,000 degrees Celsius [Oginni, 2015]. However, in the last few years FC has become a promising material also for structural purposes e.g., stabilization of weak soils, base layer of sandwich solution for foundation slabs, industrial floor and highway as well as subway engineering applications [Kadela et al., 2017], as described in detail below:

Road subbase layer: An effective way to improve the unstable ground conditions is to apply the layered system. This includes a load-bearing structure subjected to repeated and/or permanent loads and a corresponding layer of FC intermediary in the transfer of loads to (weak) subsoil. Such system should be optimal from the point of view of the ground conditions and acting loads [Kadela et al., 2017]. Presented results of numerical simulations show that the maximal tensile stress in the lower zone of subbase layer, for the pavement structure is 0.039 N/mm^2. This value is lower than the flexural strength of FC with the density of 860 kg/m^3 - 1060 kg/m^3 which is 0.55-0.67 N/mm^2. It shows potential possibility of using FC layer as a subbase for pavement structures.

Underground reactor containments: Here, FC prepared by mix foam method has been used as an isolation medium in the buried containment concept and is effective in a seismic environment. In comparison to clay and reinforced earth, FC is a stronger material, but its effect on the yield load is negligible. However, the ultimate load indicates that plasticity begins in the containment and progresses to nearly full plasticization before yielding in the surrounding FC is initiated [Mohrenholtz et al., 1982].

Seismic isolation material for tunnels: Long term earthquake observations have demonstrated that a tunnel closely follows the motion of the soil mass during an earthquake. Therefore, coating a tunnel with a soft material would be a possible measure to minimize damage to tunnels. FC has unique properties such as low density, low strength, high impact resistance and thermal and noise insulation. In addition to its seismic isolation effect, FC used as a coating material for tunnel should ensure the stability and water tightness of the tunnel [Zhao et al., 2013].

Skyscrapers: The application of structural light-weight concrete in skyscrapers of residential and commercial complexes, as well as office buildings would reduce the overall weight of the buildings, reduce the amount of material used and reduce seismic and wind loads [Lee et al., 2014]. In order to obtain higher compressive strength, it is essential that the matrix of the concrete should be improved. Therefore, it is judged that creating pores through foaming agent in addition to incorporation of admixtures for higher strength requirement would be more efficient to produce structural light-weight concrete.

Other typical usage of FC are used under concrete paving, to protect roadways from frost heave, to provide insulation for placements and systems of shallow foundations, to prevent shallow piles from frost jacking and to avoid frost heave beneath pile caps, as backfill beneath buried oil field modules and as grout to fill in abandoned pipes, to fill spaces beneath slabs, lower the temperature beneath hot oil tanks and the tank support, and lessen thermal stress and gradient in hot concrete pits [Amran et al., 2015].

1.6 OUTLINE OF THE THESIS

The thesis is divided into seven chapters. The first chapter (Chapter 1) provides a brief overview of FC, its benefits, and its applications. The second chapter (Chapter 2) provides a critical review of the effect of surfactant and admixtures on the mechanical and permeation properties of FC and highlights the major research gaps. Furthermore, the potential of foam concrete interlocking block (FCIB) is also highlighted. The objectives and scope of the current study are derived from the critical review and presented in the third chapter (Chapter 3).

The first phase of experimental investigations involves studies on the relative fresh state, hardened state and permeability properties of FC produced using FA and polypropylene (PP) fiber along with variation in foam content as discussed in fourth chapter (Chapter 4). The fifth chapter (Chapter 5) depicts a more in-depth experimental programme on the combined effect of different levels of FA (as replacement for sand) and PP fiber on spreadability and mechanical properties of FC. Further, the sixth chapter (Chapter 6) demonstrates the development of FCIB (with design density of 1500 kg/m^3) produced with FA and PP fiber-based mixes for dry-cast segmental retaining walls. The performance of FCIB and FCIB triplets in terms of compressive strength, shear resistance and permeation are studied to assess the suitability for the intended application. The last

chapter (Chapter 7) presents the typical conclusions drawn from the studies and the scope for future research.

भारतीय प्रौद्योगिकी संस्थान गुवाहाटी
Indian Institute of Technology Guwahati

CHAPTER 2
LITERATURE REVIEW

2.1 GENERAL

FC, generally classified as a cellular light-weight concrete with density ranging from 400–1850 kg/m^3, is produced by the introduction of stable air voids into the cement paste (or mortar). In comparison to traditional concrete, the presence of above-mentioned entrained air voids in FC results in significant improvement in the permeability. FC with high permeation nature has promising scope for use in retaining wall and backfill for dissipation of pore water pressure and slope stabilization [Tosun, 2014]. However, the literature review concludes that the quantum of research reported in aforementioned areas is very limited. In this chapter, the prospective use of FC as a pore water pressure dissipation measure for slope stabilization towards prevention of landslides will be discussed. Based on the existing literature, it is evident that till late 70s, FC was mostly used for non-structural applications [Fu et al., 2020]. However, in later years, FC was also proven potential in various semi-structural applications such as stabilization of weak soils, seismic isolation medium for underground reactor containments and tunnel linings and subbase layer in case of road pavements [Mohrenholtz et al., 1982, Zhao et al., 2013, Tosun, 2014, Kadela et al., 2017]. In the recent years, numerous works have been done [Falliano et al., 2018, Othman et al., 2021, Hao et al., 2022] in terms of further enhancement in the strength of FC to enhance its structural applications. It should be mentioned that the two main aspects influencing the mechanical properties and permeability of FC are bubble stability and matrix composition. Hence, the effect of various additives on the mechanical properties and permeability of FC are reviewed in the further sections of this chapter.

2.2 INFLUENCE OF MIX COMPOSITION ON THE PERMEABILITY OF CONCRETE AND EFFICIENCY OF PERMEABILITY TESTING METHODOLOGY OF FC

Permeability of different types of concrete is another essential prerequisite for diverse uses. It is a commonly established fact that the permeation characteristics of concrete is very much dependent on the composition of concrete [Ahmad et al., 2012]. In this line,

studies have proven that aggregate characteristics such as aggregate size, texture and proportion of coarse to fine aggregate significantly affect the permeation characteristics of concrete [Nyame and Buenfeld, 1986, Cao et al., 2019]. Moreover, the permeability of different types of concrete and the corresponding methodology adopted as reported in literature are summarized in table 2.1. In this context, as per Yu et al., 2018, the permeability of concrete reported as intrinsic permeability (K in m^2) can be transformed to a water permeability coefficient (Kw in m/s) using the equation 2.1. Hence, the water permeability of the reported values have been calculated using the equation 2.1 and reported in table 2.1. Further, an in-depth review on permeation characteristics of FC is needed. However, FC, being most commonly used as mortar or paste (without coarse aggregates) with more amount of finer material can help in designing more permeable concrete than conventional normal weight concrete as depicted in figure 2.1. Further, few studies have identified that the oxygen and water vapor permeability (0.01 to 0.08 kgsMN/m^3 for 1500 to 800 kg/m^3) of FC increases with increasing porosity [Kearsley and Booyens, 1998, Kearsley and Wainwright, 2001, Yuan et al., 2021]. Hence, selection of FC with higher air content will result in more permeable FC as porosity and permeability are highly interdependent factors [Kearsley and Wainwright, 2001, Hilal et al., 2014, Yuan et al., 2021]. Further, it is to be noted that the entrained air voids which exhibit the filler effect similar to that of aggregates, however do not reduce the permeability of FC by obstructing the flow of water [Kearsley and Wainwright, 2001, Yuan et al., 2021]. In this line, the mixes used in the investigation by Kearsley and Wainwright, 2000, 2001, were based on equal water/binder ratio rather than equal workability, and that is why the anticipated decrease in porosity with increased ash content was not observed. Further, as the ash/cement ratio rises, the FC mixtures' water vapour permeability increases as well. This trend becomes more significant at lower densities [Kearsley and Wainwright, 2001]. Furthermore, as per Gopalakrishnan et al., 2020, the water absorption of FC (density: 1200 kg/m^3) has increased from 9.8% to 17.5% along with its water permeability up to 80% (at the age of 28 days) due to replacement of cement by FA (up to 50%) and river sand by quarry dust (up to 50%). Furthermore, the water absorption of FC produced using alkali activated FA and ground granulated blast furnace slag (also known as geopolymer FC) has varied from 14.9% to 124% with variation in density from 1200 kg/m^3 to 200 kg/m^3 at the age of 28 days [Hao et al., 2022]. In this line, the permeability of grout consisting of cement and FA has increased in the order of 10^2, due to the additional pore formed on the fiber's surface enhancing the drainage path connectivity and reducing

tortuosity. However, the usage of superplasticizer (SP) in the same product has been reported to reduce its permeability through pore refinement [Huang, 2001].

$$Kw = \frac{K\rho g}{\nu} \tag{2.1}$$

Where, Kw= Water permeability of concrete (in m/s), K= intrinsic permeability (in m^2), ρ = density of the fluid, kg/m^3, g = acceleration due to gravity, 9.81 m^2/s, ν = dynamic viscosity of the fluid, s/m^2. Further, for water at 20 °C, the term $\rho g/\nu$ equals $9.79 \times 10^6\ m^{-1}\ s^{-1}$, when a steady-state flow Q is reached [Yu et al., 2018].

Table 2.1: Permeability of various types of concrete reported in the literature.

Reference.	Type of Concrete	Mix composition	Permeability Methodology	Permeability
Yuan et al., 2021	FC of dry density 200 kg/m^3	Neat cement pastes with water to cement ratio (W/C) = 0.45	High-resolution X-ray microcomputed tomography (micro-CT)	9.3 cm/s
	FC of dry density 400 kg/m^3			3.4 cm/s
	FC of dry density 600 kg/m^3			1.1 cm/s
Hilal et al., 2014	FC (density between 1300 kg/m^3 to 1900 kg/m^3)	Cement: sand of 1:1.12, 1: 1.7 and 1: 2.28 and W/C ≈ 0.5	Constant head method and falling head method (air permeability) and calculated using empirical formula proposed by Katz and Thompson, 1986.	In the order of 10^{-12} to 10^{-16} m^2
Loosveldt et al., 2002	Mortar	Cement: Fine sand: Coarse sand = 1: 1.5: 0.65 at W/C of 0.4	Water permeability method	0.137 to 2.741 x 10^{-9} cm/s (calculated using eq. 2.1 by Yu et al., 2018)

Chandrappa and Biligiri, 2016	Pervious concrete	Cement/aggregate = 0.2, 0.2 and 0.33 W/C = 0.25, 0.3 and 0.35	Falling head permeameter apparatus	0.076 to 3.5 cm/s
Sun et al., 2019	Pervious concrete	Aggregate/cement (A/C) = 2.5, 3, 3.5, 4 and 4.5, W/C = 0.25, 0.3, 0.35, 0.4, 0.45 and 0.5, SP/cement = 0.00625	Falling head method in accordance with Chinese Technical Specifications for Pervious Concrete Pavement [CJJ/T 135-2009]	0 to 0.4 cm/s
Liu et al., 2011	Light-weight aggregate concrete	W/C of 0.38, Cement content = 500 kg/m^3, 100% replacement of various size fractions of normal weight aggregate with light-weight aggregate (expanded clay), SP ranging between 2.1 to 2.7 L/m^3 of concrete.	Water permeability in accordance with BS EN 12390-8	0.9 x10^{-11} cm/s to 4.0 x10^{-11} cm/s
Kondraivendhan et al., 2013	Conventional concrete	Silica fume/cement = 0.05, 0.1 and 0.15, Slag/cement = 0.1, 0.3 and 0.5, A/C = 3 and 4, W/C = 0.45, 0.5 and 0.6	Estimation using pore size distribution parameters	In the order of 10^{-13} cm/s
Pereira-de-Oliveira et al., 2014	Self-compacting concrete	Cement, natural and recycled coarse and fine aggregate, SP and water with a W/C = 0.57	Air and water permeability as per Castro-Gomes et al., 2002	In the order of 10^{-9} cm/s (calculated using eq. 2.1 by Yu et al., 2018)
Huang, 2001	Grout	Cement: FA = 1: 2.33, water-to-solid ratio (W/S) ranging between 0.4 To 0.8, PP fiber/cement + FA = 0.01, SP/cement + FA = 0.01	Methodology prescribed by Soongswang et al., 1988	In the order of 10^{-9} to 10^{-6} cm/s and 10^{-10} to 10^{-8} cm/s (with/without PP fiber)

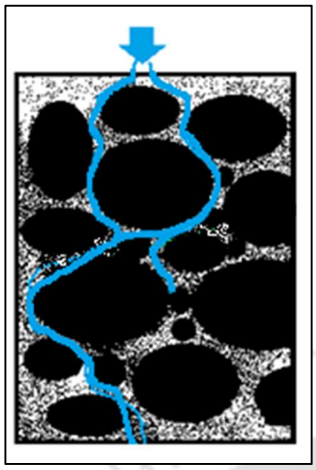

Figure 2.1: (A) Water permeation through conventional concrete.

Figure 2.1: (B) Water permeation through FC.

In this regard, it is to be noted that the literature on tortuosity, permeation related characteristics and clogging potential of FC is also very limited. As per Yuan et al., 2021, and She et al., 2017, based on studies on permeation characteristics of FC, it was established that pore size, pore shape, aspect ratio of pores and specific surface area of pores have significant effect on tortuosity and permeability. Further, in order to address the problem of clogging, it is necessary to design the FC with lesser tortuosity and higher permeability as the particles moving in pores (that are more tortuous) have greater probability of retaining and accumulating within pores [Kia et al., 2017]. Furthermore, FC usually has microstructure with void sizes generally ranging from 100 to 200 microns and hence the particles bigger than 200 microns are prevented from entering the pores, thereby reducing the chances of getting clogged by bigger particles. Moreover, as the density of air voids in FC is more, rate of clogging is expected to be lesser.

Also, it can be noted from table 2.1 that mostly water permeability method is used to measure the permeability of different types of concrete (other than the FC). Based on the limited studies on permeability of FC as summarized in table 2.1, it can be seen that air / water vapour permeability or the Micro CT scanner methods are the commonly adopted methods. Further, the water permeability of mortar has been found to be systematically lower (in the order of 10^{-1} to 10^{-2}) in comparison to air permeability [Loosveldt et al., 2002]. This can be attributed to the theory of gas slippage (the Klinkenberg effect), the rehydration of non-reacted cement, migration of fine elements, dissolution/ precipitation and water absorption in the smallest pores of the cement matrix [Klinkenberg, 1941,

Loosveldt et al., 2002]. In addition, this difference in water and air permeability increased with decrease in the permeability of concrete [Bamforth, 1987]. As per Milla et al., 2021, measuring the actual water permeability of concrete with economical and rapid test methodologies is important. Particularly for concrete structures such as retaining walls, dams, reservoirs, and marine structures, interaction with water is more common rather than gas/ air/ water vapour, hence it is more rational to measure the permeability of FC using the water permeability method. The water permeability of concrete can be determined as per BS EN 12390-8 and DIN 1048-5: 1991 standards in which the field conditions (in terms of water head) are replicated by applying hydraulic pressure [Milla et al., 2021]. These methods are however limited to determining the depth of penetration. Alternatively, the IS 3085: 2021 provides guidelines for the measurement of the water permeability of concrete in accordance with Darcy's law of fluid permeability through a porous medium. Further, the standard also provides guidelines for ensuring that sealing the edges of the concrete specimen is watertight. According to IS 3085: 2021, sealant is a substance that is applied to a surface to prevent air, water, and other substances from entering or escaping from it. These sealants are generally used in permeability test in order to define and control the flow direction of fluids in specimen. Molten sealant, epoxy coating, duct tape, and polyurethane rubber ring are some of the sample sealing technologies used by researchers to assure unidirectional flow [Soongswang et al., 1988, RILEM TC 116-PCD, Chandrappa and Biligiri, 2016, Milla et al., 2021, IS 3085: 2021]. The limitation of use of molten sealant as recommended by IS 3085: 2021 is that there are more possibilities of ingress of its liquid phase into the porous structure of FC which can clog the accessible pores, thus leading to inaccurate permeability of FC. Studies have proved that amongst all edge sealing systems, tapes and films offer the best overall performance whereas mixes were found to have a higher risk of hydrophobation [Svennberg and Segerholm, 2006]. Further, the duct tape sealing mechanism is usually adopted when the pressure head levels are in the range of 0 cm to 50 cm [Chandrappa and Biligiri, 2016, Sun et al., 2019]. Hence, the RILEM TC 116-PCD sealing guidelines using a polyurethane rubber ring compressed onto the specimen is the most suitable for porous concrete samples such as FC or pervious concrete subjected to hydraulic pressure. Here it is to be noted that, as per RILEM TC 116-PCD guidelines (for measurement of gas permeability of concrete) the maximum pressure head to be applied on the specimen to be tested is 3.0 bar (3.06 kg/cm^2) whereas, as per IS 3085: 2021 method the corresponding pressure head is 15 kg/cm^2. Thus, available guidelines for the measurement of

permeability are applicable to much lower pressure than those proposed in IS 3085: 2021. Hence, in order to apply a higher-pressure head (similar to that of IS 3085: 2021) on porous samples such as FC, an improvised sealing system, in accordance with the RILEM TC 116-PCD sealing guidelines, is needed.

2.3 EFFECT OF BUBBLE STABILITY ON THE MECHANICAL PROPERTIES OF FC

As per IS 7597: 2019, the compounds known as foaming agents are those that provide a liquid the potential to generate foam when added. Foaming agent are a specific class of compounds that contain both hydrophobic and hydrophilic groups. They have special properties that allow them to enrich at the interface to lower interfacial tension or self-assemble spontaneously in solutions with different morphologies [Ghosh, 2009]. These foaming agents demonstrate their adaptability by being used in a wide range of industries, including drilling mud emulsification, foaming in the chemical industry, cleaning in automobiles, and solubilization in the pharmaceutical industry, etc. [Porter, 1994, Rosen, 2004]. The generation of stable foam, which is necessary for the creation of high-quality FC, cannot be achieved by all foaming agents. Further, the qualities of foam, such as its density, output rate, capacity, and stability, are greatly influenced by the foaming agent choice, and these properties ultimately impact the characteristics of FC [Sahu et al., 2018]. Furthermore, the amount of air voids created in cement pastes or mortar by the foaming agent controls the density of FC.

In most FC applications, the volume of the bubbles ranges from 6% to 35% of the total final mixture [Atoyebi et al., 2018]. Furthermore, the properties of concrete in both its fresh and hardened forms are significantly influenced by the amount of foaming agent present [Jones and McCarthy, 2005b, Aldridge et al., 2005]. Also, the strength, toughness, thermal and sorptivity characteristics of the FC have been greatly influenced by the quality of the foaming agent [Nambiar and Ramamurthy, 2006, Panesar, 2013]. Typically, the foaming agent is composed of hydrolyzed proteins, detergents, synthetic materials, saponin, resin soaps, and glue resins [Bing et al., 2012]. In the global construction sector, protein and synthetic foaming agents are most frequently utilized. The formation of the protein foaming agent occurs in an enclosed, more grounded cell of air-void structure, allowing for the inclusion of a larger volume of bubble and producing a more stable bubble network. The synthetic ones, on the other hand, give up a more prominent extension and thus a lesser density. [Tikalsky et al., 2004, Bing et al., 2012]. It has been

discovered that using chemical foam volume excessively reduces the flow and density of FC ultimately resulting in the reduction of its mechanical properties [Aldridge et al., 2005]. Also, the amount of time spent mixing FC has a significant impact on its flow, indicating that prolonged mixing may cause the enclosed cell of air-voids to be damaged by lowering its air content [Richard, 2013].

Reportedly, the mechanical properties of FC are often influenced by the amount of foam present, rather than the water to cement ratio [Welker et al., 2000]. In particular, the type and dosage of foaming agents, have a significant impact on the mechanical properties of FC [Tikalsky et al., 2004, Nambiar and Ramamurthy, 2006]. It is found that the addition of air-voids in FC has less influence on elastic modulus than on hardened strength [Bing et al., 2012]. Overall, it is advised to add the chemical foaming agent in a viscous state as soon as the product is manufactured to ensure the consistency of the foam. Commonly, foam stabilizer and foaming agent are added to the FC to increase consistency [Aldridge et al., 2005, Nambiar and Ramamurthy, 2006, Bing et al., 2012]. In this context, Laukaitis et al., 2005 and Siva et al., 2015, stated that addition of additives can prevent bubbles from collapse and stabilize the mix and this will subsequently ensure uniform cellular structure and enhanced strength of FC. Further, it has also been observed that the inclusion of fine fillers in concrete, such as FA, sieved river sand (<300 μm) and pulverized sand, improves foam stability by preventing the coarsening effect and forming a homogeneous covering surrounding the lamellae [Nambiar and Ramamurthy, 2006, 2008, Awang et al., 2012]. Hence, in the following section, a review on the effect of FA on the properties of FC is presented.

2.4 EFFECT OF FA ON THE MECHANICAL PROPERTIES AND CONSISTENCY OF FC

To boost the tremendous capability of FC in structural applications, the mechanical performance of FC has to be improved through the improvement of pore structure and matrix composition. Here it is to be noted that, as per Indian standard codal guidelines, the minimum requirement of compressive strength for load-bearing applications of FC ranges from 6.5 N/mm^2 to 25.0 N/mm^2 for density ranging from 1200 kg/m^3 to 1800 kg/m^3 [IS 2185-4: 2019]. In this line, strong efforts are made by various researchers to enhance the properties of FC through use of various waste products and additives such as FA (up to 75%), silica fume (up to 20%), nano silica (1.5%), ground granulated blast furnace slag (up to 40%), glazed hollow beads (up to 4%), quarry dust (up to 60%)

[Kearsley and Wainwright, 2000, 2001, Jones and McCarthy, 2005a, Nambiar and Ramamurthy, 2006, Hu et al., 2016, She et al., 2018, Gokce et al., 2019, He et al., 2019, Jose et al., 2020, Lu et al., 2020, She et al., 2020, Chen et al., 2021] as summarized in table 2.2. For instance, Kearsley and Wainwright, 2000, 2001, produced FC with partial replacement of cement with FA and based on the experimental outcomes reported that the oxygen and water vapour permeability of such FC increases with increase in porosity as well as FA content. However, no significant reduction in long-term strength of such modified FC was observed. In a recent work by Chen et al., 2021, for FC with density less than 1000 kg/m^3 the partial replacement of cement with FA up to 50%, has resulted in a limited increase in compressive strength at the age of 28 days. However, further increase in FA replacement level is reported to have negative effect with a maximum decrease up to 29% in compressive strength. Further, it is to be noted that the water absorption of such modified FC had increased from 10% to 30% with increase in FA content. Adding to above, it is surprising to note that very few researchers have used class F FA as potential alternative for sand in FC [Jones and McCarthy, 2005a, Nambiar and Ramamurthy, 2006, He et al., 2019, Gandhi et al., 2023]. Based on the limited studies, researchers have concluded that the use of FA rather than sand results in the enhancement of compressive strength as well as water absorption.

In this line, Zhihua et al., 2007, stated that modification of cement-sand matrix with ultra-fine mineral admixtures such as slag (16%) and FA (84%) as replacement for sand increased the viscosity and prevented the segregation of fresh FC mixture. Further, from mechanical behavior perspective, it facilitated faster development of strength and resulted in 4 to 11 times enhancement in strength of FC when compared to control mixes without admixtures. In another work, Hilal et al., 2014, have studied the combined effect of cement replacement with silica fume and sand replacement with FA at 10% and 20% replacement levels respectively in FC with different design densities viz. 1300 kg/m^3, 1600 kg/m^3 and 1900 kg/m^3. Based on their experimental outcomes, it was proved that combined effect of above mineral admixtures has enhanced the spreadability from 180 mm to 350 mm and also significantly improved the mechanical performance which is evident from 100% to 200% increase in compressive strength, 40% to 100% increase in flexural strength and 40% to 95% increase in split tensile strength of FC. Though there are many studies reported on use of FA as binder replacement, however, there are only limited studies available on use of FA as filler and on the water demand requirement for

different levels of FA additions, and on the consistency and stability of FC mixes. Further, it is to be noted that the incorporation of FA and other fine mineral admixtures necessitates the addition of high range water reducing admixtures to achieve the required dispersion and consistency. In this line, there are also few studies reported on incompatibility issues between SP and foaming agent in terms of collapse of foam particularly when a higher dosage of SP is used in FC. For instance, Dhasindrakrishna et al., 2021, studied the impact of variation in dosage of SP (0.05% to 0.47% by weight of cement + FA) on foam stability through assessment of various stages of FC stability such as failure initiation, partial collapse and complete collapse. Based on their experimental outcomes, it was established that the stability of fresh FC rises with foam content as long as the interstitial paste's rheological properties stay constant. Hence from the compatibility perspective, in line with earlier literature, dosage of SP in FC was limited to 0.2% by weight of cement as the rheological behavior of FC changed from shear thinning to shear thickening at higher dosages of SP [McGovern, 2000, Brady et al., 2001, Dhasindrakrishna et al., 2021]. In this line, a few studies have also highlighted that the incompatibility issue was more noticed with protein-based foaming agent than with synthetic ones [McGovern, 2000, Brady et al., 2001]. From the review it is evident that the effect of the addition of SP on the consistency and stability of FC mixes with various mineral admixtures is another important facet to be studied in detail.

Table 2.2: Summary of various properties of FC with FA and other admixtures as reported in the literature.

Reference.	**FC Density**	**Mix-proportion**	**Properties (Age at time of testing)**
Hu et al., 2016	400 kg/m^3	Cement / FA ratio = 1.5 (by weight), water-binder ratio = 0.6, Glazed Hollow Beads were added at a dosage of 0.8%, 1.6%, 2.4%, 3.2%, and 4% by weight of gross binder material.	Compressive strength: 1.8 N/mm^2 to 2.4 N/mm^2 (28 days)
Kadela et al., 2017	500 kg/m^3 to 1300 kg/m^3	Neat cement pastes with foam Water$_{eff}$/ cement = 0.44 (Water$_{eff}$ includes water and liquid foaming agent)	Compressive strength: 1 N/mm^2 to 15 N/mm^2 (28 days) Flexural strength: 0.1 N/mm^2 to 0.9 N/mm^2 (28 days)

Falliano et al., 2018	300 kg/m^3 to 850 kg/m^3	Neat cement paste and foam Water$_{eff}$ / cement = 0.3	Compressive strength: 0.1 N/mm^2 to 10.2 N/mm^2 (28 days)
Jose et al., 2020	1600 kg/m^3 to 1800 kg/m^3	Water: powder (cement + FA + G) ratio =0.55, 0.65 Sand to powder ratio = 3, 4. G = Ground Granulated Blast Furnace Slag replacing cement at10% to 40% by weight, FA replacing cement at 10% to 40% by weight, Q = Quarry dust replacing sand at 20% to 60% by weight.	Compressive strength: 2.1 N/mm^2 to 13.3 N/mm^2
Othman et al., 2021	1400 kg/m^3 to 1800 kg/m^3	Cement to sand ratio = 0.5 to 2 (by weight) W/C = 0.4 to 0.6 Processed spent bleaching earth as partial cement replacement	Compressive strength: 3.0 N/mm^2 to 23 N/mm^2 (28 days)
Gopalakrishnan et al., 2020	1200 kg/m^3	Partially replacing cement by FA at 0 to 50% levels by weight Partially replacing river sand by quarry dust at 0 to 50% levels by weight Water to binder ratio = 0.4	Compressive strength: 5.3 N/mm^2 to 11.2 N/mm^2 (28 days) Split tensile strength: 0.7 N/mm^2 to 1.7 N/mm^2 (28 days) Water Absorption: 9.8% to 17.5% (28 days)
Chourasia et al., 2020	800 kg/m^3	FA (580 kg), cement (140 kg), water (80 kg), and foaming agent (88 L) are the main ingredients of the developed FC panels.	Compressive strength of cube: 3.2 N/mm^2 Panel compressive strength = 1.20 N/mm^2 Water Absorption of panels: 41 %
Hao et al., 2022	200 kg/m^3 to 1200 kg/m^3	Alkali activated FC Matrix consists of FA (30%), granulated blast furnace slag (30%), sodium silicate (27%), sodium hydroxide (2%) and water (11%) in mass %.	Compressive strength: 0.5 N/mm^2 to 45 N/mm^2 (28 days) Flexural strength: 0.22 N/mm^2 to 13.9 N/mm^2 (28 days) Water Absorption: 14.1% to 124% (28 days)

2.5 EFFECT OF PP FIBER ON THE MECHANICAL PROPERTIES OF FC

Several studies have reported that the use of fiber can further enhance the strength of FC as summarized in table 2.3. For instance, strong efforts are made by various researchers to enhance the properties of FC through use of various natural and synthetic fibers. The natural fibers such as wood fibers (up to 0.4%), flax fibers, bamboo fibers (up to 1%), sisal and coir fibers (up to 0.75%), banana fiber (up to 0.55%), coconut and pineapple leaves fibers (up to 0.4%), hemp and kenaf fibers (up to 1%) natural fiber henequen (treated or untreated) (up to 1.5%) have been used in the FC [Yan et al., 2014, Mydin et al., 2015, Kavitha and Kala, 2016, Mydin et al., 2016, Grubesa et al., 2018, Xu et al., 2019, Liu et al., 2020, Afraz and Ali, 2021, Khan et al., 2022]. On the other hand, the various synthetic fibers employed in the enhancement of mechanical properties of FC are PP fiber (up to 1.5%), steel fibers (up to 0.4%), basalt fiber (up to 1 kg/m^3 of concrete), asbestos fibers (up to 2%), plastic (up to 0.25%), polyvinyl alcohol fibers (up to 0.3%) and carbon fibers (up to 1%) [Awang and Ahmad, 2012, Kudyakov and Steshenko, 2015, Mhedi et al., 2018, Falliano et al., 2019, Amran et al., 2020b, Raj et al., 2020, Khan et al., 2022]. Further, it is reported that, among the various natural and synthetic fibers used in FC, the synthetic fibers have greater strength than natural fibers [Khan et al., 2022]. Here it is to be noted that, the addition of PP fiber increased resistance to fire, sulphates, chlorides, and carbonation as well as decreased water absorption, leading to the enhancement in durability of FC. Additionally, PP fibers increased the drying shrinkage, shear resistance and crack resistance of the FC [Hadipramana et al., 2013, Liu et al., 2021]. Furthermore, higher modulus of elasticity values was observed by Mellin, 1999, when PP fiber was added to FC (PP fibers 0.50% by mix volume) [Brady et al., 2001]. In another work, Awang and Ahmad, 2014, attempted to evaluate the durability of FC using synthetic and natural fibers such as steel, PP fiber, AR-glass, oil palm fiber, and kenaf fiber. As per their findings, FC with PP fiber exhibited the highest reduction in shrinkage and thermal conductivity. Further, steel fibers, basalt and asbestos fibers, and plastic fibers have negative influence on the homogeneity, compressive strength, durability and production cost of FC [Raj et al., 2019, Khan et al., 2022]. On a similar note, in other works by Raupit et al., 2017 and Hazlin et al., 2017, use of PP fiber in FC showed enhancement in the tensile strength. In addition, such FC also showed sufficient flexural strength post failure. As per Fedorov and Mestnikov, 2018, the increase of strength with

increase in fiber content up to the optimum dosage is due to the cumulative action of two factors. Primarily, the cement matrix in fiber reinforced FC directly transmits the load to the fibers. Secondly, the enhanced fiber-matrix microstructure due to additional binder content can be attributed to the gain of strength. Above enhancement in the tensile strength of FC by PP fiber was later used for seismic isolation applications [Li et al., 2020]. It must be mentioned here that though addition of PP fiber enhanced the tensile strength, as per Huang, 2001; Karahan and Atis, 2011; Hazlin et al., 2017, the use of PP fiber also increased the water absorption capacity and permeability.

Table 2.3: Summary of various properties of FC with fiber (without mineral admixtures) as reported in the literature.

Reference.	FC Density	Mix-proportion	Properties (Age at time of testing)
Hadipramana et al., 2013	1400 kg/m^3, 1600 kg/m^3, and 1800 kg/m^3	Cement, sand and water PP fiber at dosage 0.33 kg/m^3 and 0.25 kg/m^3 of concrete	Compressive strength: 3.65 N/mm^2 to 14.79 N/mm^2 (28 days) Split tensile strength: 3 N/mm^2 to 5 N/mm^2 (28 days)
Falliano et al., 2019	500 kg/m^3 to 1100 kg/m^3	Neat cement pastes with W/S = 0.3 Short fiber = 6 to 48.5 kg/m^3 of concrete	Compressive strength: 1.5 N/mm^2 to 12.84 N/mm^2 (28 days) Flexural strength: 0.09 N/mm^2 to 3.94 N/mm^2 (28 days)
Castillo-Lara et al., 2020	700 kg/m^3	Cement: limestone aggregate (passing through 600 μm) = 2:1 Water = 240 kg/m^3 of concrete Foam = 29 kg/m^3 of concrete Fiber (PP / henequen) = 0.5%, 1% or 1.5% (by volume)	Compressive strength: 1.42 N/mm^2 to 2.14 N/mm^2 (28 days) Flexural strength: 0.225 N/mm^2 to 0.447 N/mm^2 (28 days)

2.6 COMBINED EFFECT OF FA AND PP FIBER ON THE MECHANICAL PROPERTIES OF FC

In earlier sections, the effects of FA and PP fiber on the permeability and mechanical properties of cement-sand based FC were reviewed. Individually, these mix components have been shown to significantly improve the characteristics of FC, according to the existing literature. Therefore, this section addresses the combined effect of these matrix modifications on the characteristics of FC as reported in the literature (table 2.4).

According to Yoosuk et al., 2021, the compressive strength and flexural strength (at the age of 7 days) of high calcium FA geopolymer FC (density: 800 kg/m^3 to 1500 kg/m^3) with 8 molar NaOH, has increased by a maximum of 24% and 93% at PP fiber content of 0.5% and 2.5% respectively. Further, at higher dosage of PP fiber (up to 3%) a significant decrease in these mechanical properties was observed. Similarly, the toughness of such

FC has increased up to 2 kNmm with increase in fiber content with a maximum at 2.5% fiber content. In this regard, Yoosuk et al., 2021, elucidated that up to the optimum dosage, the enhancement in mechanical properties was due to the effect of fiber bridging across the cracks. However, beyond the optimum level of PP fiber content, a drop in workability and the lack of uniform fiber distribution resulted in a rise in porosity and a reduction in mechanical properties. Further, Yoosuk et al., 2021 also stated that, the addition of PP fiber created interfacial transition zones between fibers and matrices. On a similar note, in other work by Li et al., 2022, the compressive strength of FA-based FC (density: 200 kg/m^3) of the same age tends to increase first and then decreased with the increase in PP fiber (length: 15 mm and diameter: 100 μm) content. In this regard, Li et al., 2022 have stated that, with the addition of 0.1% PP fiber, a three-dimensional spatial mesh structure was established in such FC. This resulted in the fiber's role of bridging the skeleton, safeguarding the foam from rupturing, and enhancing foam stability. Further, the fiber and hydration products were closely connected into a whole, improving the compressive strength of FC [Amran et al., 2020a, Agustini et al., 2021, Li et al., 2022]. However, when higher dosage of fiber say 0.4% was adopted, fiber could not be equally distributed throughout the matrix. This led to the rupture of foam and uneven hydration ultimately resulting in damaged pore structure and reduction in compressive strength. In line with earlier discussion, Bing et al., 2012, also stated that the workability of the mixes was significantly decreased when PP fiber was added, and additional SP was needed to make the mixes flowable. In similar works by Raj et al., 2020, it is stated that the mechanical properties of cement/ FA-based FC have increased up to 90% with increase in fiber content up to 0.3%. Also, the impact strength and abrasion resistance of such FC has increased with increase in Poly vinyl alcohol fiber content. Further, this modification has changed the product's failure mode from brittle to ductile behaviour [Amran et al., 2020a, Raj et al., 2020, Agustini et al., 2021]. However, at higher dosages these mechanical properties have exhibited a decreasing trend. As per Awang and Ahmad, 2014, the inclusion of PP fiber has significantly reduced the drying shrinkage of 1000 kg/m^3 FC, along with noteworthy enhancement in its mechanical properties. Further, the replacement of 30% of cement with FA along with PP fiber has exhibited further enhancements in the aforementioned properties.

Recent work by Beskopylny et al., 2023 found that 10% replacement of cement by FA in FC consisting cement, sand and PP fiber exhibited 12% increase in compressive strength and 23% increase in flexural strength. Further replacement of cement with FA (above

10% and up to 70%) in above FC however led to reduction in the compressive strength (up to 41%) and flexural strength (up to 56%). From the aforementioned literature review, it is evident that the combined inclusion of fiber and FA has exhibited significant enhancements in the properties of FC thorough synergistic effect. Hence, in order to enhance the mechanical properties and permeability of FC, PP fiber and FA are chosen as the potential mix components.

Table 2.4: Summary of literature on FC highlighting combined effect of FA and fiber on hardened state properties.

Reference.	**FC Density**	**Mix-proportion**	**Properties (Age at time of testing)**
Bing et al., 2012	800 kg/m^3 to 1500 kg/m^3	Cement: FA = 1:1 Silica fume = 15% (cement replacement by weight) PP fiber: 0.8%	Compressive strength: 5 N/mm^2 (7 days) to 55 N/mm^2 (90 days) Split tensile strength: 0.5 N/mm^2 to 1.4 N/mm^2 (28 days)
Awang et al., 2015	1000 kg/m^3	Cement: sand: water = 1:1.5:0.45 PP fiber or kenaf fiber at 0.25% and 0.4% dosage by volume 30% cement replacement with FA by weight	Compressive strength: 2.0 N/mm^2 (7 days) to 4.0 N/mm^2 (90 days) Split tensile strength: 0.6 N/mm^2 to 0.9 N/mm^2 (28 days) Flexural strength: 0.6 N/mm^2 (7 days) to 1.2 N/mm^2 (90 days)
Rasheed and Prakash, 2015	900 kg/m^3	FA: cement: water: foam 833: 277: 277: 1.4 kg/m^3 Poly-olefin macrofiber or Poly-olefin fibrillated fiber at a dosage of <0.55% by volume	Compressive strength: 3.9 N/mm^2 to 8.4 N/mm^2 (28 days) Split tensile strength: 6.3 N/mm^2 to 10.7 N/mm^2 (28 days)
Jessie and Kotteeswaran., 2018	1400 kg/m^3 to 1650 kg/m^3	Cement: FA: water = 1:0.925:0.75 (by weight) Glass, PP fiber, polyester, rice husk ash, coconut coir ash at dosages of 0.15%, 0.3%, 0.5% by weight of cement	Compressive strength: 4 N/mm^2 to 10 N/mm^2 (28 days)

Raj et al., 2020	1600 kg/m^3	Cement: Bottom Ash = 1:1, W/S =0.35, Fiber content (%) = 0.15 to 0.5	Compressive strength: 6 N/mm^2 to 17 N/m m^2 (28 days) Split tensile strength: 2 N/m m^2 to 4.5 N/m m^2 (28 days) Flexural strength: 1 N/m m^2 to 2.6 N/m m^2 (28 days) Water absorption = 1 g/100 c m^2 to 25 g/100 cm^2
Amran et al., 2020a	1000 kg/m^3 to 1900 kg/m^3	Cement: FA = 1:1 Silica fume = 15% of cement replacement by weight PP fiber = 7.2 kg/m^3	Compressive strength: 10 N/mm^2 to 70 N/mm^2 (28 days) Split tensile strength: 2 N/mm^2 to 9 N/mm^2 (28 days) Flexural strength: 2 N/mm^2 to 13 N/mm^2 (28 days)
Agustini et al., 2021	1250 kg/m^3, 1650 kg/m^3	Alkaline activator/ FA = 0.35 10 Molar of sodium hydroxide solution Sodium silicate: Sodium hydroxide = 1:2 PP fiber = 0%, 0.25%, 0.5%	Compressive strength: 6 N/mm^2 to 25 N/mm^2 (28 days) Split tensile strength: 2.5 N/mm^2 to 8 N/mm^2 (28 days)
Yoosuk et al., 2021	800 kg/m^3 to 1500 kg/m^3	Liquid alkaline to FA ratio of 0.70 sodium silicate/sodium hydroxide ratio of 1 Sand to FA ratio of 1 Sodium hydroxide concentration of 2 to 8 molars, PP fiber contents of 0%, to 3.0% by weight of FA Foam content of 0%, 1%, and 2%	Compressive strength: 7.65 N/mm^2 to 20.94 N/mm^2 (7 days) Flexural strength: 1.27 N/mm^2 to 3.85 N/mm^2 (7 days) Toughness: 0 kNmm to 2 kNmm
Li et al., 2022	200 kg/m^3	Cement: FA = 3:2 Silica fume = 0% to 8% dosage Hydrogen peroxide = 4% to 6% dosage PP fiber: 0% to 0.4%	Compressive strength: 0.2 N/mm^2 (7 days) to 0.7 N/mm^2 (90 days)
Beskopylny et al., 2023	800 kg/m^3	Water / binder + sand = 0.47 Sand / binder = 0.3 Replacing cement with FA at levels ranging from 0% to 70% PP fiber at 1% by weight of cement.	Compressive strength: 2 N/mm^2 to 3.8 N/mm^2 (28 days) Flexural strength: 0.4 N/mm^2 to 1.13 N/mm^2 (28 days)

Batra et al., 2023	1000 kg/m^3	Cement: sand = 1:2 (by weight) W/S = 0.3 Solids = cement + sand + FA + silica fume + PP fiber Replacing cement with silica fume at 10% level (by weight) Replacing sand with FA at 45% level (by weight) PP fiber added at dosage of 0.2% by total volume	Compressive strength: 0.5 N/mm^2 to 2 N/mm^2 (28 days) and 0.5 N/mm^2 to 3.5 N/mm^2 (56 days) Split tensile strength: 0.1 N/mm^2 to 0.5 N/mm^2 (28 days) and 0.1 N/mm^2 to 0.6 N/mm^2 (56 days) Energy absorption: 1596.88 Joules to 2228.17 Joules
Gandhi et al., 2023	1000 kg/m^3, 1500 kg/m^3	Cement: sand = 1:2 (by weight) W/S = 0.3, 0.35 Replacing sand with FA at 45% by weight Replacing total solids with PP fiber at 0.2%	Compressive strength: 1.0 N/mm^2 to 9 N/mm^2 (28 days) and 1 N/mm^2 to 14 N/mm^2 (56 days) Split tensile strength: 0.5 N/mm^2 to 1.5 N/mm^2 (28 days) and 0.5 N/mm^2 to 6 N/mm^2 (56 days) Energy absorption: 0.1% to 0.38%

2.7 POTENTIAL BENIFITS OF FCIB

Appropriately designed masonry type of construction is considered to be a cost-effective and low-energy alternative. Interlocking blocks (IB), also known as mortarless bricks, is a construction technique that pioneers the concept of dry stacking bricks. IB is globally appreciated because of its special attributes such as enhancement in construction productivity, savings in manpower and material cost, enhanced mechanical and reduced shrinkage properties along with self-alignment and robustness [Whelan, 1985, Anand et al., 2003, Forghani et al., 2016, Thamboo et al., 2020, Shi et al., 2021]. Further, the allowable axial compressive stress for masonry made of IB is higher than that of traditional masonry for a given block strength [Anand and Ramamurthy, 2000]. Several researchers have developed various forms of IB classified based on their geometry (hollow, solid, curved and provisions for reinforcement), function (load bearing, partition or cladding walls) and method of construction [Ali et al., 2012]. The basic idea behind interlocking concept is to restrict the relative movement between the adjacent blocks and enhance mechanical interactions to achieve the required stability [Lecci et al., 2021]. For instance, Wang et al., 2019 has developed a block with imperfection in all 3 directions to establish the interlocking effect and has studied the stability of an Igloo. These imperfections may take the shape of interlocking

characteristics including projections and recesses, tongues and grooves, and nibs and cuts. However, the absence of mortar in the IB is expected to result in reduced lateral load resistance. Hence, to address this, Ali et al., 2012 and Thamboo et al., 2020, recommended provision of horizontal interlocking features along with the vertical interlocking features which could enhance lateral resistance against horizontal as well as vertical bending. Furthermore, the lateral resistance and stability of structure against static and dynamic forces can be enhanced with additional measures such as reinforcement, post-tensioning, internal grouting and surface rendering [Anand and Ramamurthy, 1999, 2000, Ali et al., 2012, Thamboo et al., 2020]. Also, the geometry of the blocks needs to be carefully designed with a tolerance of ± 0.25mm accuracy, as the IB units demand high levels of dimensional accuracy that adhere to the "standard" unit dimension [Thamboo et al., 2020]. In this line, it is to be noted that imperfections in surface geometry and contact surface could cause negative impact on mechanical properties leading to failure [Shi et al., 2021]. Further, to address the doubts related to water permeation behavior of IB masonry, studies conducted by Anand et al., 2003 and Forghani et al., 2016 have shown that the performance is comparable with that of conventional masonry. Also, the use of mortar paste along with the IB is reported to enhance the compressive strength of the system by 30% while maintaining the inherent characteristics of masonry construction [Ahmad, 2014].

The use of FC as light-weight blocks for masonry construction is more prevalent owing to its reduced density, increased thermal, and acoustic efficiency, better elasticity, compressibility, high energy absorption, durability and fire resistance [Chourasia et al., 2020]. Further, the use of these larger-sized light-weight blocks as an alternative to traditional small-sized bricks helps to reduce mortar joints in masonry construction and subsequently makes the construction process less labor-intensive and time-consuming [Anand and Ramamurthy, 1999, 2000]. Adding to the aforementioned positive attributes, cutting off the unnecessary mass of masonry through the use of light-weight materials will enable the structure to withstand seismic forces and help to go for the greater elevation of structures [Bertero et al., 1980, Bhattacharyya and Agarwal, 2014, Talukdar et al., 2017]. In this line, recent studies have proposed that FC has greater potential for use in light-weight IB masonry for seismic-resistant structures [Chourasia et al., 2020]. Comparative analysis of the performance of burnt solid clay units with interlocking FC panels in confined masonry building demonstrated that the base shear coefficient of confined masonry building enhanced from 0.95 to 1.79 with the added benefit of reduced

masonry wall cross-sectional area by 64% highlighting the superior performance of FC panels. According to the researchers, the interlocking pattern with the top and bottom vertical grooves, caused the FC panels to interlock with efficiency and this helped to limit crack propagation and preserved the system's structural integrity during seismic activity [Chourasia et al., 2020]. However, it is to be noted that for immediate implementation and easy acceptance by the end users, simpler design of IB with close resemblance with the conventional bricks is always appreciated as several innovative systems never made it past the design stage due to their complex configurations [Crofts, 1993, Anand and Ramamurthy, 2000]. Based on the literature review, among the various types of IB reported, Bamba brick classified as perforated block with keys on 2 surfaces and interlocking in 2 directions sounds to be a better option for load bearing and seismic resistance [Kintingu, 2009, Lin, 2020, Xie et al., 2022]. Further, the interlocking in Bamba brick is reported to be more effective in shear resistance as these IB have 50% of its area in shear in the form of interlocking keys provided on 2 surfaces and hence can be considered superior to other interlocking patterns reported in literature. Here it is to be noted that, the minimum compressive strength requirement for dry cast segmental retaining wall units in accordance with ASTM C1372-23 is 20.7 N/mm^2.

2.8 SUMMARY OF LITERATURE REVIEW

Since porosity and permeability are closely related, FC with a larger air content can result in more pervious microstructure which can be utilized for various applications such as horizontal and vertical drains, retaining walls, pavements, etc., where higher permeation is necessitated [Kearsley and Wainwright, 2001, Hilal et al., 2014, Yuan et al., 2021]. Further, with void diameters typically ranging from 100 to 200 microns, FC has a higher density of air voids. As a result, the rate of clogging is anticipated to be lower since particles larger than 200 microns are prevented from entering the pores. Earlier, FC was only designed to attain a low compressive strength (between 1 and 10 N/mm^2), which makes it ideal for use in trench reinstatement and void fill. As a result, the material is rarely used in structural sections. However, many studies have been conducted recently [Falliano et al., 2018, Othman et al., 2021, Hao et al., 2022] to improve FC's strength further for structural applications. In this context, the use of additives and admixtures can stabilize the mixture and stop bubbles from collapsing, ensuring homogeneous cellular structure and subsequently enhances strength of FC. Moreover, the addition of fine fillers such as FA and sieved river sand (less than 300 μm), has been found to enhance the foam

stability by averting the coarsening effect and creating a uniform layer around the lamellae and subsequently improved FC strength [Nambiar and Ramamurthy 2006, 2008, Awang et al., 2012]. On the other hand, FC's tensile strength, ductility, water absorption capacity, and permeability were all improved by the inclusion of PP fiber as reported by various researchers [Huang, 2001, Karahan and Atis, 2011, Hazlin et al., 2017]. Moreover, FA and PP fiber (when combined) have shown a synergistic impact in increasing FC's strength and reducing its shrinkage. Hence, in the present study, various combinations of FA and PP fiber are being studied for enhancement in the mechanical properties and permeability of FC. It should be noted that for porous concrete samples, like FC or pervious concrete subjected to hydraulic pressure, the RILEM TC 116-PCD sealing guidelines, which use a polyurethane rubber ring compressed onto the specimen, are the most appropriate. This is because molten sealants in accordance with IS 3085: 2021, may infiltrate the sample resulting in reduced permeability of sample due to clogging. Further, the RILEM TC 116-PCD guidelines for the measurement of permeability are applicable to much lower pressure than those proposed in IS 3085: 2021. Therefore, an improvised sealing system in compliance with the RILEM TC 116-PCD sealing standards is required in order to apply a higher-pressure head (equivalent to that of IS 3085: 2021) on porous samples, such as FC.

From the literature review on IB it is evident that, economy, robustness and sustainability are the potential benefits of FCIB. Here it is to be noted that, the choice of IB pattern plays a major role in load bearing capacity for the intended application. Further, the Bamba type interlocking pattern, with 50% of its area in shear resistance, can be considered superior to other interlocking patterns reported in literature. Moreover, the literature review indicates that the combination of highly permeable FC with superior interlocking pattern, satisfying the ASTM C1372-23 requirements, can be a potential product for the intended application of dissipation of pore water pressure behind retaining wall.

2.9 MAJOR GAPS IN EXISTING WORK

Based on the review, it is observed that more systematic research is necessitated in the following areas as the available literature is limited. The limited literature available on the permeability of FC indicate that, in contrast to other types of concrete, air/ water vapour permeability or the Micro CT scanner methods are more frequently used instead of water

permeability method. This may be explained by the FC's high porosity, which makes it challenging to seal in order to achieve unidirectional flow and precise measurement of its water permeability. Hence, a reliable sealing method is required to measure the water permeability of FC.

On the other hand, several studies have suggested the potential of FC mostly in non-structural and semi-structural applications which can be attributed to its reduced mechanical properties. In this regard, though FA and PP fiber (either alone or in combination) have the potential to enhance the strength and permeability, there aren't many studies reported in this context. Hence, in this work, the mechanical properties and permeability of FC are being studied by experimenting with different FA and PP fiber combinations. Furthermore, the literature review also highlights that the reduced density of FC can be utilized in the production of IB which can result in added benefits such as savings in manpower, material and time. However, the literature available in this context is very scarce. Hence, research on FCIB is necessary in order to effectively implement this.

2.10 MOTIVATION FOR THE WORK

With enhanced mechanical and permeation characteristics, FC can have good potential in various applications such as controlling stormwater runoff, ensuring drainage paths for recharging groundwater, vertical and horizontal drains in landfills, and pore pressure dissipation through retaining walls [Tosun, 2014, Guntakal and Selvan, 2017, Park et al., 2022]. On a similar note, the authors have published two review articles Kamisetty et al., 2022, 2023a, on possible structural application of FC in construction of retaining wall facilitating pore water pressure dissipation. Further, it is to be noted that generation of FC requires sand in large quantities. With ongoing issues related to unavailability of suitable sand in huge quantities, the production of FC using sand may be proved unsustainable. Replacement of sand with FA will not only reduce the dependency of FC’s production on sand but will also utilize hazardous industrial waste like FA in FC production, which otherwise is an environmental concern [Jones and McCarthy, 2005a, Nambiar and Ramamurthy, 2006, Raut and Deo, 2017, He et al., 2019, Gandhi et al., 2023]. In the light of very limited works on strength and permeability of FC with combination of FA (as filler) and PP fiber [Siddique, 2003, Hazlin et al., 2017, Raut and Deo, 2017], the present work investigates the effect of partial replacement of sand with Class F FA and

incorporation of PP fiber on spreadability, strength and water permeability of FC. The high porosity of FC makes it challenging to adopt the conventional method of water permeability testing, particularly with respect to the existing sealing techniques. Ingress of molten sealants into porous structure of FC [IS 3085:2021], suitability of RILEM TC 116-PCD technique only for low pressure (up to 3 kg/cm^2) are the major limitations commonly reported with the presently adopted sealing techniques. Further, review indicates that appropriate sealing mechanism for rational measurement of permeability of porous materials like FC needs to be identified. Hence, to address the above issue, the present study is first of kind of study to propose a novel sealing mechanism for measurement of water permeability of FC at higher pressures. Furthermore, the literature review indicates various potential benefits of FC and IB individually. However, the literature available on the use of FC for IB for the intended application of dry cast segmental retaining wall is very scarce. Hence, the present study aims to develop a potential FCIB as dry cast segmental retaining wall unit.

भारतीय प्रौद्योगिकी संस्थान गुवाहाटी
Indian Institute of Technology Guwahati

CHAPTER 3

OBJECTIVES AND METHODOLOGY

3.1 GENERAL

From the review of factors leading to landslides in north east India, the need for an innovative mitigation measure and the potential of FC for its use in dry-cast segmental retaining walls have been highlighted. The primary objective of the present study is to develop dry cast segmental retaining wall units with desired strength and permeation characteristics. The detailed objectives and scope for present study have been defined as outlined in the following sections.

3.2 OBJECTIVES

Following are the detailed objectives of the present study:

- To evaluate the effect of variation in foam content on the fresh state (consistency and stability) and hardened state properties (compressive strength, split tensile strength and water permeability) of FC mixes with FA (as replacement for sand) and PP fiber.
- To carry out extensive experimental investigations on the effect of various levels of replacement of sand with FA and total solids replacement with PP fiber on the fresh state (consistency and stability) and mechanical characteristics (compressive strength, split tensile strength and flexural strength) of FC with design density 1500 kg/m^3.
- To ascertain the performance (water absorption, water permeability, compressive strength and shear resistance) of FCIB and masonry prisms produced with selected FC mixes which satisfied the criteria of strength and permeation as obtained from earlier studies.

3.3 SCOPE OF WORK

The scope of the study is limited to the following with respect to raw materials and methods to be adopted.

- The study is restricted to synthetic surfactant comprising of 5% sodium lauryl sulphate (SLS) and 0.2% carboxymethyl cellulose (CMC) (as additive).

- A constant cement sand ratio of 1:2 is adopted throughout the study. Ordinary Portland cement (OPC) 43 grade conforming to IS 269: 2020, sieved river sand finer than 300 μm, FA (class F) obtained from NTPC Bongaigaon and PP fiber have been used.
- FC design fresh density ranging from 1000 to 1800 kg/m^3 have been adopted for permeability studies to study the effect of foam content in accordance with DIN 1048-5: 1991, IS 3085: 2021.
- SP (Fosroc auramix 300) has been used in the present study. Dosage of SP has been varied accordingly for different mixes to achieve the desired spreadability of minimum 40% in accordance with ASTM C796-19 [Nambiar and Ramamurthy, 2008].
- The selection of satisfactory mixes is carried out using the guidelines mentioned in ASTM C1372-23 with respect to compressive strength for use in dry-cast segmental retaining walls.

3.4 OUTLINE OF THE PRESENT RESEARCH WORK

The current study is conducted by adopting the following methodology as depicted in figure 3.1.

- An in-depth review on the influence of various admixtures on mechanical and permeation behaviour of FC is carried out.
- Firstly, the experimental investigations on the effect of variation in foam content on the fresh state properties (consistency and stability), mechanical properties (compressive strength and split tensile strength) and water permeability of FC with FA and PP fiber for design density ranging from 1000 kg/m^3 to 1800 kg/m^3 shall be studied at the age of 28 days and 56 days. In order to investigate the permeation behaviour of porous concrete such as FC, a novel sealing mechanism has been developed and utilized to measure the water permeability in accordance with IS 3085: 2021.
- This is followed by extensive experimental investigations on the influence of variation in FA levels (sand replacement), PP fiber levels (total solids replacement), SP (at constant W/S = 0.3) and W/S (to achieve recommended fresh state properties) on the performance (spreadability and mechanical properties) of FC with design density of 1500 kg/m^3 in accordance with ASTM guidelines.

- Finally, the most suitable mixes with desired compressive strength in accordance with ASTM C1372-23, shall be used for production of FCIB. The performance of FCIB and masonry prisms constructed using FCIB will be ascertained through further investigations such as water permeability, compressive strength, and shear resistance.

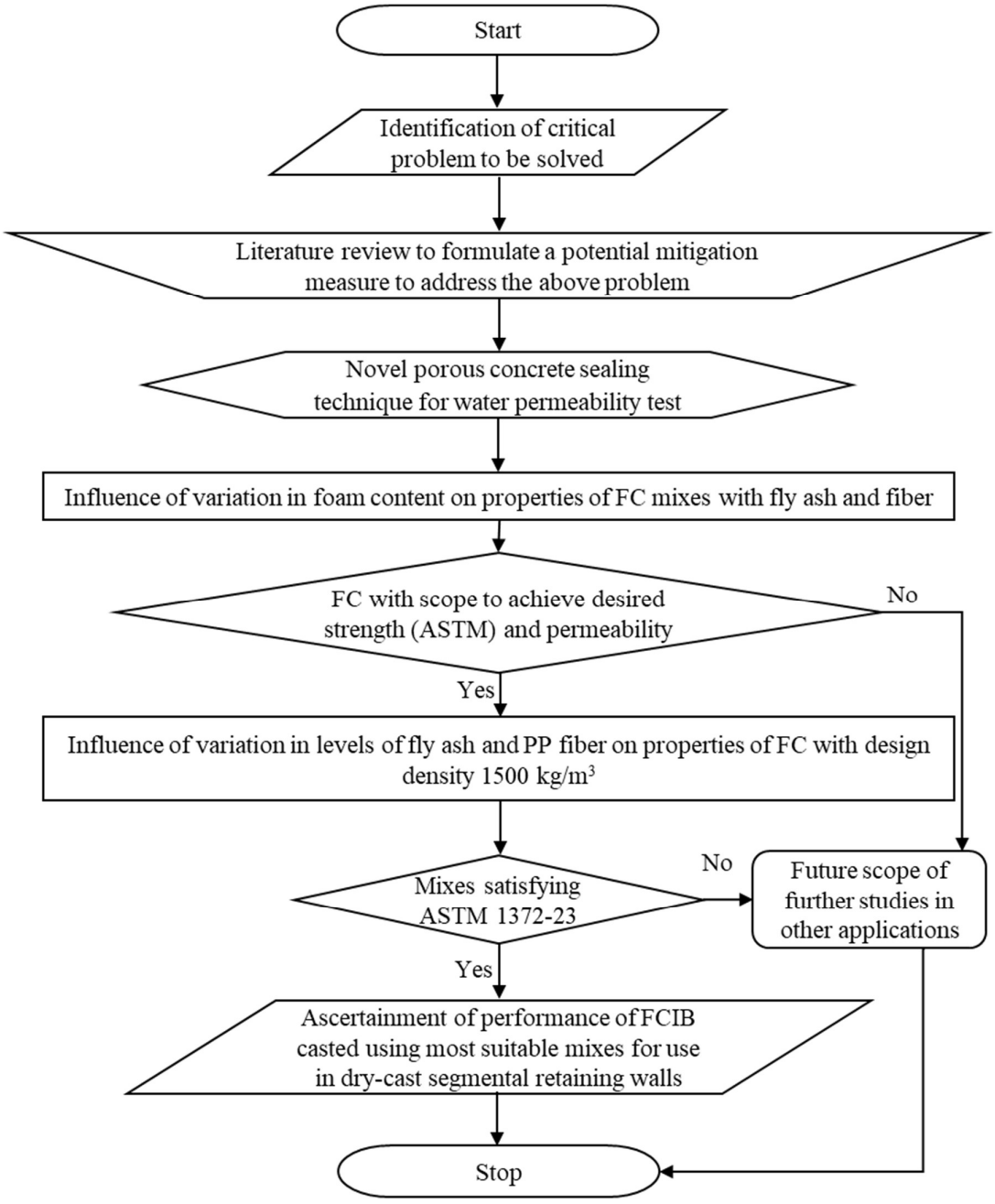

Figure 3.1: Proposed methodology.

भारतीय प्रौद्योगिकी संस्थान गुवाहाटी
Indian Institute of Technology Guwahati

CHAPTER 4

INFLUENCE OF VARIATION IN FOAM CONTENT ON PROPERTIES OF FC MIXES WITH FA AND PP FIBRE

4.1 GENERAL

Strength and permeability are the two critical properties of interest for various applications of FC. These properties are well known to be highly dependent on parameters such as density, mix composition and microstructure of FC. Among various measures to enhance the strength and permeation characteristics of FC, incorporation of FA and PP fiber has been proven to be effective solutions by various studies. In terms of permeability, though the measurement of air / water permeability has been suggested by various methods, usually such measurements are limited to a pressure of 3 bar. For higher pressures (as recommended in IS 3085: 2021codal provisions) no to limited work is available. In this chapter, variation in spreadability, permeability, compressive strength and split tensile strength of FC due to replacement of 50% of sand with Class F FA and incorporation of PP fiber is investigated on a systematic basis for FC with varying foam volume. For the measurement of permeability at higher pressures (>3 bar), use of novel sealing mechanism using 5 mm thick rubber membrane as sealant with iron spiral cylinder and clamp as casing, is attempted in this work. The present study is first of kind of study using the above-mentioned sealing mechanism for measurement of permeability of FC at higher pressures. Further, only scanty literature is available on permeation behavior of FC with FA (as filler) and PP fiber.

4.2 MATERIALS AND METHODOLOGY

4.2.1 MATERIALS

Materials for the current investigation include OPC-43 grade (supplied by Dalmia Ltd.) that conforms to IS 269: 2020 and sand that passes through a 300 µm sieve at a constant cement-to-sand ratio of 1:2. Additionally, Class-F FA (procured from National Thermal Power Corporation, Bongaigaon, India) having a specific gravity of 2.16 and passing through a 75 µm screen is utilized as replacement for sand. PP fiber utilized in the present

study is purchased from Jogani Impex LLP and has specific gravity of 0.91, tensile strength of 390 N/mm^2, length of 12 mm, and diameter of 22 µm. A foam generator (Greenstone) is utilized to produce pre-formed foam with an initial foam density of 50 kg/m^3 from a surfactant solution mixture of SLS and CMC (purchased from LOBA chemicals) at 5% and 0.2% concentrations respectively.

4.2.2 MIX PROPORTION

The present study is limited to FC with design densities of 1000, 1500 and 1800 kg/m^3 (foam volume varying from 9% to 50%). According to ASTM C796-19, the mix proportions needed to achieve these target densities were computed and are shown in Table 4.1. Further, Table 4.2 provides details on the terminology for various mix codes. The W/S of the above-mentioned design densities are fixed at 0.35, 0.3, and 0.25 respectively considering the stability of mixes based on previous literature and preliminary trials [Sahu and Gandhi., 2021]. A constant cement-to-sand ratio of 1:2, by mass has been adopted throughout the study. Concrete mixes are prepared by replacing 50% of sand (by weight) with FA and/or 0.05% of total solids with PP fiber (by weight) and these replacement levels are chosen based on literature considering strength and shrinkage aspects. Further, the corresponding base mixes are also prepared by adopting a similar method by excluding the foam component. For all the proposed mixes, the following methodology of preparation is consistently adopted as the mixing process has a substantial impact on the material property. In order to create a homogeneous base mix of the mix components (except foam), the horizontal single shaft mixer with spiral arm is utilized to mix the components for 2 minutes at 35 rpm. Afterward, the predetermined amount of foam is added to the base mixture, and the foam is mixed into the slurry until it is fully mixed into the base mixture. To achieve a homogeneous blend, the complete mixing procedure could take atleast 5 minutes.

Table 4.1: Mixture proportions for 1 m^3 of concrete.

Mix code	Target fresh Density (in kg/m^3)	W/S	Cement (in kg)	Sand (in kg)	FA (in kg)	PP fiber (in kg)	Foam content (in kg)
C1	2169	0.35	535	1071	0	0	0
C2	2259	0.30	579	1158	0	0	0

C3	2349	0.25	626	1253	0	0	0
C1Fa	2034	0.35	502	502	502	0	0
C2Fa	2114	0.30	542	542	542	0	0
C3Fa	2193	0.25	585	585	585	0	0
C1Ps	2167	0.35	535	1070	0	0.803	0
C2Ps	2257	0.30	578	1157	0	0.868	0
C3Ps	2346	0.25	625	1251	0	0.939	0
C1FaPs	2033	0.35	502	502	502	0.753	0
C2FaPs	2112	0.30	541	541	541	0.812	0
C3FaPs	2192	0.25	584	584	584	0.877	0
FC1	1000	0.35	247	494	0	0	25.053
FC2	1500	0.3	385	769	0	0	12.709
FC3	1800	0.25	480	960	0	0	6.598
FC1Fa	1000	0.35	247	247	247	0	23.941
FC2Fa	1500	0.3	385	385	385	0	10.976
FC3Fa	1800	0.25	480	480	480	0	4.435
FC1Ps	1000	0.35	247	494	0	0.370	25.039
FC2Ps	1500	0.3	384	769	0	0.577	12.686
FC3Ps	1800	0.25	480	960	0	0.72	6.570
FC1FaPs	1000	0.35	247	247	247	0.370	23.927
FC2FaPs	1500	0.3	384	384	384	0.577	10.954

FC3FaPs	1800	0.25	480	480	480	0.72	4.408

Table 4.2: Nomenclature for mix codes.

Mix code	Meaning
FC1, FC2, FC3	FC1, FC2, FC3 represent FC mixes with design densities 1000 kg/m^3, 1500 kg/m^3 and 1800 kg/m^3 respectively
C1, C2, C3	C1, C2, C3 represent base mixes corresponding to FC1, FC2, FC3 respectively.
Fa	Fa represents mixes with 50% by weight of sand replaced with FA
Ps	Ps represent mixes with 0.05% by weight of total solids replaced with PP fiber
FC3FaPs	For example: This mix code represents FC of 1800 kg/m^3 (FC3) which consists of 50% by weight of sand replaced with FA (Fa) and 0.05% by weight of total solids replaced with PP fiber (Ps).

4.2.3 METHODOLOGY

4.2.3.1 FRESH STATE PROPERTIES, MECHANICAL PROPERTIES AND MICROSTRUCTURE INVESTIGATION

The essential FC fresh state properties to determine the ideal mix proportions are stability and spreadability. The density of FC is measured twice to determine its stability: once before moulding, known as fresh density, and once after demoulding, known as demoulded density. A standard container with a defined volume is immediately filled with FC (without any compaction), and the weight of the sample within the container is then used to compute the fresh density. Similarly, based on sample weight and sample volume after hardening, the demoulded density is computed. Spreadability of FC is assessed using an ASTM standard cone (confirming to ASTM C230-17) in accordance with ASTM C1611-21 [Nambiar and Ramamurthy, 2008, Khwairakpam and Gandhi, 2022].

The mechanical properties of FC are examined in terms of compressive strength and split tensile strength. For each mix proportion, 6 samples of 50 mm cubical specimens and 6 samples of 100 mm in diameter and 200 mm in height cylindrical specimens are prepared in order to determine the compressive strength and split tensile strength respectively. Specimens are demoulded and put through water curing after 24 hours until the age of testing. Specimens are tested at two distinct ages (3 specimens each), namely 28 and 56 days, in order to evaluate the variation of strength with age. Three days before the test,

the specimens are removed from the curing tank, let to air dry, and then tested for compressive strength and split tensile strength in accordance with ASTM C796-19 and ASTM C496-17 respectively.

In the present study, the microstructure of hardened FC samples is studied with SEM images as well as with images captured with optical microscope. For SEM images study, a 2 mm cubical chunk has been cut from the specimen and polished, cleaned with compressed air and the images are captured using SIGMA 300 field emission scanning electron microscope [Castillo-Lara et al., 2020]. For optical microscopic study, the FC specimens are prepared by lapping of specimens with abrasive paper of fineness grade 1000 followed by cleaning with compressed air and drying in oven at 50 ˚C for 3 days. The cut surfaces of 50 mm cubes are treated with coats of black ink followed by filling of pores with white powder as discussed in detail in various works [Chandini and Anand., 2018, Khwairakpam and Gandhi, 2022]. The prepared specimen with air voids of white color and remaining regions in black color is captured and binarization is done using Tcapture image analysis software.

4.2.3.2 PERMEABILITY OF FC

As per literature review, the permeability of FC is to be examined in accordance with IS 3085: 2021. The codal guidelines suggest that the size of the specimen to be tested for permeability has to be a cylindrical sample with a minimum diameter of 100 mm or 5 times the maximum size of aggregate whichever is greater, and the height of the specimen should be equal to its diameter. In this study, as the maximum size of aggregate used for making FC is 300 µm, the size of the cylindrical specimen is chosen as 100 mm diameter and 100 mm height. Six specimens with these dimensions have been prepared for each mix as mentioned earlier in section 4.2.2 and tested for permeability of FC at the above-mentioned ages (3 specimens for each age). Additionally, the sample sealing method recommended by RILEM TC 116-PCD is to be adopted as the use of molten sealant as recommended by IS 3085: 2021 might result in ingress of its liquid phase into the porous structure of FC and eventually clog the accessible pores as discussed earlier. Further, based on the preliminary studies, it is found that the hydraulic pressure that needs to be applied to the FC sample should be higher than the RILEM recommendation of 3 bar pressure to facilitate the completion of test within the maximum time limit as prescribed in IS 3085: 2021. However, the compressibility of air being higher than the rubber

membrane, and hence the application of higher-pressure head on the specimen might affect the sealing efficiency of system recommended by RILEM TC 116-PCD with rubber ring compressed by air. Therefore, an iron clamp and spiral cylindrical casing system is used as an alternative to compress the rubber tube onto the sidewalls of the sample (instead of compressed air as suggested by RILEM TC 116-PCD) in order to improve the sealing efficiency at high pressure, as shown in figure 4.1A. For this purpose, the sample is inserted into a 5 mm thick rubber tube and later fastened with an iron clamp into the spiral cylindrical casing as shown in figure 4.1B.

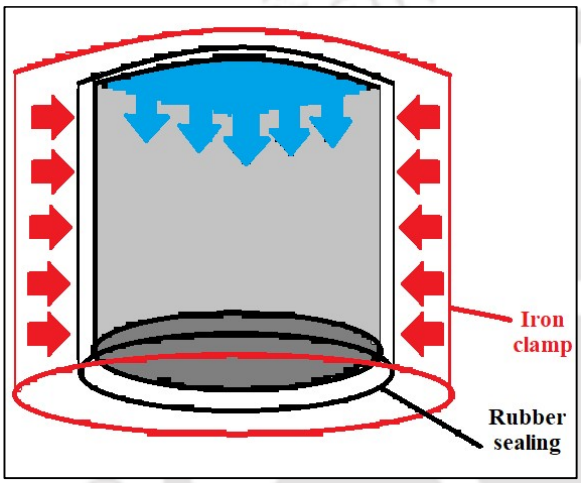

Figure 4.1: (A) Schematic representation of sealing of sample for permeability test.

Figure 4.1: (B) Setup with rubber tube and iron clamp for sealing the sample.

Further, the efficiency of sealing mechanism is inspected as described in IS 3085: 2021 and presented in figure 4.2A. As seen in figure 4.2A, the sealing membrane's effectiveness as a sealer is demonstrated by the fact that air bubbles emerge from the sample's core rather than its interface. The sealed sample is now placed into the permeability device's top cap and bottom clamp funnel as shown in figure 4.2B. Every four hours, the water outflow is monitored while the sample is under a hydraulic pressure of 1, 3, and 5 kg/cm^2 for the FC design densities of 1000, 1500, and 1800 kg/m^3 respectively. Every three consecutive readings were compared until a guaranteed steady state flow is achieved, and the discharge quantity is utilized to compute the permeability of FC using equation 4.1 below, in accordance with IS 3085: 2021.

$$Kw = \frac{Q}{\frac{A.H.T}{L}} \tag{4.1}$$

*Where, Kw= Water permeability of concrete, Q= quantity of discharge, A= cross-sectional area of the specimen, T= time taken for discharge, H= pressure head =10*P (in m), P= pressure applied on the water to percolate into the specimen, L= thickness of the specimen [IS 3085: 2021].*

Additionally, the specimen is immediately split apart to check whether the entire cross-section had participated in permeability. The entire cross-section was discovered to be moist, as shown in figure 4.2C. Further, the compressive stress generated in the sealing system was found to be lesser than the compressive strength of samples used in the present study and hence it can be assumed that the impact of sealing system on the compressive strength and permeability results is not significant.

Figure 4.2: (A) Testing efficiency of sealing mechanism.

Figure 4.2: (B) Experimental setup to measure concrete permeability.

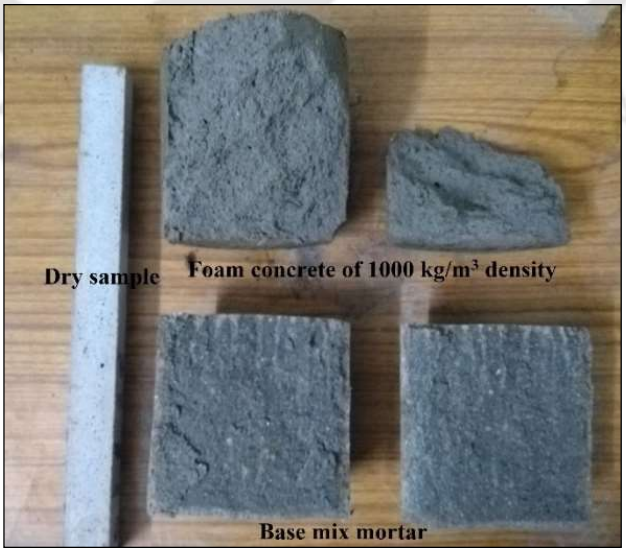

Figure 4.2: (C) Cross section of sample showing water permeation.

4.3 RESULTS AND DISCUSSION

4.3.1 FRESH STATE PROPERTIES (DENSITY AND SPREAD PERCENTAGE)

The proposed FC mixes and the corresponding base mixes are tested for fresh state properties as described in section 4.2. The fresh densities and demoulded densities of various mixes are presented in figures 4.3A, 4.3B, 4.3C. From the aforementioned figures it is evident, that all the FC mixes adopted in this study, have achieved target fresh densities meeting the tolerance limits (i.e., ± 50 kg/m^3 of target density) in accordance to ASTM C869-11 standard and hence can be considered as stable mixes [Nambiar and Ramamurthy, 2008, Amran et al., 2020a, Castillo-Lara et al., 2020]. The difference between fresh and demoulded densities is very much higher for base mix when compared to FC mixes. For instance, a maximum difference of 19% is observed for base mixes while for FC mixes, it is only 7%. Hence, the loss of water from concrete to atmosphere is relatively easier from base mixes when compared to FC mixes. Further, for FC mixes with FA (e.g., FC3Fa), the difference between the fresh and demoulded densities, is found to be 3% while the corresponding difference for contemporary mixes without FA is found to be 7%. The lesser variation in density in FA mixes can be attributed to the higher water retention capacity of FA resulting from its high-water absorption nature [Gokce et al., 2019]

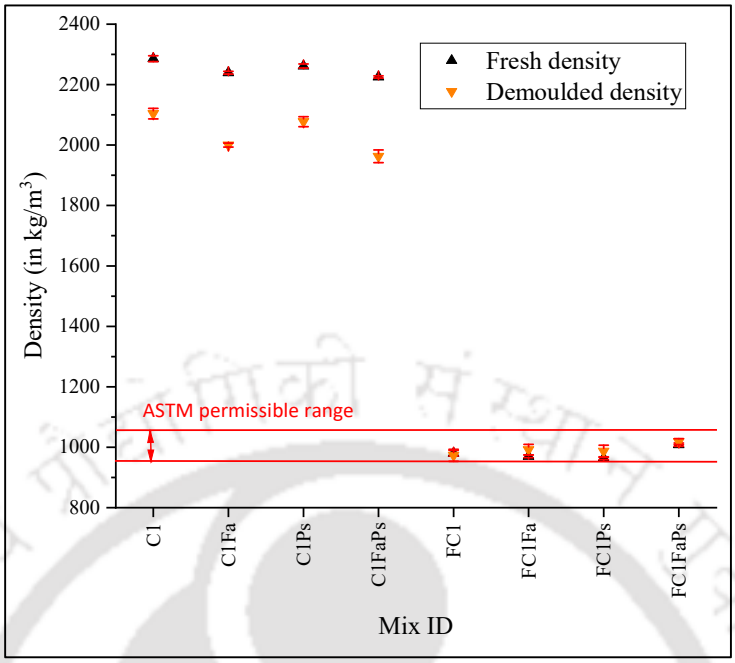

Figure 4.3: (A) Variation in density of concrete for base mixes and FC mixes (Target fresh density 1000 kg/m³).

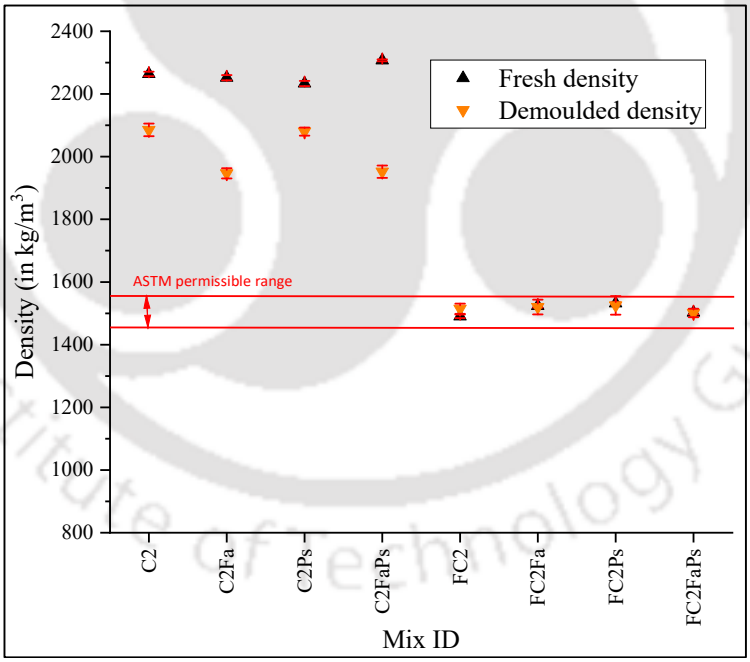

Figure 4.3: (B) Variation in density of concrete for base mixes and FC mixes (Target fresh density 1500 kg/m³).

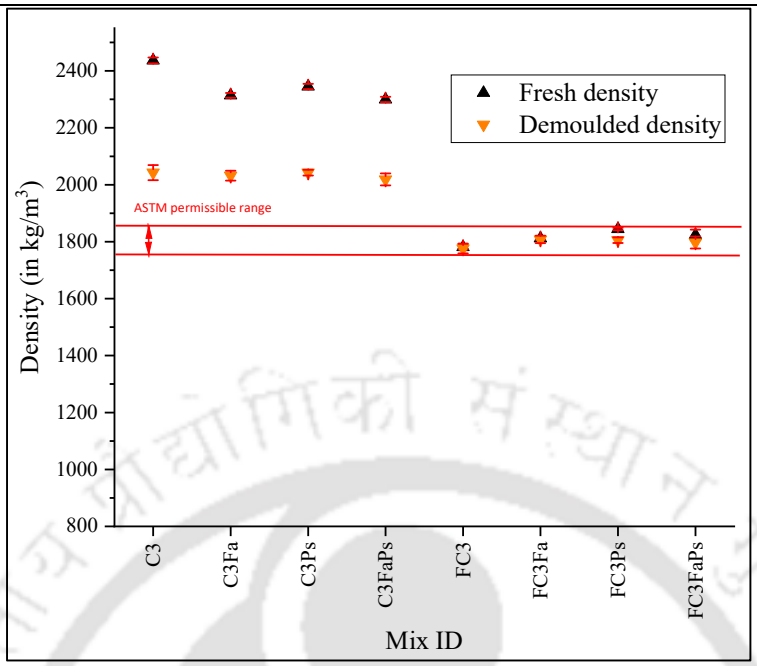

Figure 4.3: (C) Variation in density of concrete for base mixes and FC mixes (Target fresh density 1800 kg/m³).

Further, previous studies have proved that cohesiveness and density of the FC mixes have significant impact on its workability [Makul and Sua-iam, 2016, Krishna et al., 2021]. The results on average spread percentage of various mixes derived from the present study are exhibited in figures 4.4A, 4.4B, 4.4C. General comparison between FC and base mixes indicate relatively lesser spread for FC mixes which is in line with observations reported in literature [Markin et al., 2019, Sahu et al., 2021]. This can be ascribed to more cohesive nature of FC when compared to mixes without foam (base mix). Further, comparative analysis of mixes with FA and corresponding mixes without FA (e.g., comparing C1 Vs C1Fa and FC1 Vs FC1Fa) shows drastic reduction in spread percentage in mixes with FA of the order of 64% for base mixes and 95% for FC mixes which is in line with observations reported in literature [Zawawi et al., 2020]. The finer size particles of FA resulting in higher water demand can be ascribed to reduction in spread percentage. Adding to above, greater cohesiveness and reduced density of FA-based mixes also contributes to substantial reduction in spread percentage [Nambiar and Ramamurthy, 2008, Marthong and Agarwal, 2012]. Similarly, the inclusion of fiber has reduced spread percentage by 17% to 70% for base mixes and 9% to 34% for FC. This behaviour of reduction in spread percentage due to PP fiber addition can be ascribed to the water adsorption by fiber eventually leading to reduction in water content needed for

workability [Zhang and Li, 2013, Amran et al., 2020a]. In addition, fibers also restrict the movement of particles which in turn affects the workability [Gencel et al., 2021]. Further, the combined mixes with FA and fiber (e.g., C1FaPs and FC1FaPs) has exhibited an aggravated reduction in spread percentage of the order of 59% to 89% for base mixes and 76% to 95% for FC mixes. Results indicate that the addition of fibers and FA resulted in a significant reduction in spread percentage in FC mixes when compared to base mixes. Also, the higher viscosity of SLS + CMC surfactant solution and the cohesive nature of the mixes can be attributed to relatively lesser workability of FC mixes. Particularly at higher densities of FC though the concrete exhibited mouldability, but failed to exhibit spreadability. This can be attributed to the lower W/S adopted at higher densities in addition to greater solid content.

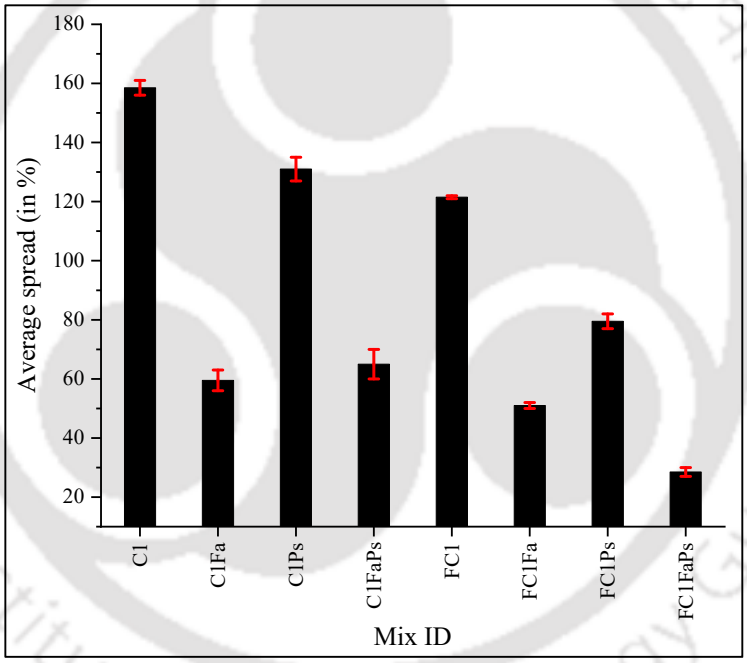

Figure 4.4: (A) Spread percentage of base mixes and FC mixes (Target fresh density 1000 kg/m³).

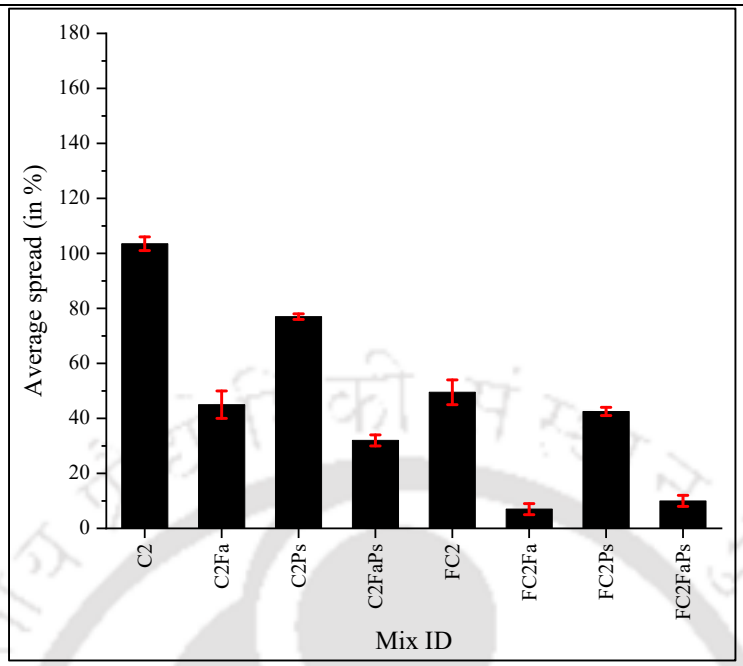

Figure 4.4: (B) Spread percentage of base mixes and FC mixes (Target fresh density 1500 kg/m^3).

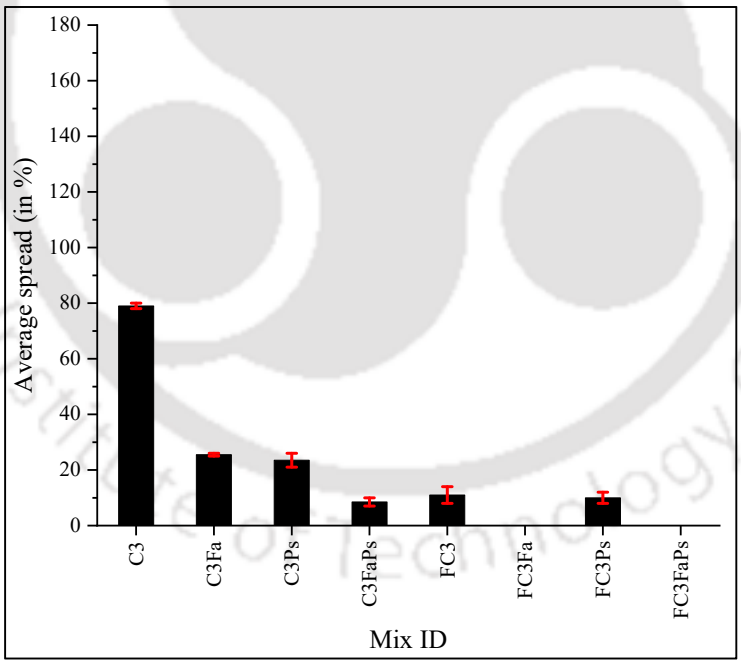

Figure 4.4: (C) Spread percentage of base mixes and FC mixes (Target fresh density 1800 kg/m^3).

4.3.2 MECHANICAL PROPERTIES OF FC

4.3.2.1 COMPRESSIVE STRENGTH

Effect of mix composition on compressive strength of base mix

Results on compressive strength of various base mixes tested at different ages are presented in figures 4.5A, 4.5B, 4.5C. Replacement of 50% of fine aggregate (300 μm) with FA results in maximum increase of 84% in compressive strength (C3 Vs C3Fa). This increase is more predominant in samples at later age of 56 days which is in line with observations reported in literature [Siddique, 2003, Kou et al., 2008, Zawawi et al., 2020]. The delayed pozzolanic reaction and production of more calcium silicate hydrate (C-S-H) gel contributes to the above-mentioned rise in strength as established in literature [Kou et al., 2008]. On the other hand, replacement of the 0.05% of total solids (by weight) with PP fiber has shown up to 10% reduction in compressive strength (C3 Vs C3Ps). The above reduction in strength due to addition of fibers is not noticeable in mixes with lower W/S. On contrary, combination mixes with both FA and PP fiber have shown an increase in compressive strength of mortar by 47% to 89% when compared to corresponding C1, C2 and C3 mixes. Significant increase in paste content due to addition of FA and subsequent increase in binder property and bonding of paste and fiber contributes to enhancement in strength. From this it can be observed that the combination mixes are exhibiting enhanced mechanical properties [Bing et al., 2012, Gandhi et al., 2023]. Further, the results on the compressive behavior (load vs displacement curves) also supports the above observation. For instance, based on the comparative analysis of the compressive behavior (load vs displacement curves) of base mixes (figures 4.5D, 4.5E, 4.5F, 4.5G, 4.5H, 4.5I) it is evident that the post peak behaviour of combination base mixes with both FA and PP fiber (figure 4.5G) shows enhanced ductility behaviour due to the bridging of opening cracks with fibers than that of base mixes without additives (figure 4.5D). The above observations are in line with the results reported by researchers on fiber reinforced concrete [Caggiano et al., 2016].

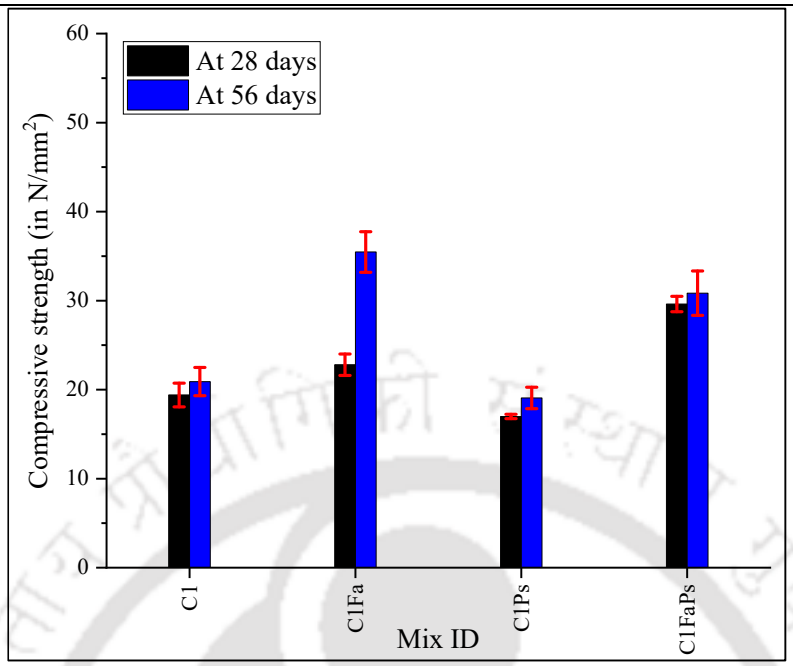

Figure 4.5: (A) Variation in compressive strength of base mixes (For FC target fresh density 1000 kg/m^3).

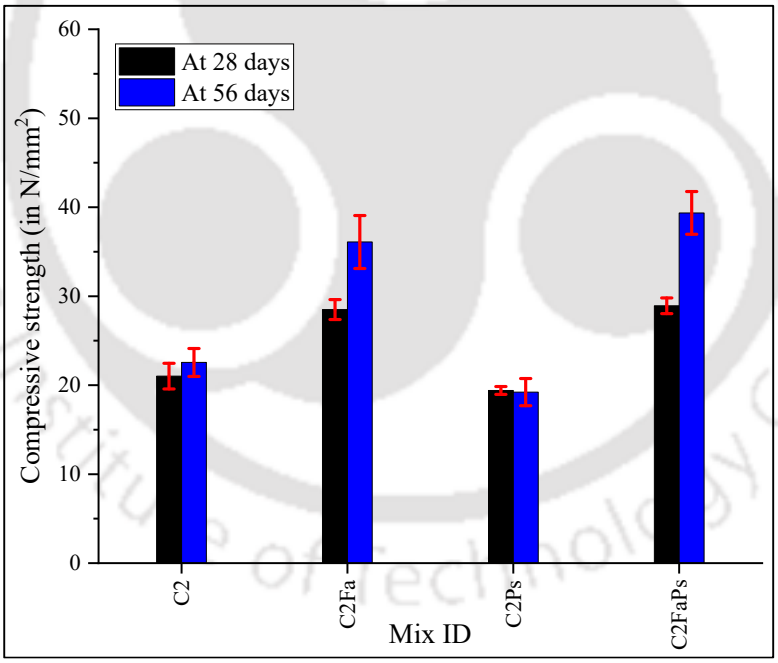

Figure 4.5: (B) Variation in compressive strength of base mixes (For FC target fresh density 1500 kg/m^3).

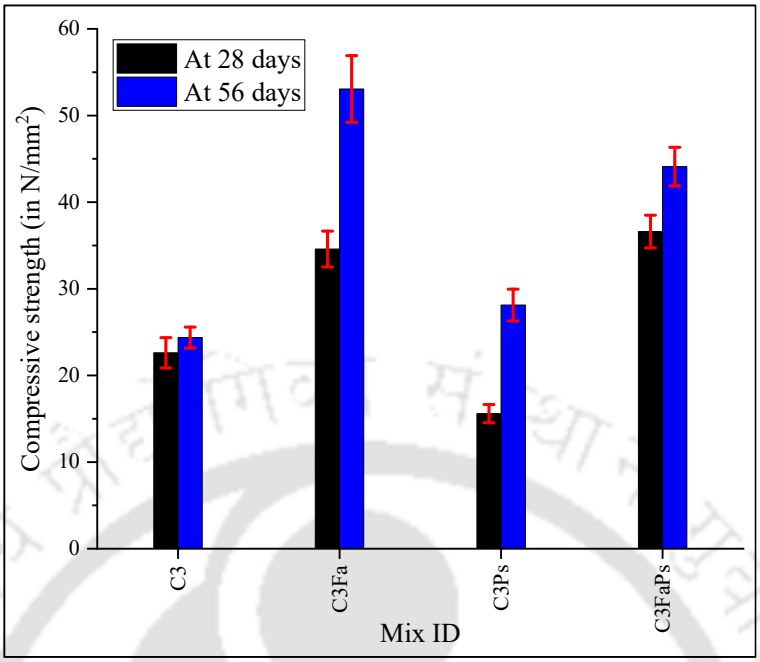

Figure 4.5: (C) Variation in compressive strength of base mixes (For FC target fresh density 1800 kg/m^3).

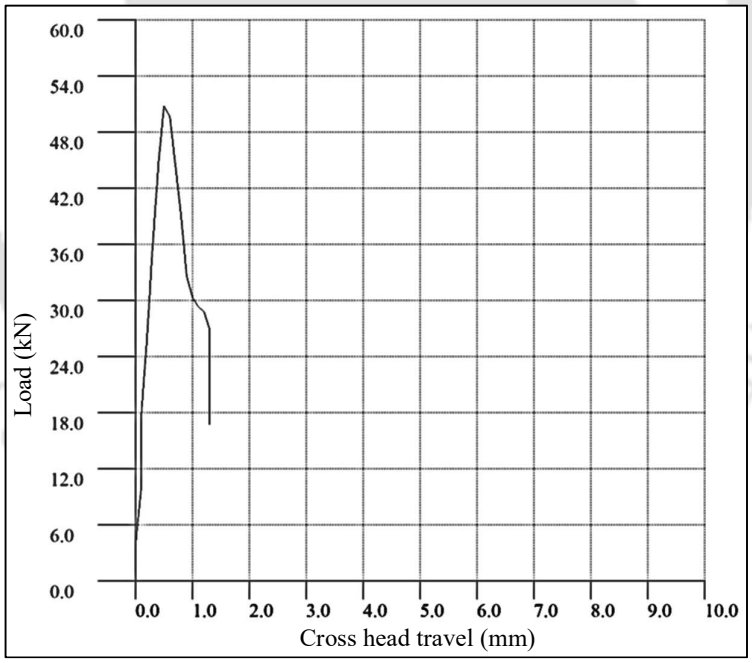

Figure 4.5: (D) Typical compressive behavior (load vs displacement) of base mixes without additives (For FC target fresh density 1000 kg/m^3).

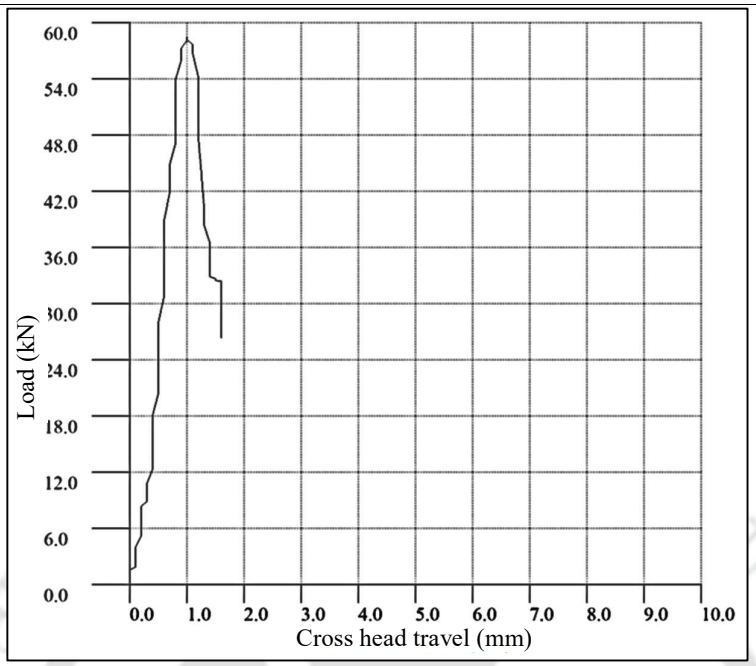

Figure 4.5: (E) Typical compressive behavior (load vs displacement) of base mixes without additives (For FC target fresh density 1500 kg/m³).

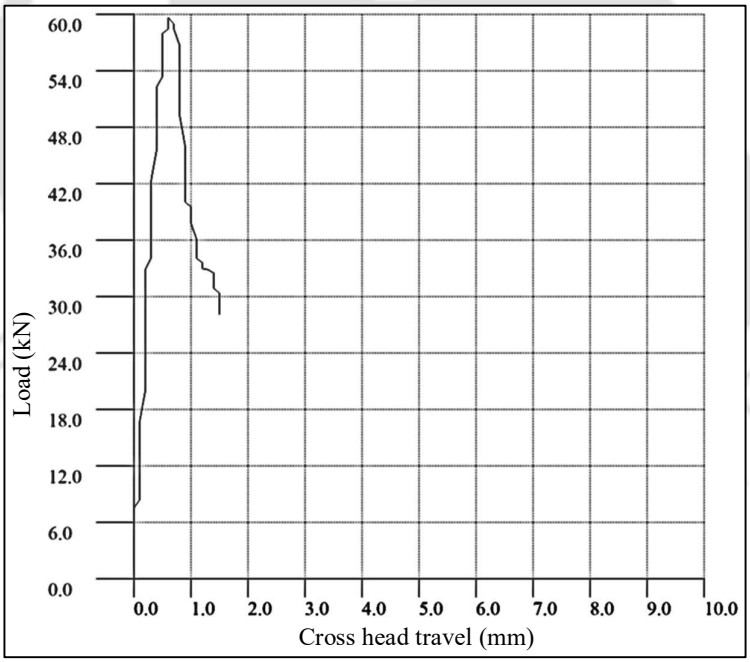

Figure 4.5: (F) Typical compressive behavior (load vs displacement) of base mixes without additives (For FC target fresh density 1800 kg/m³).

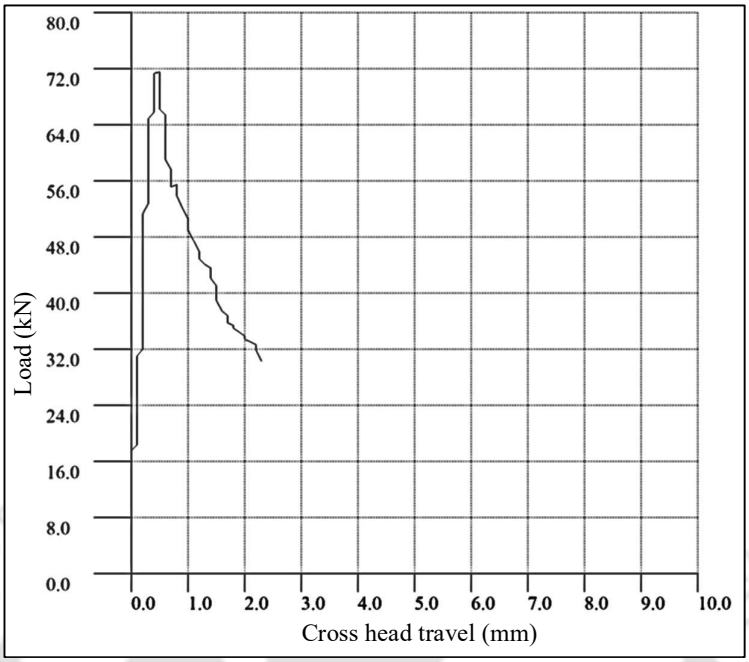

Figure 4.5: (G) Typical compressive behavior (load vs displacement) of base mixes with additives (For FC target fresh density 1000 kg/m^3).

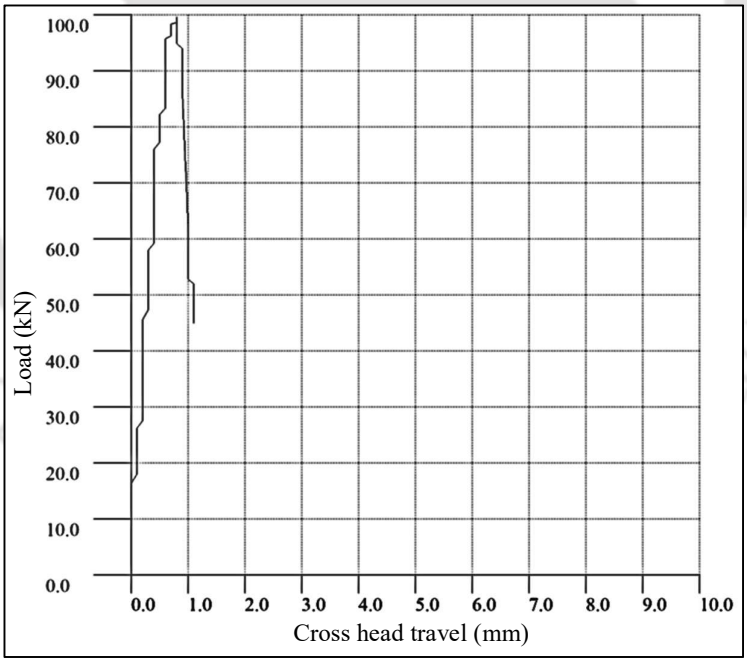

Figure 4.5: (H) Typical compressive behavior (load vs displacement) of base mixes with additives (For FC target fresh density 1500 kg/m^3).

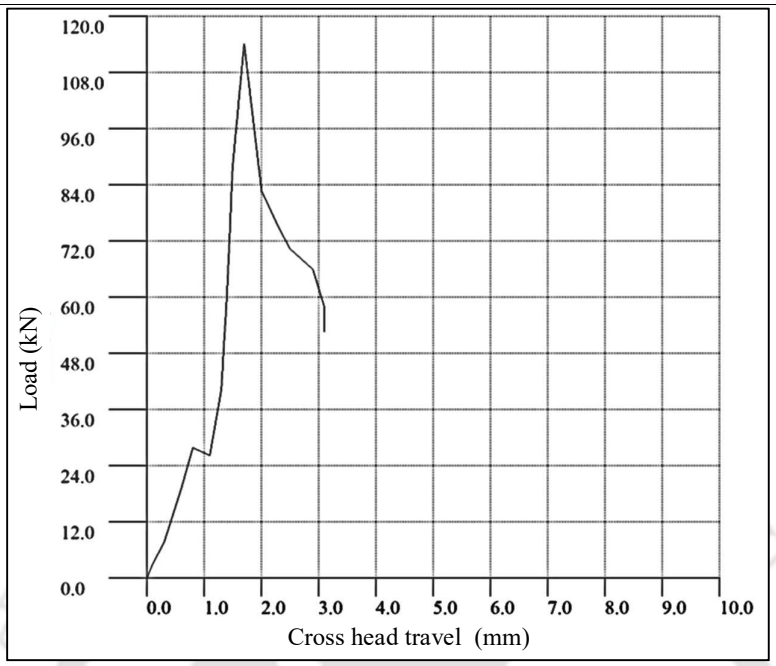

Figure 4.5: (I) Typical compressive behavior (load vs displacement) of base mixes with additives (For FC target fresh density 1800 kg/m^3).

Effect of mix composition on compressive strength of FC

Figures 4.6A, 4.6B, 4.6C, 4.6D, 4.6E, 4.6F, 4.6G, 4.6H, 4.6I shows the variation in compressive strength for different FC mixes along with the typical compressive behavior (load vs displacement curves). The comparative analysis on the effect of various mix constituents on the compressive strength of FC is discussed in detail in the following sections.

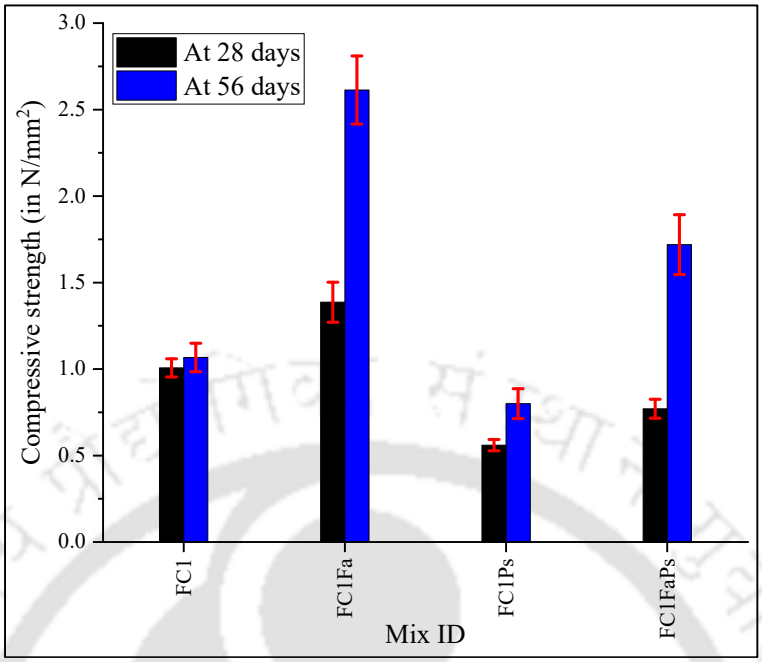

Figure 4.6: (A) Variation in compressive strength of FC mixes (Target fresh density 1000 kg/m³).

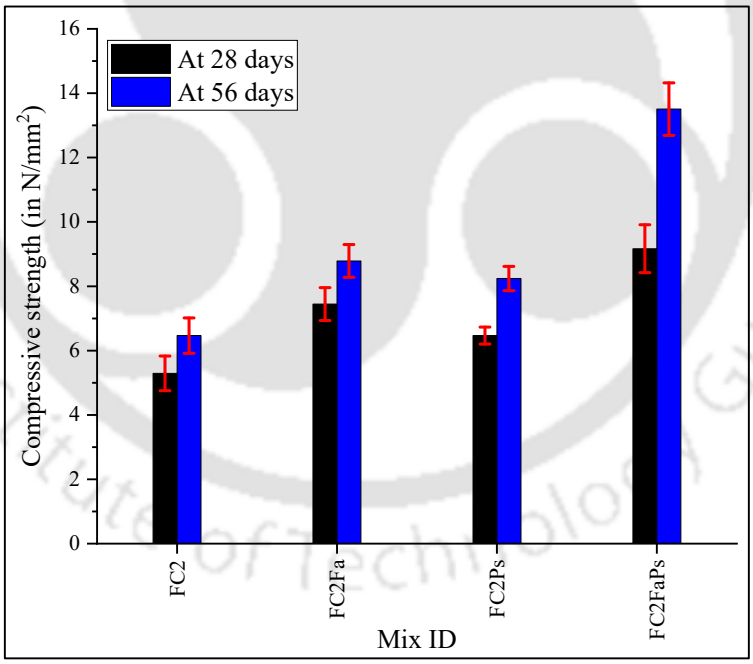

Figure 4.6: (B) Variation in compressive strength of FC mixes (Target fresh density 1500 kg/m³).

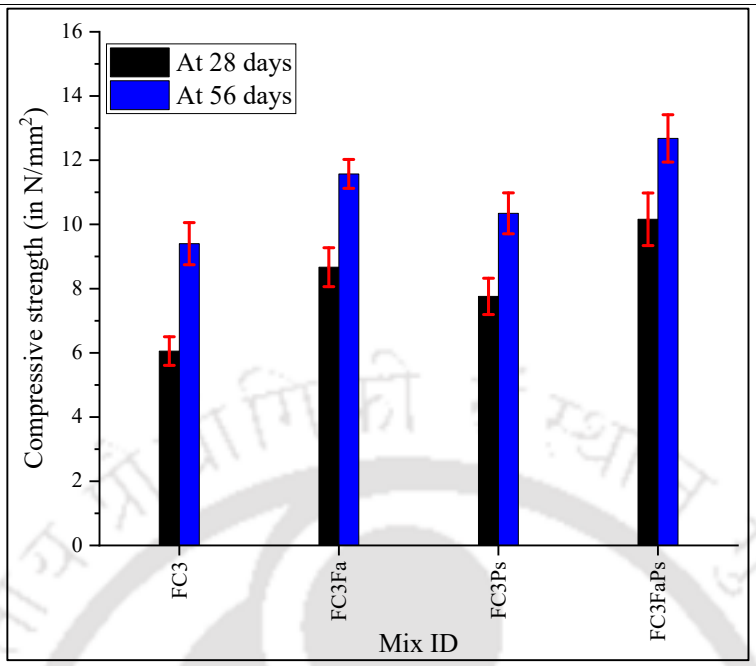

Figure 4.6: (C) Variation in compressive strength of FC mixes (Target fresh density 1800 kg/m³).

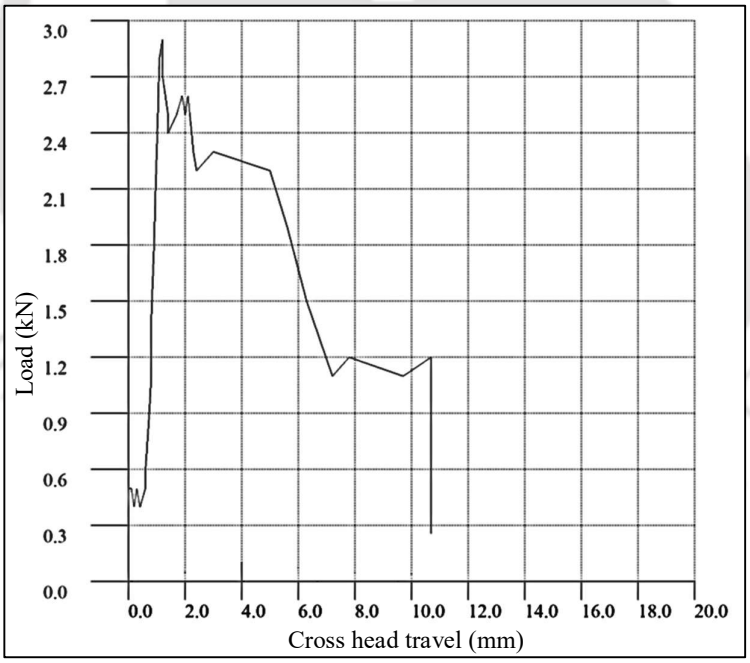

Figure 4.6: (D) Typical compressive behavior (load vs displacement) of FC mixes without additives (Target fresh density 1000 kg/m³).

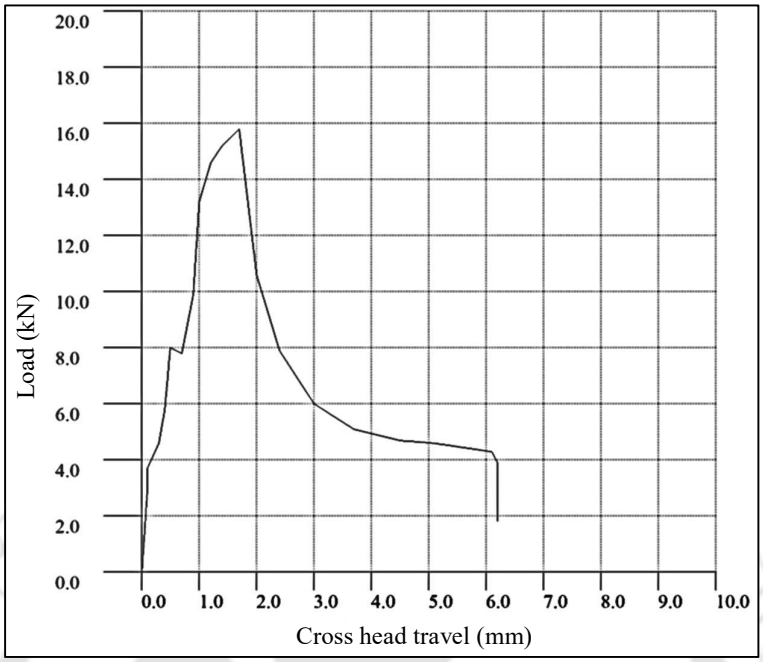

Figure 4.6: (E) Typical compressive behavior (load vs displacement) of FC mixes without additives (Target fresh density 1500 kg/m^3).

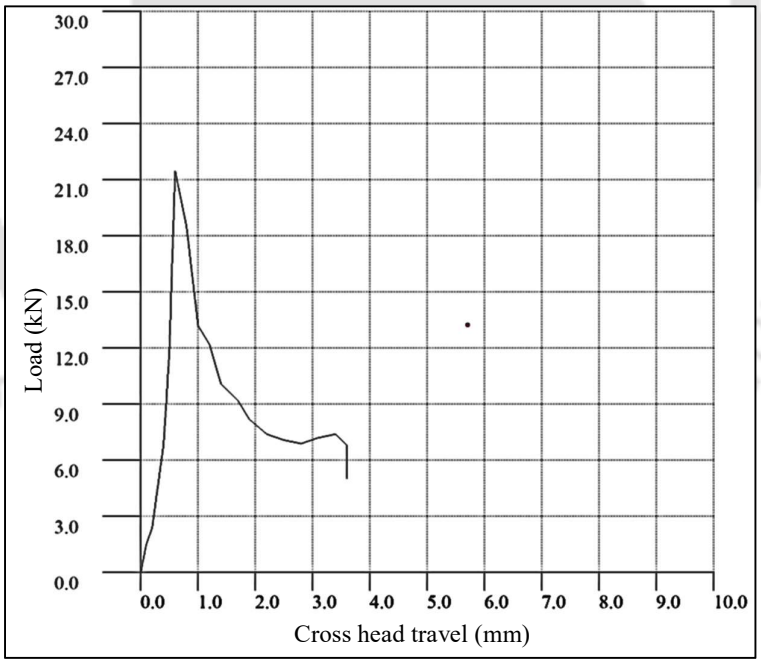

Figure 4.6: (F) Typical compressive behavior (load vs displacement) of FC mixes without additives (Target fresh density 1800 kg/m^3).

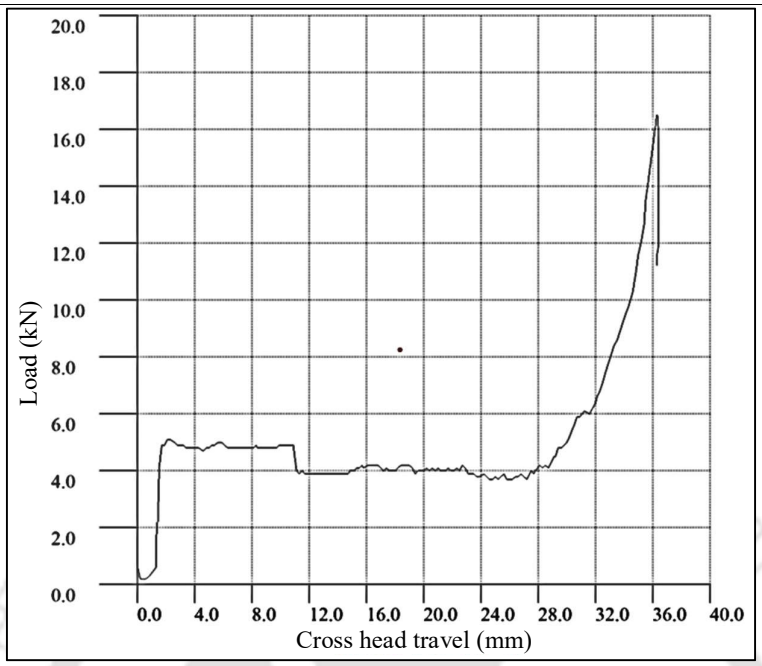

Figure 4.6: (G) Typical compressive behavior (load vs displacement) of FC mixes with additives (Target fresh density 1000 kg/m^3).

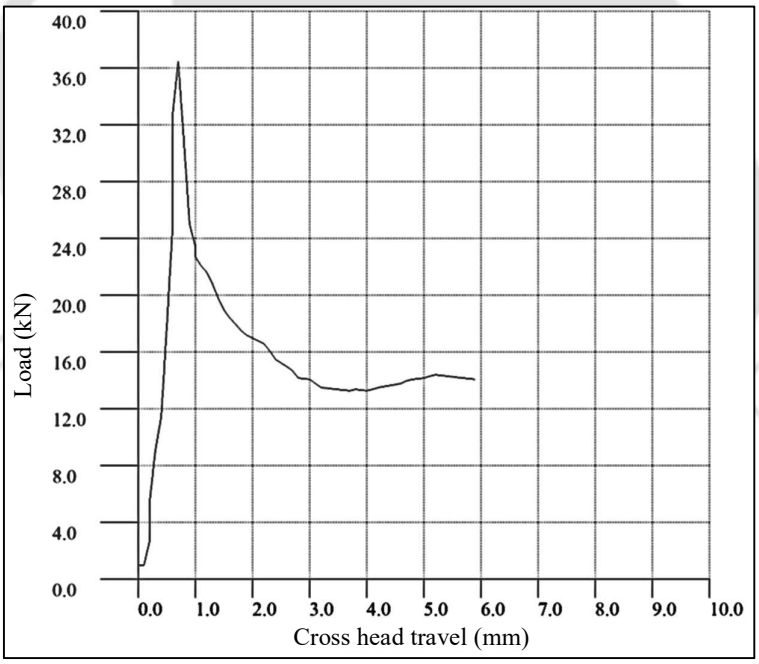

Figure 4.6: (H) Typical compressive behavior (load vs displacement) of FC mixes with additives (Target fresh density 1500 kg/m^3).

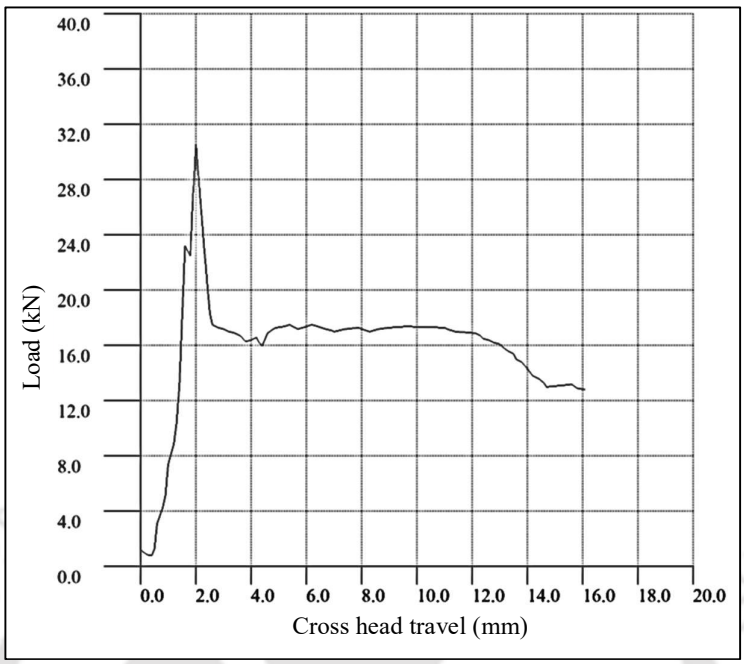

Figure 4.6: (I) Typical compressive behavior (load vs displacement) of FC mixes with additives (Target fresh density 1800 kg/m^3).

The inclusion of foam has shown a drastic reduction in the compressive strength of FC. Comparative analysis of results on the compressive strength of FC mixes (figures 4.6A, 4.6B, 4.6C) and corresponding base mixes (figures 4.5A, 4.5B, 4.5C), indicate that for different design densities, significant reduction in the range of 70% to 90% is observed due to addition of foam. However, the addition of foam has enhanced ductility behaviour of FC in the post peak region as evident from the load vs displacement curves in figures 4.6D, 4.6E, 4.6F, 4.6G, 4.6H, 4.6I. Also, the above enhancement of ductility is found to increase with increase in foam volume. Replacement of 50% of sand with class F FA in FC mixes results in enhancement in compressive strength which is more significant at later ages (56 days) as established in the literature [Raut and Deo, 2017]. For instance, 38% and 114% enhancement in compressive strength is observed at 28 days and 56 days respectively due to replacement of sand with FA for FC density of 1000 kg/m^3. Since the pozzolanic reaction occurs in a delayed manner, the FA which replaced the sand is not able to contribute much to strength at early age when compared to sand-based mixes. However, after sufficient progress of pozzolanic reaction at later age (56 days), significant improvement in strength occurred in mixes with 50% sand replaced with FA. Adding to the above, increase in fine paste content due to sand replacement with FA and subsequent improvement in aggregate-binder interface also contributes to strength

enhancement. The increase in strength is found to be more evident for design densities 1000 kg/m^3 and 1500 kg/m^3. Basically, mixes with higher air content (say 1000 kg/m^3 design density) have thinner and weaker pore walls due to lesser amount of solid content eventually leading to poor strength. However, addition of FA results in significant improvement in pore wall strength due to densification of matrix derived from additional C-S-H gel formed due to pozzolanic reaction of FA [Pan et al., 2007, Ganesan et al., 2015]. This results in significant enhancement in strength in lower density (1000 kg/m^3, 1500 kg/m^3) mixes when compared to higher density mixes (1800 kg/m^3). However, in higher density mixes due to lesser amount of air, the strength of concrete is considerably good even before replacement of sand with FA as the amount of solid content is high.

The inclusion of PP fiber at dosage of 0.05% by weight of total solids has shown positive as well as negative impact on compressive strength depending upon the testing age and the amount of foam in the mix. For instance, for 1000 kg/m^3 design density, significant reduction ranging from 25% to 44% in compressive strength is observed due to addition of PP fiber. Further, the reduction is more significant in early age when compared to later age due to improvement of matrix quality with age. The higher reduction in compressive strength noted in lower density FC mix with higher air content can be ascribed to lesser paste content which results eventually in poor bonding between fibers and matrix [Gencel et al., 2021]. Hence, the mixes FC1Ps is found to be unsatisfactory in terms of strength. On the other hand, for mixes with more paste content (say 1500 kg/m^3 design density) significant increment of 27% in compressive strength is observed which highlights the better bonding between fiber and paste [Amran et al., 2020a].

The combined effect of 0.05% replacement of total solids with PP fiber and 50% replacement of aggregates with FA has resulted in an overall increase in compressive strength of FC. For instance, for design density 1000 kg/m^3, addition of FA and fibers results in 30% reduction in strength at early age (28 days). However, at a later age (56 days) a significant increment of 57% is observed. Hence, for lower density mixes, the combined effect of FA and fibers is good unlike FCPs mixes. The corresponding increments observed for 1500 kg/m^3 and 1800 kg/m^3 design densities are 103% and 37% which is in line with the existing literature [Amran et al., 2020a]. Hence, the above experimental outcomes prove that the synergetic effect of addition of FA and PP fiber results in significant improvement in compressive strength due to improvement of

microstructure [Amran et al., 2020a]. Adding to above, the error bars indicate that the dispersion of values is not high and the coefficient of variation of the compressive strength results are comparable with values reported by other researchers for FC [Panesar, 2013, Sahu and Gandhi, 2021]. Further, based on the results on load vs displacement behavior of FC mixes (figures 4.6D, 4.6E, 4.6F, 4.6G, 4.6H, 4.6I) it is evident that the ductility of combination FC mixes with both FA and PP fiber (figure 4.6G) outperforms the FC mixes without additives (figure 4.6D). The above trend can be attributed to role of fibers in prevention of micro cracks propagation as discussed in literature on fiber reinforced FC [Awang et al., 2015].

4.3.2.2 SPLIT TENSILE STRENGTH

Effect of mix composition on split tensile strength of base mix

Results on split tensile strength of various base mixes tested as per ASTM C496-17 at different ages are presented in figures 4.7A, 4.7B, 4.7C. Further, results of comparative analysis of split tensile strength and compressive strength are presented in figures 4.7D, 4.7E, 4.7F. Replacement of 50% of fine aggregate (300 μm) with FA results in maximum increase of 47% in split tensile strength and it is more evident in mixes with lower W/S as highlighted in earlier literature [Siddique, 2003]. Improvement in microstructure due to pozzolanic effect of FA contributes to the above-mentioned rise in strength as established in literature [Halse et al., 1984]. Further, in line with observations on compressive strength, replacement of the 0.05% of total solids by weight with PP fiber has shown up to 11% reduction in split tensile strength. However, the combination mixes with both FA and PP fiber shows contradictory trend exhibiting increase in split tensile strength of mortar when compared to corresponding C1, C2 and C3 mixes, and the above increment is predominant in mixes with lower W/S. The reasons for the above trend can be cited as better bonding of paste and fiber due to increased paste content. In line with earlier discussion, it is evident that the combination mixes outperform in terms of split tensile strength also. Furthermore, it is to be noted that the split tensile strength to compressive strength ratio (f_t/f_c) for all the base mixes is between 0.06 to 0.08 which is in line with the conventional concrete [Mahajan and Bhagat, 2021].

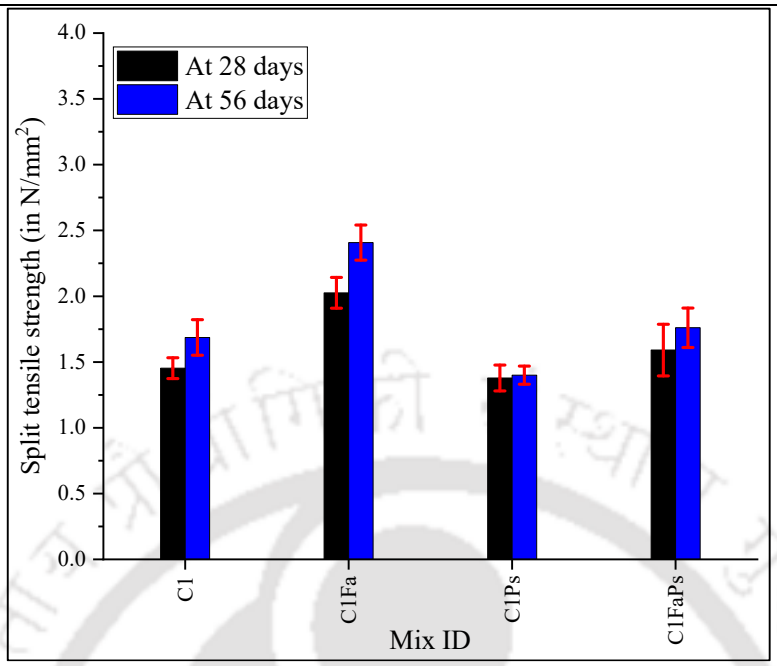

Figure 4.7: (A) Variation in split tensile strength of base mixes (For FC target fresh density 1000 kg/m³).

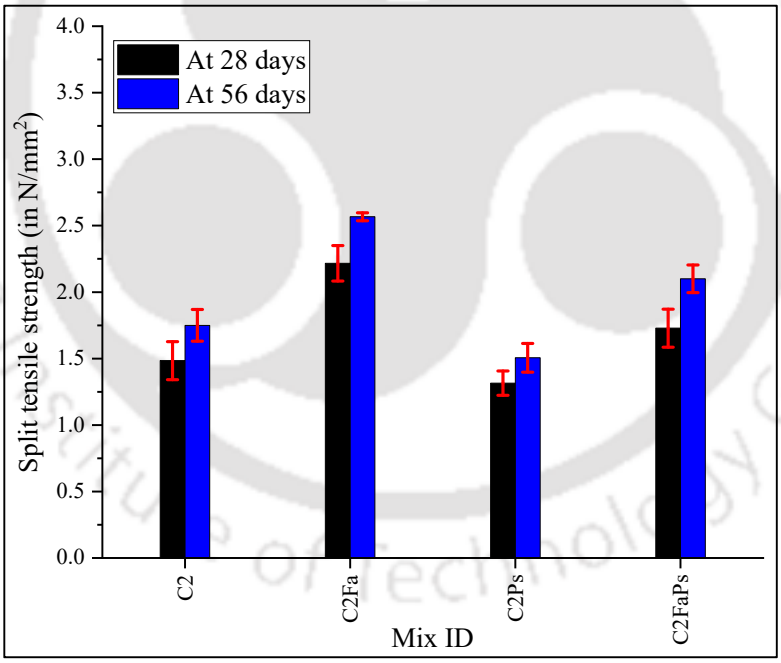

Figure 4.7: (B) Variation in split tensile strength of base mix (For FC target fresh density 1500 kg/m³).

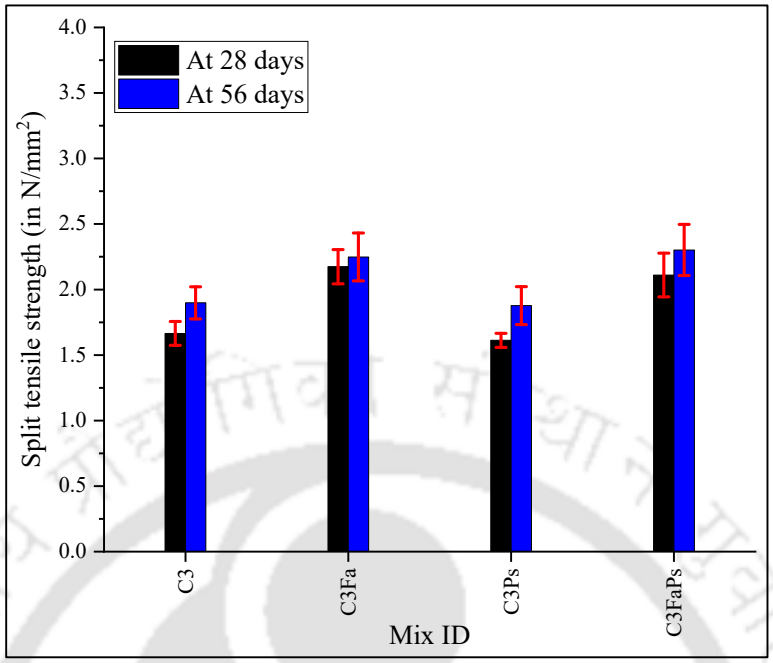

Figure 4.7: (C) Variation in split tensile strength of base mix (For FC target fresh density 1800 kg/m^3).

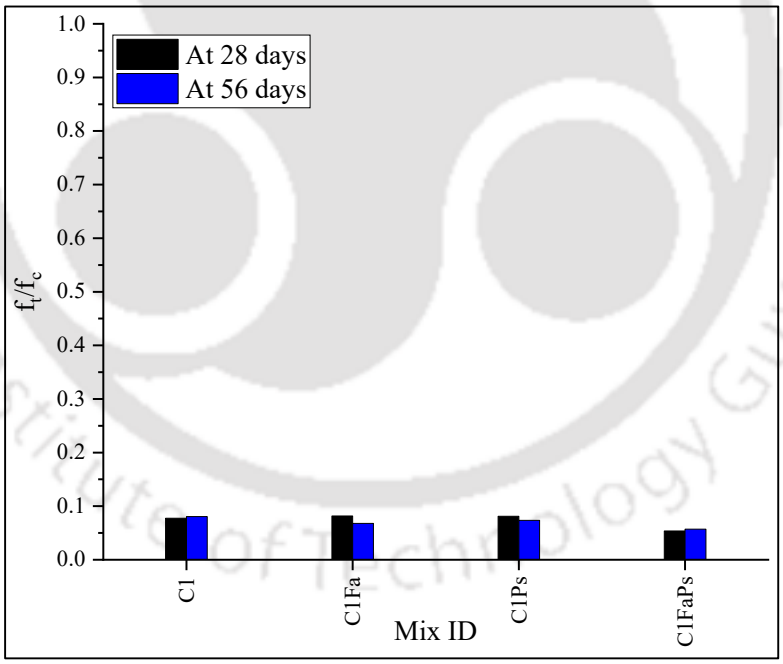

Figure 4.7: (D) Split tensile strength to compressive strength ratio of base mixes (For FC target fresh density 1000 kg/m^3).

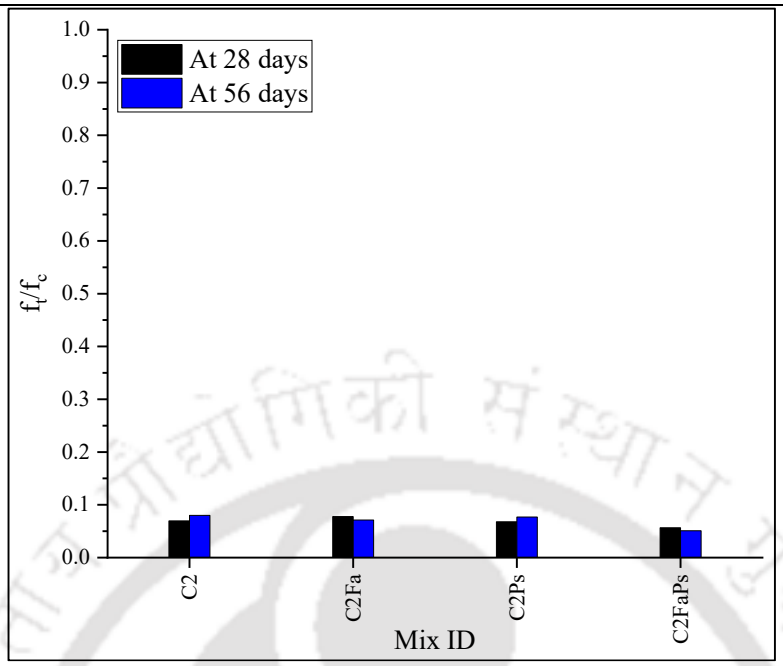

Figure 4.7: (E*) Split tensile strength to compressive strength ratio of base mixes (For FC target fresh density 1500 kg/m³).*

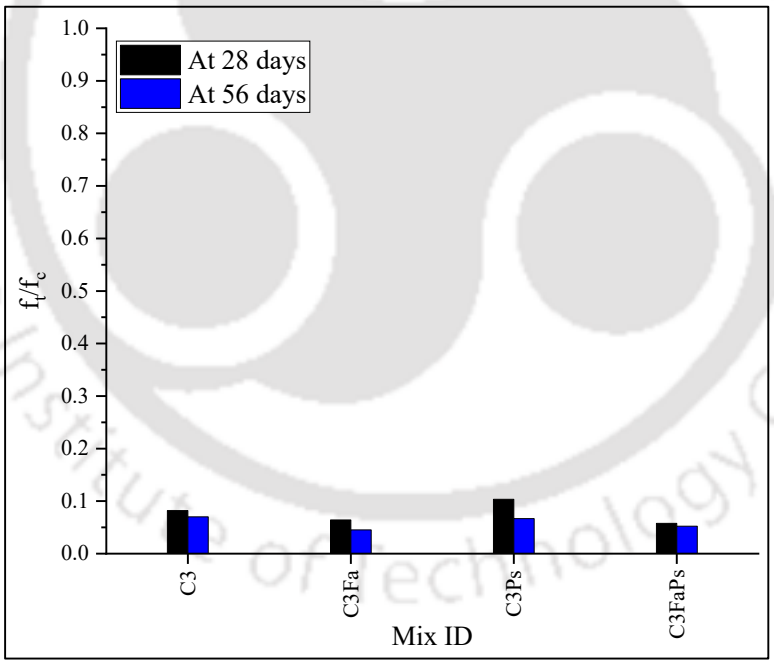

Figure 4.7: (F) Split tensile strength to compressive strength ratio of base mixes (For FC target fresh density 1800 kg/m³).

Effect of mix composition on split tensile strength of FC

Results on split tensile strength of various FC mixes tested as per ASTM C496-17 at different ages are presented in figures 4.8A, 4.8B, 4.8C. Further, results of comparative

analysis of split tensile strength and compressive strength are presented in figures 4.8D, 4.8E, 4.8F. The comparative analysis on the effect of various mix constituents on the split tensile strength of FC is discussed in detail in the following sections.

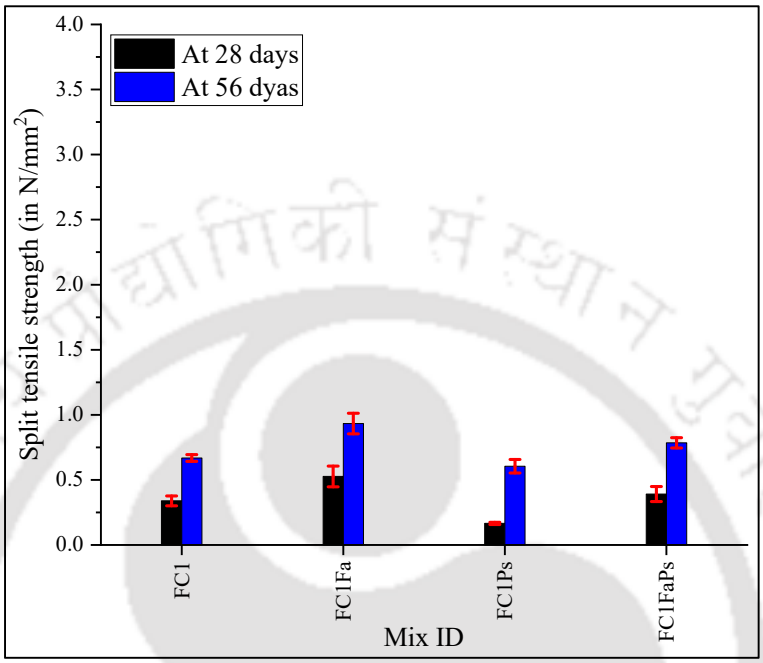

Figure 4.8: (A) Variation in split tensile strength of FC mixes (Target fresh density 1000 kg/m³)

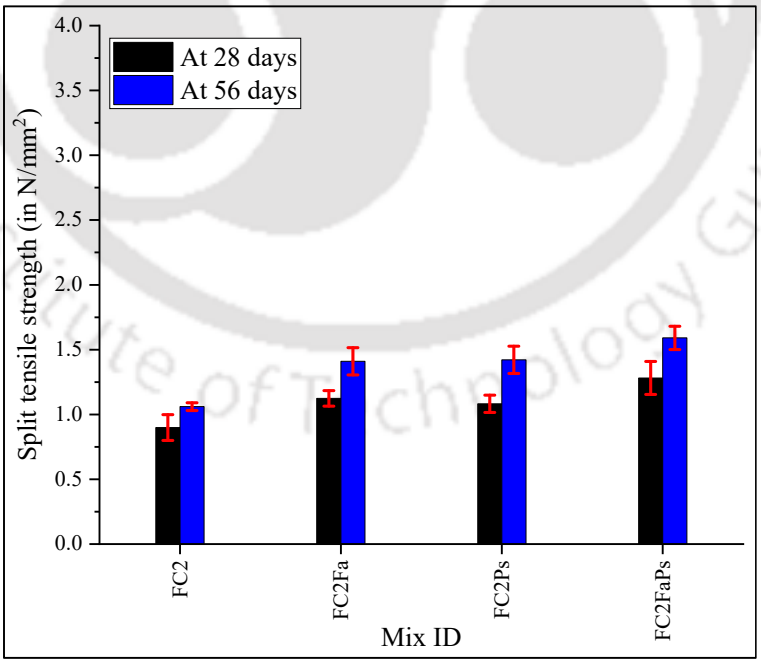

Figure 4.8: (B) Variation in split tensile strength of FC mixes (Target fresh density 1500 kg/m³)

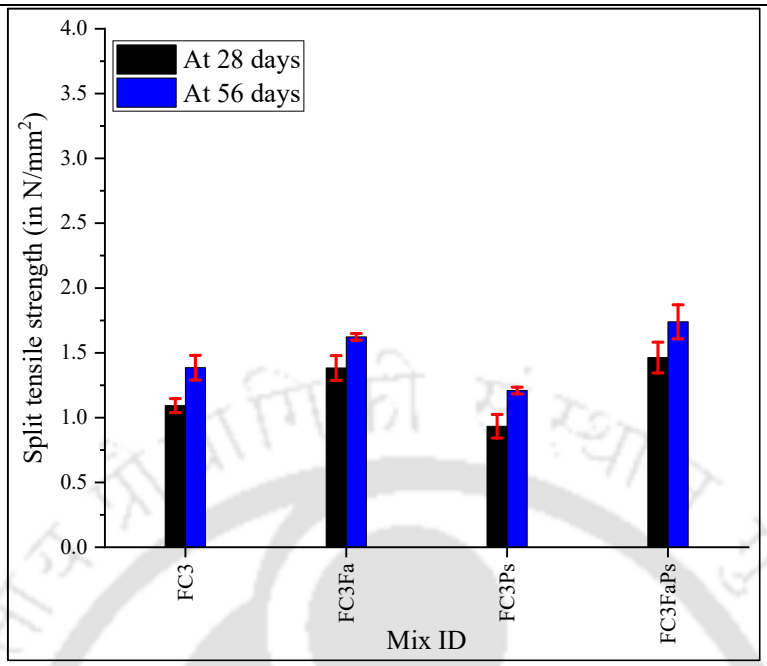

Figure 4.8: (C) Variation in split tensile strength of FC mixes (Target fresh density 1800 kg/m^3)

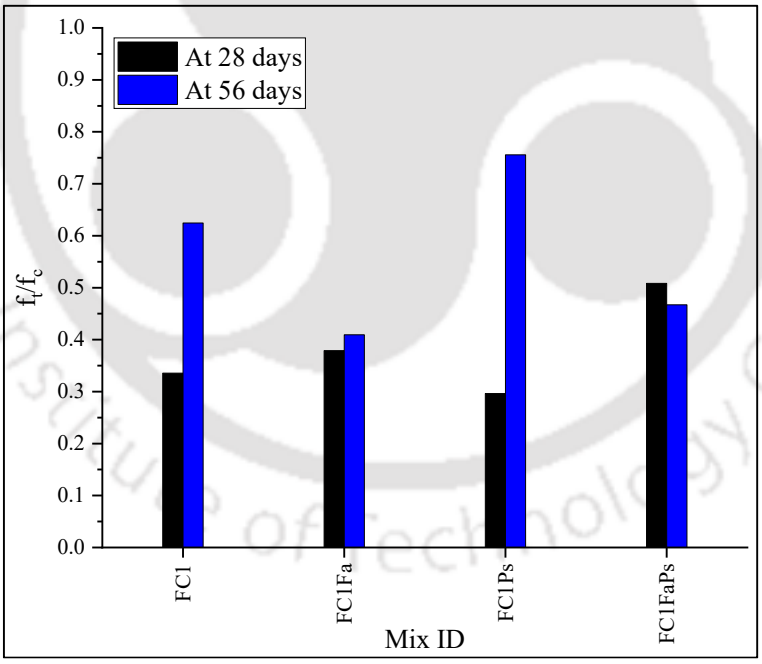

Figure 4.8: (D) Split tensile strength to compressive strength ratio of FC mixes (Target fresh density 1000 kg/m^3).

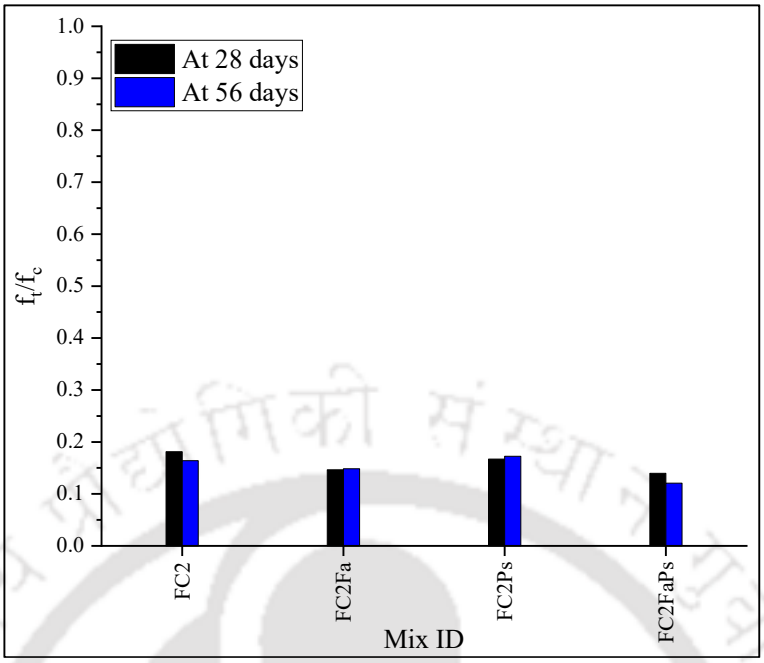

Figure 4.8: (E) Split tensile strength to compressive strength ratio of FC mixes (Target fresh density 1500 kg/m^3).

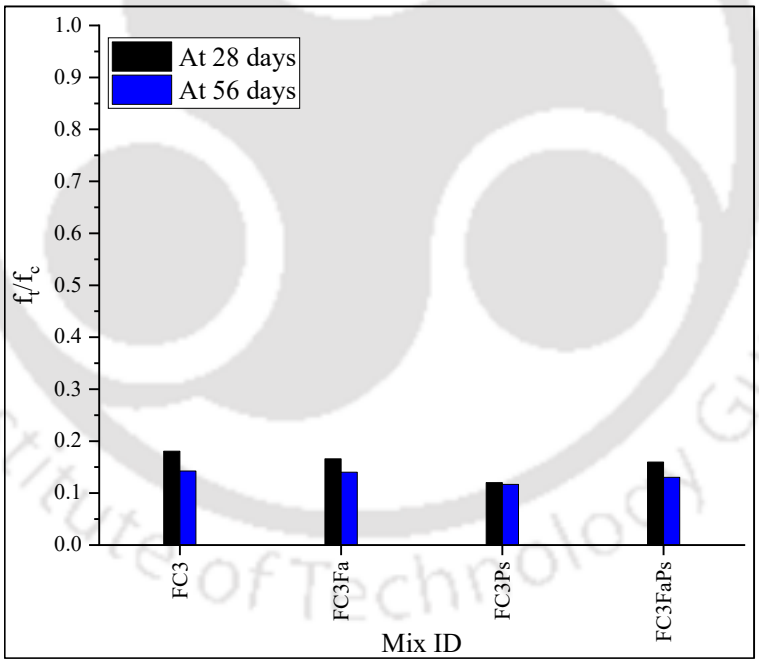

Figure 4.8: (F) Split tensile strength to compressive strength ratio of FC mixes (Target fresh density 1800 kg/m^3).

In line with earlier observations, experimental outcomes show an increment of 16% to 37% in split tensile strength due to replacement of sand with class F FA in FC mixes and the results are in agreement with earlier published literature [Raut and Deo, 2017]. The increase in strength is found to be more significant in mixes with design density 1000

kg/m^3. However, the lower f_t/f_c ratio of mixes with FA when compared with the corresponding mixes without FA can be attributed to the increased brittle nature of FC mixes with FA.

Similar to earlier discussion on compressive strength, inclusion of PP fiber has shown minor decrement in split tensile strength for FC mix with design density l000 kg/m^3 and this can be ascribed to reduced paste content and poor bonding of fiber in the above mix. On the other hand, for mixes with 1500 kg/m^3 design density (FC2Ps), split tensile strength is found to be maximum due to the better bonding between fiber and paste as established in the literature [Hazlin et al., 2017]. However, f_t/f_c ratio of 1500 kg/m^3 (FC2Ps) is found to be lesser than that of 1000 kg/m^3 (FC1Ps). The above trend indicates that the ductility of 1000 kg/m^3 concrete with higher amount of foam is very much higher than that of mixes with lesser amount of foam [Jones and Zheng, 2013, Hilal et al., 2016, Gandhi et al., 2023]. Hence the air content in the concrete plays a significant role in the ductility of concrete as indicated by f_t/f_c ratio.

Combined mixes with both PP fiber and FA (FC1FaPs) exhibits 17% increase in strength when compared to FC1 along with f_t/f_c ratio of 0.47 in case of 1000 kg/m^3 design density FC. The corresponding increments for 1500 kg/m^3 and 1800 kg/m^3 design densities are 50% and 26% respectively. Hence, the above experimental outcomes prove that the synergetic effect of FA and PP fiber results in significant improvement in split tensile strength due to improvement of microstructure and enhancement in ductility behaviour of FC as highlighted in the previous literature [Gandhi et al., 2023].

4.3.3 EFFECT OF MIX COMPOSITION ON PERMEABILITY OF FC

The permeability test has been conducted on the FC samples at the age of 28 days and 56 days using the methodology in accordance with IS 3085: 2021 and the test results are presented in figures 4.9A, 4.9B, 4.9C. Further, from the literature it is evident that the permeability of base mixes can be expected in the range of 10^{-10} cm/s which requires a pressure head greater than 7 kg/cm^2. However, the sealing mechanism adopted in the present study has failed for base mix indicating there is a need for further enhancement in the sealing mechanism to experimentally determine the permeability of impermeable concrete. Hence permeability of base mixes is not reported in this study.

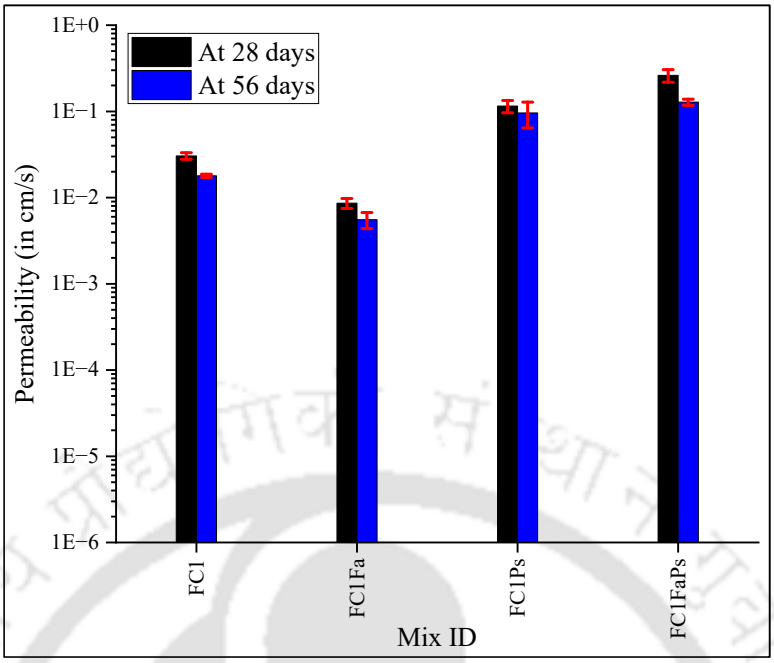

Figure 4.9: (A) Variation in permeability of FC mixes (Target fresh density 1000 kg/m^3).

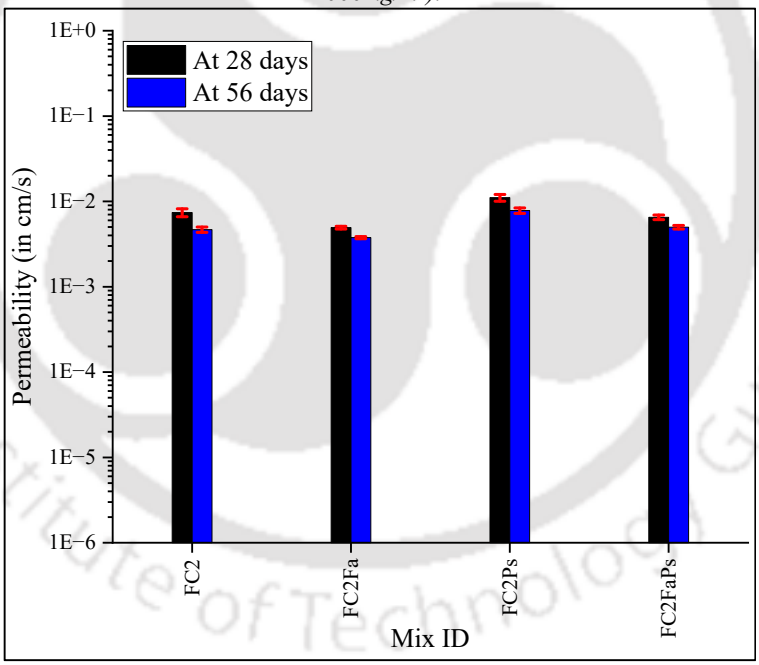

Figure 4.9: (B) Variation in permeability of FC mixes (Target fresh density 1500 kg/m^3).

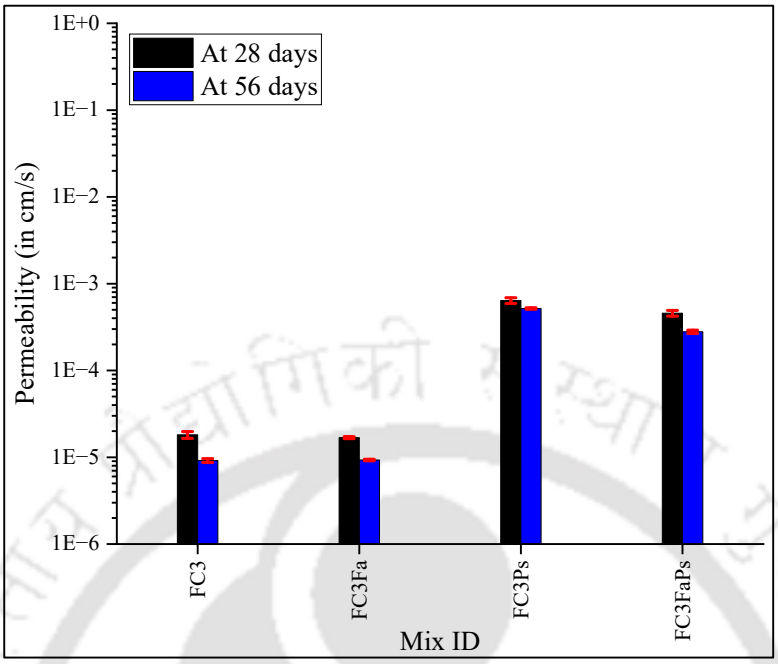

Figure 4.9: (C) Variation in permeability of FC mixes (Target fresh density 1800 kg/m³).

The FC mixes FC1, FC2 and FC3 are found to exhibit average permeability of 10^{-1} cm/s, 10^{-3} cm/s and 10^{-5} cm/s respectively which is in line with the existing literature as presented in Table 2.1. It is evident from the results that increase in foam content enabled greater permeation of air voids. In mixes with higher air content, the decrease in solid content, subsequent decrease in inter-void thickness and closer proximity of air voids favours possibility of interconnection of entrained air voids [Gencel et al., 2021, Yuan et al., 2021]. The above observations are verified with the images of microstructure of concrete samples of mixes with different densities i.e., FC1(figure 4.10C) and FC3 (figure 4.10G) captured with optical microscope at same magnification level of 0.7X. From the images it is evident that, permeability being a function of porosity, connectivity between pores increases with increase in foam volume. Hence, it is to be noted that, though entrained air voids are considered as aggregates in some literature, they do not reduce permeability through obstruction of flow like conventional aggregates. On the other hand, permeability is increased due to increase in W/S requirement particularly in mixes with higher foam volume [Kearsley and Wainwright, 2001, Kolias and Georgiou, 2005]. Replacement of 50% of sand with Class F FA in FC mixes results in significant reduction in permeation characteristics, particularly in mixes with higher foam content. For

instance, for FC with design density 1000 kg/m^3, replacement of sand with FA results in 30% and 69% reduction in permeability at 28 days and 56 days respectively. The above-mentioned reduction in permeability due to FA incorporation can be attributed to the improvement in microstructure due to formation of additional C-S-H gel as a result of the pozzolanic reaction and the improvement is found to be more significant at later ages [Zawawi et al., 2020]. Further, the cauliflower structure of C-S-H gel (figures 4.10A, 4.10B) is expected to enhance the tortuosity resulting in lesser permeation as highlighted by Zhu et al., 2021 and Yang et al., 2018. Comparative analysis of images of microstructure of FC mixes FC1 (figure 4.10C) and FC1Fa (figure 4.10D) captured with optical microscope also highlights the above improvement in microstructure in mixes with FA with reduced pore volume and lesser connected porosity. Adding to above, in line with observations of Tikalsky et al., 2004, the existence of more number of interfacial voids and cracks in the microstructure of FC with only sand as filler (FC2) can be attributed to its higher permeability. However, it is to be noted that in mixes with relatively lesser foam content, the variation in permeation due to FA addition is not significant. This could be attributed to the lesser inclusion of pores which eventually reduces the possibility of permeation [Kearsley and Booyens, 1998].

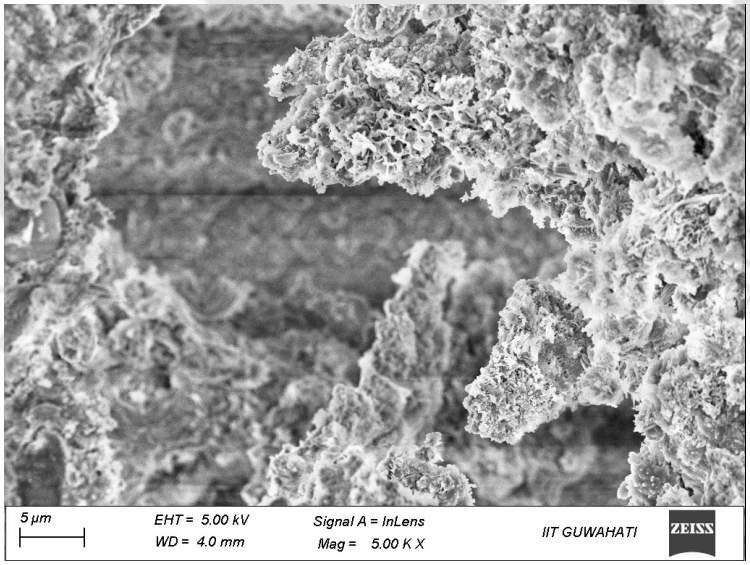

Figure 4.10: (A) SEM image of chunk of FC2 mix at 5.00 KX magnification at the age of 56 days.

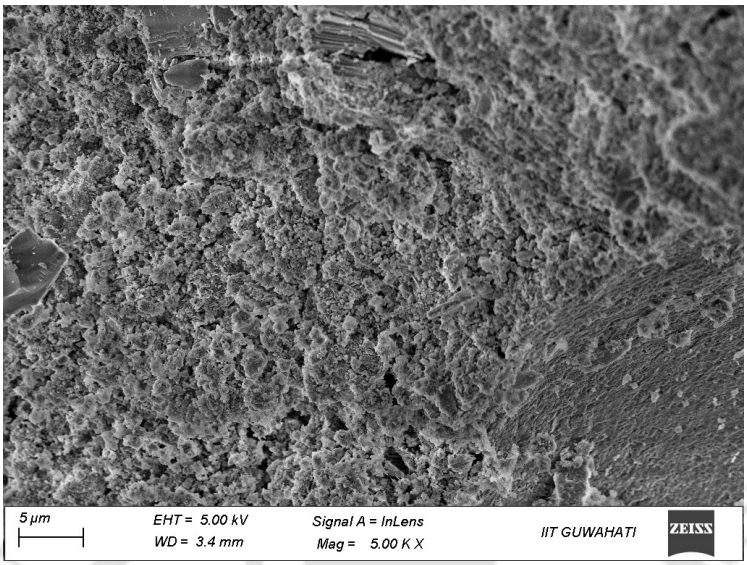

Figure 4.10: (B) SEM image of chunk of FC2Fa mix at 5.00 KX magnification at the age of 56 days.

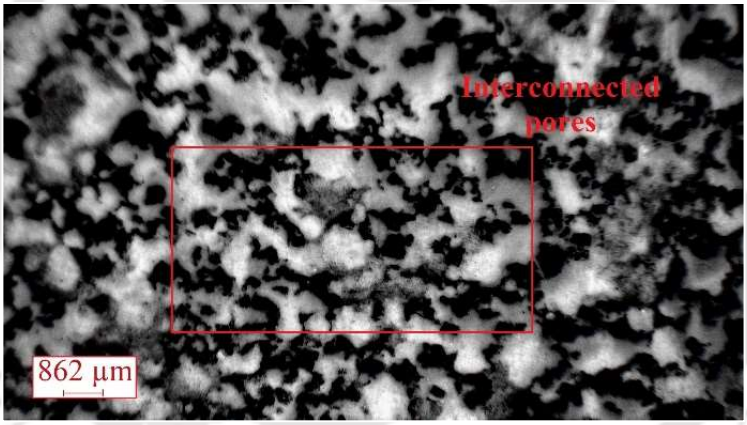

Figure 4.10: (C) Optical microscopic image of FC1 mix at 0.7X magnification at the age of 56 days.

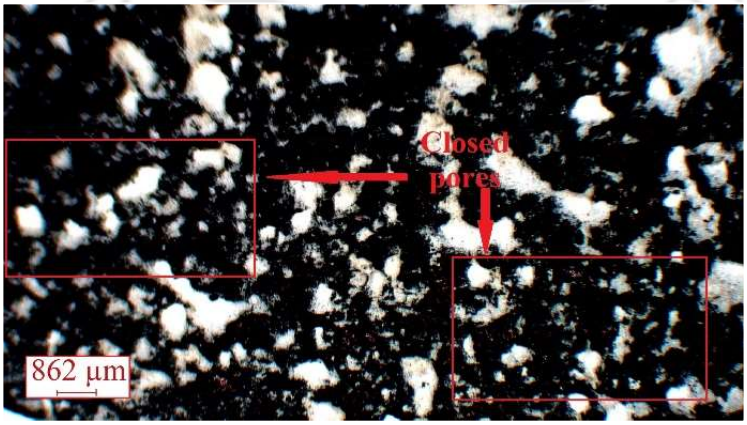

Figure 4.10: (D) Optical microscopic image of FC1Fa mix at 0.7X

magnification at the age of 56 days.

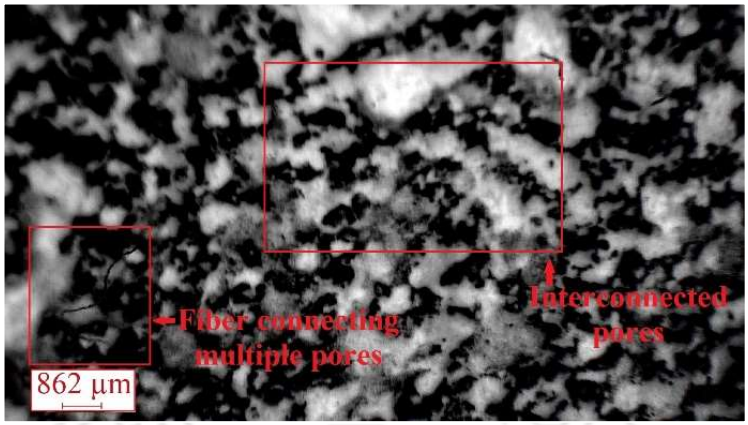

Figure 4.10: (E) Optical microscopic image of FC1Ps mix at 0.7X magnification at the age of 56 days.

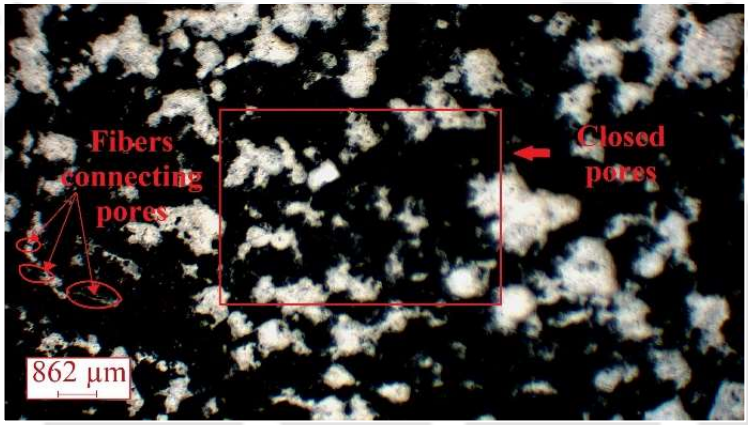

Figure 4.10: (F) Optical microscopic image of FC1FaPs mix at 0.7X magnification at the age of 56 days.

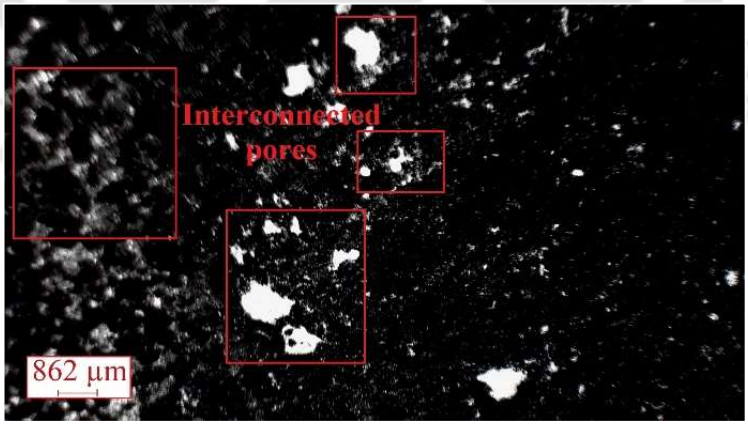

Figure 4.10: (G) Optical microscopic image of FC3 mix at 0.7X magnification at the age of 56 days.

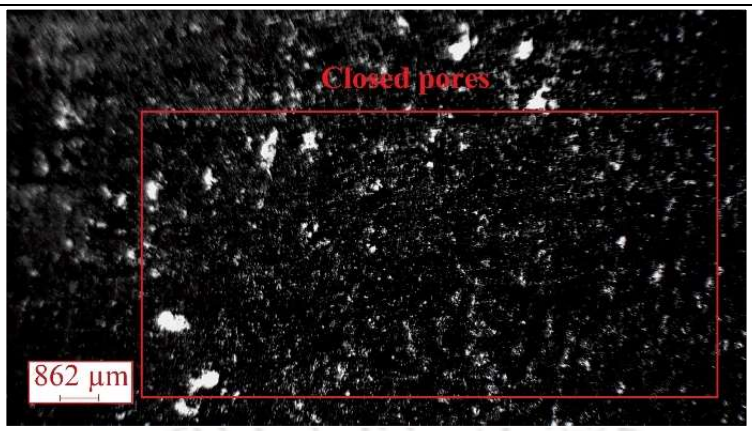

Figure 4.10: (H) Optical microscopic image of FC3Fa mix at 0.7X magnification at the age of 56 days.

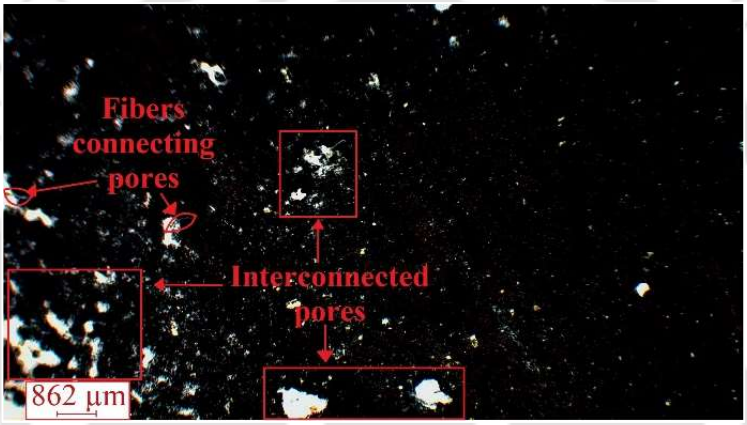

Figure 4.10: (I) Optical microscopic image of FC3Ps mix at 0.7X magnification at the age of 56 days.

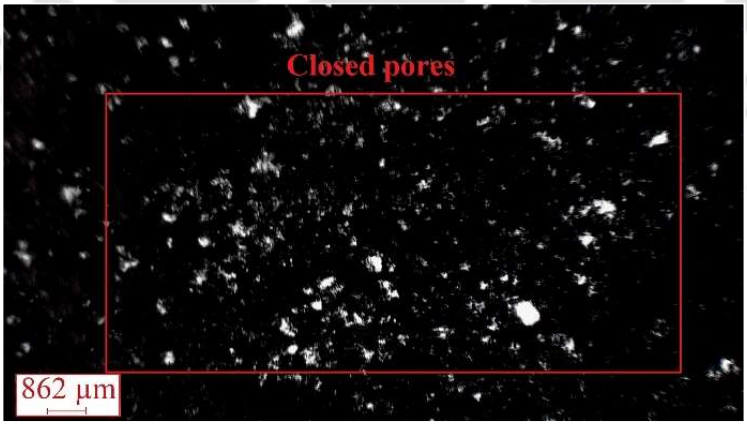

Figure 4.10: (J) Optical microscopic image of FC3FaPs mix at 0.7X magnification at the age of 56 days.

Addition of PP fiber at 0.05% by weight of total solids has shown significant increment in permeability of FC mixes. For instance, permeation of mixes FC1Ps, FC2Ps and FC3Ps

are 3.8, 1.5 and 35 times greater than that of FC1, FC2 and FC3 mix at 28 days. Similarly, the corresponding improvement in permeation at 56 days are found to 5.4, 1.7 and 56 times respectively. The enhancement in permeability due to fiber addition can be attributed to the interconnectivity between pores established due to the additional pores formed on the fiber-matrix interface as presented in figure 4.11A [Jones and McCarthy, 2005a, Gencel et al., 2021]. Further, the greater connectivity between pores is established due to the passage of a single fiber through multiple pores as observed in the microscopic image in figure 4.11B. The high-water adsorption capacity of the fiber also contributes to increment in porosity and pore connectivity due to drying at later stages [Huang, 2001]. Further, since solid content and fiber content are directly correlated, FC3 mixes with higher fiber contents due to the presence of more solid content at higher densities, are exhibiting higher increments in permeability [Gencel et al., 2021].

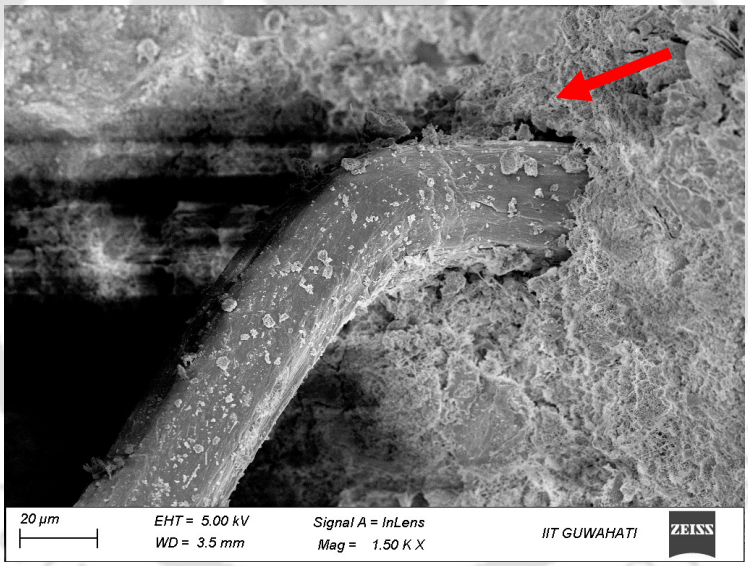

Figure 4.11: (A) SEM image of the fiber-matrix interface at 1.50 KX magnification.

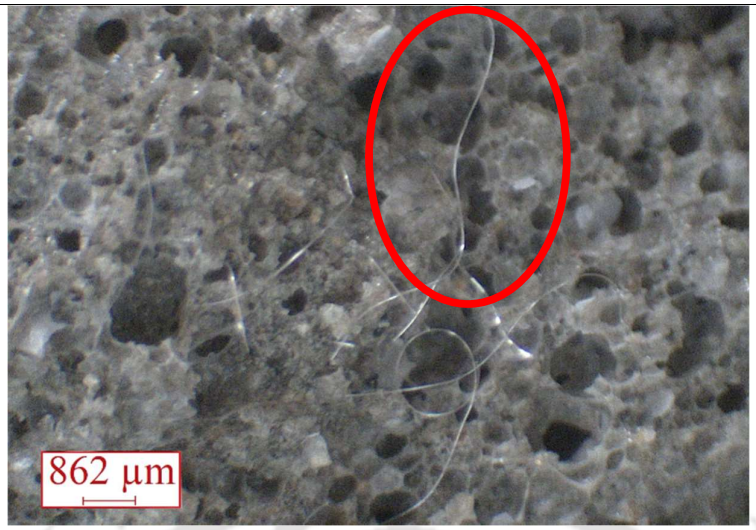

Figure 4.11: (B) Optical microscopic image of FC1Ps mix at 0.7X depicting pore connectivity.

In mixes with both FA and PP fiber, the effect of PP fiber is more predominant on permeation when compared to that of FA. For instance, permeation of FC1FaPs is higher than that of FC1Ps, FC1Fa and FC1. Hence the enhancement of permeation due to fiber addition outperforms the decrement in permeation due to FA addition and subsequently results in overall increment of permeation in combined mixes particularly FC1FaPs. The above observation is evident in the comparative analysis of images of microstructure of concrete samples captured with optical microscope (figures 4.10D, 4.10E and 4.10F). Figure 4.10F shows that though the porosity is reduced due to FA addition, however the addition of fibers has resulted in increase of connectivity between pores. However, in mixes with lesser foam volume, the difference in permeation between mixes say FC3Ps and FC3FaPs is not significant. Whereas the comparative analysis of FC mixes with FA and fiber (FC1FaPs, FC2FaPs, FC3FaPs) with the corresponding FC mixes (FC1, FC2, FC3) shows an enhancement of permeability by 8.6, 0.9 and 25 times at early age (28 days) and 7.2, 1.1 and 30 times at later age (56 days). The above observations indicate the inclusion of PP fiber is predominantly influencing the permeation behaviour of FC as discussed in the earlier section.

4.4 SUMMARY

To summarize, the current study is an attempt to determine the mix composition of FC which could result in desired strength as well as permeability for its intended application in retaining walls to facilitate dissipation of pore water pressure. Firstly, the effect of

variation in foam content for particular level of sand replacement with FA and particular PP fiber level has been studied on various properties of concrete. From the experimental outcomes, it is evident that though the lower density FC i.e., 1000 kg/m^3 have exhibited high permeability in the order of 10^{-1} cm/s, but the maximum compressive strength attained is only 2.6 N/mm^2. However, it is to be noted that for use in retaining wall applications, minimum strength of atleast 20.7 N/mm^2 is needed as per ASTM C1372-23 guidelines. On the other hand, relatively higher density FC mix i.e., 1800 kg/m^3 exhibited a maximum compressive strength of 13.5 N/mm^2 which needs to be further enhanced for its use in the intended application. Nevertheless, permeability of the above mix is relatively lower in the order of 10^{-5} cm/s which is not satisfactory for the intended application. Whereas the intermediate density FC mix i.e., 1500 kg/m^3 are exhibiting a maximum compressive strength of 14.2 N/mm^2 along with a satisfactory permeability of 10^{-3} cm/s. Hence, the further studies are attempted to improve the strength and permeability of 1500 kg/m^3 density FC through variation in FA level and fiber content as discussed in upcoming chapter.

CHAPTER 5

COMBINED EFFECT OF DIFFERENT LEVELS OF FA (AS REPLACEMENT FOR SAND) AND PP FIBER ON SPREADABILITY AND MECHANICAL PROPERTIES OF FC

5.1 GENERAL

The preliminary studies on the effect of foam, FA (FA) (50% replacement of sand) and PP fiber (0.05% replacement of total solids) on the fresh state, mechanical and permeability of FC with different design densities viz. 1000 kg/m^3, 1500 kg/m^3 and 1800 kg/m^3 are discussed in Chapter 4. Experimental outcomes have revealed that FA has a positive influence on the mechanical properties and negative influence on the spreadability and permeability. Further, foam and PP fiber enhance the permeability of FC while decreasing its spreadability and mechanical properties. The main objective of the present study is to determine the mix composition of FC which could result in desired strength as well as permeability for its intended application in IB for retaining walls to facilitate dissipation of pore water pressure. From the experimental outcomes discussed in previous chapter, it is evident that though the lower density FC i.e. 1000 kg/m^3 has exhibited high permeability in the order of 10^{-1} cm/s, but the maximum compressive strength attained is only 2.6 N/mm^2. However, it is to be noted that for use in retaining wall applications, minimum strength of atleast 20.7 N/mm^2 is needed as per ASTM C1372-23 guidelines. On the other hand, relatively higher density FC mix i.e. 1800 kg/m^3 exhibited a maximum compressive strength of 13.5 N/mm^2 which needs to be further enhanced for its use in the intended application. Nevertheless, permeability of the above mix is relatively lower in the order of 10^{-5} cm/s which is not satisfactory for the intended application. Whereas, the intermediate density FC mix i.e. 1500 kg/m^3 are exhibiting a maximum compressive strength of 14.2 N/mm^2 along with a satisfactory permeability of 10^{-3} cm/s. Hence in the current chapter, the further studies are attempted to improve the strength and permeability of 1500 kg/m^3 density FC through variation in FA level and fiber content.

5.2 MATERIALS, MIX PROPORTION AND METHODOLOGY

The following constituent materials are used in the present study for the production of FC:

- OPC-43 grade (supplied by Dalmia Ltd.).
- Sand that is passed through a 300 μm sieve.
- Class-F FA, purchased from National Thermal Power Corporation, Bongaigaon, India.
- PP fiber purchased from Jogani Impex LLP.
- SLS purchased from LOBA chemicals.
- CMC purchased from LOBA chemicals.

The properties of these materials are explained in details in chapter 4. Additionally, SP (Auramix 300), polycarboxylic ether (PCE) based admixture, procured from FOSROC chemicals has been used to achieve the desired spreadability [Nambiar and Ramamurthy, 2008 and Beskopylny et al., 2023].

The present study is limited to FC with design density of 1500 kg/m^3. According to ASTM C796-19, the mix proportions needed to achieve these target densities were computed and are shown in Table 5.1. Further, Table 5.2 provides details on the terminology for various mix codes. The W/S of the above-mentioned design density is primarily fixed at 0.3 considering the stability of mixes based on previous literature and preliminary trials [Sahu and Gandhi, 2021]. A constant cement-to-sand ratio of 1:2, by mass has been adopted throughout the study. Concrete mixes are prepared by replacing 25%, 50%, 75% and 100% of sand (by weight) with FA and/or 0.2%, 0.4%, 0.6%, 0.8% and 1% of total solids with PP fiber (by weight) and these replacement levels are chosen based on literature considering strength and shrinkage aspects. Further, in the earlier literature it is established that the addition of 1% PP fiber to grout mix has increased the permeability in the order of 10^2 indicating that fiber-matrix interface is providing convenient flow paths for water permeation [Huang, 2001]. For all the proposed mixes, the methodology described in chapter 4 has been followed for the preparation of stable and homogeneous FC mix.

Table 5.1: Nomenclature for the proposed FC2 mixes.

Mixes with varying SP (at constant W/S of 0.3) (S)							
Design density	**Total solids replacement with PP Fiber**		**Sand replacement with FA**				
			F0	**F1**	**F2**	**F3**	**F4**
			0%	**25%**	**50%**	**75%**	**100%**
1500 kg/m^3 (FC2)	**P0**	**0.0%**	SFC2F0P0	SFC2F1P0	SFC2F2P0	SFC2F3P0	SFC2F4P0
	P1	**0.2%**	SFC2F0P1	SFC2F1P1	SFC2F2P1	SFC2F3P1	SFC2F4P1
	P2	**0.4%**	SFC2F0P2	SFC2F1P2	SFC2F2P2	SFC2F3P2	SFC2F4P2
	P3	**0.6%**	SFC2F0P3	SFC2F1P3	SFC2F2P3	SFC2F3P3	SFC2F4P3
	P4	**0.8%**	SFC2F0P4	SFC2F1P4	SFC2F2P4	SFC2F3P4	SFC2F4P4
	P5	**1.0%**	SFC2F0P5	SFC2F1P5	SFC2F2P5	SFC2F3P5	SFC2F4P5
Mixes with varying W/S (without SP addition) (W)							
Design density	**Total solids replacement with PP Fiber**		**Sand replacement with FA**				
			F0	**F1**	**F2**	**F3**	**F4**
			0%	**25%**	**50%**	**75%**	**100%**
1500 kg/m^3 (FC2)	**P0**	**0.0%**	WFC2F0P0	WFC2F1P0	WFC2F2P0	WFC2F3P0	WFC2F4P0
	P1	**0.2%**	WFC2F0P1	WFC2F1P1	WFC2F2P1	WFC2F3P1	WFC2F4P1
	P2	**0.4%**	WFC2F0P2	WFC2F1P2	WFC2F2P2	WFC2F3P2	WFC2F4P2
	P3	**0.6%**	WFC2F0P3	WFC2F1P3	WFC2F2P3	WFC2F3P3	WFC2F4P3
	P4	**0.8%**	WFC2F0P4	WFC2F1P4	WFC2F2P4	WFC2F3P4	WFC2F4P4
	P5	**1.0%**	WFC2F0P5	WFC2F1P5	WFC2F2P5	WFC2F3P5	WFC2F4P5

Table 5.2:Nomenclature for mix codes.

Mix code	Description
FC2	FC2 signify FC mixes with design density 1500 kg/m^3
F0, F1, F2, F3, F4	F0, F1, F2, F3, F4 represent mixes with FA replacing sand at 0%, 25%, 50%, 75% and 100% by weight respectively.
P0, P1, P2, P3, P4, P5	P0, P1, P2, P3, P4, P5 represent mixes with PP fiber replacing total solids at 0%, 0.2%, 0.4%, 0.6%, 0.8% and 1% by weight respectively.
S	S represent mixes with required SP dosage to achieve the recommended fresh state properties of minimum 40% spread and density within ASTM permissible limits of 1500 ±50 kg/m^3.
W	W represent mixes with required W/S to achieve the recommended fresh state properties of minimum 40% spread and density within ASTM permissible limits of 1500 ±50 kg/m^3.
WFC2F2P1	For Example: This mix code denotes FC with required W/S for the preparation of stable self-compacting FC with design density 1500 kg/m^3 (FC2) and comprises of 50% by weight of sand replaced with FA (F2) and 0.2% by weight of total solids replaced with PP fiber (P1).

Further, the methodology discussed in chapter 4 is followed to measure the fresh density, demoulded density, compressive strength and split tensile strength of the proposed FC mixes. Additionally, to assess the flexural strength, three number of prism specimens of size 40 mm* 40 mm* 160 mm are casted for each mix and are tested at ages 28 days and 56 days as mentioned in ASTM C348-21.

5.3 DETAILED INVESTIGATIONS ON EFFECT OF VARIATION OF MIX PROPORTION PARAMETERS ON FC BEHAVIOUR

5.3.1 FRESH STATE PROPERTIES

Cohesiveness and density of the mix has significant impact on workability of concrete. Further, the consistency of the FC is crucial to achieve the desired design density [Nambiar and Ramamurthy, 2008, Beskopylny et al., 2023]. The replacement of solids with foam, FA, and PP fibre individually have decreased the spread of FC mixes, in accordance with previous investigations as discussed in chapter 4. This can be ascribed to the finer particle size and higher water demand of FA, the higher cohesiveness of FC mixes, the reduction in water content brought on by water absorption of FA, and the

restriction of particle movement by PP fibre. Further, the combined effect of replacement of solids with foam, FA, and PP fiber (e.g. CFaPs and FCFaPs) showed an aggravated reduction in spread percentage of FC mixes as a consequence of the synergistic effect. Hence, as a next step, the influence of various FA and PP fiber levels (individually) on the fresh state properties of FC2 mixes at constant W/S of 0.3 are being assessed in the following sections. Further, the required W/S (without SP dosage) or SP dosage (at W/S = 0.3) are being derived by trial-and-error method, in order to achieve the minimum required spreadability of 40% for stable FC mixes with various FA and PP fiber levels (individually). Additionally, the combined effect of various FA and PP fiber levels (for the cases of variation in SP at constant W/S of 0.3 and variation in W/S without SP) on fresh state properties of FC2 mixes is being evaluated.

5.3.1.1 CONSISTENCY AND DENSITY OF FC

Effect of FA

Firstly, studies on the effect of sand replacement with FA on the spreadability of FC are carried out at a constant W/S of 0.3, so that only the effect of variation in FA level on fresh state behavior can be observed. From figure 5.1 it is evident that there is a significant reduction of 36% in spread when 25% of sand is replaced with FA (comparing FCF0P0 and FCF1P0). The decrease in spreadability due to the replacement of sand with FA can be ascribed to the finer FA particles which necessities more water thereby resulting in stiffer mix [Zhihua et al., 2007]. Further for mixes with complete replacement of sand with FA (FCF4P0), the spread is almost zero indicating that the W/S needs to be increased to meet the water demand of finer FA particles.

Earlier studies reported in literature have proved that FC mixes with spreadability in the range of 40% to 60% met the stability and workability requirements [Nambiar and Ramamurthy, 2008]. In this line, a stable FC mix is defined as a mix that has actual fresh density and demoulded density within ± 50 kg/m^3 of the target fresh density [Khwairakpam and Gandhi, 2022]. Surprisingly all the above-mentioned mixes casted at W/S of 0.3 met the density requirements in both fresh and demoulded states even though the consistency requirements are not met. However, considering the practical requirements for complete filling of mould or formwork at site, the consistency of the above mixes needs to be enhanced.

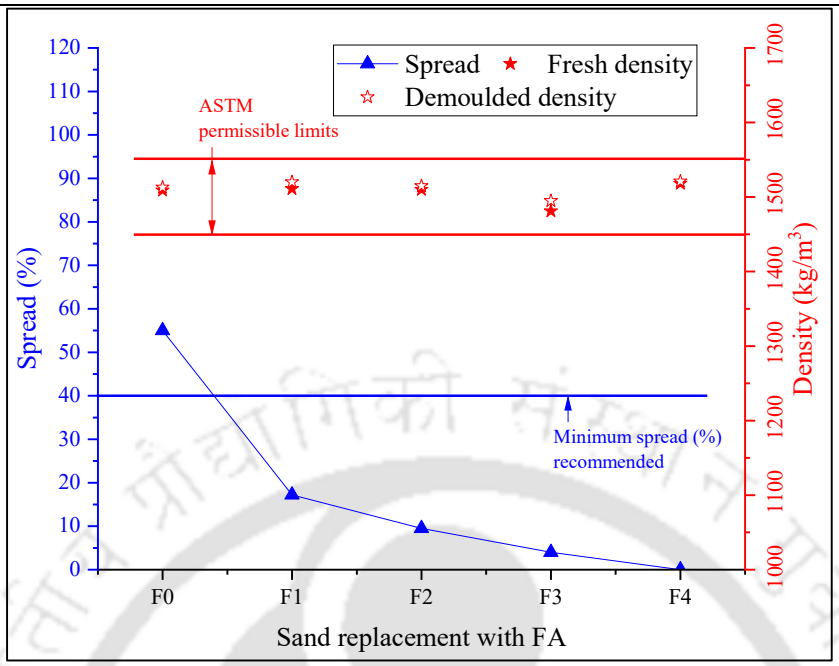

Figure 5.1: Effect of variation in level of FA on consistency and density of FC2 mixes at constant W/S of 0.3 (without SP addition).

With the above points in view, further trials are carried out to determine W/S needed for mixes with different sand replacement levels with FA (25% to 100%) to meet the above-mentioned consistency requirements. The results (figure 5.2) show that, the increase in sand replacement with FA from 0% to 100% results in 52% increment in W/S to achieve minimum spread of 40%. Also, all the above mixes are found to be stable with fresh density and demoulded density within ± 50 kg/m^3 of target fresh density (figure 5.2). Detailed analysis of experimental outcomes indicates that, to achieve the desired consistency in terms of spreadability (minimum spread requirement of 40%), for the first 25% replacement of sand with FA an increment of 0.025 of W/S is needed for FC with design density 1500 kg/m^3. For the second 25% replacement of sand with FA another increment of W/S of 0.025 is done. However, with the above increment in W/S the spreadability requirement is met just marginally as shown in figure 5.2. Hence, for the subsequent replacement levels i.e. 75% and 100% slightly higher increments in W/S say 0.03 and 0.045 are added respectively to achieve the desired consistency. The finer size particles of FA resulting in higher water demand can be ascribed to greater W/S requirement in order to achieve the desired spread percentage [Zhihua et al., 2007]. Adding to above, greater cohesiveness and reduced density of FA also contributes to

substantial increment in W/S for obtaining the required consistency [Nambiar and Ramamurthy, 2008, Marthong and Agarwal, 2012].

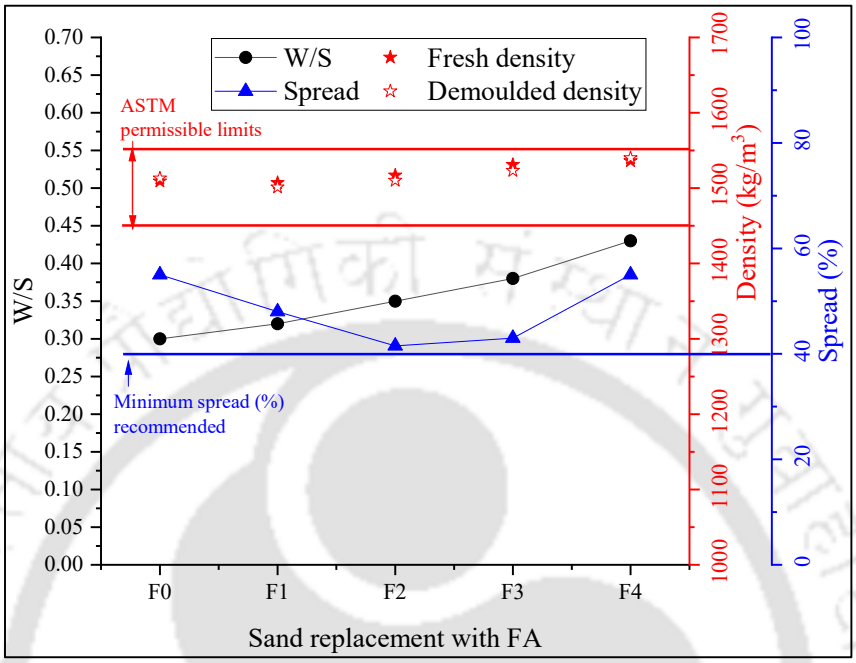

Figure 5.2: Effect of variation in W/S and FA level on the consistency and density of WFC2 mixes (without SP addition).

As a next step, further trials are carried out to determine SP dosage needed for mixes with different sand replacement levels with FA (25% to 100%) at constant W/S of 0.30. In the literature, it is well established that PCE-based SP is more efficient in water demand reduction due to the steric hindrance effect [Wang et al., 2021]. Hence, PCE-based SP is adopted in the present study. The experimental outcomes indicate that, to achieve the desired consistency in terms of spreadability, for every 25% replacement of sand with FA there is a constant requirement of 0.25% of SP dosage (% by weight of cement) for FC with design density 1500 kg/m^3. In line with previous results, all mixes are found to be stable with fresh density and demoulded density within ± 50 kg/m^3 of target fresh density as shown in figure 5.3.

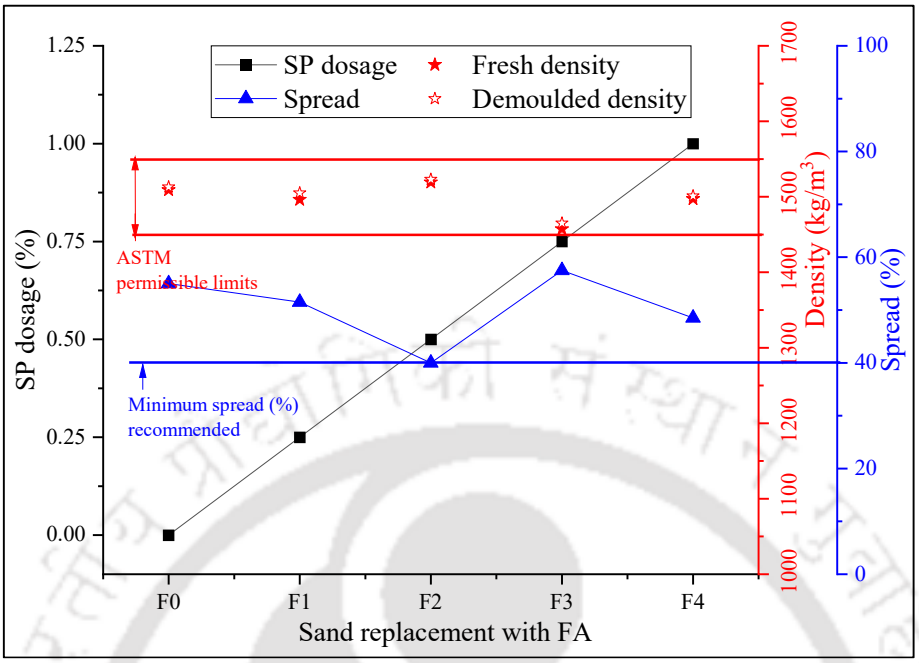

Figure 5.3: Effect of variation in SP dosage and FA level on the consistency and density of SFC2 mixes.

Effect of PP fiber

Figure 5.4 shows the effect of variation in PP fiber on spreadability and density of FC mixes with different levels of total solids replacement with PP fiber at a constant W/S of 0.3. The inclusion of PP fiber has shown negative impact on the spreadability of FC as evident in figure 5.4. For instance, the inclusion of 0.2% PP fiber as replacement for total solids has reduced spread percentage by 27.5%. Further, for the mixes with PP fiber content greater than 0.6% (% by weight of total solids) spread % is almost zero. This behaviour of reduction in spread percentage due to PP fiber addition can be ascribed to the water adsorption by PP fiber eventually leading to reduction in water content available for workability of mixes [Zhang and Li., 2013]. Furthermore, the restriction of flow due to mesh like structure formation which is an inherent property of PP fiber reinforced concrete can also be attributed to this behaviour [Li et al., 2022]. Nevertheless, the FC density of all the studied mixes with respect to PP fiber variation are within the ASTM permissible limits of ±50 kg/m^3. Further, a slight decreasing trend is observed in the density of PP fiber reinforced FC mixes, however these variations are not significant.

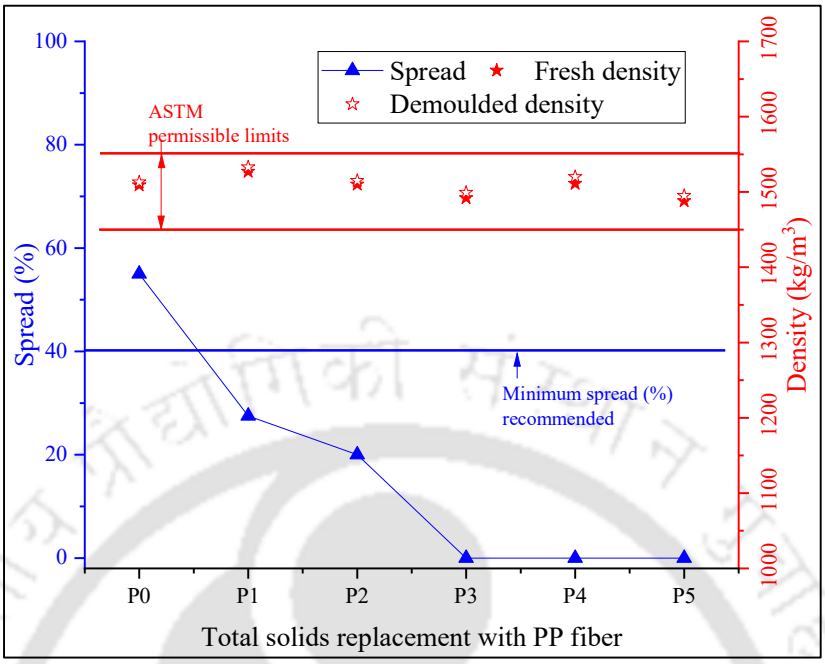

Figure 5.4: Effect of variation in level of PP fiber on spread and density of FC2 mixes at constant W/S of 0.3 (without SP addition).

As a next step, to enhance the spreadability of PP fiber reinforced FC mixes, the W/S ratio is increased for different levels of PP fiber as shown in figure 5.5. Results show that for every 0.2% increment in PP fiber (for mixes without FA), a systematic increase in requirement of W/S by 0.005 has been observed to achieve the desired spreadability of WFC2 mixes. In line with earlier observations, for the proposed mixes, the addition of PP fibers is found to affect the water demand and spreadability due to the water adsorption by PP fibers and restriction of the particle movement, with the later effect being more predominant. However, it is to be noted that the above impact of fibre on spreadability and water demand is relatively lesser when compared to its effect in mixes with varying levels of FA. Also, all the proposed FC mixes are exhibiting equivalent spread % except for the mix with 1% PP fiber content (P5), which can be attributed to its slightly lower density. Further, it is to be noted that with the adopted W/S ratios for varying fibre content, all the PP fibre reinforced FC mixes are able to meet the minimum spreadability requirement of 40% and their densities are within the ASTM permissible limits.

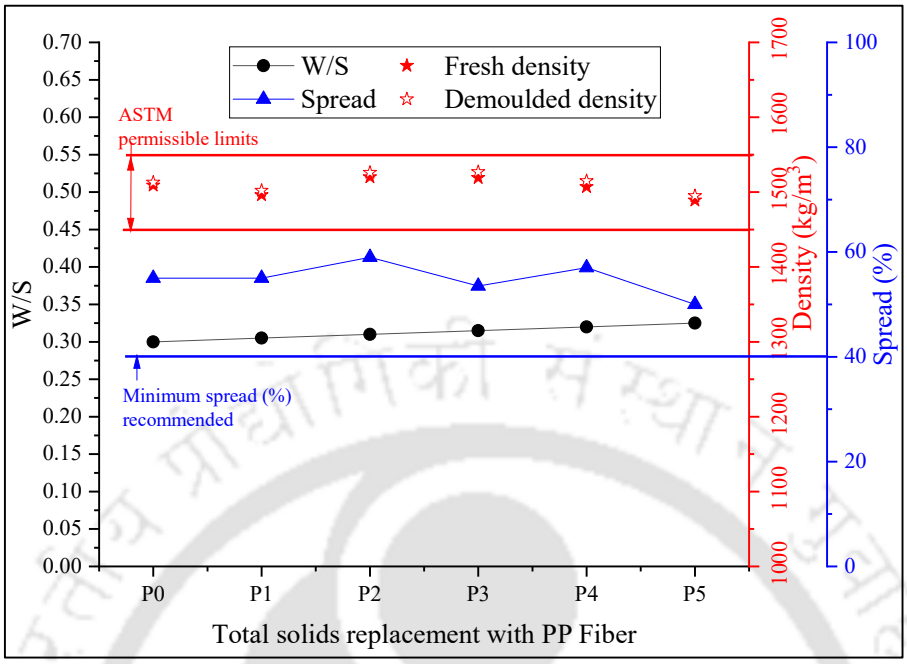

Figure 5.5: Effect of variation in W/S and PP fiber level on the consistency and density of WFC2 mixes (without SP).

Having studied the effect of variation of W/S, as a next step at constant W/S of 0.3, SP is varied to study its effect on spreadability and density. From figure 5.6, it is evident that, for every 0.2% replacement of total solids with PP fiber (for mixes without FA), a constant SP dosage of 0.05% is demanded for all the FC mixes studied. The above can be ascribed to the water adsorption of PP fiber and the associated decrement in spreadability due to the addition of fibre [Zhang and Li, 2013, Amran et al., 2020a]. Further, a decreasing trend is noted for the spread % of FC mixes with PP fiber content increasing from 0.2% to 0.8%. This can be attributed to the restriction of flow due to mesh like structure formation with PP fibers which is an inherent property of PP fiber reinforced concrete [Li et al., 2022]. Whereas, few exceptions with relatively higher flow are observed at 0.2% and 1% PP fiber dosage which can be attributed to the addition of slightly higher SP dosage than the required dosage at 0.2% PP fiber content and reduced foam content at 1% PP fiber content. Considering the effect of variation in SP dosage on the spreadability and density, replacement of total solids with various levels of fiber in FC, is able to meet the minimum spreadability requirement of 40% and their densities are within the ASTM permissible limits.

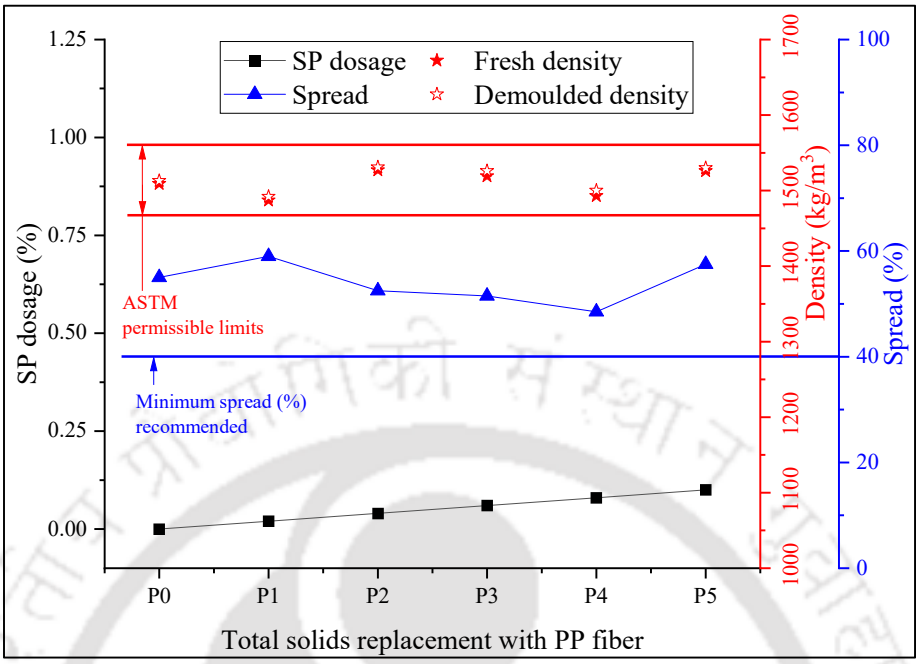

Figure 5.6: Effect of variation in SP dosage and PP fiber level on the consistency and density of SFC2 mixes.

Combined effect of FA and PP fiber

For the further studies on the combination mixes with FA as replacement for sand (at 25%, 50%, 75% and 100% replacement levels) and PP fiber added at different levels viz. 0.2%, 0.4%, 0.6%, 0.8% and 1% by weight of total solids, increment in W/S requirement (adopted from studies conducted on individual parameter variation as discussed earlier (figures 5.2, 5.5)), is presented in figure 5.7A. For example, as per individual parameter variation as discussed earlier, the additional W/S required for FC2, F1 and P1 are 0.3, 0.025 and 0.005 respectively, hence the adopted W/S for WFC2F1P1 is the addition of all (i.e. 0.3 + 0.025 + 0.005 = 0.33). From the fresh state properties of the proposed FC combination mixes (figure 5.7B), it has been observed that all the mixes are meeting the minimum spread of 40% as recommended in the literature. The small variations in the spread % can be attributed to various reasons such as PP fiber matrix interactions, variations in mesh formations, and reduced foam content [Markin et al., 2019, Sahu et al., 2021, Li et al., 2022]. Further, the spread % is mostly high for mixes with FA content less than 50% and PP fiber less than 0.4%. On the other hand, for combination mixes with PP fiber content greater than 0.6% (P3, P4 and P5), the spread observed is relatively lesser and this can be attributed to the synergistic effect of increase in cohesiveness of mix due

to FA addition and dense mesh like structure by PP fiber [Zhihua et al., 2007, Li et al., 2022].

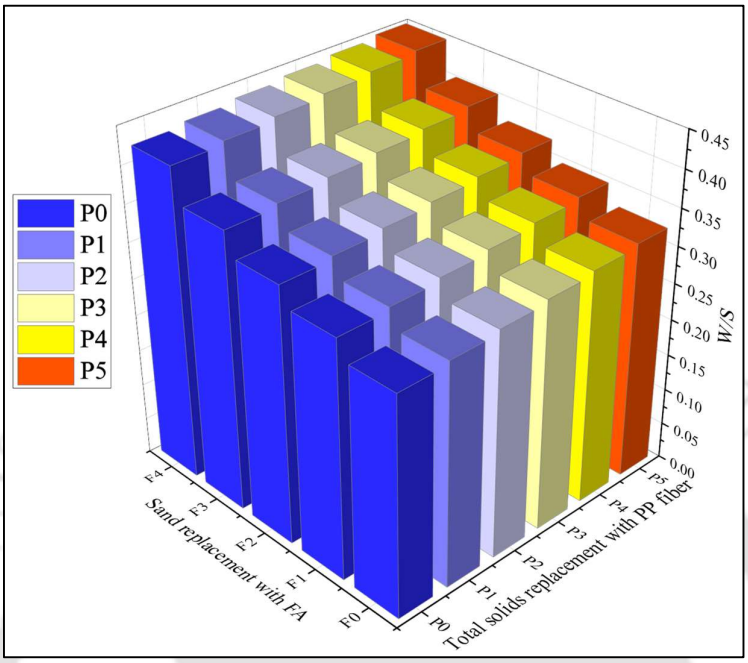

Figure 5.7: (A) Variation in W/S of WFC2 mixes for various combinations of PP fiber and FA.

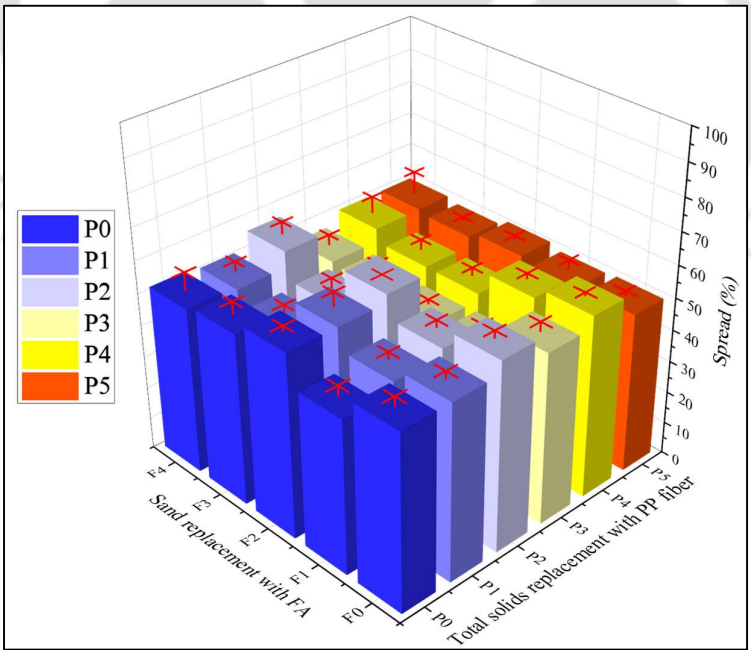

Figure 5.7: (B) Effect of variation in W/S, FA level and PP fiber level on the consistency of WFC2 mixes.

Close observation on variation in density of combination mixes indicate that the densities of all the proposed FC mixes (figure 5.8), are within the ASTM permissible limits with minimal variations with respect to the design density of 1500 kg/m^3. However, relatively higher variation in density is noted with variation in PP fiber content for combination mix with 100% sand replaced with FA. Particularly mix (WFC2F4P5) with higher W/S, more PP fiber (1%) and higher FA content (say 100%) is found to exhibit minimum density due to lower density of constituents used.

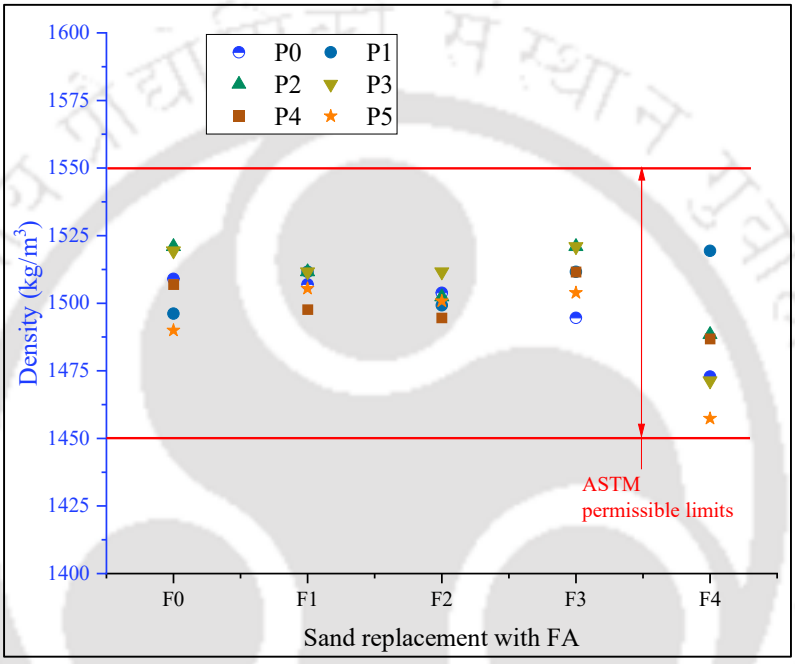

Figure 5.8: Effect of variation in W/S, FA level and PP fiber level on the density of WFC2 mixes.

As a next step, to study the effect of SP dosage on the combination mixes, SP requirement is adopted from studies conducted on individual parameter variation as discussed earlier (figure 5.3, 5.6, 5.9A). For example, as per studies on individual parameter variation as discussed earlier, the SP dosages required for FC2, F1 and P1 are 0%, 0.25% and 0.05% respectively, hence the adopted SP dosage for SFC2F1P1 is the addition of both (i.e., 0% + 0.25% + 0.05% = 0.3%). From the experimental results on fresh state properties of the proposed FC combination mixes, it has been observed that all the mixes are meeting the minimum spread requirement of 40% as recommended in the literature (figure 5.9B). Adding to above, the variations noticed in the spread % values indicate that the dispersion of values is not high. Further, comparative analysis indicates that mostly the mixes with either high FA content or high PP fiber content or combination of both exhibit high

spread % and this can be attributed majorly to the reduced foam content in those mixes which otherwise increases the viscosity of FC mixes.

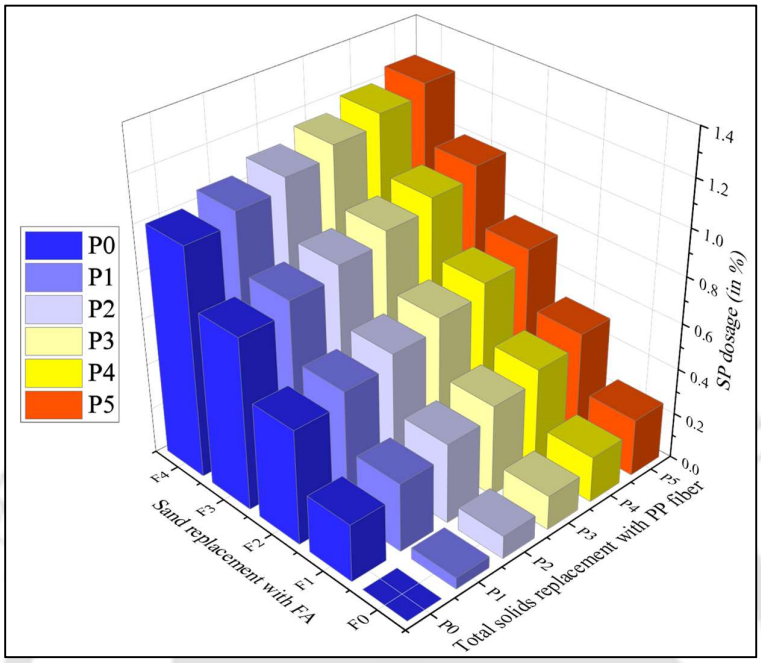

Figure 5.9: (A) Variation in SP dosage of SFC2 mixes for various combinations of PP fiber and FA.

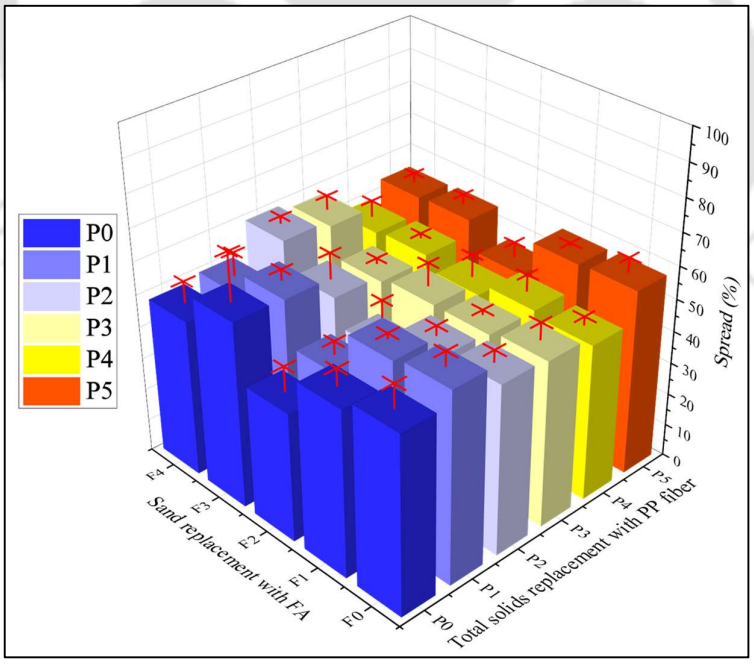

Figure 5.9: (B) Effect of variation in SP dosage, FA level and PP fiber level on the consistency of SFC2 mixes.

Furthermore, considering the effect on density, for the proposed combination mixes density is found to be within the ASTM permissible limits of ±50 kg/m^3. Here an interesting fact is observed by comparing the variation of density of FC mixes with 25% replacement of sand with FA with varying PP fiber content. The above variations in density with respect to PP fiber content are relatively lower (figure 5.10). Whereas, with the increment in FA content the variations in density with respect to PP fiber content is found to increase. Furthermore, these variations are higher when compared to those in the case of mixes studied with varying W/S above. This can be attributed to the reduction in foam content in mixes with increase in PP fiber content and FA [Markin et al., 2019, Sahu et al., 2021]. For instance, the FC mixes with high PP fiber content (1% total solids replacement with PP fiber) are mostly exhibiting maximum FC density. This can be attributed to the relatively low density of PP fiber among the solid components of the FC mixes, ultimately resulting in higher decrement in foam content. Furthermore, these variations in spread % and density of combination FC mixes can be attributed to the combinations of various forces contributing to the compatibility of mix components such as absorption force by FA, cement and sand, adsorptive force by PP fiber, steric hindrance effect by SP and the surfactant solution's capacity to maintain bubble stability in foam [Zhihua et al., 2007, Zhang and Li, 2013, Markin et al., 2019, Amran et al., 2020a, Sahu et al., 2021, Li et al., 2022]. From the above discussion it is clearly evident that the usage of FA has exhibited greater demand in terms of both SP as well as water content when compared to that of PP fiber.

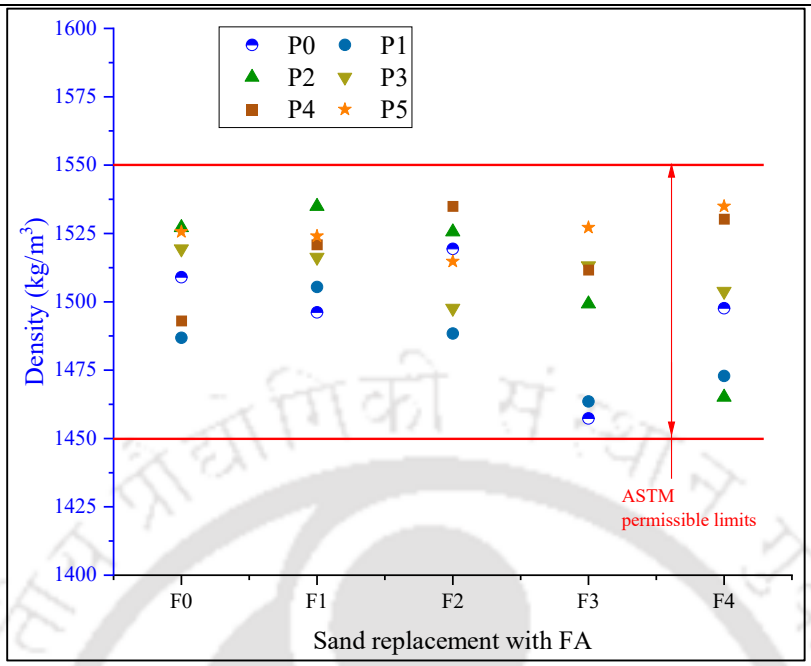

Figure 5.10: Effect of variation in SP dosage, FA level and PP fiber level on the density of SFC2 mixes.

5.3.2 MECHANICAL PROPERTIES OF FC

In general, the mechanical properties of concrete play a critical role in determining the safety and performance of structures. Compressive strength, split tensile strength and flexural strength are the vital mechanical properties defining the applicability of certain type of concrete for its desired application. As per earlier studies in chapter 4, the mechanical properties of all the mixes studied (at 56 days of testing) have significantly increased, when FA replaces 50% of the fine aggregate (300 µm) attributing to its pozzolanic effect, whereas replacement of the 0.05% of total solids (by weight) with PP fiber has shown minor reduction in strength. Further, combination mixes with both FA and PP fiber (i.e. FCFaPs) have shown a significant improvement in mechanical behaviour indicating the dominant role of FA from strength perspective. Hence as a next step, studies on the combined effect of various proportions of FA (0%, 25%, 50%, 75% and 100%) as sand replacement and PP fiber (0%, 0.2%, 0.4%, 0.6%, 0.8% and 1%) as total solids replacement by weight on the mechanical properties are carried out in this section.

5.3.2.1 COMPRESSIVE STRENGTH OF PROPOSED FC MIXES

The proposed FC mixes have been found exhibiting satisfactory fresh state properties within the recommended limits as discussed in the previous section. Hence, as a next step,

in accordance with ASTM C109/ C109M-21, the compressive strength of the proposed FC mixes is being investigated in this section. The initial discussion focuses on the distinct impact of FA or PP fibre, as well as the necessary dosage of W/S or SP, on the FC's compressive strength. Subsequently, the combined impact of FA and PP fibre on the suggested FC mixes' compressive strength is being investigated. Further, the results of the compressive strength of these FC mixes tested at different ages are presented in figures 5.11 – 5.13.

Effect of FA on compressive strength of proposed FC mixes

The results of the compressive strength of the FC mixes with varied levels of sand replacement with FA along with the required W/S or SP dosage (derived from earlier studies resulting in mixes with desired stability and consistency) tested in accordance with ASTM C109/ C109M-21 are shown in figure 5.11A, 5.11C. Further, various comparative analyses such as A: comparative analysis of 28 days strength of all the FC mixes with the FC2F0P0 mix at 28 days, B: comparative analysis of 56 days strength of all the FC mixes with the FC2F0P0 mix at 56 days, C: comparative analysis of 56 days strength of all the FC mixes with the corresponding 28 days strength are shown in figure 5.11B, 5.11D. Obviously, as expected, the mixes without FA (FC2F0P0) exhibits the lowest compressive strength of 4 N/mm^2 while the mixes with incremental FA content exhibits incremental trend in compressive strength. Also, the difference between 28 days and 56 days compressive strength is very much less for the mixes without FA, when compared to that of mixes with FA. Figure 5.11A and 5.11C shows that, as the FA content increases in the FC mix, significant increase in compressive strength is observed. For instance, increase in FA level from 0 to 100% along with either increase in W/S from 0.3 to 0.425 (figure 5.11A) or SP dosage from 0% to 1% (figure 5.11C) results in increase in compressive strength from 4 N/mm^2 to 17 N/mm^2 and 4 N/mm^2 to 25 N/mm^2 respectively. The above increase in strength due to FA addition (as observed in scatter B of figure 5.11B, 5.11D) can be attributed to the pozzolanic reaction which is basically a reaction between amorphous silica in FA and Ca $(OH)_2$ (a by-product of cement hydration) to form additional C-S-H gel. However, it is to be noted that pozzolanic reaction is a slow reaction and the pozzolanic activity increases rapidly after 28 days [Feng et al., 2018]. Hence, the initial strength gains due to FA addition as observed in scatter A of figures 5.11B (linear trend), 5.11D (exponential trend), can be attributed

mostly to the improvement in microstructure resulting from enhanced packing of finer particles of FA [Ramamurthy et al., 2009]. Additionally, the usage of SP instead of increasing W/S, further increases the compressive strength exponentially (by comparing scatter A of figures 5.11B and 5.11D) through enhancement in the microstructure of FC. This can be attributed to the reduction of additional pores due to reduced water content and densification resulting from steric hindrance effect of PCE based SP [Dhasindrakrishna et al., 2021, Wang et al., 2021]. Also, due to delayed pozzolanic reaction, a significant enhancement of strength at later age is observed as established in literature [Pan et al., 2007, Ganesan et al., 2015]. For instance, increment of 90% and 142% in compressive strength is observed for increase in age from 28 days to 56 days particularly for mixes WFC2F2P0 and SFC2F1P0 (as observed in scatter C of figures 5.11B, 5.11D). For mixes in which W/S is increased with increase in FA level (WFC2 mixes), it is noticed that beyond 50% replacement level, there is not much further improvement in strength due to limited progress of pozzolanic activity (as observed in scatter C of figure 5.11B). On the other hand, in the case of mixes where SP dosage is increased instead of increase in W/S (SFC2 mixes), beyond 25% replacement level of sand with FA, there is reduction in strength enhancement from 28 days to 56 days which can be ascribed to the limited progress of pozzolanic activity (as observed in scatter C of figure 5.11D). This can be ascribed to the limited availability of $Ca(OH)_2$ for pozzolanic reaction due to its encapsulation within the web-like structure of C-S-H gel. Further, it is to be noted that the thickness of this encapsulation increases with age of concrete affecting the availability of $Ca(OH)_2$ for pozzolanic reaction [Sevim and Sengul, 2021]. The above observations are in agreement with earlier study by Xu and Sarkar, 1994 on cement: FA (1: 1.5) paste who had reported based on chemical analysis, that the $Ca(OH)_2$ is available in unreacted form even at the age of 90 days in tested samples. This indicates that, though there is $Ca(OH)_2$ available in the mixes with FA content greater than 50%, it could not be accessed by the reactive silica for pozzolanic reaction as discussed earlier. Further, among all the mixes only SFC2F4P0 mix (at 56 days of curing) satisfies the ASTM C1372-23 requirement of 20.7 N/mm^2 compressive strength for its desired application for dry-cast segmental retaining wall units.

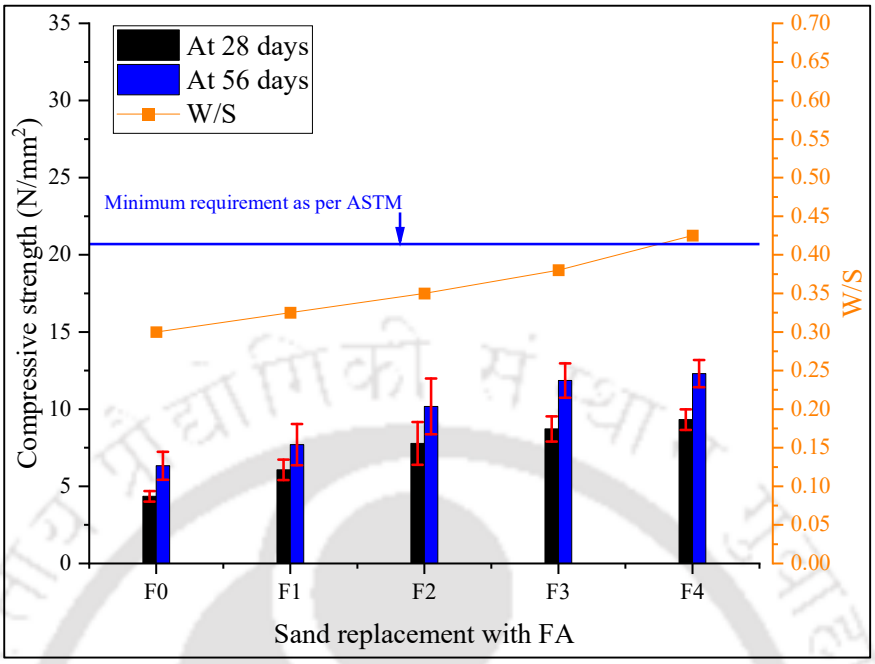

Figure 5.11: (A) Combined effect of W/S and FA level on the compressive strength of WFC2 mixes.

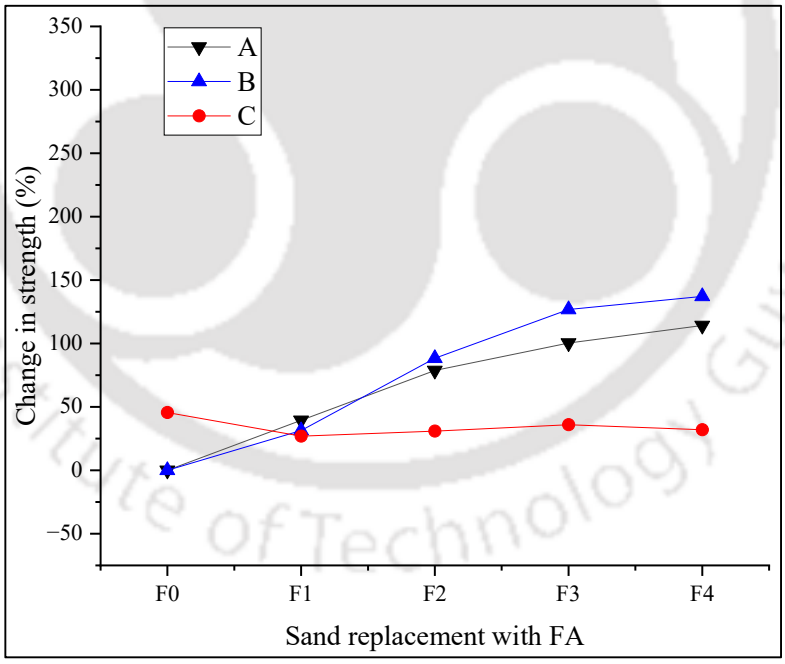

Figure 5.11: (B) Comparative analysis between compressive strength of the proposed WFC2 mixes (with variation in FA level) at different testing ages.

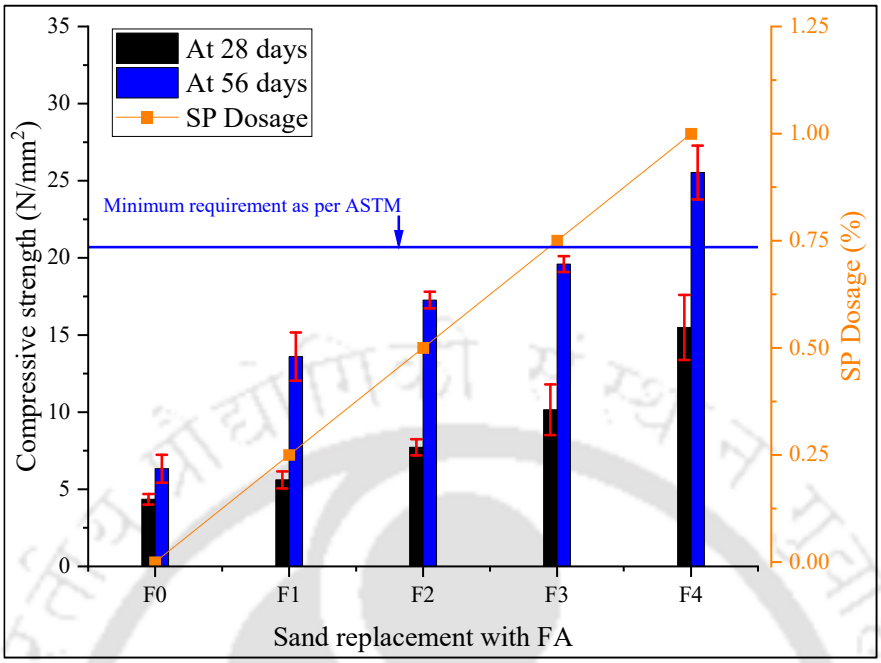

Figure 5.11: (C) Combined effect of SP dosage and FA level on the compressive strength of SFC2 mixes.

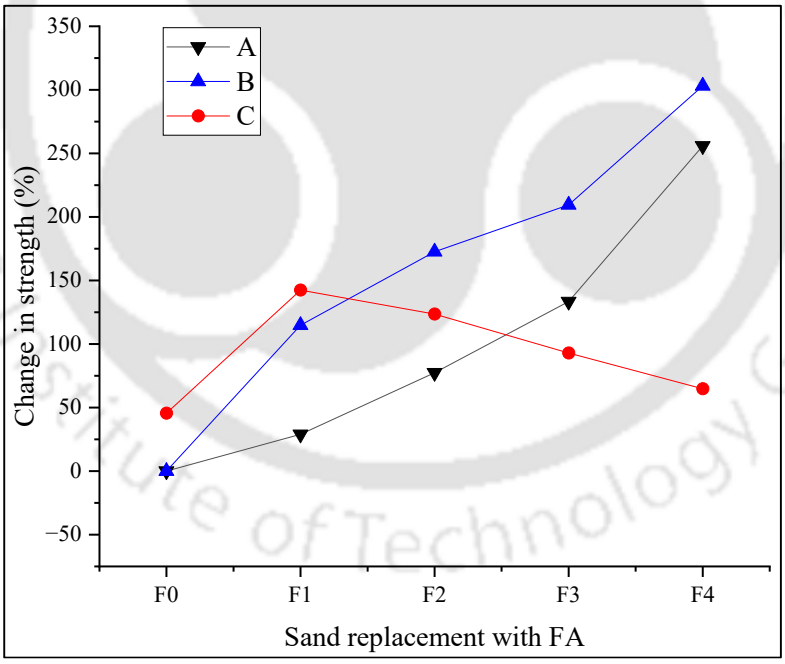

Figure 5.11: (D) Comparative analysis between compressive strength of the proposed SFC2 mixes (with variation in FA level) at different testing ages.

Note: In figure 5.11B, 5.11D description of adopted various legends is provided below.

A: Comparison of all the mixes with FC2F0P0 at 28 days, B: Comparison of all the mixes with FC2F0P0 at 56 days, C: Comparison between 28 days and 56 days compressive strength of all mixes.

Effect of PP fiber on compressive strength of proposed FC mixes

The results of the compressive strength of the FC mixes with varied levels of PP fiber along with the required W/S or SP dosage (derived from earlier studies resulting in mixes with desired stability and consistency) tested in accordance with ASTM C109/C109M-21 are shown in figure 5.12A, 5.12C. Further, various comparative analyses such as A: comparative analysis of 28 days strength of all the FC mixes with the FC2F0P0 mix at 28 days, B: comparative analysis of 56 days strength of all the FC mixes with the FC2F0P0 mix at 56 days, C: comparative analysis of 56 days strength of all the FC mixes with the corresponding 28 days strength are shown in figure 5.12B, 5.12D. Experimental outcomes show that the mix with 1% PP fiber content (WFC2F0P5) exhibits the lowest compressive strength of <3 N/mm^2 while the mixes with incremental PP fiber content exhibits an inverted 'U' trend for both 28 days and 56 days compressive strength, with a maximum for SFC2F0P2 mix. Close observations shows that mixes SFC2F0P1 and SFC2F0P2 are exhibiting up to 5% and 60%, and 131% and 171% enhancement in compressive strength at 28 days and 56 days respectively when compared to SFC2F0P0 mix. The above increase in strength due to PP fiber addition (as observed in scatter B of figure 5.12B, 5.12D) can be attributed to the enhanced fiber matrix interaction due to the usage of SP as established in the literature [Huang, 2001, Hadipramana et al., 2013, Falliano et al., 2019, Castillo-Lara et al., 2020]. Additionally, the increase in surface area through increase in PP fiber content (up to 0.4%), exhibits a positive influence on the fiber-matrix interactions. Hence, the initial strength gains due to PP fiber addition as observed in scatter A of figures 5.12B, 5.12D respectively, can be attributed to the improvement in microstructure of fiber-matrix zone resulting from enhanced packing due to usage of SP [Huang, 2001]. Additionally, the usage of SP instead of additional W/S, further increases the compressive strength exponentially (by comparing scatter A of figures 5.11B and 5.11D) through enhancement in the microstructure of FC. This can be attributed to the reduction of additional pores due to reduced water content and enhanced packing due to the steric hindrance effect by SP [Huang, 2001].

Further increase in the PP fiber content shows a negative influence on compressive strength of FC. This can be attributed to the substantial reduction in the amount of matrix owing to the low density of PP fiber. Adding to above, at higher dosage of PP fiber, close vicinity of individual PP fibers leads to increase in amount of transition zone (i.e. weaker

zone) between PP fiber and matrix and ultimately affects the strength of FC (figure A.1) [Noushini et al., 2013, 2014, Zhang et al., 2019, Xu et al., 2020]. However, a slightly higher compressive strength of SFC2F0P5 (figure 5.12C) is observed at the age of 28 days as an exception to the above-mentioned trend. Another noteworthy observation is that the difference between 28 days and 56 days compressive strength is very much less for the mixes with either no PP fiber or high PP fiber content (SFC2F0P0, SFC2F0P5), when compared to that of mixes with intermediate PP fiber content (0.2% to 0.8%) (figure 5.12C). Here it is to be noted that, in the proposed FC mixes discussed in this section, cement is the only binder present and hence the hydration reaction of cement can be considered as one of the major contributors for the strength gain from 28 days to 56 days. Further, the mix SFC2F0P1 is exhibiting higher strength gain beyond 28 days (as observed in scatter C of figure 5.12D). This can be attributed to the PP fiber-matrix interactions which enhance the compressive strength of FC through restriction of crack propagation, which is an intrinsic property of PP fiber reinforced concrete [Yuan and Jia, 2021]. Furthermore, though the SFC2F0P2 mix is exhibiting the highest compressive strength of 12 N/mm^2, the strength gain beyond 28 days is low (figure 5.12C, 5.12D). This can be attributed to the increase in the surface area of PP fiber and subsequent reduction in the binder content affecting the bonding between PP fiber and matrix.

Moreover, in the case of SFC2F0P3 mix increase in transition zone between PP fiber and matrix due to increase in PP fiber dosage, has major effect at 28 days strength (figure A.1). Whereas, at 56 days the densification of matrix due to cement hydration reaction help to improve the PP fiber matrix interaction zones and hence strength is improved (figure 5.12C) [Yuan and Jia, 2021]. On a similar note, the SFC2F0P4 mix also exhibits lesser strength due to close vicinity of PP fibers and reduced amount of matrix for binding resulting in lowest compressive strength and lowest strength gain from 28 days to 56 days, particularly at 56 days (figure A.1, 5.12C, scatter C of figure 5.12D) [Noushini et al., 2013, 2014, Zhang et al., 2019, Xu et al., 2020, Yuan and Jia, 2021]. Further, none of the mixes are satisfying the ASTM C1372-23 recommended 20.7 N/mm^2 for dry-cast segmental retaining wall units proving them to be unsuitable for the desired application.

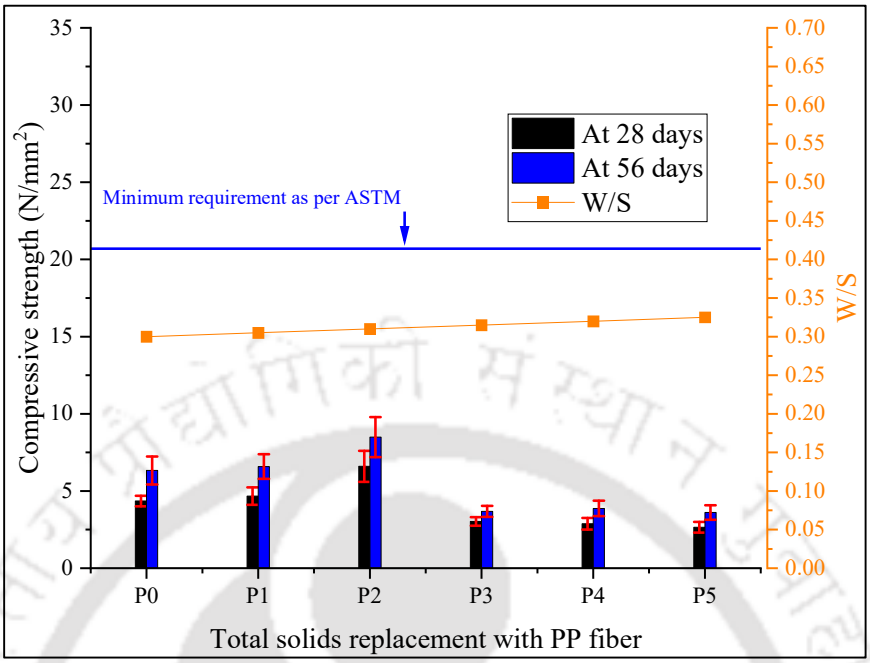

Figure 5.12: (A) Combined effect of W/S and PP fiber level on the compressive strength of WFC2 mixes.

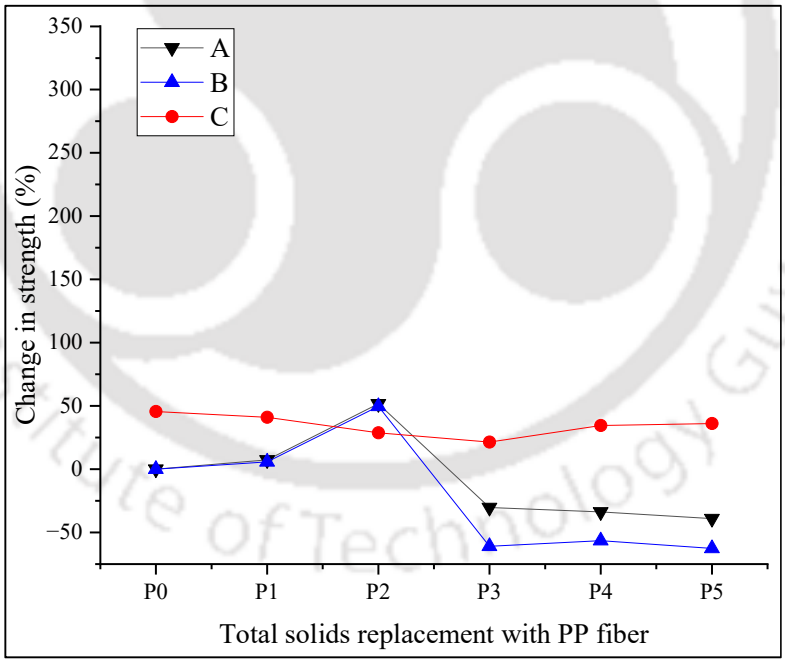

Figure 5.12: (B) Comparative analysis between compressive strength of the proposed WFC2 (with variation in PP fiber level) mixes at different testing ages.

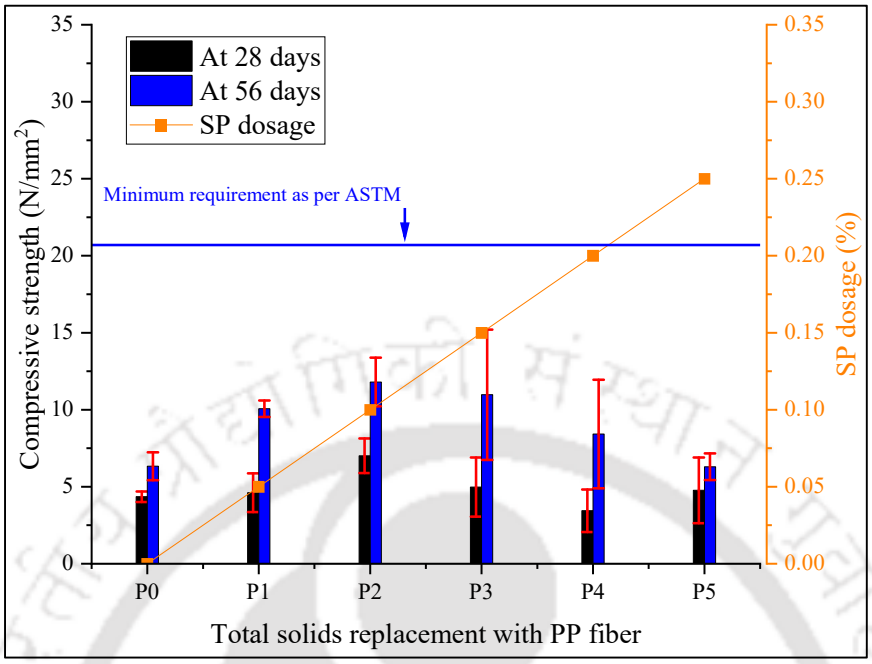

Figure 5.12: (C) Combined effect of SP dosage and PP fiber level on the compressive strength of SFC2 mixes.

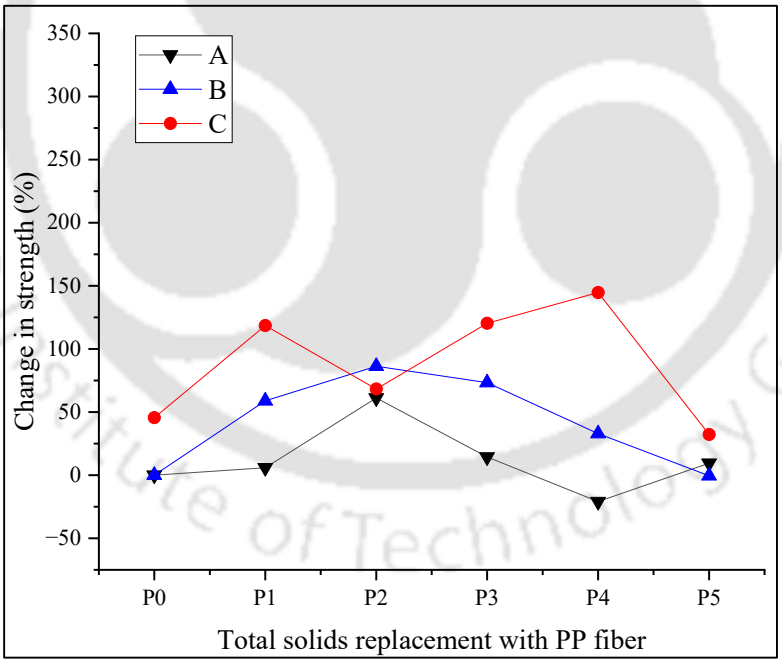

Figure 5.12: (D) Comparative analysis between compressive strength of the proposed SFC2 (with variation in PP fiber level) mixes at different testing ages.

Note: In figure 5.12B, 5.12D description of adopted various legends is provided below.

A: Comparison of all the mixes with FC2F0P0 at 28 days, B: Comparison of all the mixes with FC2F0P0 at 56 days, C: Comparison between 28 days and 56 days compressive strength of all mixes.

Combined effect of FA and PP fiber on compressive strength of proposed FC mixes

From the above results, it is evident that both FA and PP fiber are enhancing the compressive strength of FC individually. Hence as a next step, the combination mixes with the above utilized variations in W/S, SP dosage, FA and PP fiber are considered for further enhancement in compressive strength of FC for its desired application in accordance with ASTM C1372-23 (figures 5.13A - 5.13J). In line with the earlier results, the combination mixes with both FA and PP fiber have shown an increase in compressive strength of SFC2 by 61% to 462% with a maximum of 25 N/mm^2 compressive strength for the SFC2F4P2 mix at the age of 28 days (figures 5.13A, 5.13C, 5.13F, 5.13H). The increase in packing efficiency due to the combined effect of finer FA particles (<75 μm), thin PP fibers (22 μm) and the steric hindrance effect by PCE based SP can be attributed as major contributors for this enhancement in 28 days strength [Dhasindrakrishna et al., 2021, Wang et al., 2021]. Here it is to be noted that, for any given FA level, the increment in PP fiber level is exhibiting a similar inverted 'U' trend. Further, closer examination shows that, the combination mixes are exhibiting enhancement in compressive strength up to 0.4% replacement of total solids with PP fiber irrespective of the FA level. The increment of PP fiber level from 0.4% to 0.6% is exhibiting a sudden drop in the compressive strength of FC irrespective of FA level at 28 days. Moreover, though there is higher strength gain from 28 days to 56 days, the P3 mixes are significantly lower in compressive strength. This peculiar behaviour of FC can be attributed to the close vicinity of PP fiber leading to increase in weaker transition zones between fibre and matrix along with poor bonding due to reduced matrix content as discussed in earlier section (figure A.1) [Noushini et al., 2013, 2014, Zhang et al., 2019, Xu et al., 2020, Yuan and Jia, 2021]. In line with observations, further replacement of total solids with PP fiber up to 1% results in a systematic and significant reduction in compressive strength of such FC mixes (figure A.1).

Further, for any given PP fiber dosage, increase in FA level results in systematic increase in strength. However, beyond 0.6% dosage of PP fiber, the above-mentioned variation in compressive strength with increase in FA level is decreasing. Particularly in the case of P5 mixes, viz. SFC2F2P5, SFC2F3P5 and SFC2F4P5, the aforementioned variations are tending towards negligibility. This reduction in strength gain of P5 mix can be attributed to the increase in the total surface of PP fiber due to higher PP fiber content and the

reduced matrix content due to low density of PP fiber (figure A.1) [Yuan and Jia, 2021]. Here it is to be noted that, though higher PP fiber content is reducing the compressive strength, but in mixes with 100% of sand replaced with FA along with higher dosage of PP fibers (0.8% to 1%), significant enhancement of 240% and 215% in compressive strength is noted for FC mixes SFC2F4P4, SFC2F4P5 respectively when compared to that of SFC2F0P0 mix. This can be attributed to significant increase in paste content due to addition of FA and subsequent increase in binder property and bonding of paste and PP fiber [Yuan and Jia, 2021]. However, the above enhancement in strength is relatively lower when compared to combination mixes with lesser amount of PP fiber (less than 0.6%). As a significant outcome of the current study, the SFC2F4P0, SFC2F4P1, SFC2F3P1, SFC2F1P2, SFC2F2P2, SFC2F3P2, SFC2F4P2 and SFC2F4P3 are the satisfactory mixes (figure 5.13G) as per the ASTM C1372-23 recommendation of 20.7 N/mm^2 minimum compressive strength criteria for dry-cast segmental retaining wall units proving them to be eligible for further studies in the desired application. However, further testing the other properties of the proposed mixes might give a significant conclusion on the suitable FC mix for the desired application.

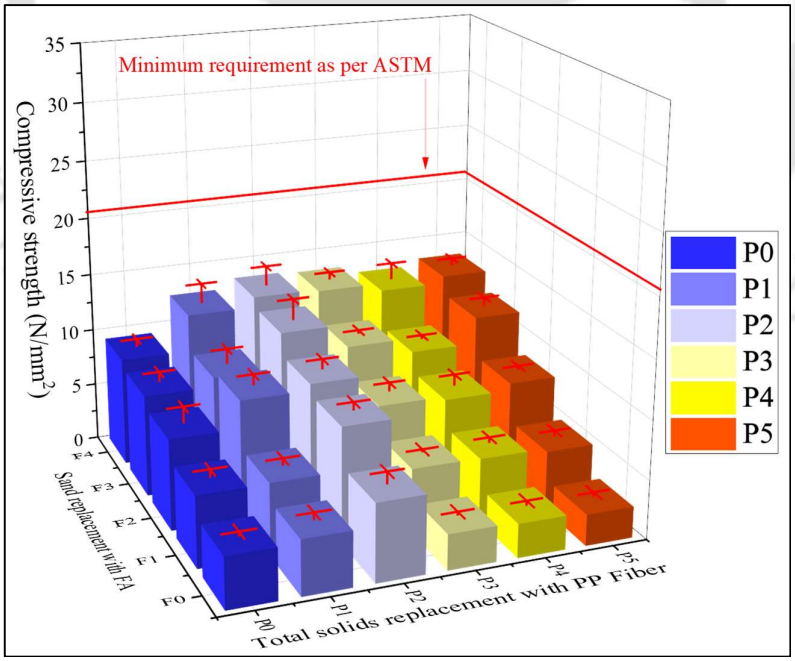

Figure 5.13: (A) Effect of variation in W/S, FA level and PP fiber level on the compressive strength of WFC2 mixes at 28 days.

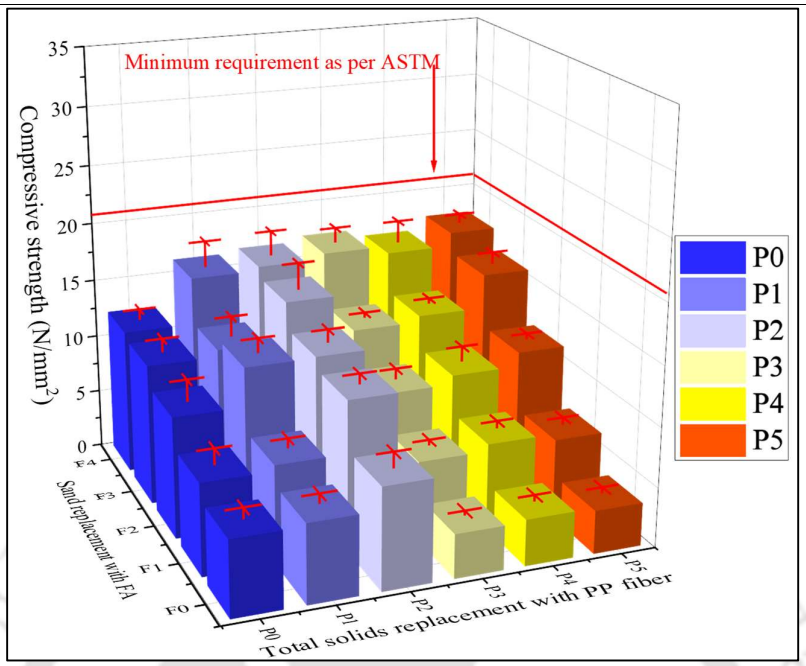

Figure 5.13: (B) Effect of variation in W/S, FA level and PP fiber level on the compressive strength of WFC2 mixes at 56 days.

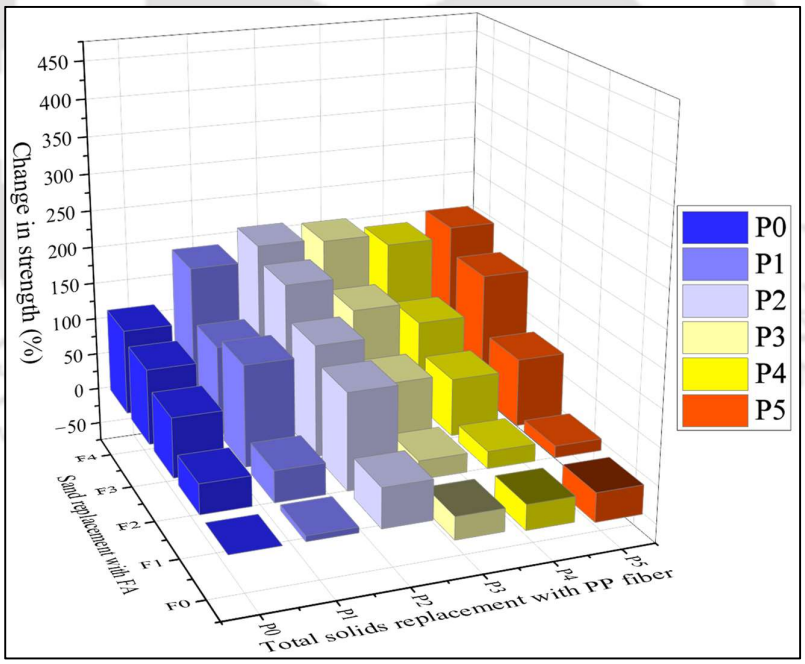

Figure 5.13: (C) Comparing the WFC2F0P0 mix and the WFC2 mixes with variations in W/S, FA level, and PP fibre level in terms of compressive strength at 28 days.

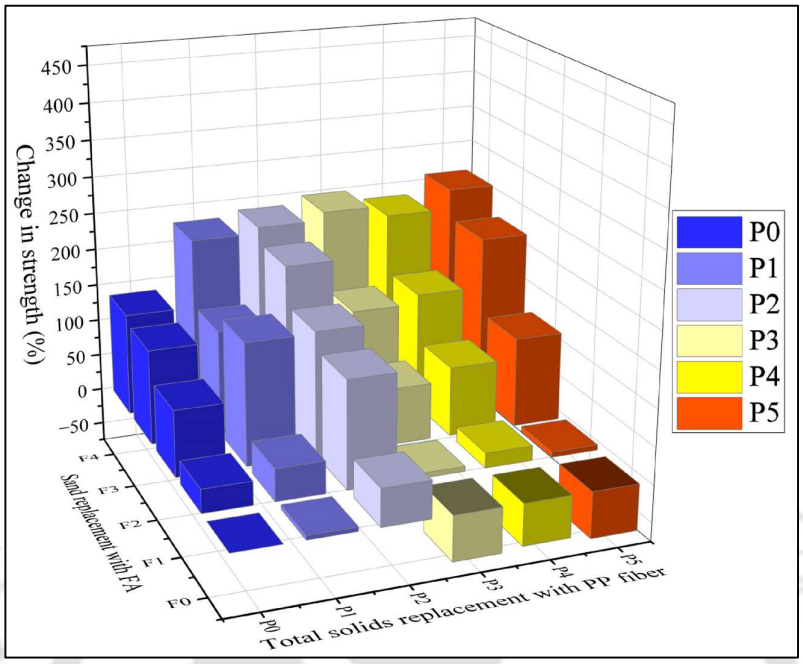

Figure 5.13: (D) Comparing the WFC2F0P0 mix and the WFC2 mixes with variations in W/S, FA level, and PP fibre level in terms of compressive strength at 56 days.

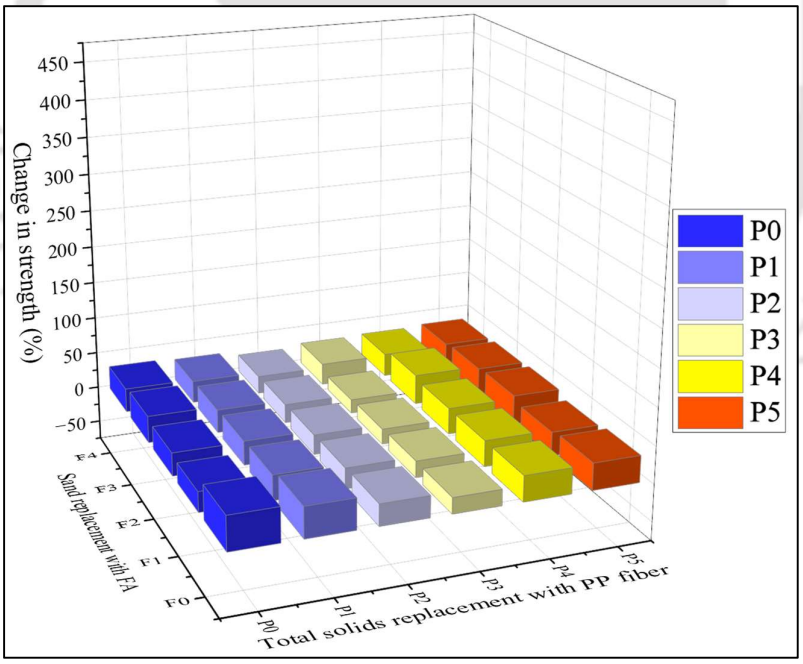

Figure 5.13: (E) Comparing the 28 days and 56 days compressive strength of the WFC2 mixes with variation in W/S, FA level and PP fiber level.

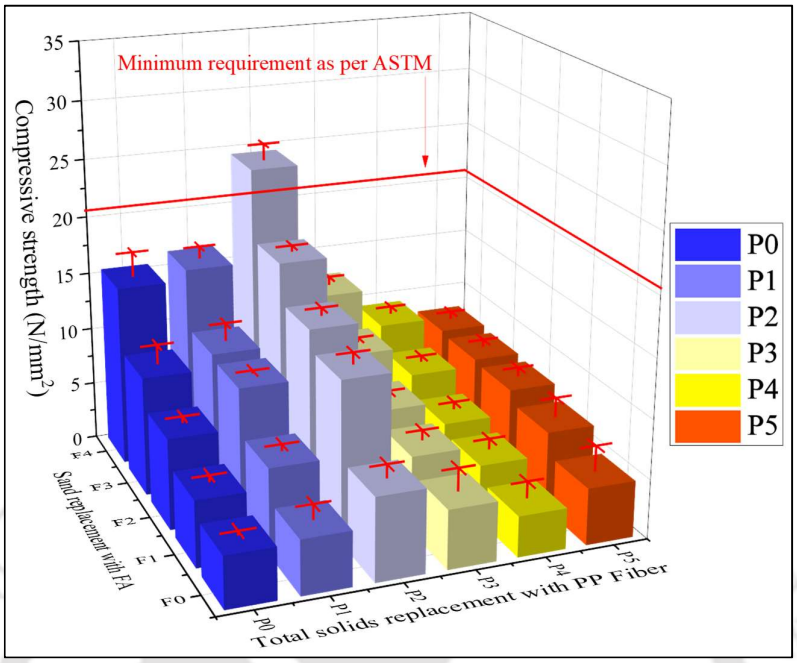

Figure 5.13: (F) Effect of variation in SP dosage, FA level and PP fiber level on the compressive strength of SFC2 mixes at 28 days.

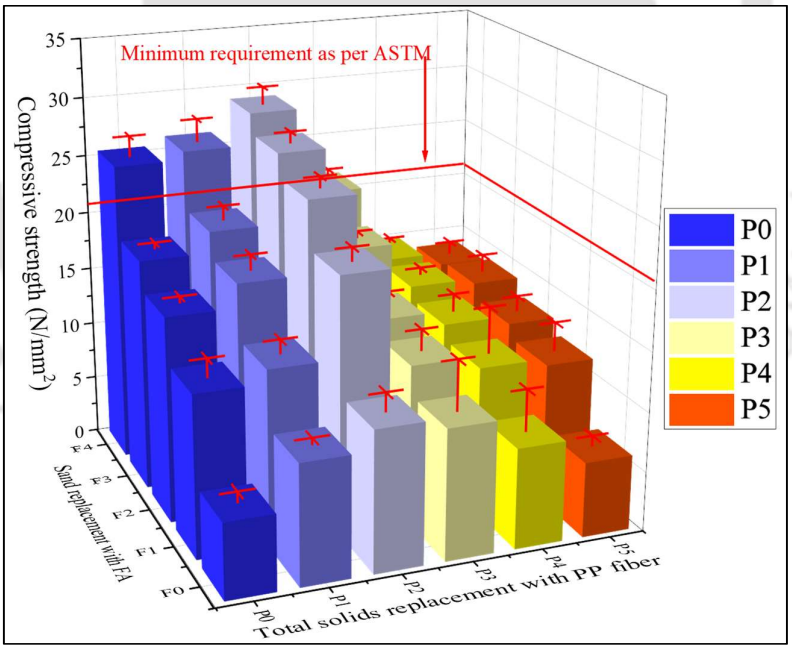

Figure 5.13: (G) Effect of variation in SP dosage, FA level and PP fiber level on the compressive strength of SFC2 mixes at 56 days.

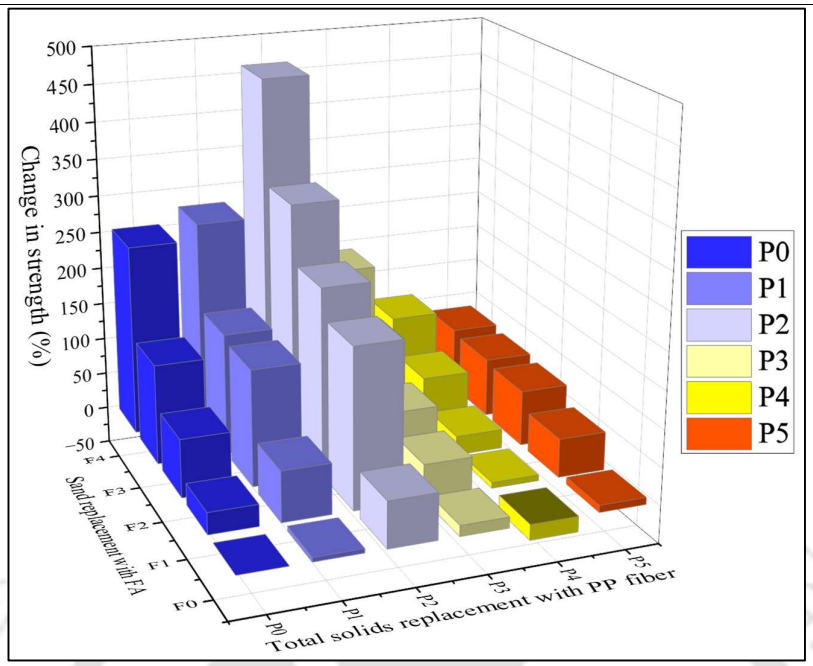

Figure 5.13: (H) Comparing the SFC2F0P0 mix and the SFC2 mixes with variations in SP dosage, FA level, and PP fibre level in terms of compressive strength at 28 days.

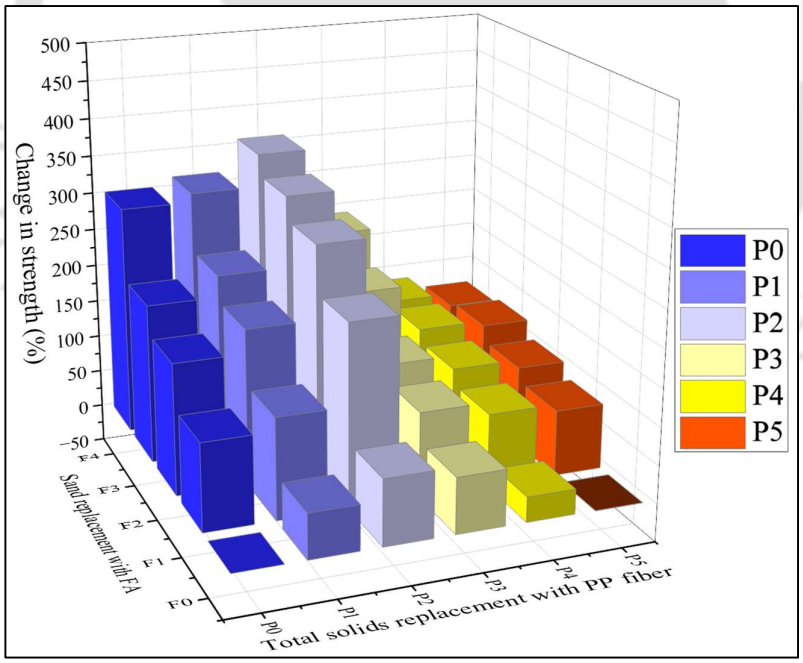

Figure 5.13: (I) Comparing the SFC2F0P0 mix and the SFC2 mixes with variations in SP dosage, FA level, and PP fibre level in terms of compressive strength at 56 days.

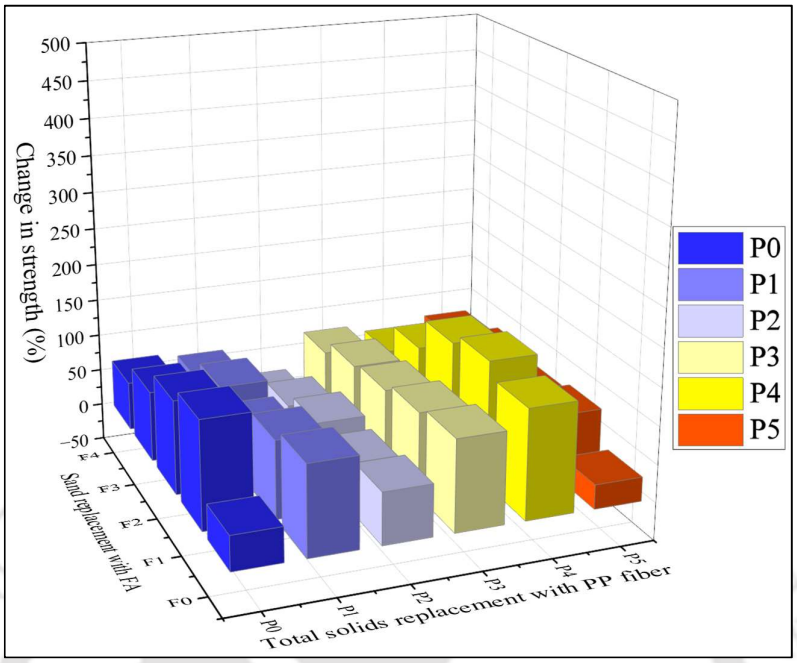

Figure 5.13: (J) Comparing the 28 days and 56 days compressive strength of the SFC2 mixes with variation in SP dosage, FA level and PP fiber level.

5.3.2.2 SPLIT TENSILE STRENGTH OF PROPOSED FC MIXES

For the assessment of proposed FC mixes for split tensile strength, cylindrical samples with dimensions of 100 mm diameter and 200 mm length have been tested as per ASTM C496-17 at 28-days and 56-days and presented in figure 5.14 – 5.17. Further, this section follows the same format as the compressive strength section in discussing the split tensile strength of the proposed FC mixes.

Effect of FA on split tensile strength of proposed FC mixes

The results of the split tensile strength of the FC mixes with varied levels of sand replacement with FA along with the required W/S or SP dosage (derived from earlier studies resulting in mixes with desired stability and consistency) tested in accordance with ASTM C496-17 are shown in figure 5.14A, 5.14D. Further, various comparative analyses such as A: comparative analysis of 28 days strength of all the FC mixes with the FC2F0P0 mix at 28 days, B: comparative analysis of 56 days strength of all the FC mixes with the FC2F0P0 mix at 56 days, C: comparative analysis of 56 days strength of all the FC mixes with the corresponding 28 days strength are shown in figure 5.14B, 5.14E. Obviously, as expected, the mixes without FA (FC2F0P0) exhibits the lowest split tensile

strength of 0.5 N/mm^2 while the mixes with incremental FA content exhibits incremental trend in split tensile strength. Also, the difference between 28 days and 56 days split tensile strength is decreasing for the mixes with increase in FA level, when compared to that of mixes without FA. Figure 5.14A and 5.14D shows that, as the FA content increases in the FC mix, significant increase in split tensile strength is observed. For instance, increase in FA level from 0 to 100% along with either increase in W/S from 0.3 to 0.425 (figure 5.14A) or SP dosage from 0% to 1% (figure 5.14D) results in increase in split tensile strength from 0.5 N/mm^2 to 1.7 N/mm^2. The above increase in strength due to FA addition (as observed in scatter B of figure 5.14B, 5.14E) can be attributed to the pozzolanic reaction which increases rapidly after 28 days [Feng et al., 2018]. Hence, the initial strength gains due to FA addition as observed in scatter A of figures 5.14B (linear trend), 5.14E (exponential trend), can be attributed mostly to the improvement in microstructure resulting from enhanced packing of finer particles of FA [Ramamurthy et al., 2009]. Additionally, the usage of SP instead of increasing W/S, further increases the split tensile strength exponentially (by comparing scatter A of figures 5.14B and 5.14E) through enhancement in the microstructure of FC. This can be attributed to the reduction of additional pores due to reduced water content and densification resulting from steric hindrance effect of PCE based SP [Dhasindrakrishna et al., 2021, Wang et al., 2021]. Also, due to delayed pozzolanic reaction, a significant enhancement of strength at later age is observed as established in literature [Pan et al., 2007, Ganesan et al., 2015]. For instance, increment of 88% and 97% in split tensile strength is observed for increase in age from 28 days to 56 days particularly for mixes WFC2F2P0 and SFC2F2P0 (as observed in scatter C of figures 5.14B, 5.14E). For mixes in which W/S is increased with increase in FA level (WFC2 mixes), it is noticed that beyond 50% replacement level, there is not much further improvement in strength due to limited progress of pozzolanic activity (as observed in scatter C of figure 5.14B). On the other hand, in the case of mixes where SP dosage is increased instead of increase in W/S (SFC2 mixes), beyond 50% replacement level of sand with FA, there is decrement in strength improvement beyond 28 days which can be ascribed to the limited progress of pozzolanic activity along with reduction in foam content and increment in brittle nature of FC (as observed in scatter C of figure 5.14E). This can be ascribed to the limited accessibility of Ca $(OH)_2$ by the reactive silica for pozzolanic reaction as discussed earlier [Sevim and Sengul, 2021, Xu and Sarkar, 1994].

Further, the analysis of split tensile strength to compressive strength ratio (f_t/f_c) for the above-mentioned mixes is presented in figures 5.14C, 5.14F. Obviously, as expected, the mixes without FA (FC2F0P0) exhibits the highest f_t/f_c of 0.15 while the mixes with incremental FA content exhibits decremental trend in f_t/f_c. This decrement in f_t/f_c reveals the increment in brittle behaviour of the FC which can be attributed to the reduction in foam content due to lower density of FA as well as close packing of matrix due to the finer particle size of FA at 28 days [Vishavkarma and Harish, 2024]. Further, though the pozzolanic reaction by FA, increases the compressive strength, but proportionate increase in split tensile strength of FC is not observed from 28 days to 56 days, subsequently resulting in lower f_t/f_c ratio and increased brittle behaviour of FC [Vishavkarma and Harish, 2024].

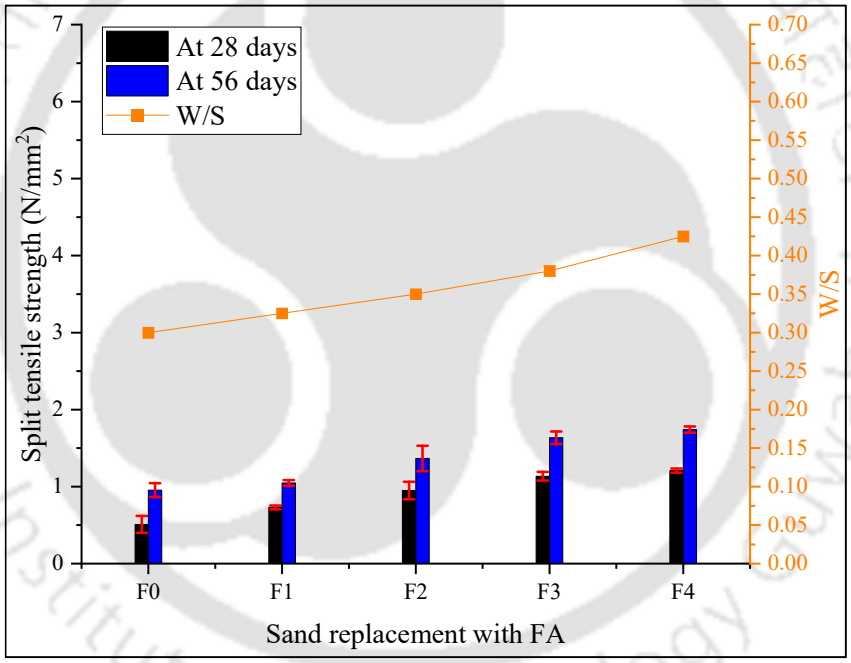

Figure 5.14: (A) Combined effect of W/S and FA level on the split tensile strength of WFC2 mixes.

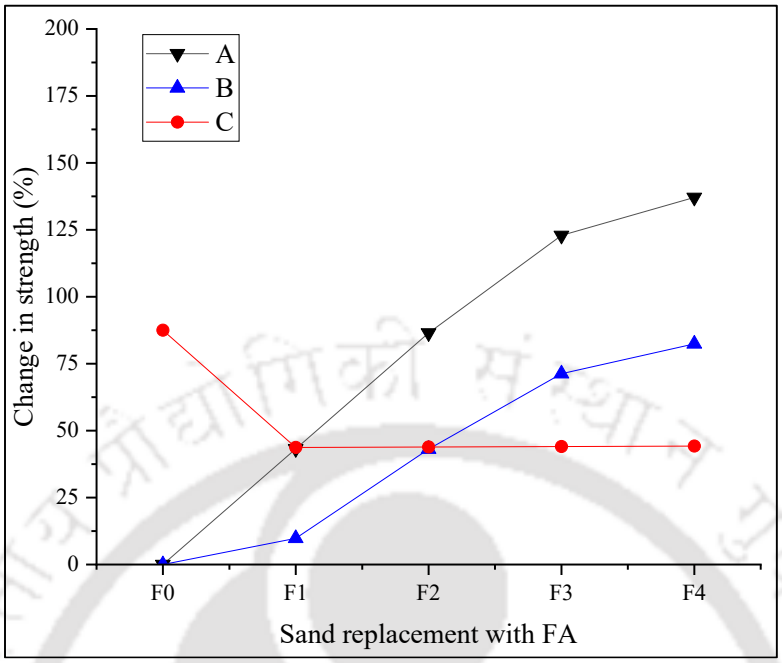

Figure 5.14: (B) Comparative analysis between split tensile strength of the proposed WFC2 mixes (with variation in FA level) at different testing ages.

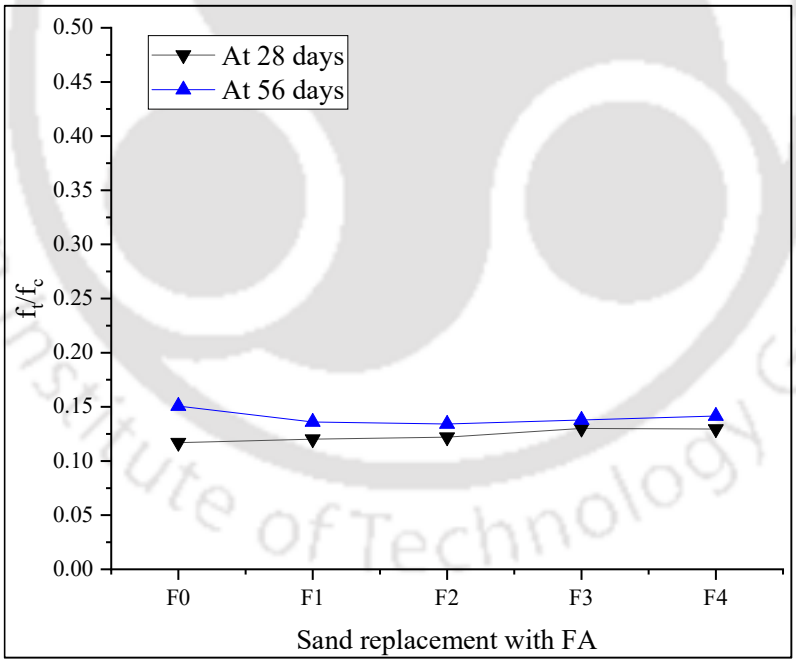

Figure 5.14: (C) Combined effect of W/S and FA level on the f_t/f_c of WFC2 mixes.

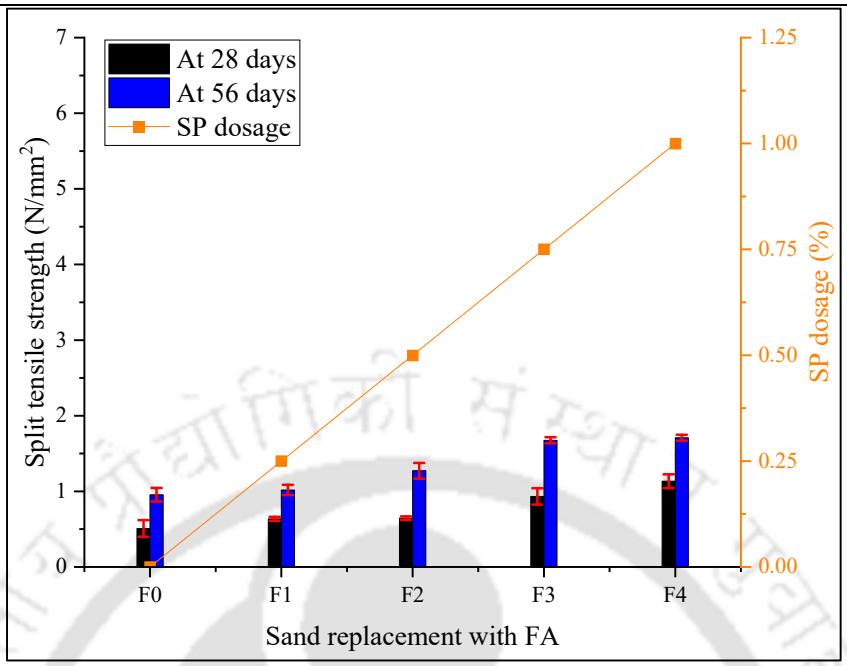

Figure 5.14: (D) Combined effect of SP dosage and FA level on the split tensile strength of SFC2 mixes.

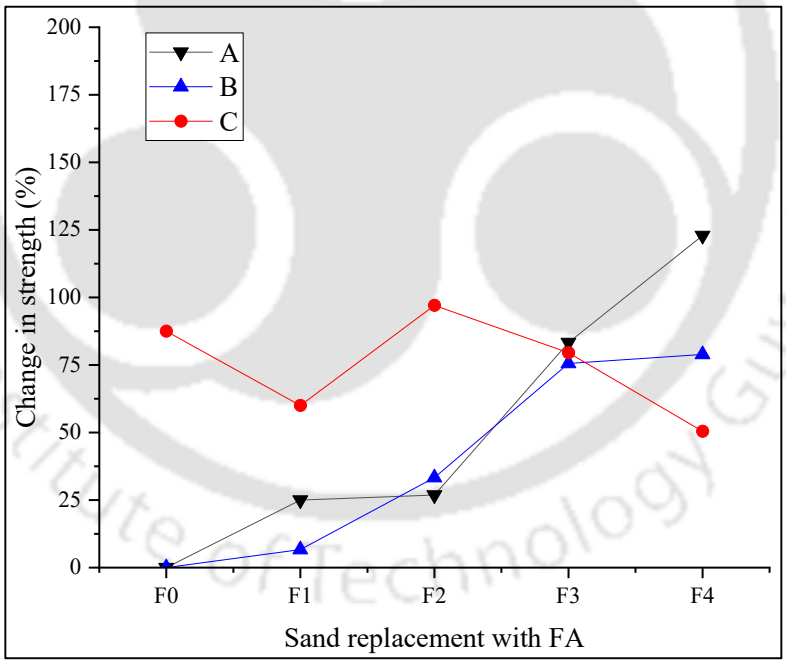

Figure 5.14: (E) Comparative analysis between split tensile strength of the proposed SFC2 mixes (with variation in FA level) at different testing ages.

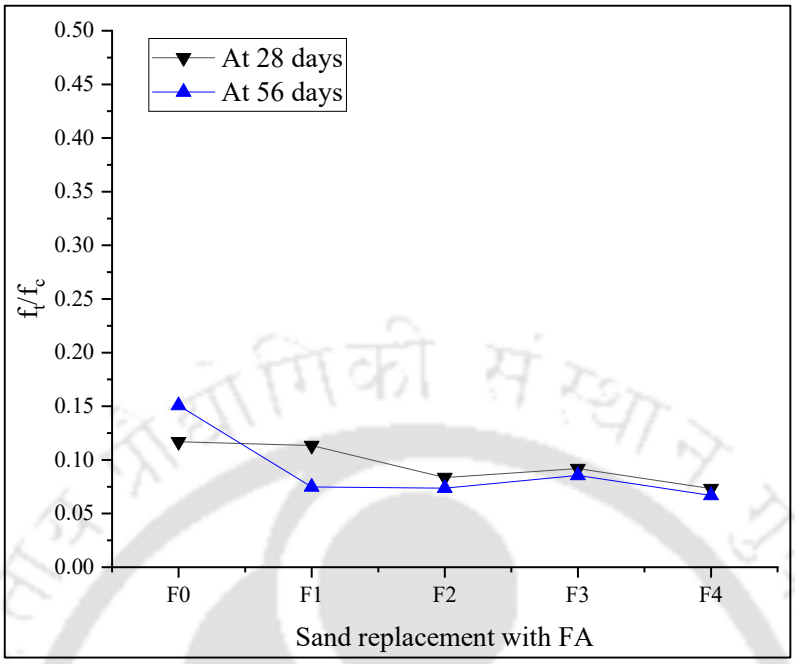

Figure 5.14: (F) Combined effect of SP dosage and FA level on the f_t/f_c of SFC2 mixes.

Note: In figure 5.14B, 5.14E description of adopted various legends is provided below.
A: Comparison of all the mixes with FC2F0P0 at 28 days, B: Comparison of all the mixes with FC2F0P0 at 56 days, C: Comparison between 28 days and 56 days split tensile strength of all mixes.

Effect of PP fiber on split tensile strength of proposed FC mixes

The results of the split tensile strength of the FC mixes with varied levels of PP fiber along with the required W/S or SP dosage (derived from earlier studies resulting in mixes with desired stability and consistency) tested in accordance with ASTM C496-17 are shown in figures 5.15A, 5.15D. Further, various comparative analyses such as A: comparative analysis of 28 days strength of all the FC mixes with the FC2F0P0 mix at 28 days, B: comparative analysis of 56 days strength of all the FC mixes with the FC2F0P0 mix at 56 days, C: comparative analysis of 56 days strength of all the FC mixes with the corresponding 28 days strength are shown in figures 5.15B, 5.15E. Furthermore, the analysis of f_t/f_c for the above-mentioned mixes is presented in figures 5.15C, 5.15F. Experimental outcomes show that the mix with 0% PP fiber content (FC2F0P0) exhibits the lowest split tensile strength of 0.5 N/mm^2 while the mixes with incremental PP fiber content exhibits an inverted 'U' trend for both 28 days and 56 days split tensile strength, with a maximum for SFC2F0P2 mix. Close observations shows that mixes SFC2F0P1

and SFC2F0P2 are exhibiting up to 48% and 116%, and 91% and 178% enhancement in split tensile strength at 28 days and 56 days respectively when compared to SFC2F0P0 mix. The above increase in strength due to PP fiber addition (as observed in scatter B of figures 5.15B, 5.15E) can be attributed to the enhanced fiber-matrix interaction due to the usage of SP as established in the literature [Raupit et al., 2017, Huang, 2001]. Additionally, the increase in surface area through increase in PP fiber content (up to 0.4%), exhibits a positive influence on the fiber-matrix interactions. Hence, the initial strength gains due to PP fiber addition as observed in scatter A of figures 5.15B, 5.15E respectively, can be attributed to the improvement in microstructure of fiber-matrix zone resulting from enhanced packing due to usage of SP [Huang, 2001]. Additionally, the usage of SP instead of additional W/S, further increases the split tensile strength in an inverted 'U' trend (by comparing scatter A of figures 5.15B and 5.15E) through enhancement in the microstructure of FC. This can be attributed to the reduction of additional pores due to reduced water content and enhanced packing due to the steric hindrance effect by SP [Dhasindrakrishna et al., 2021, Wang et al., 2021].

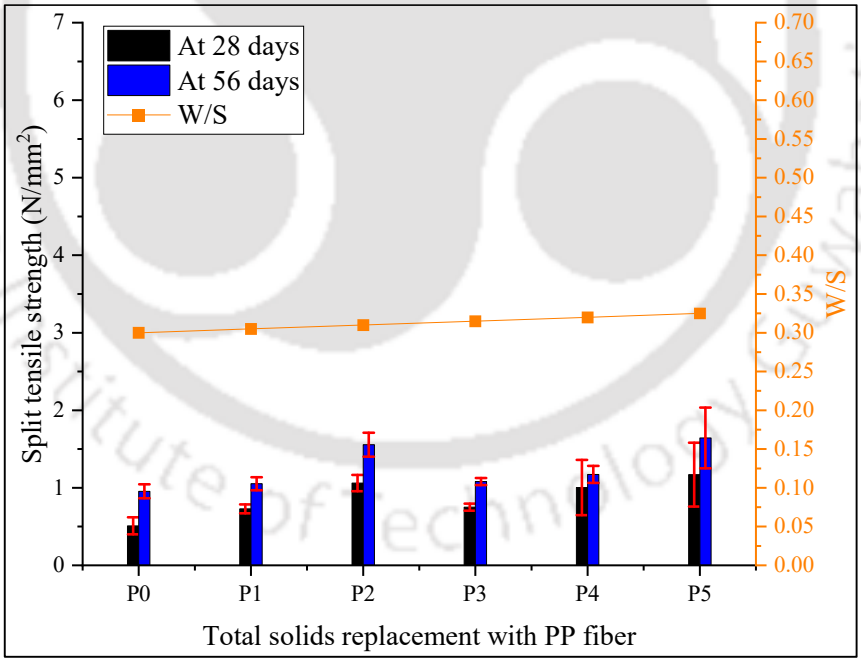

Figure 5.15: (A) Combined effect of W/S and PP fiber level on the split tensile strength of WFC2 mixes.

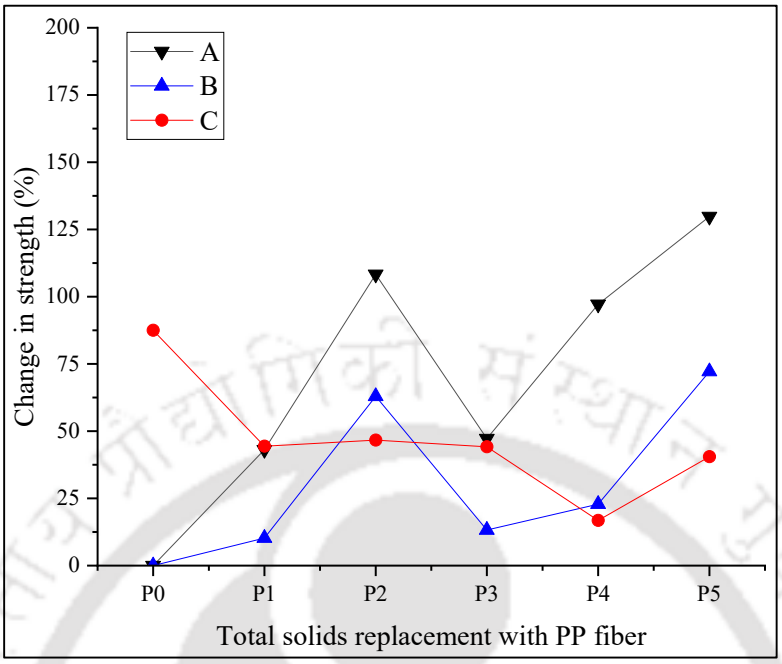

Figure 5.15: (B) Comparative analysis between split tensile strength of the proposed WFC2 mixes (with variation in PP fiber level) at different testing ages.

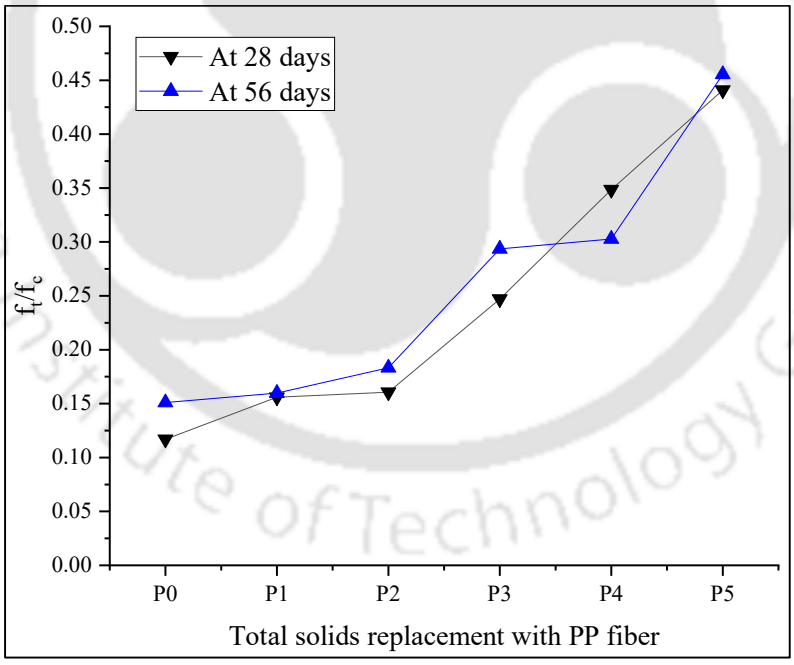

Figure 5.15: (C) Combined effect of W/S and PP fiber level on the f_t/f_c of WFC2 mixes.

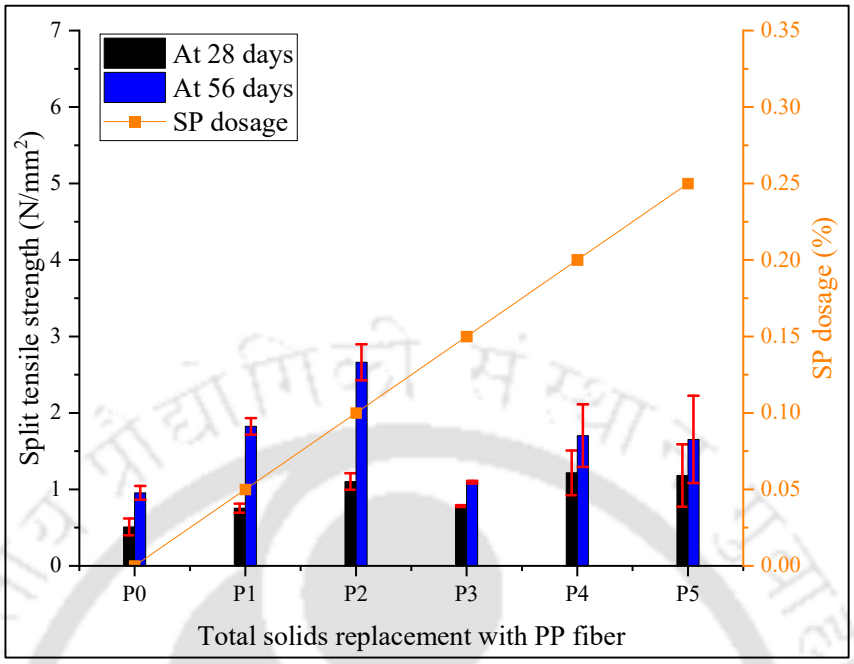

Figure 5.15: (D) Combined effect of SP dosage and PP fiber level on the split tensile strength of SFC2 mixes.

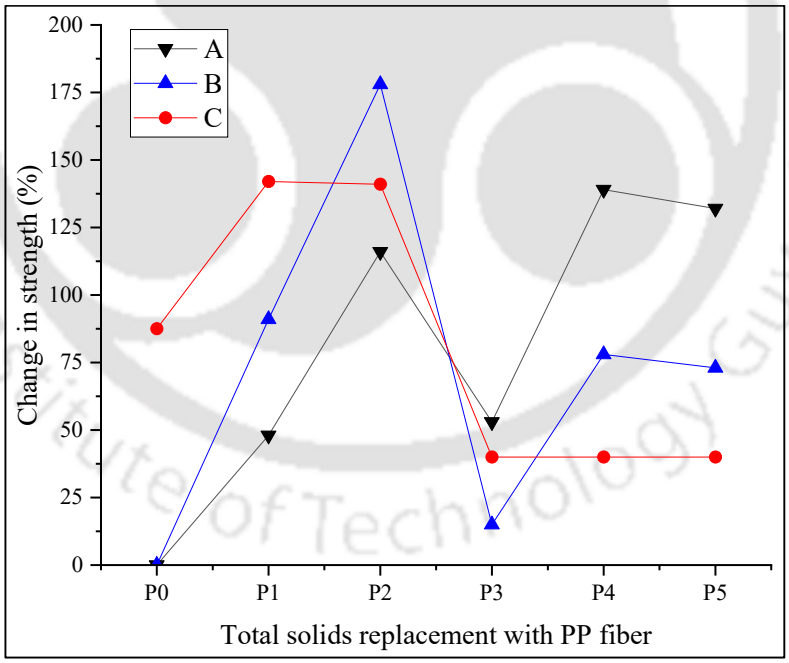

Figure 5.15: (E) Comparative analysis between split tensile strength of the proposed SFC2 mixes (with variation in PP fiber level) at different testing ages.

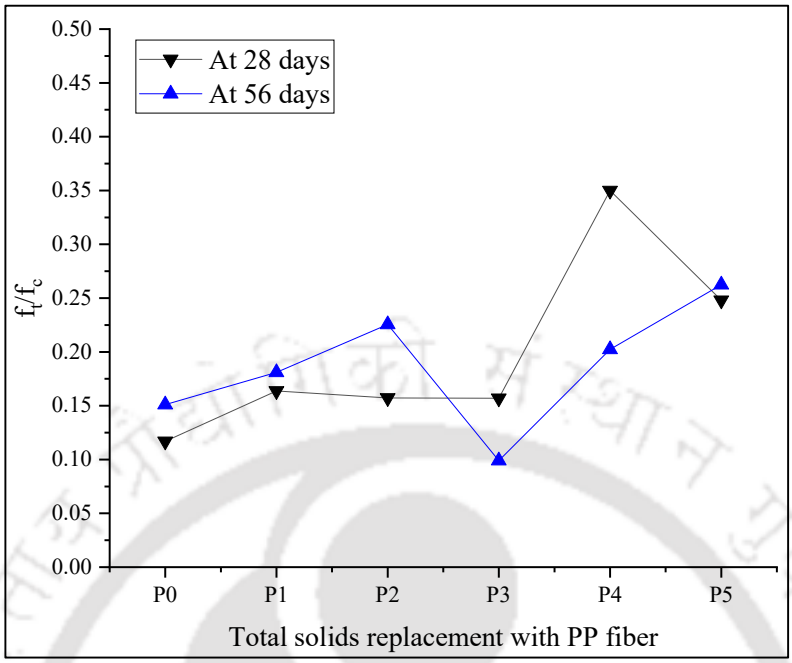

Figure 5.15: (F) Combined effect of SP dosage and PP fiber level on the f_t/f_c of SFC2 mixes.

Note: In figure 5.15B, 5.15E description of adopted various legends is provided below.
A: Comparison of all the mixes with FC2F0P0 at 28 days, B: Comparison of all the mixes with FC2F0P0 at 56 days, C: Comparison between 28 days and 56 days split tensile strength of all mixes.

Further increase in the PP fiber content shows a negative influence on split tensile strength of FC. This can be attributed to the substantial reduction in the amount of matrix owing to the low density of PP fiber. Adding to above, at higher dosage of PP fiber, close vicinity of individual PP fibers leads to increase in amount of transition zone (i.e. weaker zone) between PP fiber and matrix and ultimately affects the strength of FC (figure A.1) [Raupit et al., 2017]. However, a slightly lower split tensile strength of SFC2F0P3 is observed at the age of 28 days and 56 days as an exception to the above-mentioned trend. Another noteworthy observation is that the difference between 28 days and 56 days split tensile strength is very much less for the mixes with high PP fiber content (SFC2F0P3, SFC2F0P4, SFC2F0P5), when compared to that of mixes with lower PP fiber content (0% to 0.4%). Here it is to be noted that, in the proposed FC mixes discussed in this section, cement is the only binder present and hence the hydration reaction of cement can be considered as one of the major contributors for the strength gain from 28 days to 56 days. Further, the mixes SFC2F0P1 and SFC2F0P2 are exhibiting higher strength gain beyond 28 days. This can be attributed to the fiber-matrix interactions which enhance the

split tensile strength of FC through enhancement in ductility of FC, which is an intrinsic property of fiber reinforced concrete [Raupit et al., 2017]. Furthermore, the SFC2F0P2 mix is exhibiting the highest split tensile strength of 2.7 N/mm^2, the strength gain beyond 28 days is slightly lower than expected. This can be attributed to the increase in the surface area of PP fiber and subsequent reduction in the binder content (when compared to SFC2F0P1) affecting the bonding between PP fiber and matrix [Huang, 2001, Mydin and Soleimanzadeh, 2012, Raupit et al., 2017, Khan et al., 2022].

Moreover, in the case of SFC2F0P4 and SFC2F0P5 mixes increase in transition zone between PP fiber and matrix due to increase in PP fiber dosage, has major effect on 28 days strength. Further, the close vicinity of PP fibers and reduced amount of matrix for binding results in lower split tensile strength and lowest strength gain from 28 days to 56 days (figure A.1) [Noushini et al., 2013, 2014, Zhang et al., 2019, Xu et al., 2020].

In figures 5.15C and 5.15F, the f_t/f_c analysis for the aforementioned mixes is presented. Obviously, as expected, the mixes without PP fiber (FC2F0P0) exhibits the lowest f_t/f_c of 0.15 while the mixes with incremental PP fiber content exhibits an incremental trend in the f_t/f_c at 28 days. Further, an increment in f_t/f_c of the SFC2F0P0, SFC2F0P1 and SFC2F0P2 mixes is observed at 56 days. This increment in f_t/f_c with increase in PP fiber content, reveals the enhancement of ductility behaviour of the FC which can be attributed to the enhanced fiber-matrix interactions due to the further hydration of unreacted cement from 28 days to 56 days [Mydin and Soleimanzadeh, 2012, Raupit et al., 2017]. This is also evident by comparing the split tensile test images of the FC mixes with and without PP fiber as presented in figures 5.16A, 5.16B. The prolonged load bearing capacity exhibited by the mixes with PP fiber also reveals the enhanced ductility behaviour of fiber reinforced FC. Furthermore, the SFC2F0P3, SFC2F0P4 and SFC2F0P5 mixes exhibit a reduction in f_t/f_c at 56 days of FC with increase in PP fiber content. The above trend can be ascribed to reduction in matrix content for sufficient interaction between fibre and matrix which subsequently resulted in reduction of both split tensile strength and compressive strength [Mydin and Soleimanzadeh, 2012, Noushini et al., 2013, 2014, Raupit et al., 2017, Zhang et al., 2019, Xu et al., 2020].

Figure 5.16: (A) Post failure behaviour of FC2 mixes without PP fiber during split tensile strength test.

Figure 5.16: (B) Post failure behaviour of FC2 mixes with PP fiber during split tensile strength test.

Combined effect of FA and PP fiber on split tensile strength of proposed FC mixes

From the above results, it is evident that both FA and PP fiber are enhancing the split tensile strength of FC individually. Hence as a next step, the combination mixes with the above utilized variations in FA and PP fiber are considered for further enhancement in split tensile strength of FC for its desired application in retaining walls. The split tensile strength at 28 and 56 days, along with various comparative analyses (detailed in previous sections), of the suggested FC mixes are thus shown in figures 5.17A to 5.17N. In line with the earlier results, the combination mixes with both FA and PP fiber have shown an increase in split tensile strength of SFC2 by 573% and 512% with a maximum of 3.4 N/mm^2 and 5.8 N/mm^2 for the SFC2F4P2 mix at the age of 28 days and 56 days respectively (figures 5.17A, 5.17C). The increase in packing efficiency due to the combined effect of finer FA particles (<75 μm), enhanced ductility due to the thin PP fiber (22 μm) and enhanced fiber-matrix interactions due to the steric hindrance effect by PCE based SP can be attributed as major contributors for this enhancement in 28 days strength [Huang, 2001, Raupit et al., 2017, Dhasindrakrishna et al., 2021, Wang et al., 2021]. Here it is to be noted that, for any given FA level, the increment in PP fiber level is exhibiting a similar inverted 'U' trend. Further, the combination mixes are exhibiting

enhancement in split tensile strength up to 0.4% replacement of total solids with PP fiber irrespective of the FA level. The increment of PP fiber level from 0.4% to 0.6% is exhibiting a sudden drop in the split tensile strength of FC irrespective of FA level at 28 days. Moreover, though there is significant strength gain from 28 days to 56 days, the P3 mixes are significantly lower in split tensile strength. This peculiar behaviour of FC can be attributed to the close vicinity of PP fibers leading to increase in weaker transition zones between fibre and matrix along with poor bonding due to reduced matrix content as discussed in earlier section (figure A.1) [Mydin and Soleimanzadeh, 2012, Noushini et al., 2013, 2014, Raupit et al., 2017, Zhang et al., 2019, Xu et al., 2020]. In line with observations, further replacement of total solids with PP fiber up to 1% results in a systematic and significant reduction in split tensile strength of such FC mixes.

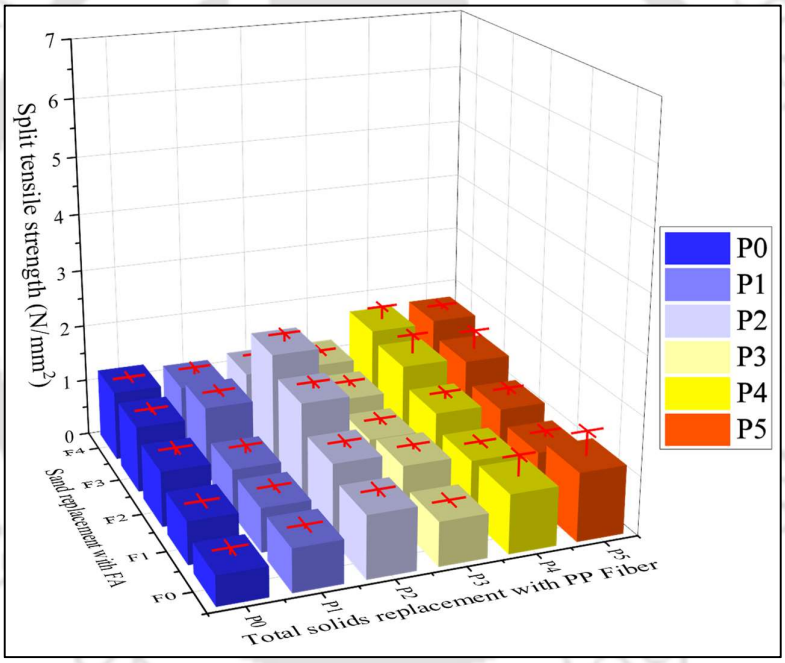

Figure 5.17: (A) Effect of variation in W/S, FA level and PP fiber level on the split tensile strength of WFC2 mixes at 28 days.

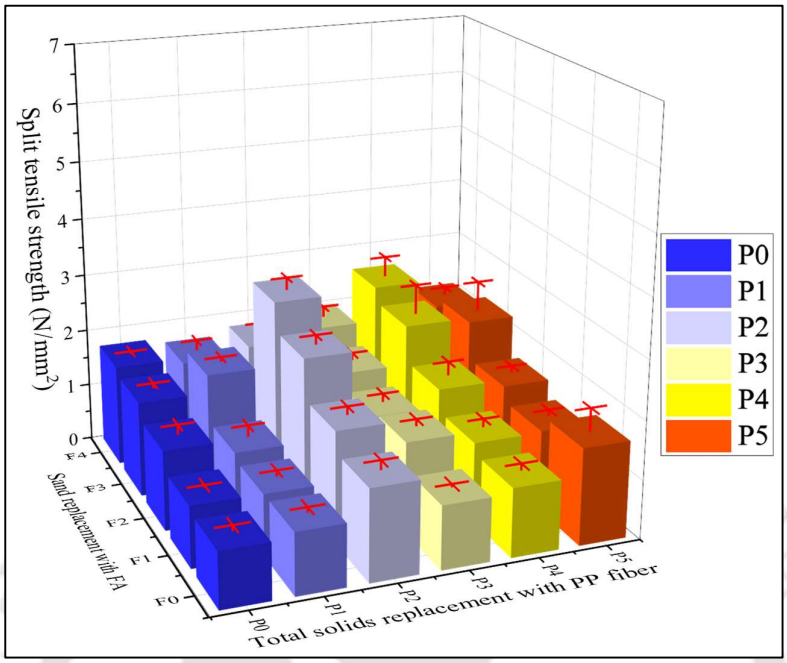

Figure 5.17: (B) Effect of variation in W/S, FA level and PP fiber level on the split tensile strength of WFC2 mixes at 56 days.

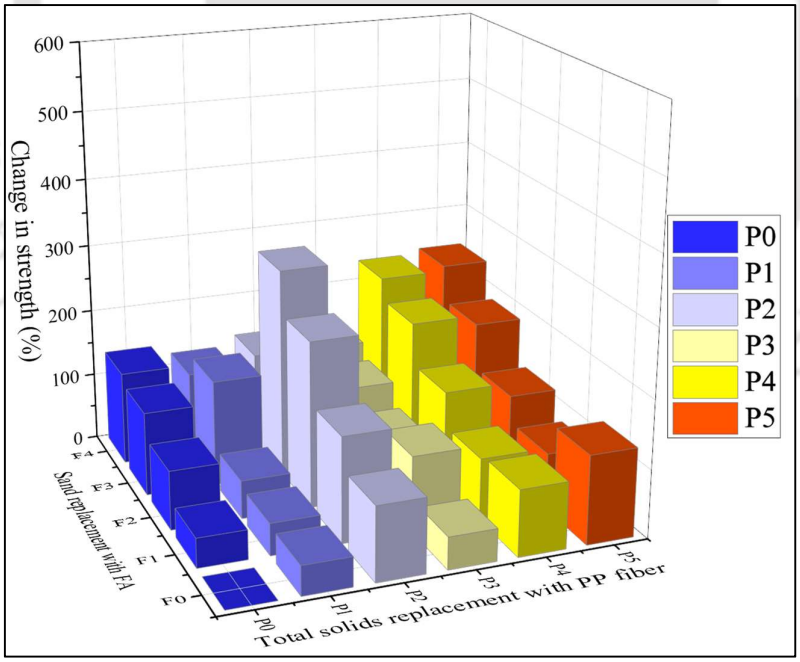

Figure 5.17: (C) Comparing the WFC2F0P0 mix and the WFC2 mixes with variations in W/S, FA level, and PP fibre level in terms of split tensile strength at 28 days.

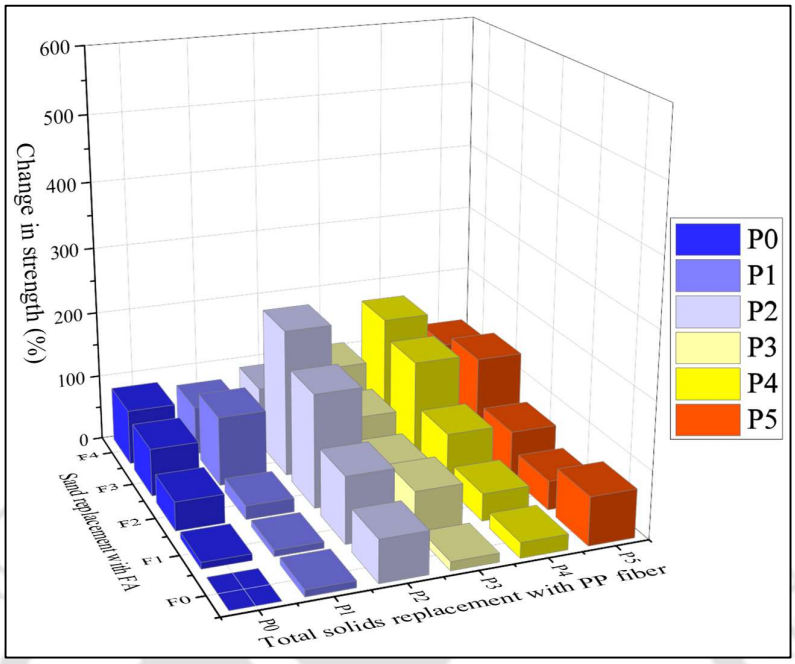

Figure 5.17: (D) Comparing the WFC2F0P0 mix and the WFC2 mixes with variations in W/S, FA level, and PP fibre level in terms of split tensile strength at 56 days.

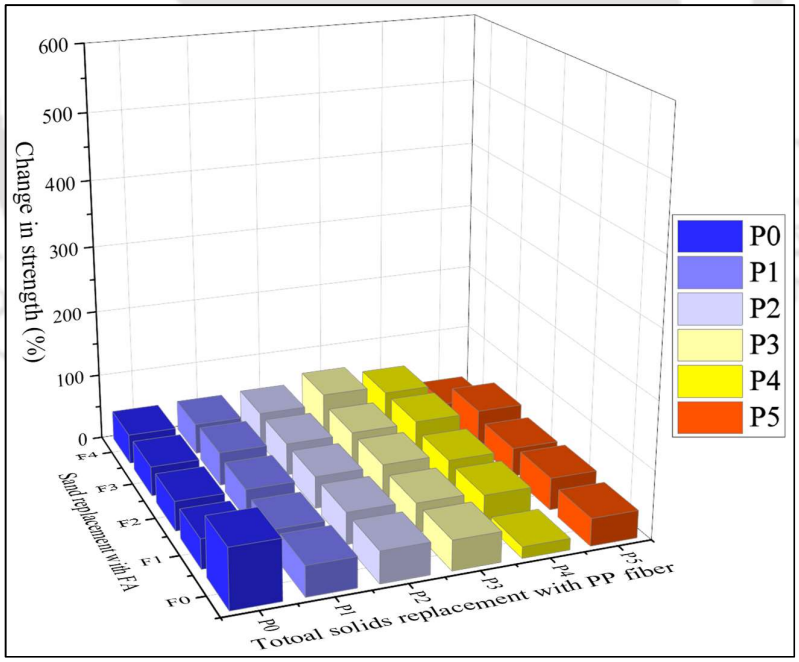

Figure 5.17: (E) Comparing the 28 days and 56 days split tensile strength of the WFC2 mixes with variation in W/S, FA level and PP fiber level.

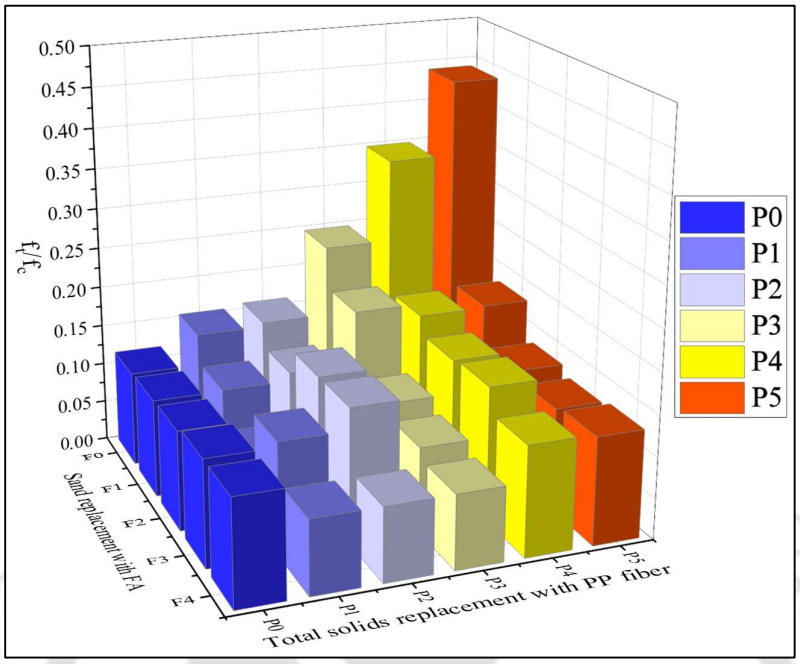

Figure 5.17: (F) Combined effect of W/S, FA level and PP fiber level on the f_t/f_c of WFC2 mixes at 28 days.

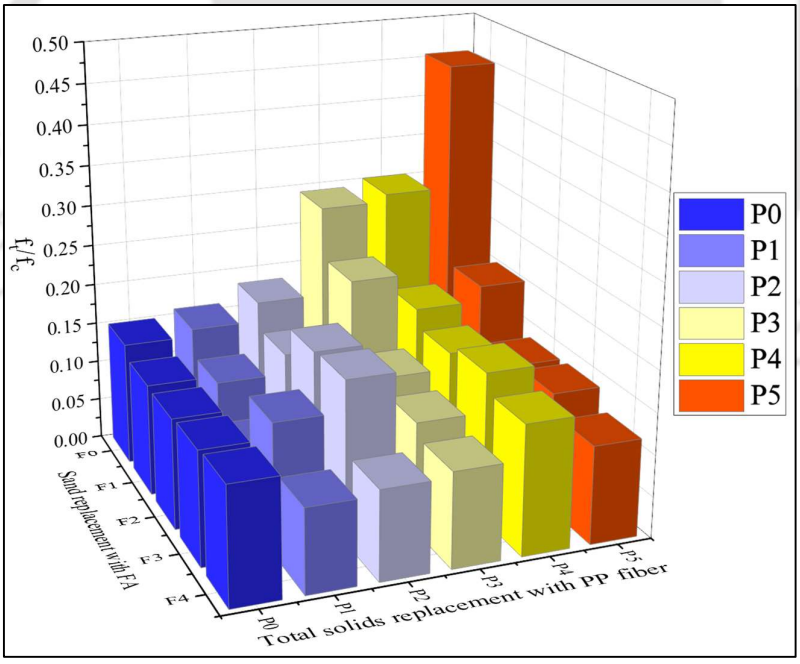

Figure 5.17: (G) Combined effect of W/S, FA level and PP fiber level on the f_t/f_c of WFC2 mixes at 56 days.

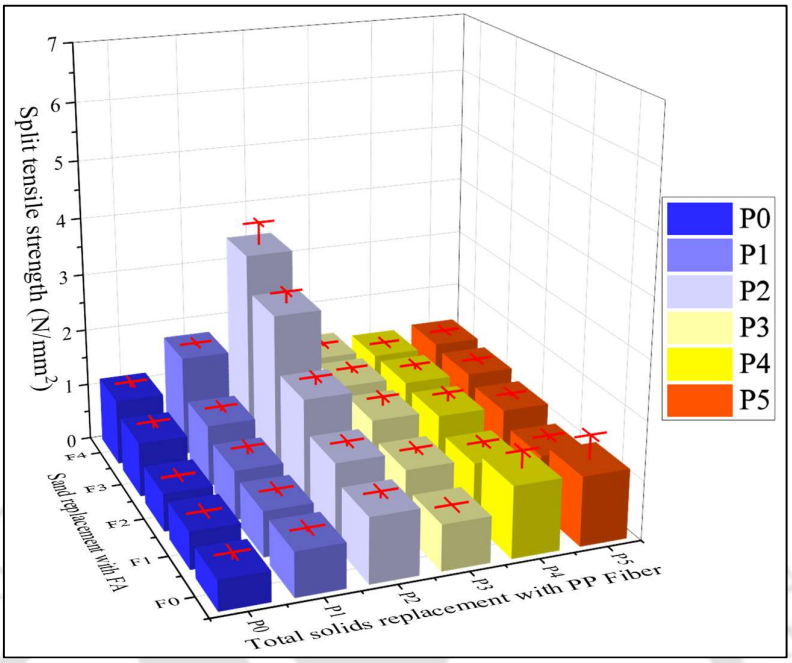

Figure 5.17: (H) Effect of variation in SP dosage, FA level and PP fiber level on the split tensile strength of SFC2 mixes at 28 days.

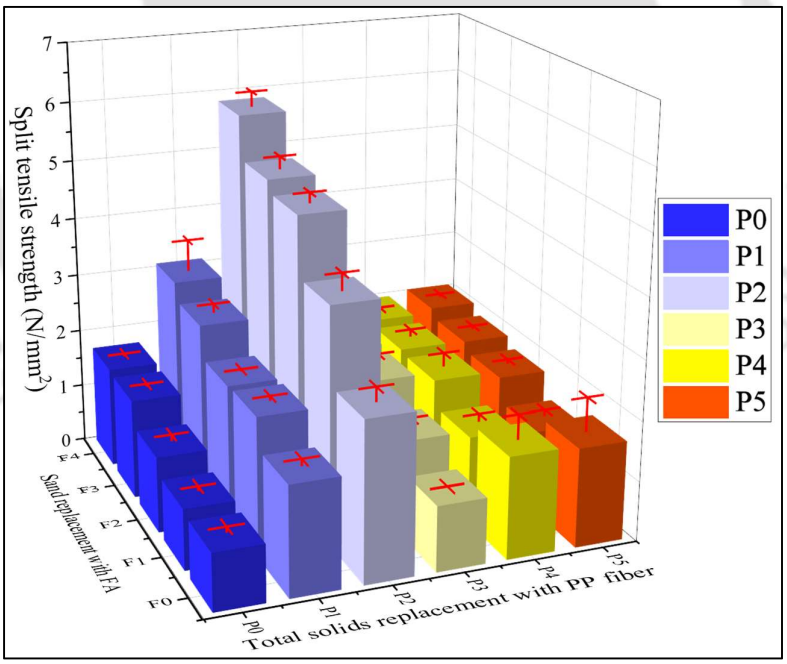

Figure 5.17: (I) Effect of variation in SP dosage, FA level and PP fiber level on the split tensile strength of SFC2 mixes at 56 days.

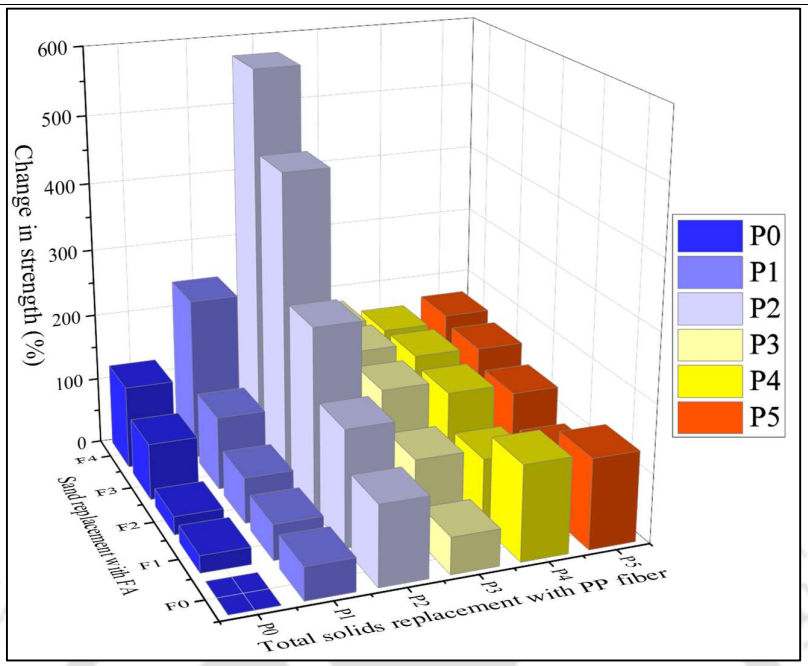

Figure 5.17: (J) Comparing the SFC2F0P0 mix and the SFC2 mixes with variations in SP dosage, FA level, and PP fibre level in terms of split tensile strength at 28 days.

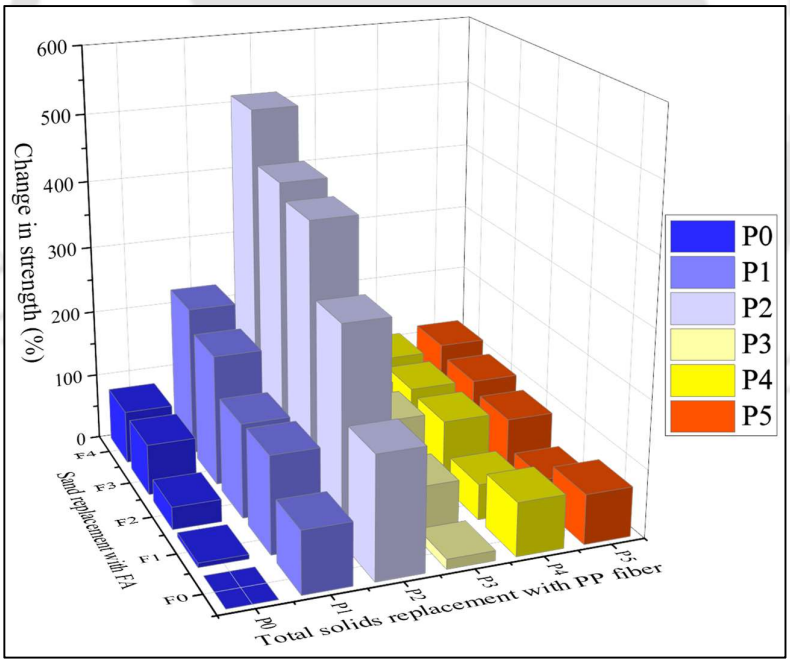

Figure 5.17: (K) Comparing the SFC2F0P0 mix and the SFC2 mixes with variations in SP dosage, FA level, and PP fibre level in terms of split tensile strength at 56 days.

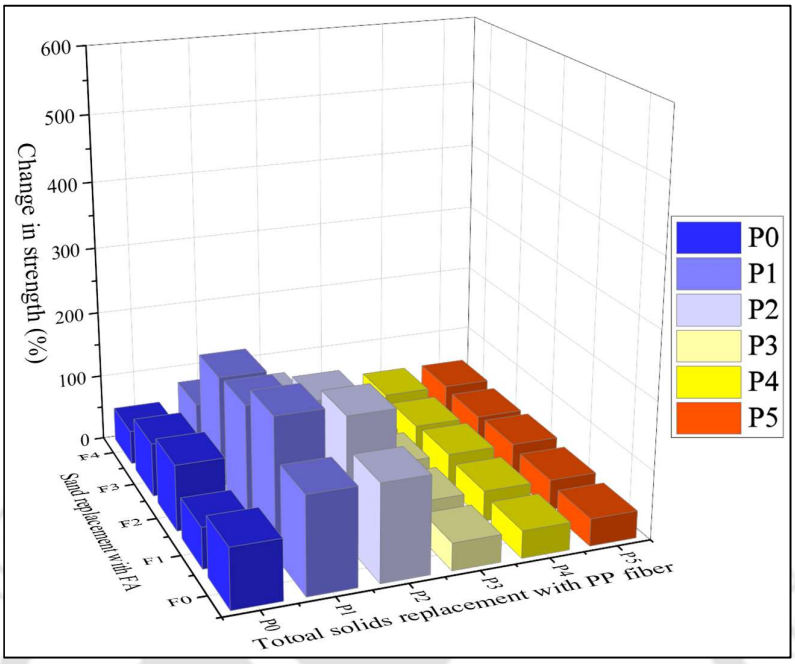

Figure 5.17: (L) Comparing the 28 days and 56 days split tensile strength of the SFC2 mixes with variation in SP dosage, FA level and PP fiber level.

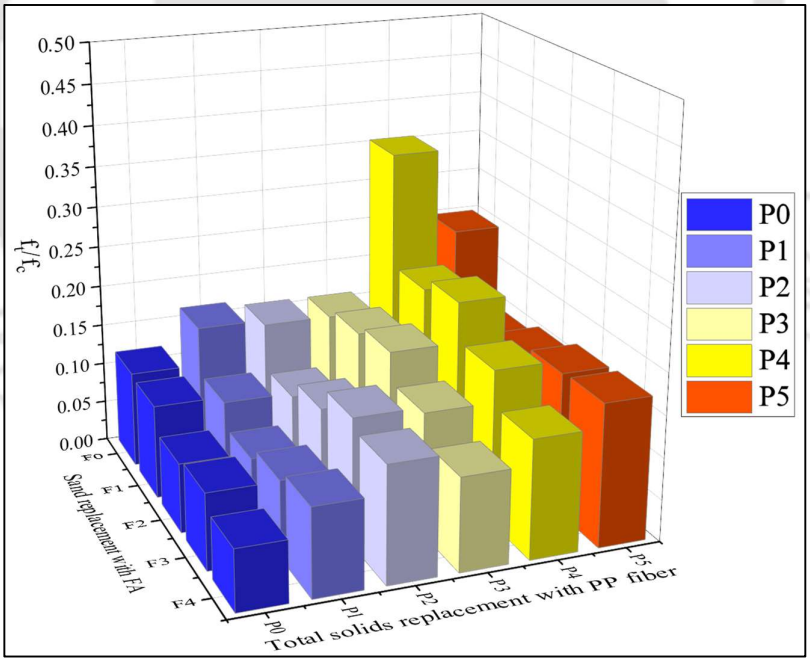

Figure 5.17: (M) Combined effect of SP dosage, FA level and PP fiber level on the f_t/f_c of SFC2 mixes at 28 days.

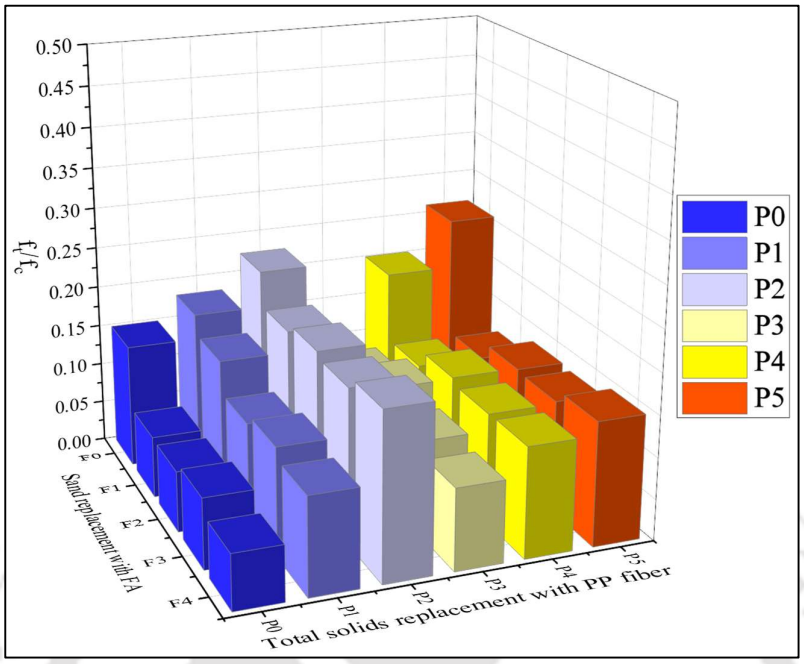

Figure 5.17: (N) Combined effect of SP dosage, FA level and PP fiber level on the f_t/f_c of SFC2 mixes at 56 days

Further, for any given PP fiber dosage, increase in FA level results in systematic increase in split tensile strength. However, beyond 0.6% dosage of PP fiber, the above-mentioned variation in split tensile strength with increase in FA level is decreasing. Particularly in the case of P5 mixes, viz. SFC2F2P5, SFC2F3P5 and SFC2F4P5, the aforementioned variations are tending towards negligibility. This reduction in strength gain of P5 mix can be attributed to the increase in the total surface of PP fiber due to higher PP fiber content and the reduced matrix content due to low density of PP fiber (figure A.1) [Mydin and Soleimanzadeh, 2012, Noushini et al., 2013, 2014, Raupit et al., 2017, Zhang et al., 2019, Xu et al., 2020]. Here it is to be noted that, though higher PP fiber content is reducing the split tensile strength, but in mixes with 100% of sand replaced with FA along with higher dosage of PP fiber (0.8 to 1%), significant enhancement of 107% and 115% in split tensile strength is noted for FC mixes SFC2F4P4, SFC2F4P5 respectively when compared to that of SFC2F0P0 mix. This can be attributed to significant increase in paste content due to addition of FA and subsequent increase in binder property and bonding of paste and PP fiber [Pan et al., 2007, Mydin and Soleimanzadeh, 2012, Noushini et al., 2013, 2014, Ganesan et al., 2015, Vishavkarma and Harish, 2024]. However, the above enhancement in strength is relatively lower when compared to combination mixes with lesser amount of PP fiber (less than 0.6%).

Further, the f_t/f_c of the combination mixes are presented in figures 5.17F, 5.17G, 5.17M, 5.17N. The close observation of these results, indicate a systematic and significant decrease in f_t/f_c with increase in FA level (0% to 100%) at 28 days for mixes without PP fiber. Whereas, for the mixes with PP fiber up to 0.4%, with increment in FA level a 'U' trend in f_t/f_c is observed which can be attributed to the enhanced fiber-matrix interactions with increase in packing efficiency [Huang, 2001, Raupit et al., 2017]. Further, at higher PP fiber levels up to 1%, with increase in FA level the f_t/f_c is mostly reducing at 28 days. On the other hand, at 56 days, with the increment in PP fiber content up to 0.4%, for all the FA levels, a systematic and significant increase in the f_t/f_c is observed. Further, the variation in f_t/f_c is found to be minimum with variation in FA level for the given PP fiber level. This reveals us that the split tensile strength is mostly improved by PP fiber at 56 days through increase in the ductility behaviour of FC due to enhancement in fiber-matrix interactions. Further, at higher PP fiber levels, a sudden drop in the f_t/f_c is observed, which can be attributed to the reduction in matrix and poor fibre matrix interaction [Huang, 2001, Mydin and Soleimanzadeh, 2012, Noushini et al., 2013, 2014, Raupit et al., 2017, Zhang et al., 2019, Xu et al., 2020, Khan et al., 2022]. From these results we can conclude that in combination mixes with PP fiber up to 0.4%, the enhancement of ductility due to PP fiber addition is more predominant when compared to the effect of the enhancement of brittle nature in FC by FA addition. As a significant outcome, among the satisfactory mixes in compressive strength section, the mixes SFC2F1P2, SFC2F2P2, SFC2F3P2 and SFC2F4P2 are exhibiting the highest split tensile strength along with the most significant enhancement in the f_t/f_c, and hence these mixes are chosen for further studies.

5.3.2.3 FLEXURAL STRENGTH OF PROPOSED FC MIXES

The flexural strength of the proposed FC mixes is tested in accordance with ASTM C348-21 and the results are exhibited in figures 5.18 – 5.21. Furthermore, this section follows the same format as the compressive strength and split tensile strength section in discussing the flexural strength of the proposed FC mixes.

Effect of FA on flexural strength of proposed FC mixes

From the results (figures 5.18A, 5.18D) it is evident that the replacement of sand with FA is exhibiting a limited but a systematic enhancement in the flexural strength of SFC2

mixes resulting in maximum enhancement of 50% at the age of 28 days (figures 5.18B, 5.18E). At later age of 56 days this enhancement is significantly increasing up to 125% (figures 5.18B, 5.18E). Further, comparative analysis of the variation in flexural strength of various FC mixes from 28 to 56 days presents a significant enhancement with increase in FA content. This enhancement at later ages can be attributed to the matrix densification due to the pozzolanic reaction by FA as observed in the compressive strength and split tensile strength results [Pan et al., 2007, Ramamurthy et al., 2009, Ganesan et al., 2015, Feng et al., 2018, Vishavkarma and Harish, 2024]. However, the flexural strength/ compressive strength ratio (f_{mor}/f_c) of the proposed mixes is exhibiting a systematic decreasing trend from 0.18 to 0.08 and 0.27 to 0.15 at 28 days and 56 days respectively, with increase in FA level (figures 5.18C, 5.18F). This can be attributed to the reduced shear capacity between the FA particles and the paste phase when compared to that of sand-paste interaction as established in the literature [Jones and McCarthy, 2005a, Ramamurthy et al., 2009, Vishavkarma and Harish, 2024].

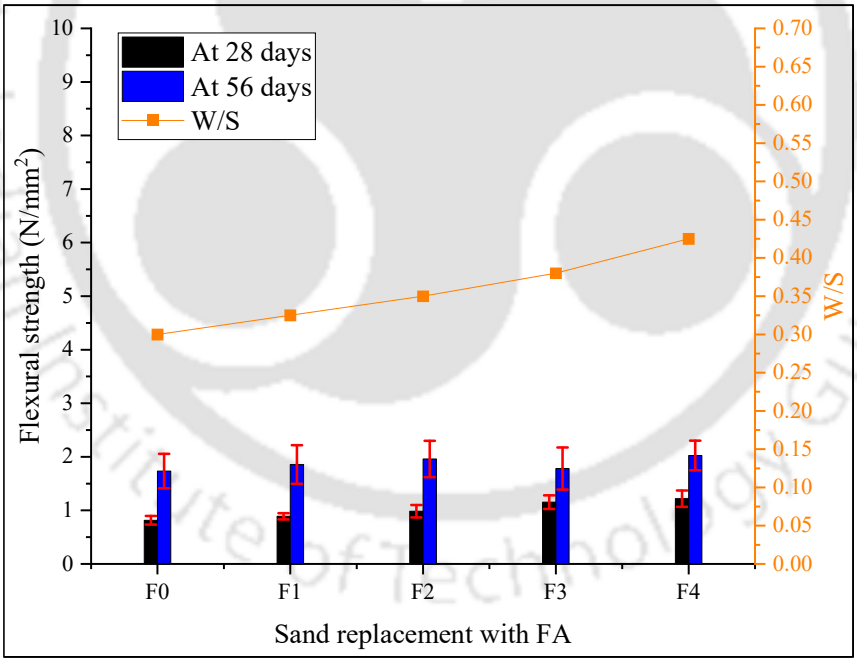

Figure 5.18: (A) Combined effect of W/S and FA level on the flexural strength of WFC2 mixes.

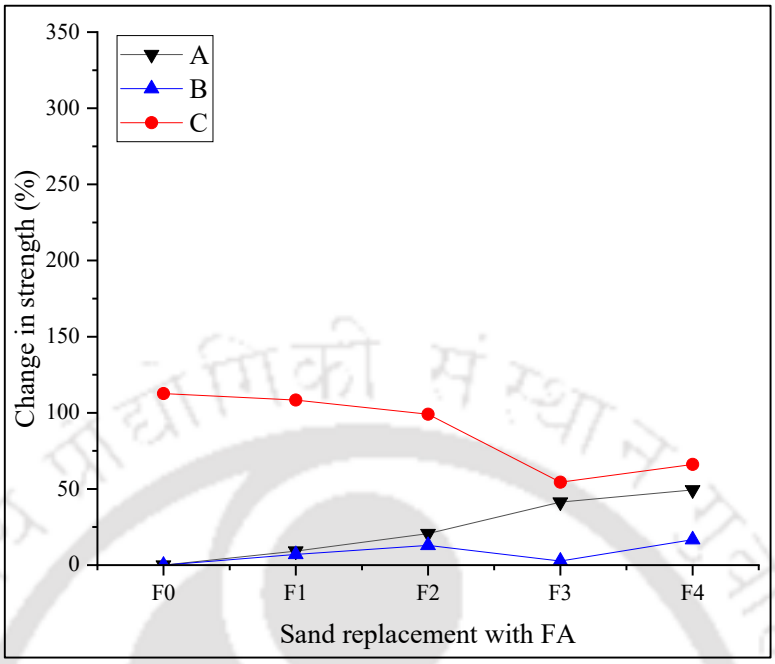

Figure 5.18: (B) Comparative analysis between flexural strength of the proposed WFC2 mixes (with variation in FA level) at different testing ages.

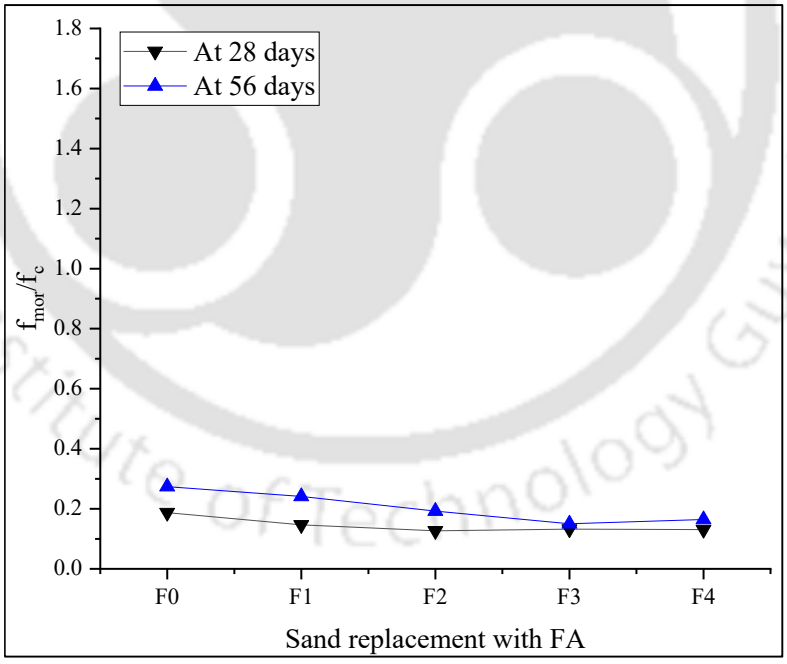

Figure 5.18: (C) Combined effect of W/S and FA level on the f_{mor}/f_c of WFC2 mixes.

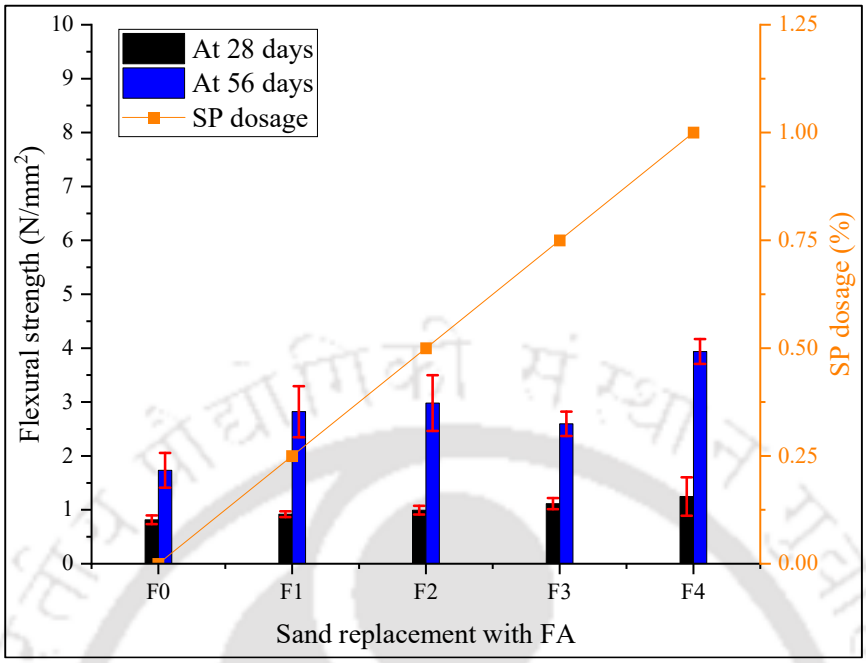

Figure 5.18: (D) Combined effect of SP dosage and FA level on the flexural strength of SFC2 mixes.

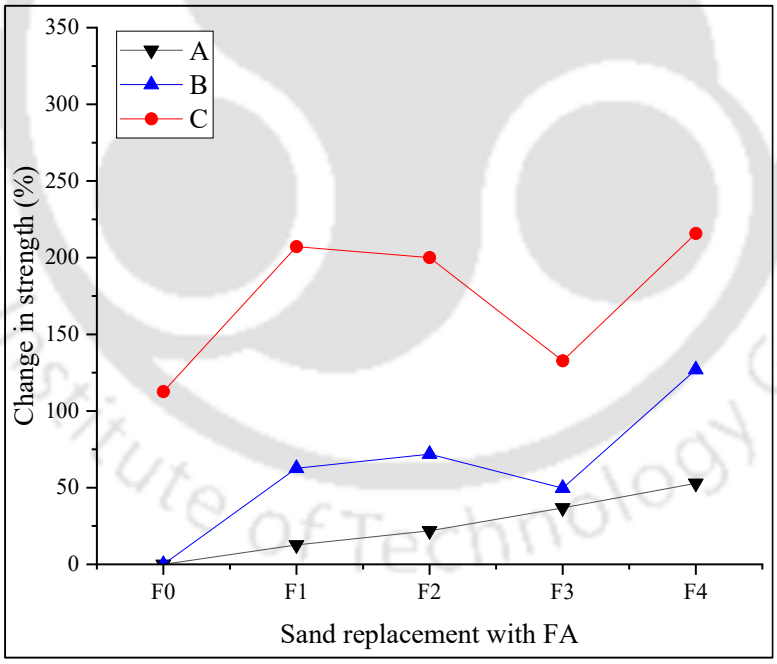

Figure 5.18: (E) Comparative analysis between flexural strength of the proposed SFC2 mixes (with variation in FA level) at different testing ages.

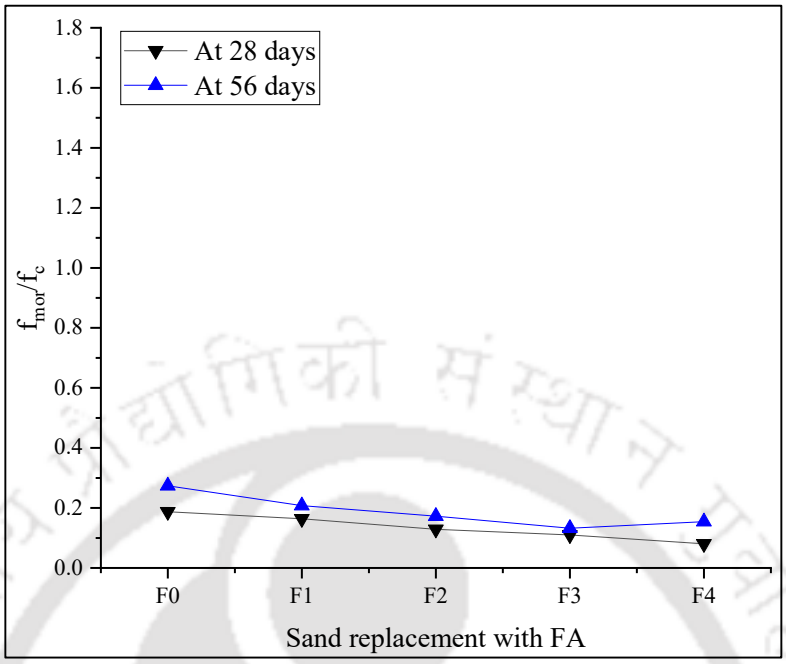

Figure 5.18: (F*) Combined effect of SP dosage and FA level on the f_{mor}/f_c of SFC2 mixes.*

Note: In figure 5.18B, 5.18E description of adopted various legends is provided below.

A: Comparison of all the mixes with FC2F0P0 at 28 days, B: Comparison of all the mixes with FC2F0P0 at 56 days, C: Comparison between 28 days and 56 days flexural strength of all mixes.

Effect of PP fiber on flexural strength of proposed FC mixes

From the results (figures 5.19A, 5.19D) it is evident that the replacement of total solids with PP fiber is exhibiting a systematic and significant enhancement in the flexural strength of SFC2 mixes resulting in maximum of 325% and 340% at the age of 28 days and 56 days respectively. These enhancements are presenting a linear trend with increase in PP fiber content at both the 28 days and 56days (scatters A, B of figures 5.19B, 5.19E). This can be attributed to the greater amount of PP fiber in the system leading to their greater participation in the enhancement of the modulus of rupture which is in line with the existing literature [Amran et al., 2020a, Mydin and Soleimanzadeh, 2012, Ahmad et al., 2022]. However, the comparative analysis of the flexural strength of FC at 56 days with respect to the corresponding 28 days strength (scatter C of figures 5.19B, 5.19E), presents a very minimal enhancement with increase in PP fiber content. The above minimum enhancement can be ascribed to the limited fiber-matrix interaction with increasing PP fiber content as discussed earlier in previous sections on compressive and split tensile strength [Mydin and Soleimanzadeh, 2012].

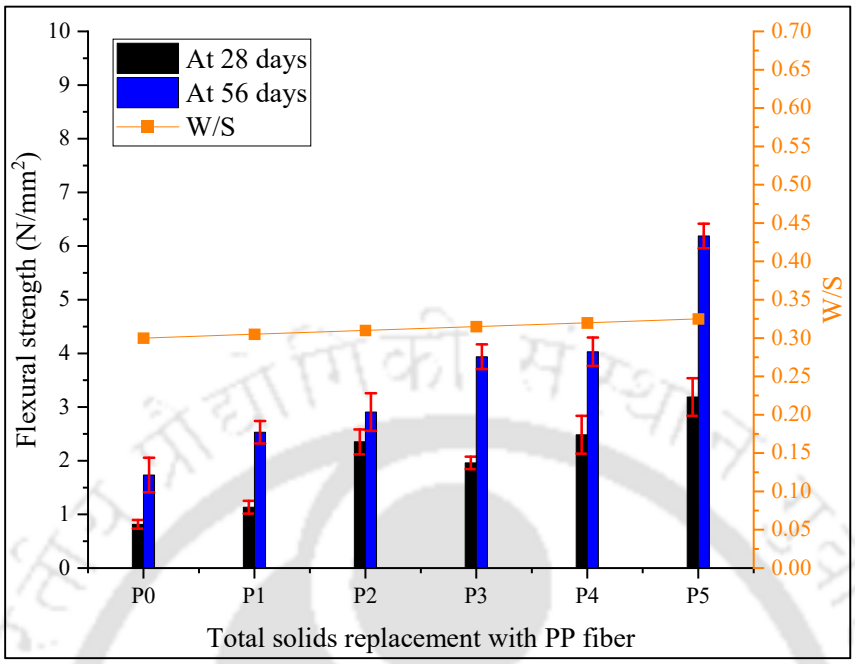

Figure 5.19: (A) Combined effect of W/S and PP fiber level on the flexural strength of WFC2 mixes.

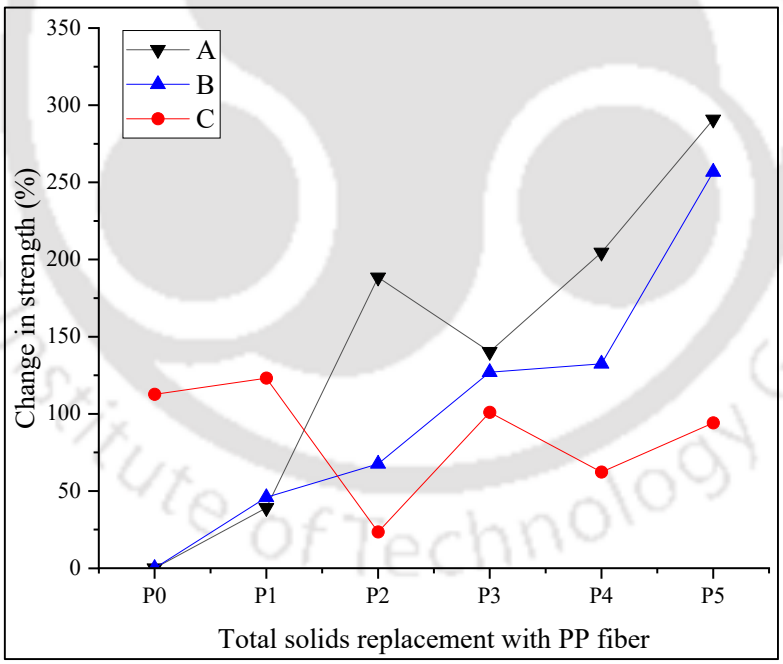

Figure 5.19: (B) Comparative analysis between flexural strength of the proposed WFC2 mixes (with variation in PP fiber level) at different testing ages.

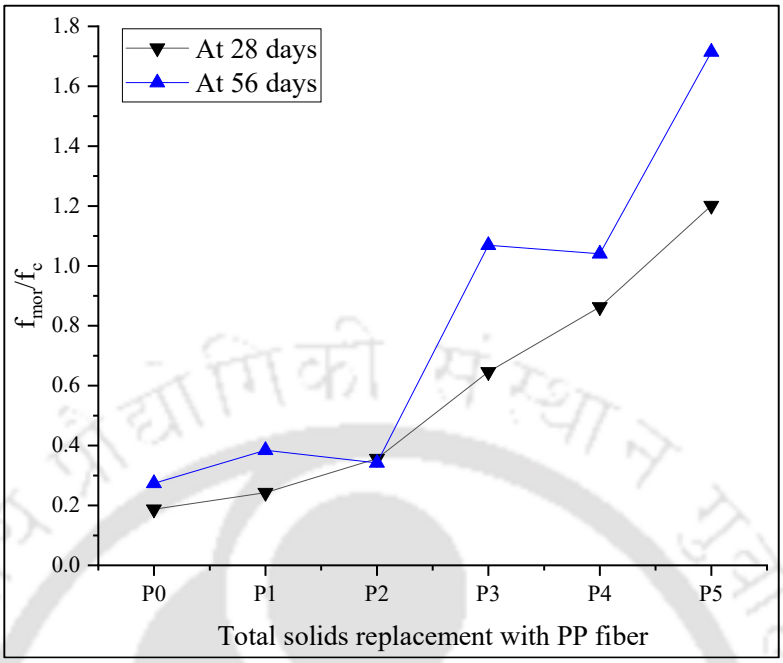

Figure 5.19: (C) Combined effect of W/S and PP fiber level on the f_{mor}/f_c of WFC2 mixes.

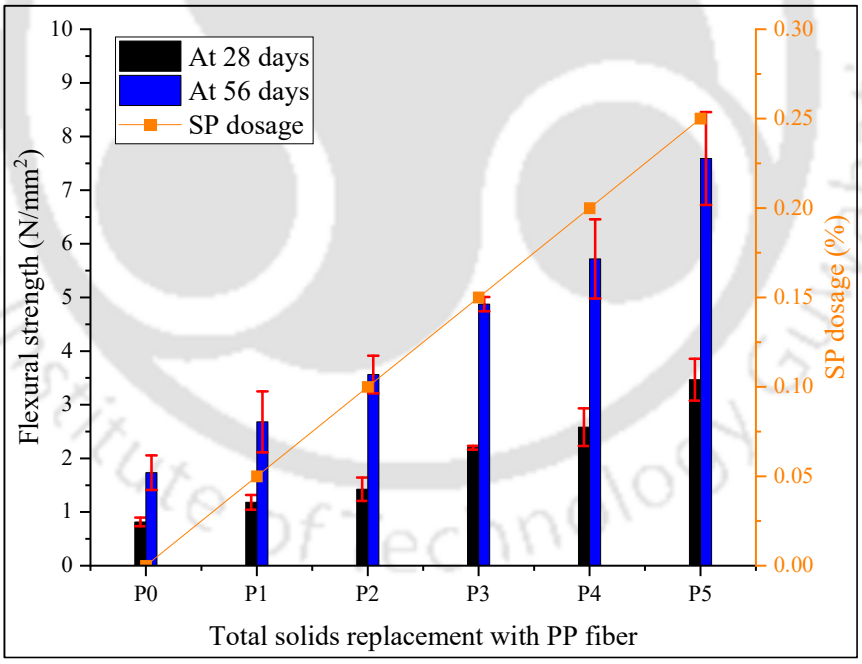

Figure 5.19: (D) Combined effect of SP dosage and PP fiber level on the flexural strength of SFC2 mixes.

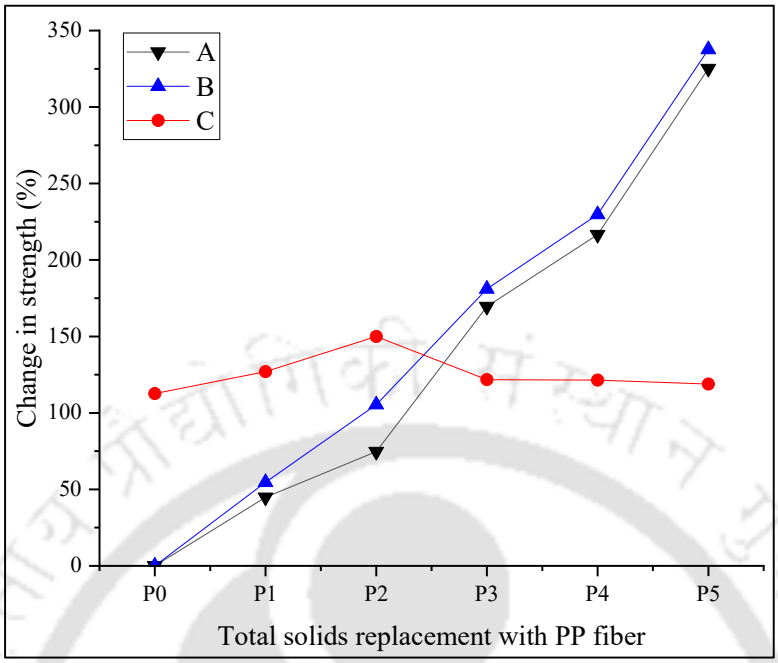

Figure 5.19: (E) Comparative analysis between flexural strength of the proposed SFC2 mixes (with variation in PP fiber level) at different testing ages.

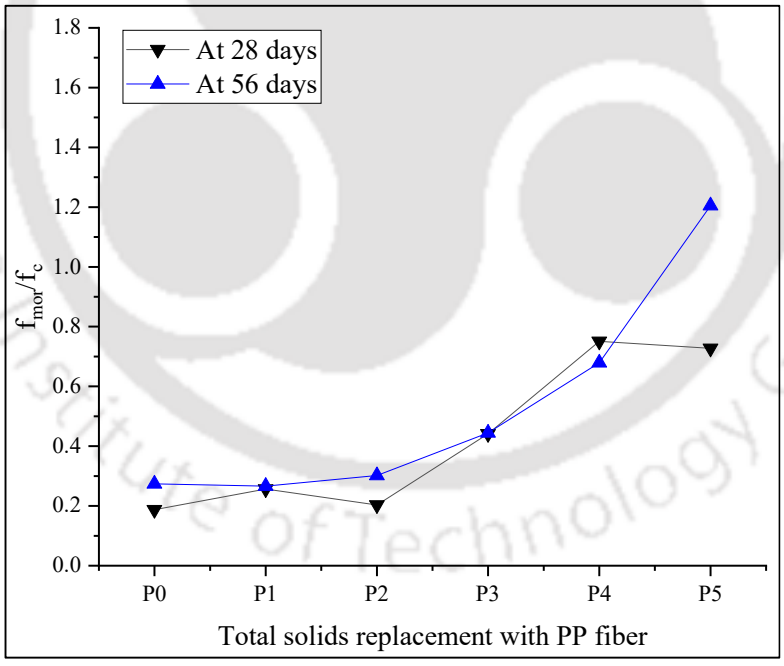

Figure 5.19: (F) Combined effect of SP dosage and PP fiber level on the f_{mor}/f_c of SFC2 mixes.

Note: In figure 5.19B, 5.19E description of adopted various legends is provided below.

A: Comparison of all the mixes with FC2F0P0 at 28 days, B: Comparison of all the mixes with FC2F0P0 at 56 days, C: Comparison between 28 days and 56 days flexural strength of all mixes.

Further, the flexural strength/ compressive strength ratio (f_{mor}/f_c) of the proposed mixes is exhibiting a systematic and significant exponential increase from 0.18 to 0.72 and 0.27 to 1.2 at 28 days and 56 days respectively, with increase in PP fiber level (figures 5.19C, 5.19F). This can be attributed to the enhanced shear behaviour of FC due to the use of chopped 12 mm PP fiber [Kearsley and Mostert, 1999, Ramamurthy et al., 2009, Ahmad et al., 2022]. Furthermore, the post failure behaviour of SFC2 mixes with and without PP fiber are presented in figures 5.20A, 5.20B. Similar to that of split tensile test, the mixes with PP fiber have presented load bearing capacity even after first crack which is clearly evident by observing the failure pattern. Hence, it is clearly evident and can be concluded that PP fiber has major influence on the ductility and post failure behaviour of FC [Mydin and Soleimanzadeh, 2012, Ahmad et al., 2022, Khan et al., 2022].

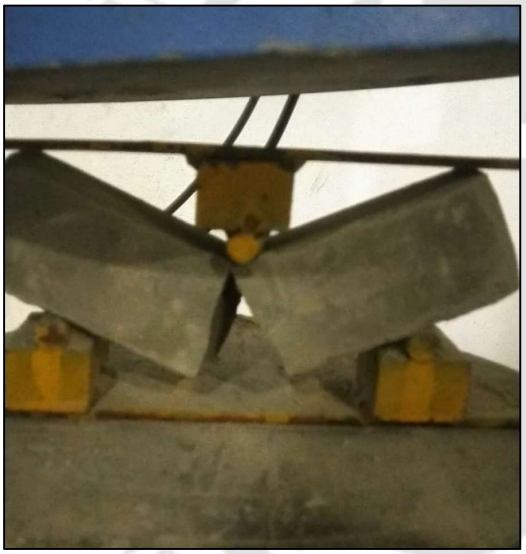

Figure 5.20: (A) Post failure behaviour of FC2 mixes without PP fiber during flexural strength test.

Figure 5.20: (B) Post failure behaviour of FC2 mixes with PP fiber during flexural strength test.

Combined effect of FA and PP fiber on split tensile strength of proposed FC mixes

From the above results, it is evident that PP fiber is enhancing the flexural strength of FC, whereas, the use of FA is exhibiting a negative influence. Hence as a next step, the combination mixes with the above utilized variations in FA and PP fiber are considered for further enhancement in flexural strength of FC for its desired application in retaining walls. The flexural strength at 28 and 56 days, along with a variety of comparative analyses (detailed in previous sections), of the suggested FC mixes are thus shown in figures 5.21A through 5.21N. In line with the earlier results, the combination mixes with

both FA and PP fiber have shown an increase in flexural strength of FC2 by 498% and 441% with a maximum of 4.9 N/mm^2 and 9.4 N/mm^2 for the mixes SFC2F4P4 and SFC2F2P5 at the age of 28 days and 56 days respectively (figures 5.21A to 5.21D, 5.21H to 5.21K). The increase in shear behaviour due to the use of PP fiber, enhanced fiber-matrix interaction due to the enhanced packing by finer FA particles (<75 µm), can be attributed as major contributors for this enhancement in 28 days strength fiber [Kearsley and Mostert, 1999, Ramamurthy et al., 2009, Mydin and Soleimanzadeh, 2012, Ahmad et al., 2022, Khan et al., 2022]. Here it is to be noted that, for any given FA level, the increment in PP fiber level is exhibiting a similar linear incremental trend both at 28 days and 56 days.

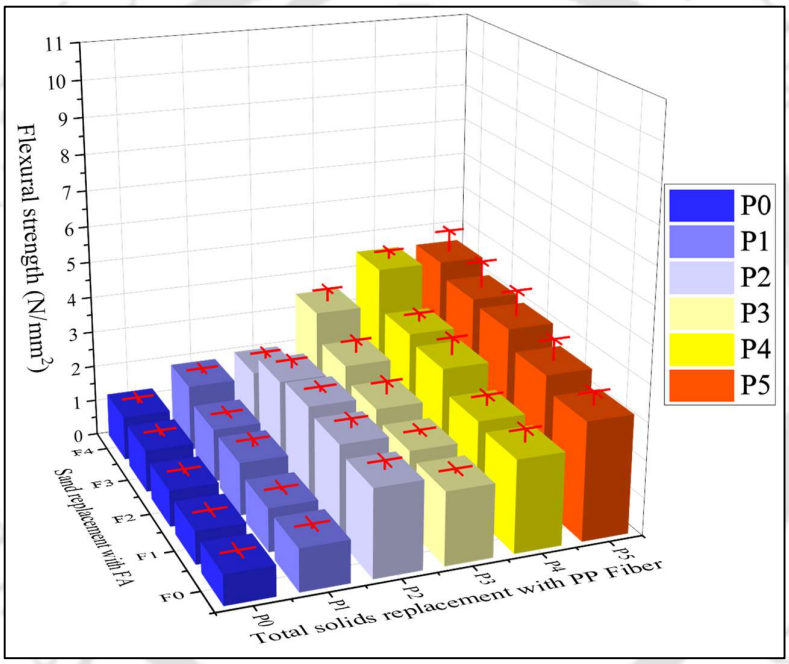

Figure 5.21: (A) Effect of variation in W/S, FA level and PP fiber level on the flexural strength of WFC2 mixes at 28 days.

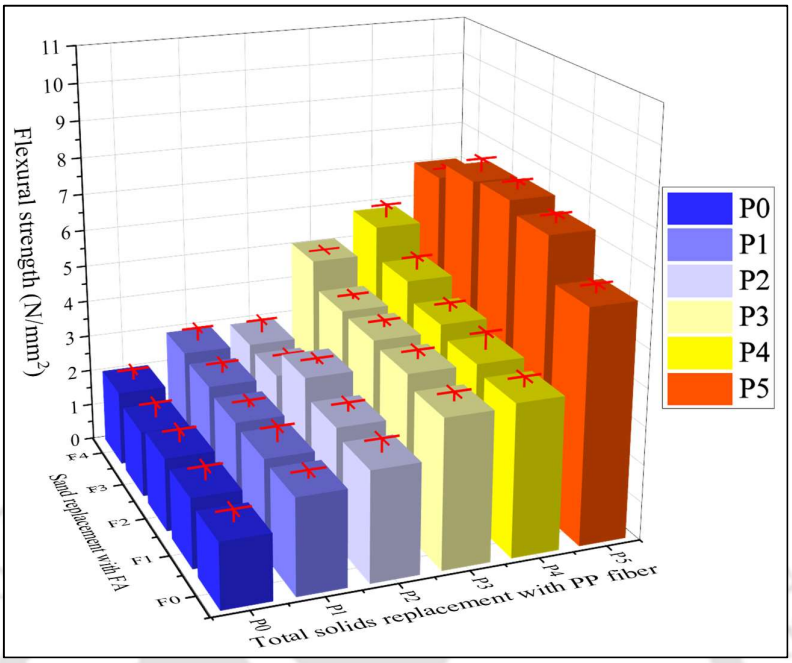

Figure 5.21: (B) Effect of variation in W/S, FA level and PP fiber level on the flexural strength of WFC2 mixes at 56 days.

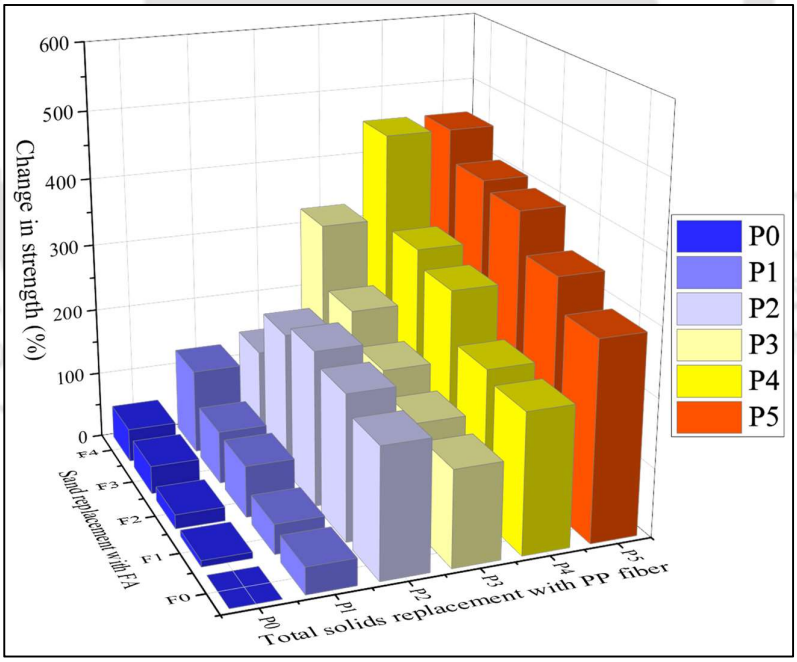

Figure 5.21: (C) Comparing the WFC2F0P0 mix and the WFC2 mixes with variations in W/S, FA level, and PP fibre level in terms of flexural strength at 28 days.

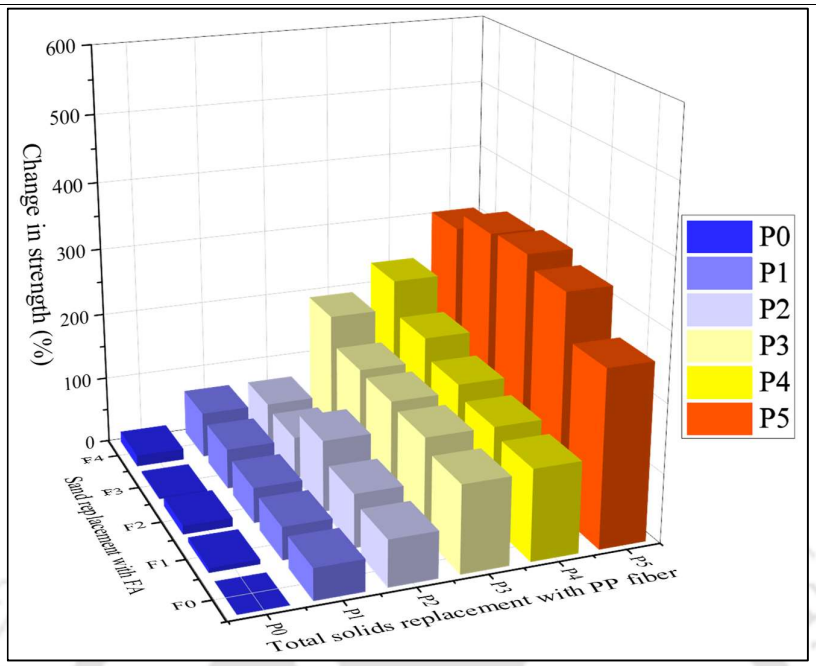

Figure 5.21: (D) Comparing the WFC2F0P0 mix and the WFC2 mixes with variations in W/S, FA level, and PP fibre level in terms of flexural strength at 56 days.

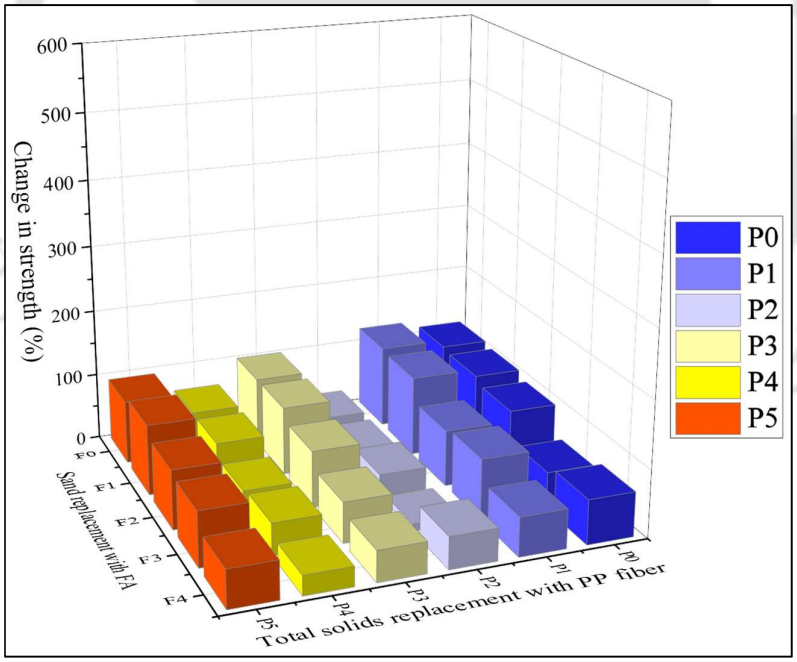

Figure 5.21: (E) Comparing the 28 days and 56 days flexural strength of the proposed WFC2 mixes with variation in W/S, FA level and PP fiber level.

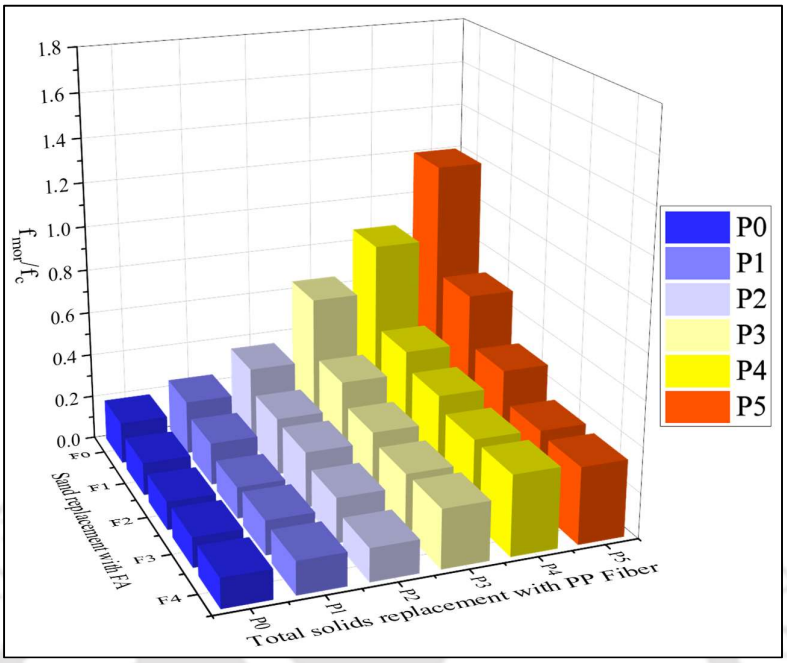

Figure 5.21: (F) Combined effect of W/S, FA level and PP fiber level on the f_{mor}/f_c of WFC2 mixes at 28 days.

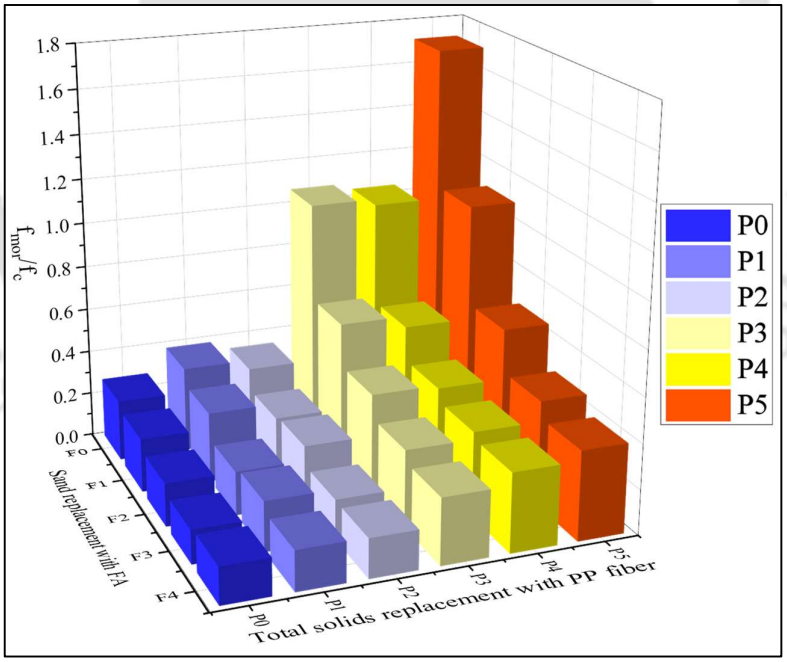

Figure 5.21: (G) Combined effect of W/S, FA level and PP fiber level on the f_{mor}/f_c of WFC2 mixes at 56 days.

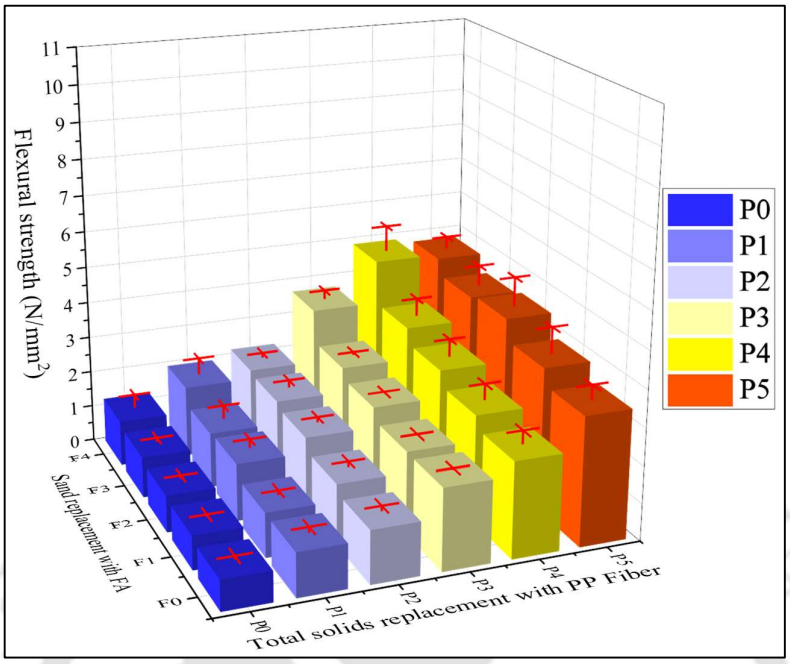

Figure 5.21: (H) Effect of variation in SP dosage, FA level and PP fiber level on the flexural strength of SFC2 mixes at 28 days.

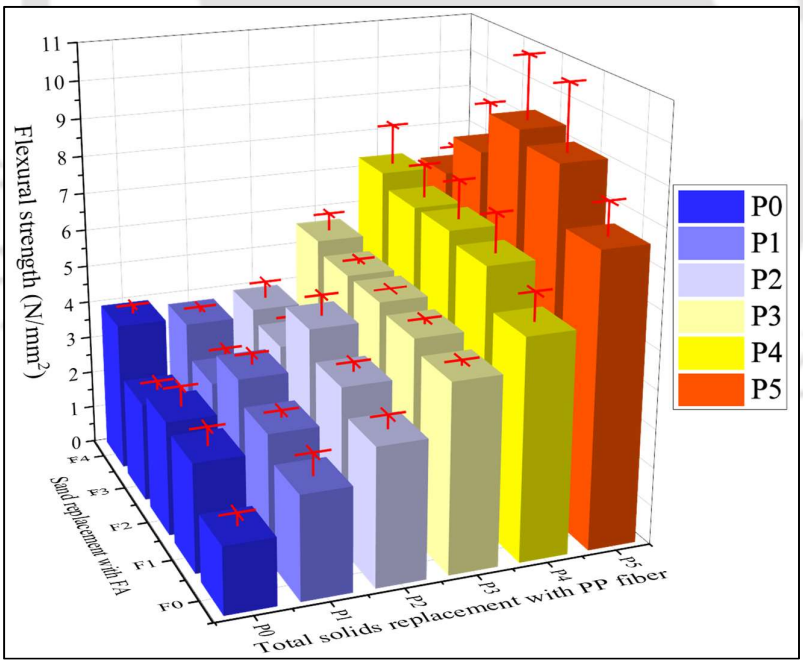

Figure 5.21: (I) Effect of variation in SP dosage, FA level and PP fiber level on the flexural strength of SFC2 mixes at 56 days.

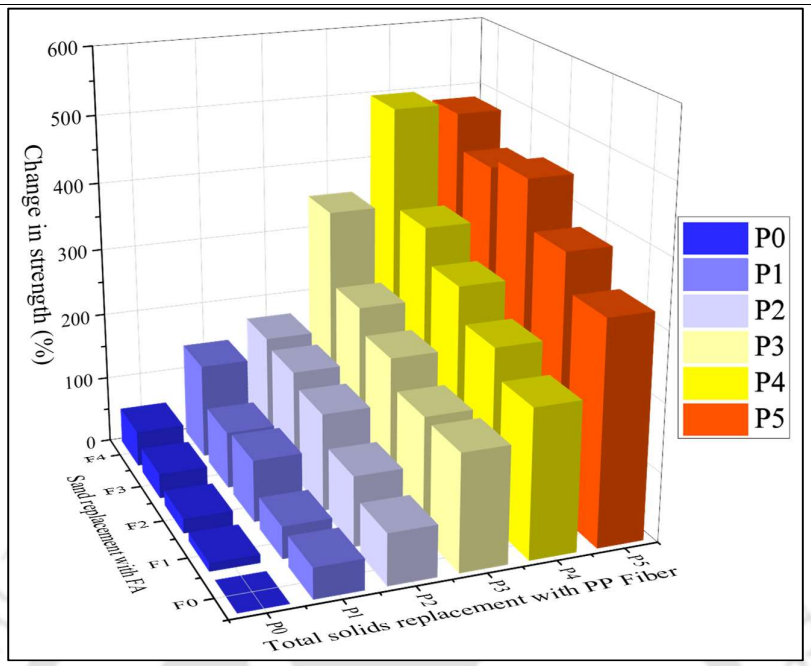

Figure 5.21: (J) Comparing the SFC2F0P0 mix and the SFC2 mixes with variations in SP dosage, FA level, and PP fibre level in terms of flexural strength at 28 days.

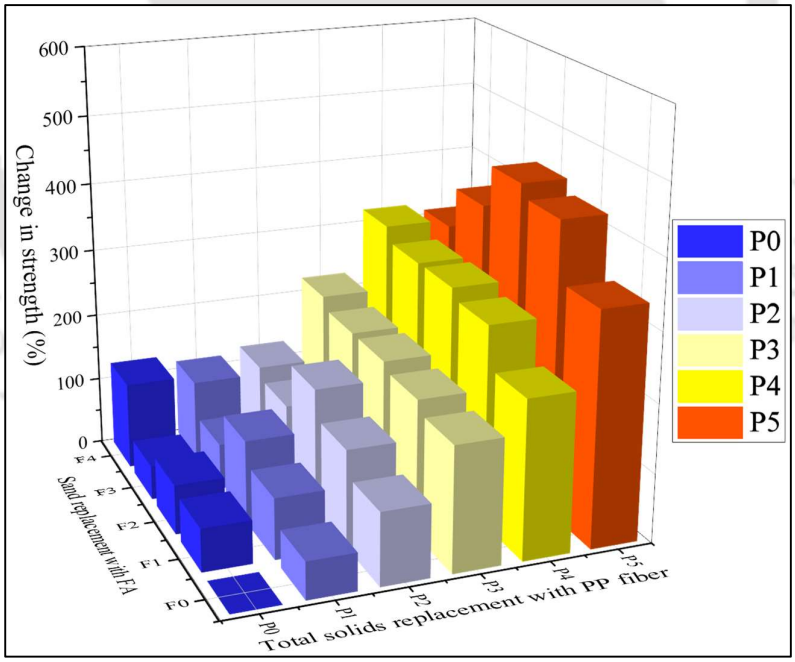

Figure 5.21: (K) Comparing the SFC2F0P0 mix and the SFC2 mixes with variations in SP dosage, FA level, and PP fibre level in terms of flexural strength at 56 days.

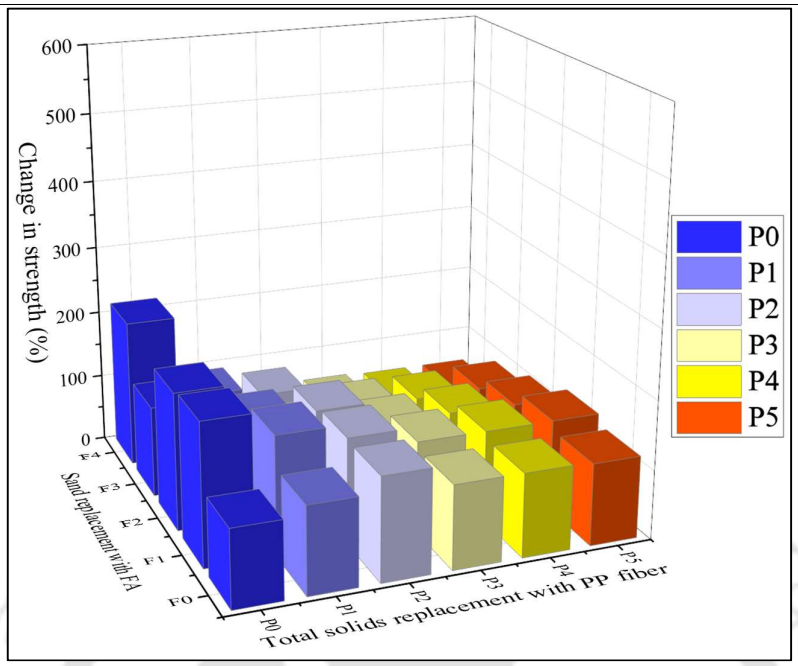

Figure 5.21: (L) Comparison between 28 days and 56 days flexural strength of the proposed SFC2 mixes with variation in SP dosage, FA level and PP fiber level.

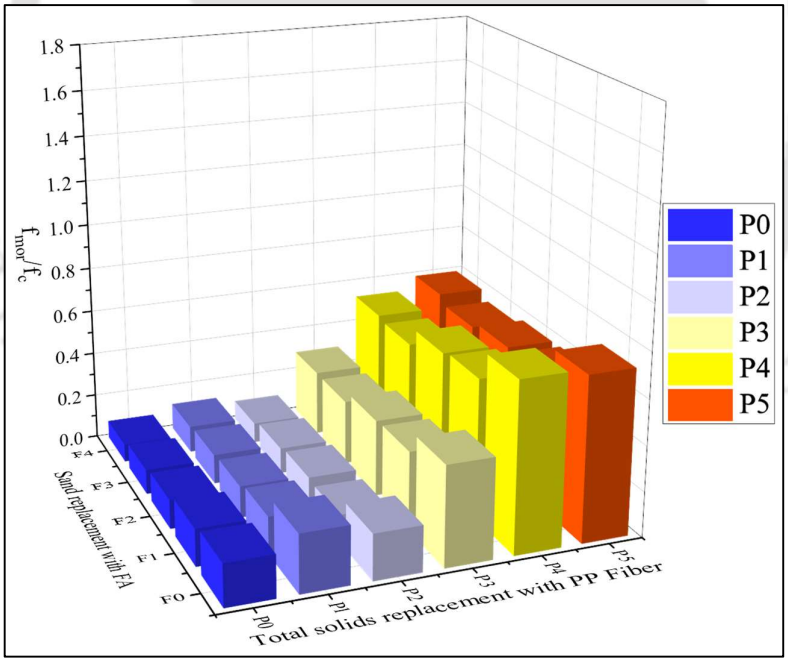

Figure 5.21: (M) Combined effect of SP dosage, FA level and PP fiber level on the f_{mor}/f_c of SFC2 mixes at 28 days.

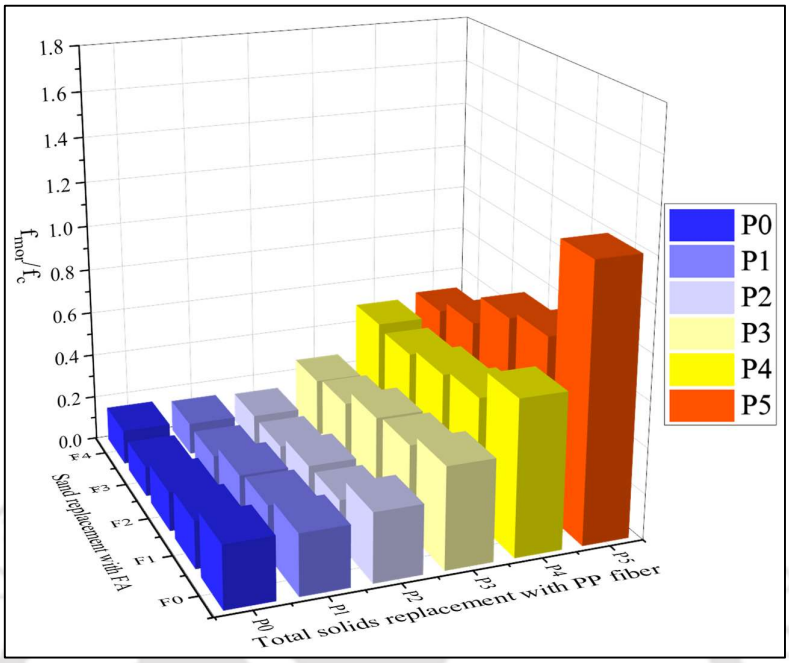

Figure 5.21: (N) Combined effect of SP dosage, FA level and PP fiber level on the f_{mor}/f_c of SFC2 mixes at 56 days.

Further, for mixes without PP fiber, increase in FA level results in a minimal linear increase in flexural strength at the age of 28 days. Furthermore, these enhancements in flexural strength are increasing with increase in PP fiber dosage. This can be attributed to the increased shear behaviour due to the enhanced packing and fiber-matrix interactions at 28 days [Kearsley and Mostert, 1999, Ramamurthy et al., 2009, Mydin and Soleimanzadeh, 2012, Ahmad et al., 2022, Khan et al., 2022]. Moreover, for any given PP fiber dosage, these combination mixes are exhibiting an inverted 'U' trend (for most of the mixes) in flexural strength with increase in FA level with maximum at 50% FA level at 56 days. This can be attributed to the enhanced packing due to finer particles and densification of matrix due to pozzolanic reaction at lower FA levels (25% and 50%) [Pan et al., 2007, Ramamurthy et al., 2009, Ganesan et al., 2015, Wang et al., 2021]. This is also evident from the 28 days to 56 days strength enhancement plots presented in figures 5.21E, 5.21L. Furthermore, at higher FA level (75% and 100%), increase in strength from 28 to 56 days is predominantly influenced by enhanced packing due to finer FA particles and limited pozzolanic reaction as established in the compressive strength section [Xu and Sarkar, 1994, Ramamurthy et al., 2009, Feng et al., 2018, Sevim and Sengul, 2021]. The f_{mor}/f_c of the combination mixes are presented in figures 5.21F, 5.21G, 5.21M, 5.21N. The close observation of these results, indicate a systematic and significant decrease in

f_{mor}/f_c with increase in FA level (0% to 100%) at 28 days for mixes without PP fiber. Further, for any given PP fiber, with increase in FA level, the f_{mor}/f_c of FC is exhibiting a similar but more significant decreasing trend at 28 days. Furthermore, these variations in f_{mor}/f_c are even more significant at 56 days. This can be attributed to the decrement in the shear capacity of FC due to the reduced sand content and increased brittle nature due to pozzolanic reaction by FA as established in the literature [Vishavkarma and Harish, 2024]. On the other hand, for any given FA level, with the increase in PP fiber dosage, the f_{mor}/f_c is increasing in an exponential trend at the age of 28 days and 56 days. Here it is to be noted, though the flexural strength of FC increases continuously, the corresponding compressive strength reduces beyond PP fiber dosage of 0.4%, which can be attributed as the reason for the aforementioned exponential trend. This enhancement in the f_{mor}/f_c can be attributed to the enhanced shear behaviour and ductility of FC due to PP fiber [Ahmad et al., 2022]. Of all the combination mixes, the SFC2F1P2, SFC2F2P2, SFC2F3P2, and SFC2F4P2 mixes are exhibiting the highest compressive strength (meeting ASTM C1372-23 guidelines), highest split tensile strength and satisfactory flexural strength along with the most significant improvement in the f_t/f_c and f_{mor}/f_c, and hence, these mixes are chosen for further studies.

5.4 SUMMARY

To summarize, the current study is an attempt to determine the mix composition of FC2 which could result in desired strength for its intended application in production of dry cast segmental retaining wall units. The effect of variation in level of sand replacement with FA and total solids replacement with PP fiber has been studied on various fresh state and mechanical properties of concrete. Firstly, the required W/S or SP dosage to produce stable FC satisfying the recommended fresh state properties have been derived. Further, these mixes have been tested for the mechanical properties viz. compressive strength, split tensile strength and flexural strength. Moreover, various comparative analyses have been done as described in previous section. The proposed matrix modifications have enhanced the compressive strength by a maximum of 573% and 512% at the age of 28 days and 56 days respectively, promoting the mixes SFC2F4P0, SFC2F4P1, SFC2F3P1, SFC2F1P2, SFC2F2P2, SFC2F3P2, SFC2F4P2 and SFC2F4P3 as satisfactory in accordance with ASTM C1372-23. Further, the testing of split tensile strength and flexural strength of the proposed FC2 mixes, revealed 306%, 221% and 498%, 912% at

the ages of 28 days and 56 days respectively. Furthermore, the f_t/f_c and f_{mor}/f_c have also enhanced with maximum at 0.45 and 1.7 respectively. Among all of the proposed FC2 mixes, the SFC2F1P2, SFC2F2P2, SFC2F3P2, and SFC2F4P2 mixes are the ones that have been selected for further research as they have the highest compressive strength (meeting ASTM C1372-23 guidelines), highest split tensile strength, satisfactory flexural strength, and the greatest improvement in the f_t/f_c and f_{mor}/f_c. However, these compressive strength results correspond to cube samples with dimension of 50 mm. On the other hand, the ASTM C1372-23 recommendations correspond to block strength. Hence, the further studies are attempted to study various IB properties viz. compressive strength and shear resistance of FCIB and triplets and permeation characteristics viz. water absorption and permeability of the selected mixes as discussed in upcoming chapter.

CHAPTER 6
STUDIES ON PROPERTIES OF FCIB PRODUCED WITH SELECTED MIXES

6.1 GENERAL

The previous chapter discussed the effect of FA (0% to 100% replacement of sand) and PP fiber (0% to 1% replacement of total solids) on the mechanical properties of FC with design density of 1500 kg/m^3. Experimental outcomes have revealed that the FA has an overall significant influence on the mechanical properties of FC. Moreover, the compressive strength and split tensile strength of FC show an inverted "U" trend (peaking at 0.4% PP fiber content), when PP fiber replaces up to 1% of the total solids by weight. Furthermore, usage of SP as well as appropriate increase in W/S to achieve predefined spreadability of 40% to 60% results in positive impact on mechanical properties of FC mixes. Here, SP is playing a predominant role in pore refinement enabling significant enhancement in the mechanical properties of FC. Further, it is important to highlight that the primary objective of this study is to identify the mix composition of FC that will produce the appropriate strength and permeability for its intended use as IB for retaining walls in order to aid in the dissipation of pore water pressure. In this context, ASTM C1372-23 guidelines require a minimum strength of atleast 20.7 N/mm^2 for use in retaining wall applications. Hence, the mixes SFC2F1P2, SFC2F2P2, SFC2F3P2 and SFC2F4P2 mixes which satisfied the aforementioned strength requirements, are selected as most suitable mixes (based on cube strength results) keeping in view of application of dry cast segmental retaining wall units. Later, the further studies are attempted as discussed in the present chapter to determine the permeation and the mechanical properties of FCIB produced using the aforementioned most suitable mixes.

6.2 MATERIALS AND METHODOLOGY

6.2.1 MATERIALS AND MIX PROPORTION

The following constituent materials are used in the present study for the production of FC:

- OPC-43 grade (supplied by Dalmia Ltd.).

- Sand that is passed through a 300 µm sieve.
- Class-F FA, purchased from National Thermal Power Corporation, Bongaigaon, India.
- PP fiber purchased from Jogani Impex LLP.
- SLS purchased from LOBA chemicals.
- CMC purchased from LOBA chemicals.
- PCE-based SP (Auramix 300) obtained from FOSROC chemicals.

The properties of these materials are explained in details in previous chapters. The present study evaluates the performance of the selected suitable mixes viz. SFC2F1P2, SFC2F2P2, SFC2F3P2 and SFC2F4P2, with design density of 1500 kg/m^3. The W/S of the above-mentioned mixes is primarily fixed at 0.3 considering the stability of mixes based on previous literature and preliminary trials [Sahu and Gandhi, 2021]. A constant cement-to-sand ratio of 1:2, by mass has been adopted throughout the study. Concrete mixes are prepared by replacing 25% (SFC2F1P2), 50% (SFC2F2P2), 75% (SFC2F3P2) and 100% (SFC2F4P2) of sand (by weight) with FA and 0.4% of total solids with PP fiber (by weight) and these replacement levels are chosen based on earlier studies.

6.2.2 METHODOLOGY

For the present study, Bamba type IB pattern reported by Kintingu, 2009, Lin, 2020, and Xie et al., 2022, for cement-soil bricks has been modified to assess the performance of FCIB. The top and bottom faces of this IB pattern possess asymmetry i.e. rotating the brick 180 degrees around its Z-axis will make the bottom view appear to be the top view, which allow them to lock one another due to their topological interlocking system. The top phase of the block has been equally divided into 8 parts as shown in figure 6.1B. Out of these, 4 parts (2, 3, 5 and 8) are extruding 10 mm above top surface (as presented in the figures 6.1A, 6.1B, 6.1C and 6.1D) with the corresponding counter parts on its bottom face. Furthermore, the slope of the internal key edges has been chosen at an angle of 45°. However, for casting of FCIB, the size of the block is chosen such that it is similar to that of the conventional clay brick used in India. The moulds are carefully fabricated so that the counter blocks superimpose perfectly maintaining the desired dimensional tolerance. In order to assess the mechanical properties of FCIB, the locks in loading surfaces are filled with 1:1 mortar to achieve levelled uniform surface and thereafter testing is done as described in the following paragraph.

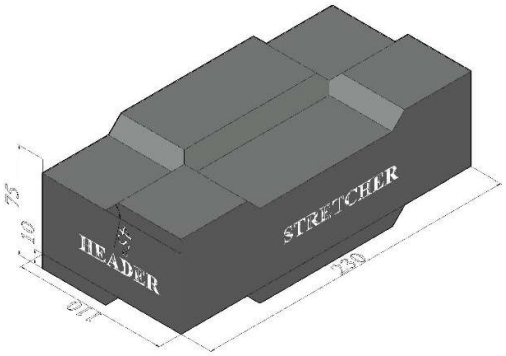

Figure 6.1: (A) Perspective view of FCIB.

Figure 6.1: (B) Plan of FCIB.

Figure 6.1: (C) Front elevation of FCIB.

Figure 6.1: (D) Side elevation of FCIB.

The methodology discussed in chapter 4 is followed to analyse the fresh density and demoulded density of the selected FC mixes. The compressive strength and water absorption of FCIB samples is measured in accordance to IS 3495-1, 2: 2019. Three number of samples are tested for each mix at ages 28 days and 56 days. The compressive strength (for blocks and triplet prisms) and shear resistance of masonry prism (for triplet prisms) produced using the FCIBs are tested at ages 28 days and 56 days as per guidelines of ASTM C1314 -23b and RILEM TC 127-MS: 1996 using the test setup as presented in figure 6.2. In order to test the permeability of above FC mixes, three cylindrical samples of 100 mm height and 100 mm diameter for each test have been casted and cured until the age of testing. The water permeability of these samples is being tested in accordance with IS 3085: 2021 using the sealing mechanism developed in earlier part of this study and at a pressure head of 3 kg/cm^2.

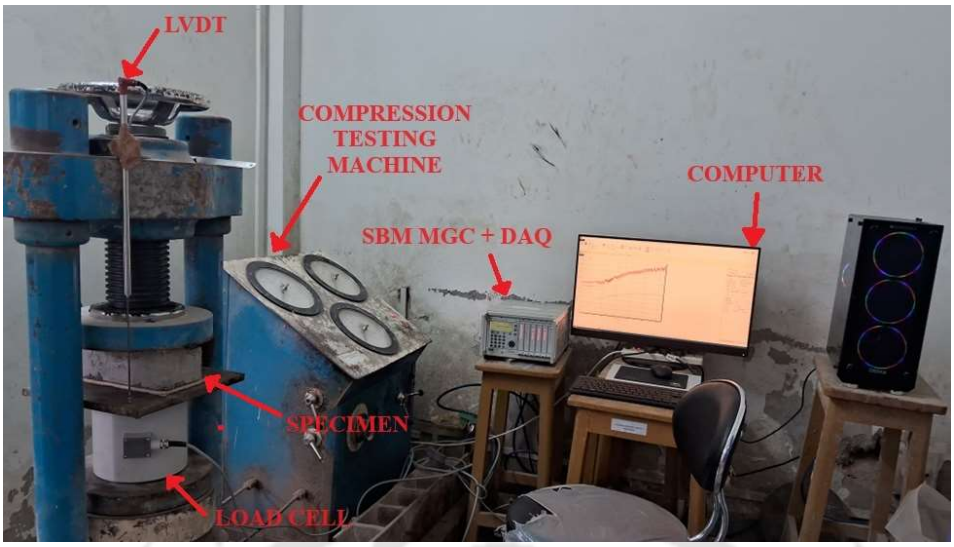

Figure 6.2: Test setup for measuring load vs. displacement vs. time for various samples of FCIB (under compression) and FCIB triplets (under compression and shear).

6.3 DETAILED INVESTIGATIONS ON EFFECT OF VARIATION OF MIX PROPORTION PARAMETERS ON FCIB BEHAVIOUR

6.3.1 FRESH STATE PROPERTIES

Cohesiveness and density of the mix has significant impact on workability of concrete. Further, the consistency of the FC is crucial to achieve the desired design density [Nambiar and Ramamurthy, 2008, Beskopylny et al., 2023]. In line with the observations reported in chapter 5, the selected FC mixes are also exhibiting the recommended spreadability of 40% to 60%. Further, the fresh and demoulded density of these mixes is also tested and found to be satisfactory.

6.3.2 MECHANICAL PROPERTIES OF FCIB

In general, the mechanical properties of masonry units play a vital role in determining the safety and performance of structures. The crucial mechanical characteristics that determine whether a particular type of IB is suitable for the given masonry application are its compressive strength and shear resistance. Firstly, FCIBs are made with the selected mixes viz. SFC2F1P2, SFC2F2P2, SFC2F3P2 and SFC2F4P2 which met the ASTM C1372-23 minimum strength requirement of 20.7 N/mm^2 as discussed in chapter 5. Later, the prisms are casted and their mechanical behaviour is studied in comparison with the cubes, blocks and triplets.

6.3.2.1 COMPRESSIVE STRENGTH OF FCIB PRODUCED USING SELECTED MIXES

The compressive strength of the FCIB produced using selected mixes are tested in accordance with IS 3495-1: 2021 at different ages (28 days and 56 days) and the results are presented in figure 6.3A. Further, various comparative analyses such as A: comparative analysis of 28 days strength of all the selected FCIB mixes with the SFC2F1P2 mix at 28 days, B: comparative analysis of 56 days strength of all the selected FCIB mixes with the SFC2F1P2 mix at 56 days, C: comparative analysis of 56 days strength of all the selected FCIB mixes with the corresponding 28 days strength are shown in figure 6.3B. Obviously, as expected, the FCIB with 25% replacement of sand with FA (SFC2F1P2) exhibits the lowest compressive strength of 8.56 N/mm^2 (at 28 days) while the mixes with incremental FA content exhibits incremental trend in compressive strength. Further, the difference between 28 days and 56 days compressive strength is mostly equivalent for all the mixes with a maximum for the mixes with 100% replacement of sand with FA. Figure 6.3A shows that, as the FA content increases in the FC mix, significant increase in compressive strength is observed. The above increase in strength due to FA addition (as observed in scatter B of figure 6.3B) can be attributed to the pozzolanic reaction. However, it is to be noted that pozzolanic reaction is a slow reaction and the pozzolanic activity increases rapidly after 28 days [Feng et al., 2018]. Hence, the initial strength gains due to FA addition as observed in scatter A of figures 6.3B (linear trend), can be attributed mostly to the improvement in microstructure resulting from enhanced packing of finer particles of FA [Ramamurthy et al., 2009]. Additionally, the appropriate dosage of SP adopted for various FCIB mixes also contribute to linear increase in compressive strength (scatter A of figure 6.3B) through enhancement in the microstructure of FC. This can be attributed to the reduction of additional pores due to reduced water content and densification resulting from steric hindrance effect of PCE based SP. Also, due to delayed pozzolanic reaction, a significant enhancement of strength at later age is observed as established in literature [Pan et al., 2007, Ganesan et al., 2015]. For instance, increment of 36% to 48% in compressive strength is observed for increase in age from 28 days to 56 days for all the mixes (as observed in scatter C of figures 6.3B). Further, among all the mixes only SFC2F4P2 mix (at 56 days of curing) satisfies the ASTM C1372-23 recommended minimum

compressive strength requirement of 20.7 N/mm^2 for its intended use as dry-cast segmental retaining wall units.

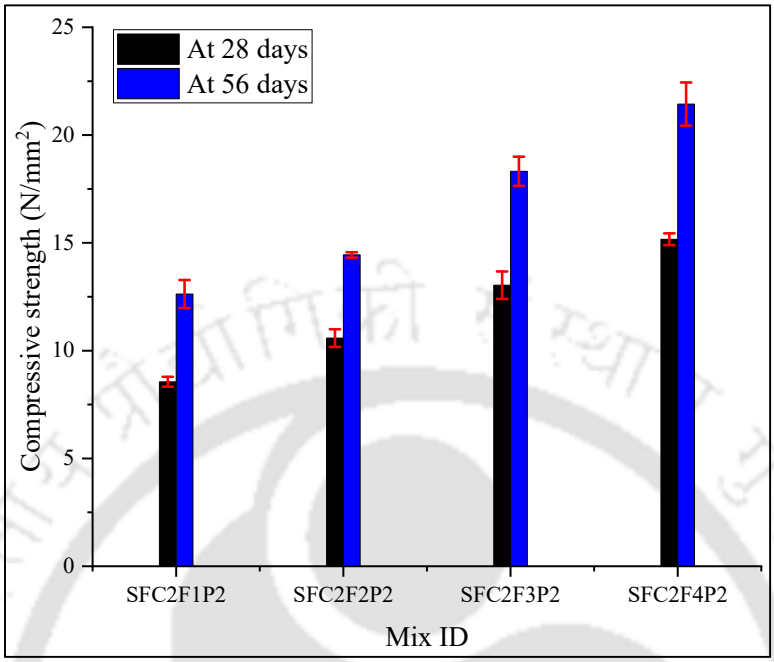

Figure 6.3: (A) Compressive strength of FCIBs produced using selected mixes.

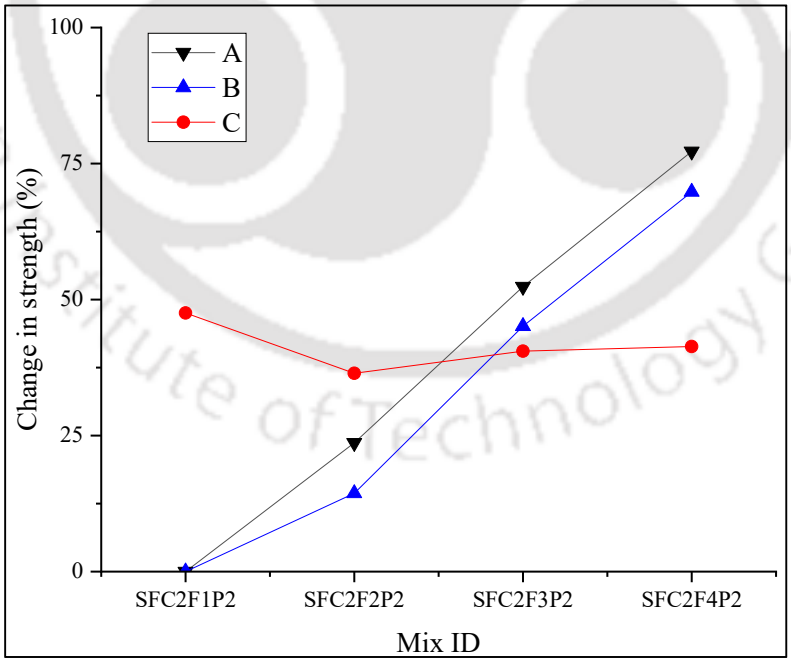

Figure 6.3: (B) Comparative analysis between compressive strength of FCIBs produced using selected mixes at different testing ages.

Note: In figure 6.3B description of adopted various legends is provided below.

A: Comparison of all the mixes with SFC2F1P2 at 28 days, B: Comparison of all the mixes with SFC2F1P2 at 56 days, C: Comparison between 28 days and 56 days compressive strength of all mixes.

The comparative analysis of compressive strength of FCIB with respect to the corresponding cubes of 50 mm dimension are presented in figure 6.4A. Further, failure patterns of FCIB and cube of 50 mm dimension under compression are presented in figures 6.4B, 6.4C. Due to the variation in IB pattern, shape and size, the compressive strength of FCIB is 57% to 74% of FC cubes of size 50 mm (tested at various ages). This is comparable with the observations of work done by Jaafar et al., 2006, who had reported block strength (with dimensions: 300 mm X 150 mm X 200 mm) as 90% of the compressive strength of 150 mm size cubes. Also, the ratio of block to cube strength obtained in the present study appears to be lesser as very small cubes of 50 mm are used for comparison. Further, though the cubes fail in a biconcave pattern, the PP fiber present in the mix is restricting its sudden failure and hence enhances the ductility behaviour of FC. Similar type of failure can also be observed in the case of FCIB by observing the load vs. time and displacement vs. time curves as presented in figures 6.4D, 6.4E. Furthermore, considering the progress of failure, the primary failure of FCIB has been observed during the initial stages at the key-lock interface as presented in figure 6.4B. Later, the brittle failure of the FCIB material has been observed through generation of multiple cracks. Finally, the ductile failure of the specimen is evident in the form of prolonged failure at fiber-matrix interface showcasing the maximum load bearing capacity, even after the occurrence of primary and secondary failures.

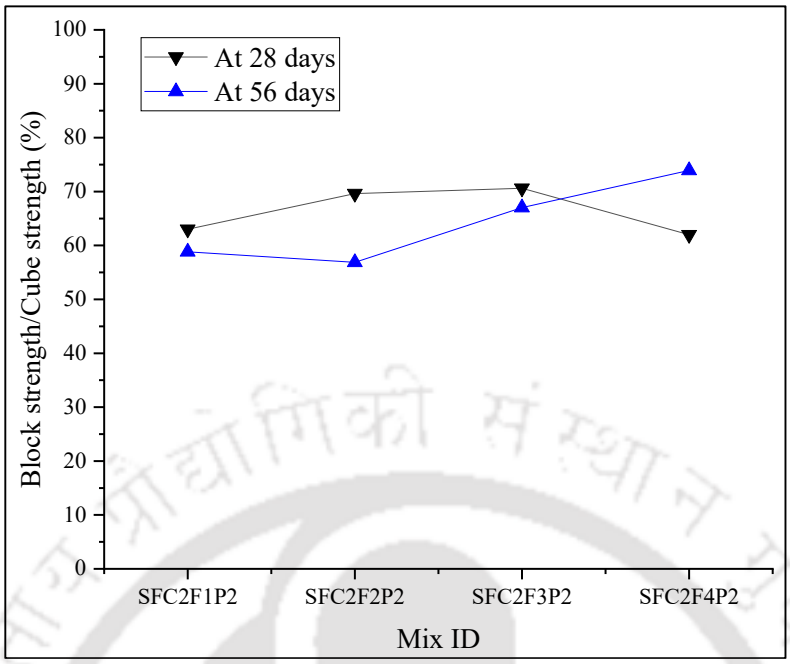

Figure 6.4: (A) Comparative analysis between compressive strength of FCIBs and the corresponding cubes of 50 mm dimension at various testing ages.

Figure 6.4: (B) Typical failure pattern of FCIB under compression.

Figure 6.4: (C) Typical failure pattern of FC cube of 50 mm dimension under compression.

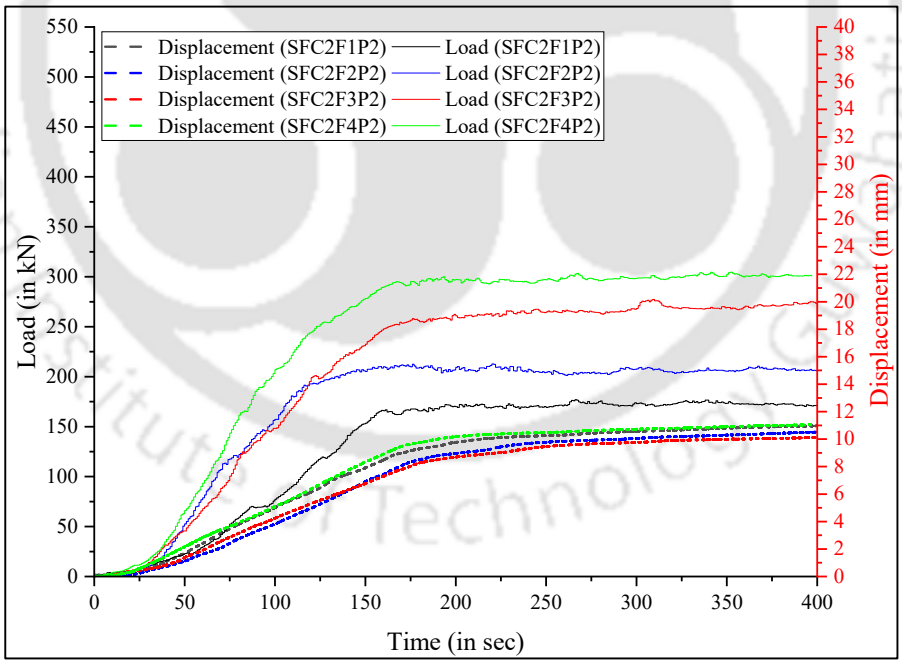

Figure 6.4: (D) Load vs. time and displacement vs. time curves of FCIB at the testing age of 28 days.

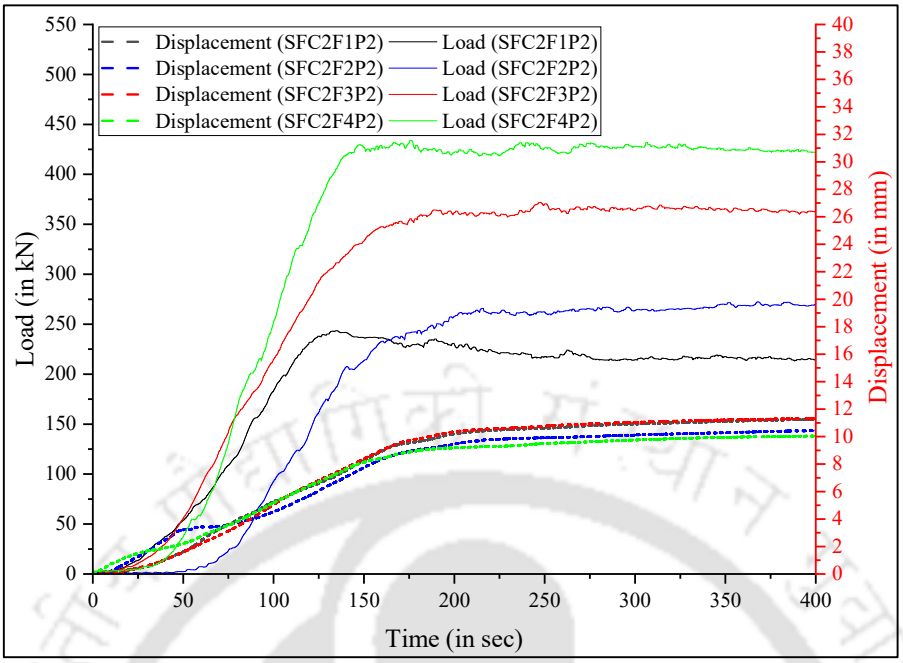

Figure 6.4: (E) Load vs. time and displacement vs. time curves of FCIB at the testing age of 56 days.

6.3.2.2 MASONRY COMPRESSIVE STRENGTH OF FCIB TRIPLETS

The results of the compressive strength of the FCIB prism (triplets) prepared using the selected mixes from chapter 5 tested in accordance with ASTM C1314 -23b are shown in figure 6.5A. Further, various comparative analyses as described in the previous section are shown in figure 6.5B. In line with the earlier results, the compressive strength of FCIB triplets is presenting similar incremental trends. The average compressive strength of the FCIB triplets with 25% replacement of sand with FA (SFC2F1P2) is 4.36 N/mm^2 (at 28 days), which is the lowest as in the case of FCIB as discussed earlier. Further, the mixes with increasing FA content show an increasing trend in compressive strength. Furthermore, at the age of 28 days, the compressive strength of triplets is exhibiting incremental trend (as observed in scatter A of figure 6.5B), owing to the improvement in microstructure due to higher packing efficiency resulting from increase in finer FA particles. Moreover, at later age, the incremental trend in pozzolanic activity (as observed in scatter C of figure 6.5B) is enhancing the compressive strength of these triplets (as observed in scatter B of figure 6.5B) [Pan et al., 2007, Ramamurthy et al., 2009, Ganesan et al., 2015, Feng et al., 2018, Vishavkarma and Harish, 2024, Ahmad et al., 2022, Khan et al., 2022].

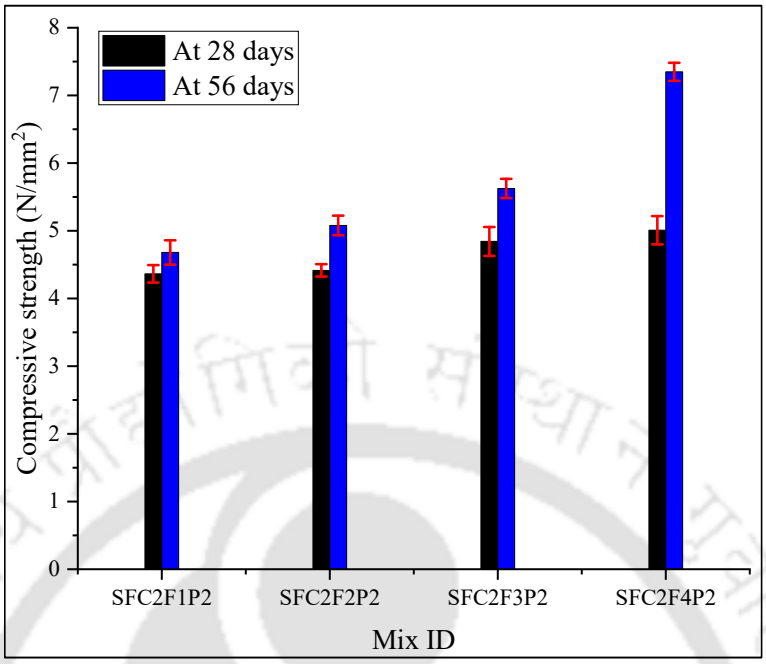

Figure 6.5: (A) Compressive strength of FCIB triplets produced using selected mixes.

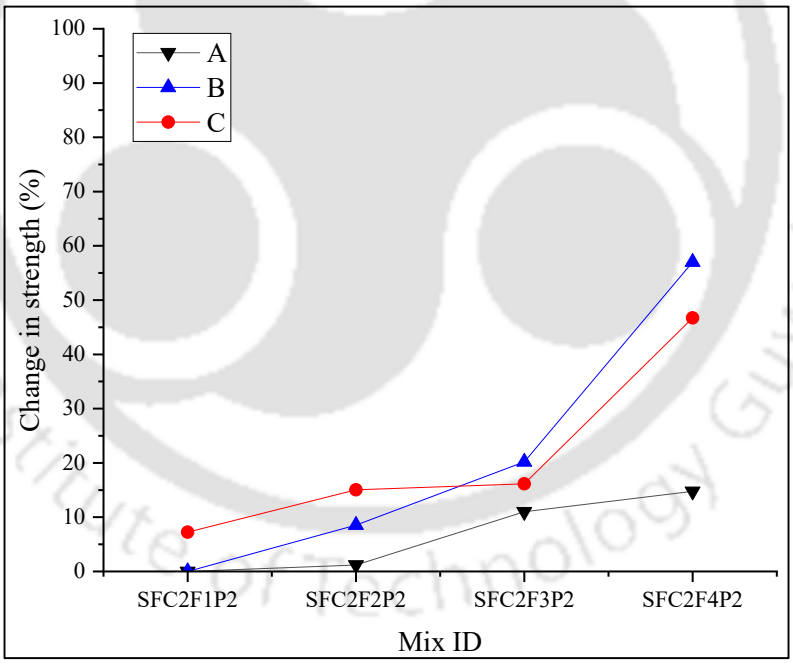

Figure 6.5: (B) Comparative analysis between compressive strength of FCIB triplets produced using selected mixes at different testing ages.

Note: In figure 6.5B description of adopted various legends is provided below.

A: Comparison of all the mixes with SFC2F1P2 at 28 days, B: Comparison of all the mixes with SFC2F1P2 at 56 days, C: Comparison between 28 days and 56 days compressive strength of all mixes.

The compressive strength of FCIB triplets is found to be 30% to 51% of FCIB as shown in figure 6.6A. The increase in aspect ratio of the FCIB triplets contributes to the above-mentioned reduction in strength when compared to FCIB. This is consistent with findings from research reported by Jaafar et al., 2006, who found that the strength of triplets accounted for 47% of the compressive strength of individual blocks. Further, at the age of 28 days, with increase in FA content, the reduction in strength of triplet when compared to that of FCIB also increases as evident from comparative analysis depicted in figure 6.6A. The above trend can be attributed to the significant positive effect of increase in FA content on FCIB when compared to that of triplet. Nevertheless, the compressive strength of triplet is more governed by geometry of triplet governing the failure pattern when compared to the effect of improvement in microstructure due to FA addition. Hence, reduced compressive strength of triplets is primarily caused by the key-lock interfaces that are three times larger when compared to that of individual FCIB as observed in figure 6.6B. As the loading progresses, the key-lock interface failure of triplet is showcasing ductile behaviour and buckling pattern of failure rather than conventional compressive failure observed in FCIB. The above failure pattern is more evident when the header face of FCIB in figures 6.6B and 6.6C are compared. Moreover, by comparing load vs. time and displacement vs. time curves of triplets (figures 6.6D, 6.6E) with that of individual FCIB, it is evident that the prolonged load bearing capacity is exhibited by FCIB as well as by the triplets which can be attributed to the enhanced ductility behaviour derived from PP fiber [Pan et al., 2007, Ramamurthy et al., 2009, Ganesan et al., 2015, Feng et al., 2018, Vishavkarma and Harish, 2024, Ahmad et al., 2022, Khan et al., 2022].

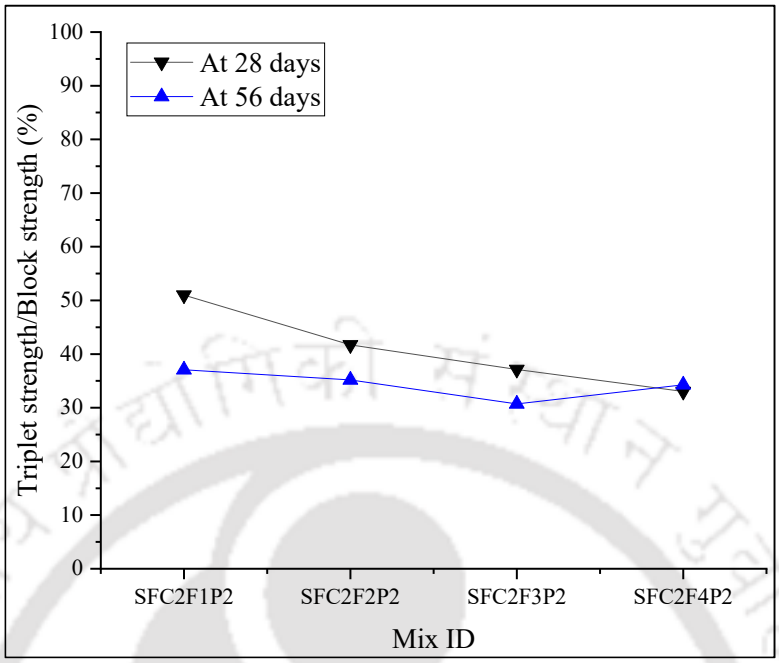

Figure 6.6: (A) Comparative analysis between compressive strength of FCIB prisms (triplets) and the corresponding FCIB at various testing ages.

Figure 6.6: (B) Typical failure pattern (stretcher face) of FCIB prisms (triplets) under compression.

Figure 6.6: (C) Typical failure pattern (header face) of FCIB prisms (triplets) under compression.

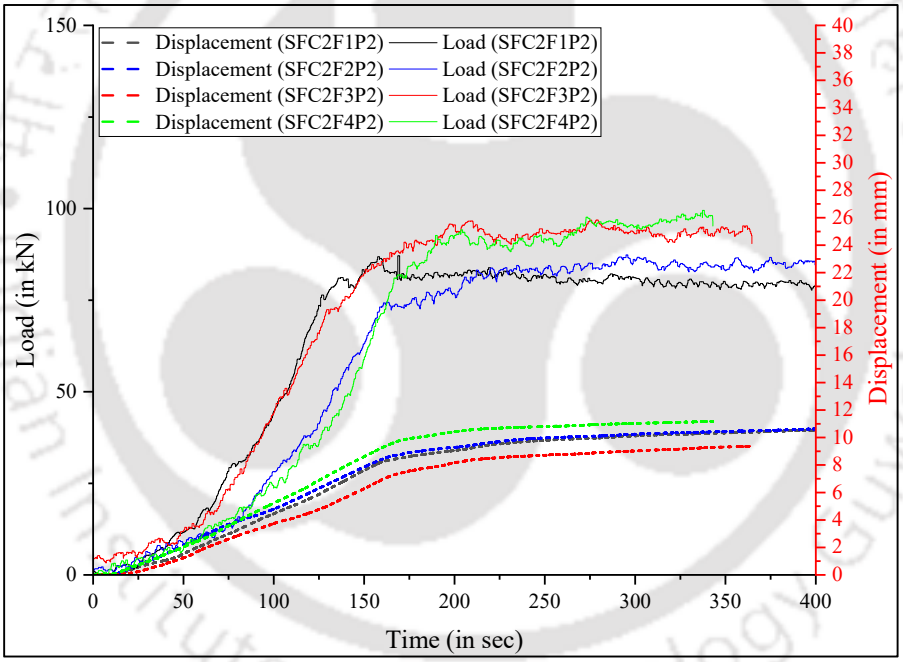

Figure 6.6: (D) Load vs. time and displacement vs. time curves of FCIB prisms (triplets) at the testing age of 28 days.

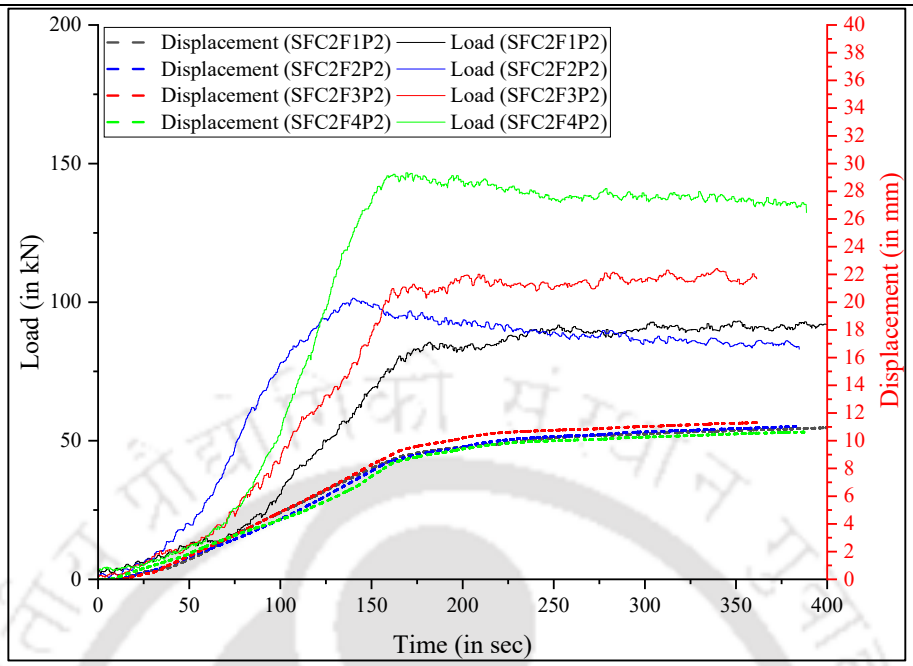

Figure 6.6: (E) Load vs. time and displacement vs. time curves of FCIB prisms (triplets) at the testing age of 56 days.

6.3.2.3 MASONRY SHEAR RESISTANCE OF FCIB TRIPLETS (PERPENDICULAR TO HEADER FACE AND STRETCHER FACE)

The shear resistance of FCIB triplets is tested in accordance with RILEM TC 127-MS: 1996 along with the confinement as suggested by Nadeem et al., 2023, using the test setup (figure 6.2) and support conditions as presented in figures 6.7A and 6.7B. These tests have been conducted for both the loading conditions independently viz. perpendicular to the header face and stretcher face and the results are presented in figures 6.7C, 6.7D. Further, various comparative analyses as described in the previous section are presented in figures 6.7E, 6.7F. Furthermore, the load vs displacement curves of the aforementioned tests are presented in figures 6.7G, 6.7H, 6.7I and 6.7J. From the aforementioned results (figures 6.7C, 6.7D), it is evident that with the increase in FA content, the shear resistance of FCIB triplets also increases following a similar trend as in the case of compressive strength of FCIB and FCIB triplets. Moreover, from the comparative analysis as presented in scatter A of figures 6.7E, 6.7F, it is evident that the enhancement in shear resistance is in greater incremental trend with increase in FA content which can be attributed to reduced foam requirement as a result of lower specific gravity of FA. Further, the lower particle size of FA and its preliminary pozzolanic

reaction also contributes to enhanced binder-aggregate ITZ resulting in higher enhancement in the shear resistance at early age [Ramamurthy et al., 2009, Feng et al., 2018]. On the other hand, at later age, though these enhancements are presenting an incremental trend as presented in scatter B of figures 6.7E, 6.7F, they are lower when compared to the early age enhancement. Mixes with higher level of FA has limited pozzolanic activity due to encapsulation of Ca $(OH)_2$ and its limited availability as discussed in earlier sections [Xu and Sarkar, 1994, Ramamurthy et al., 2009, Feng et al., 2018, Sevim and Sengul, 2021]. The above can be attributed to trend of scatter B of figures 6.7E, 6.7F showing lesser variation in shear resistance with increase in FA content. The above-mentioned observations are evident from the decremental trend in the comparative analysis of shear resistance while comparing between various ages of the sample (by observing scatter C of figure 6.7E). On a contrary, in the case of loading condition perpendicular to the stretcher face, instead of decreasing trend, 'U' trend is observed in the comparative analysis in scatter C of figure 6.7F. The geometric effect resulting from different loading pattern can be attributed to the above variation in trend. Hence, it may perhaps be concluded that the shear resistance of the proposed FCIB is greater with loading condition perpendicular to the stretcher face.

Figure 6.7: (A) Typical loading setup for testing shear resistance (perpendicular to header face) between FCIB triplets.

Figure 6.7: (B) Typical loading setup for testing shear resistance (perpendicular to stretcher face) between FCIB triplets.

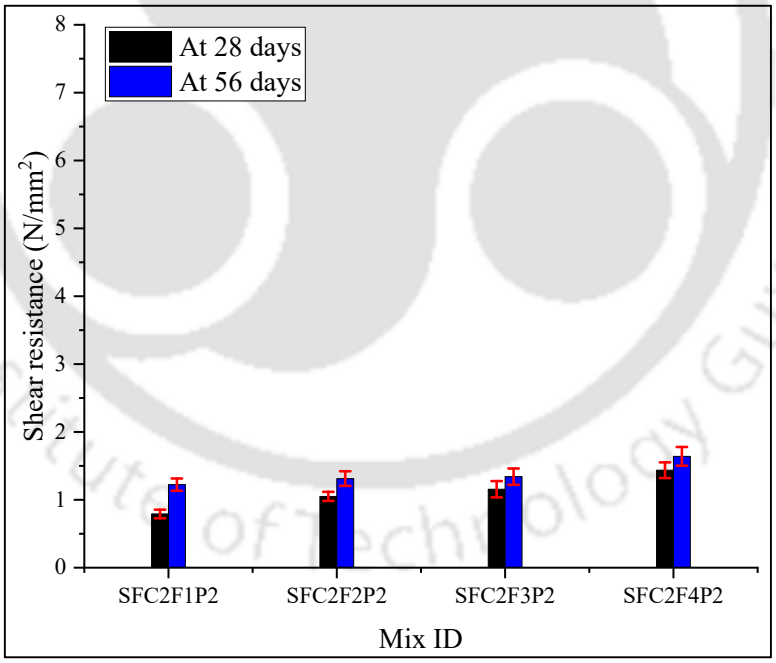

Figure 6.7: (C) Shear resistance between FCIB triplets (perpendicular to header face) produced using selected mixes.

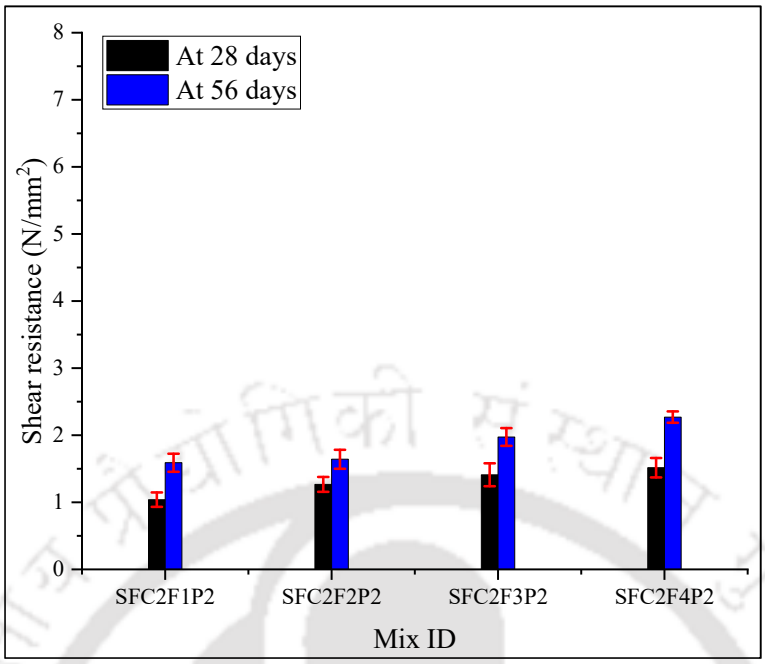

Figure 6.7: (D) Shear resistance between FCIB triplets (perpendicular to stretcher face) produced using selected mixes.

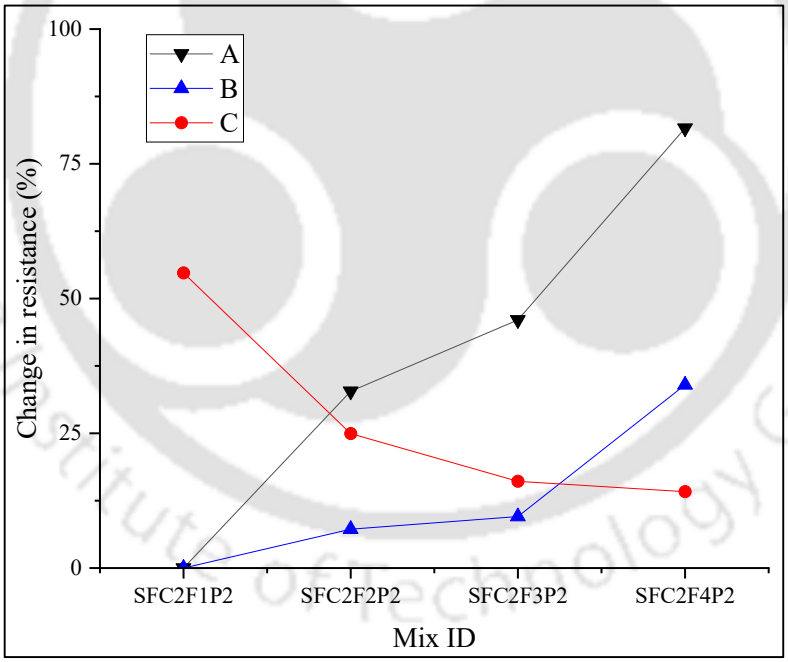

Figure 6.7: (E) Comparative analysis of shear resistance between FCIB triplets (perpendicular to header face) produced using selected mixes at different testing ages.

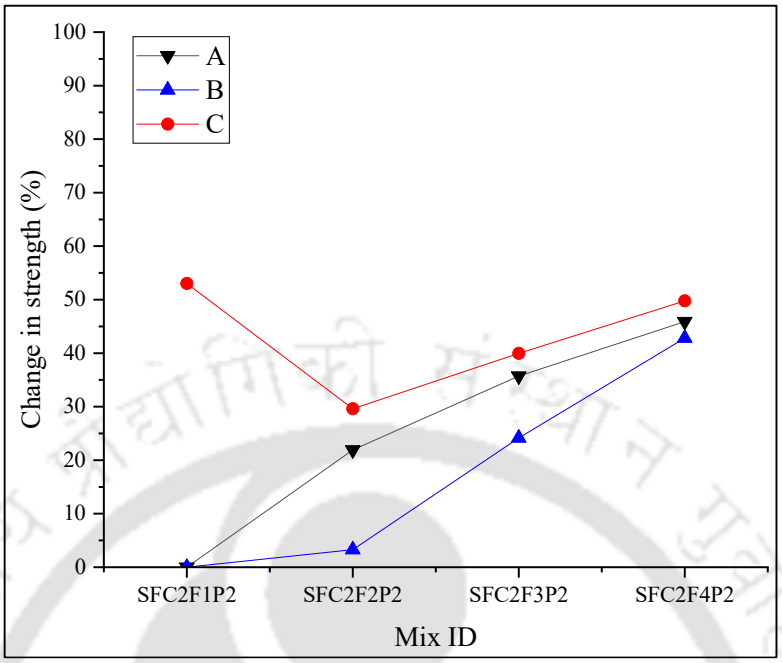

Figure 6.7: (F) Comparative analysis of shear resistance between FCIB triplets (perpendicular to stretcher face) produced using selected mixes at different testing ages.

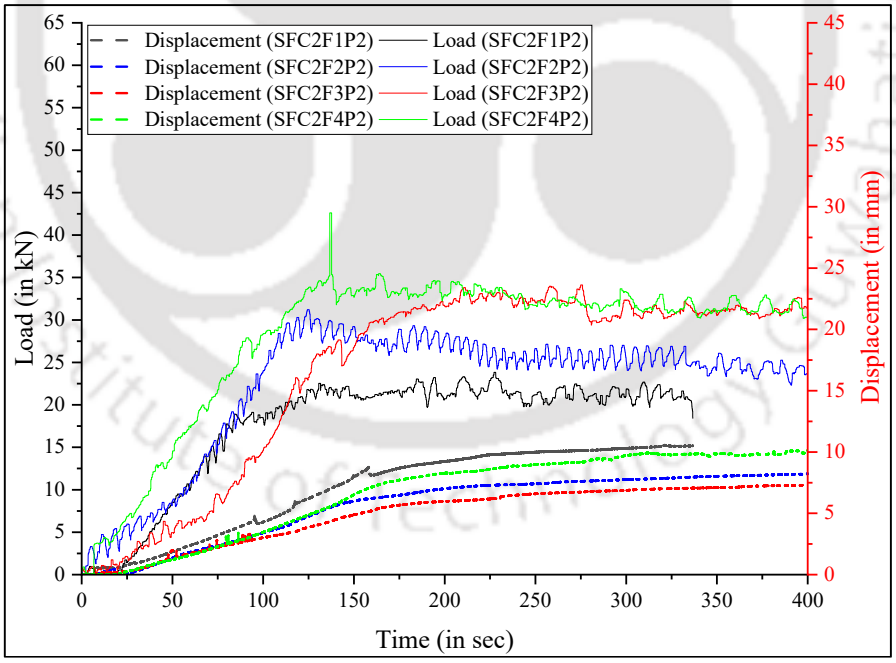

Figure 6.7: (G) Load vs. time and displacement vs. time curves of shear resistance between FCIB triplets (perpendicular to header face) at the testing age of 28 days.

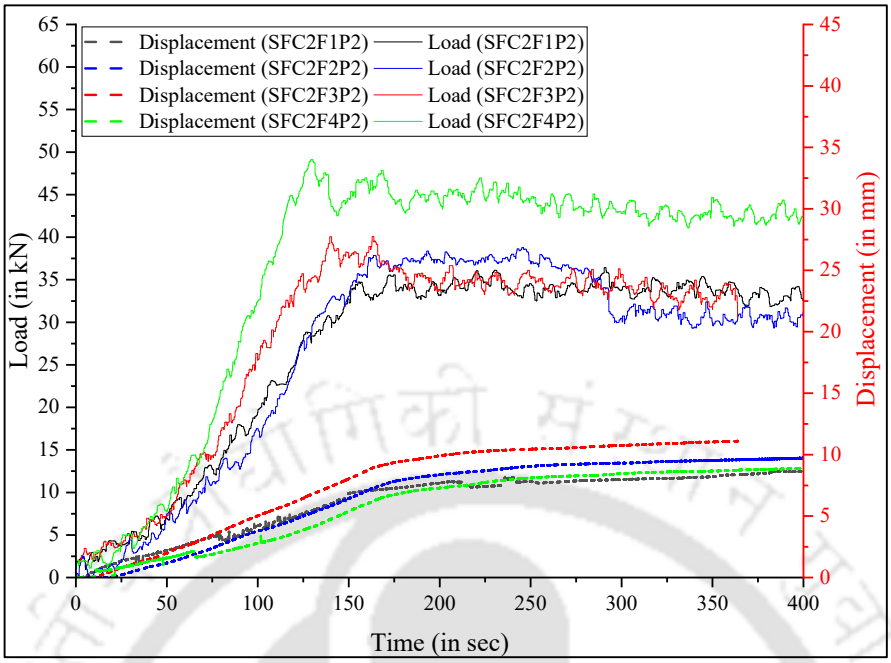

Figure 6.7: (H) Load vs. time and displacement vs. time curves of shear resistance between FCIB triplets (perpendicular to header face) at the testing age of 56 days.

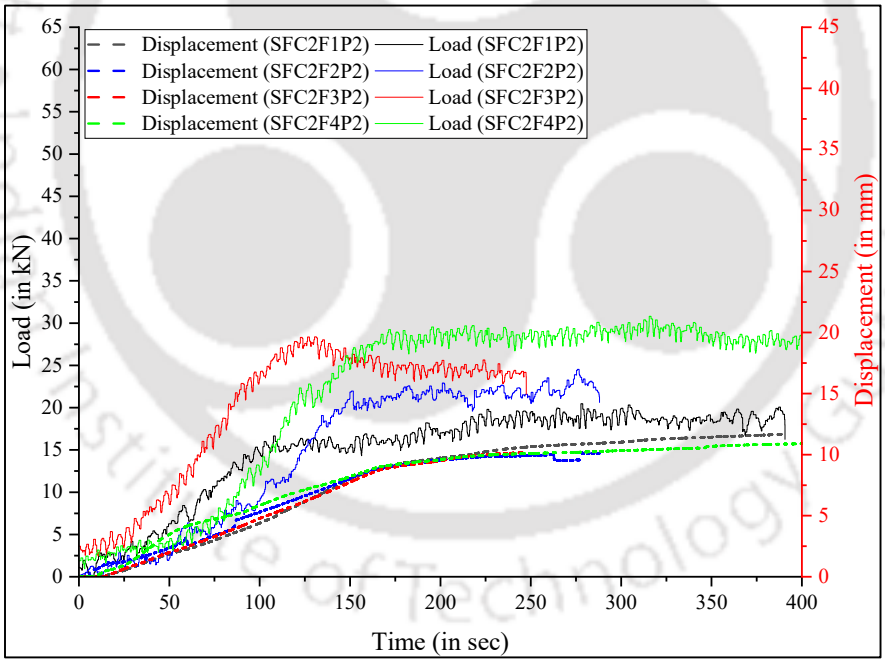

Figure 6.7: (I) Load vs. time and displacement vs. time curves of shear resistance between FCIB triplets (perpendicular to stretcher face) at the testing age of 28 days.

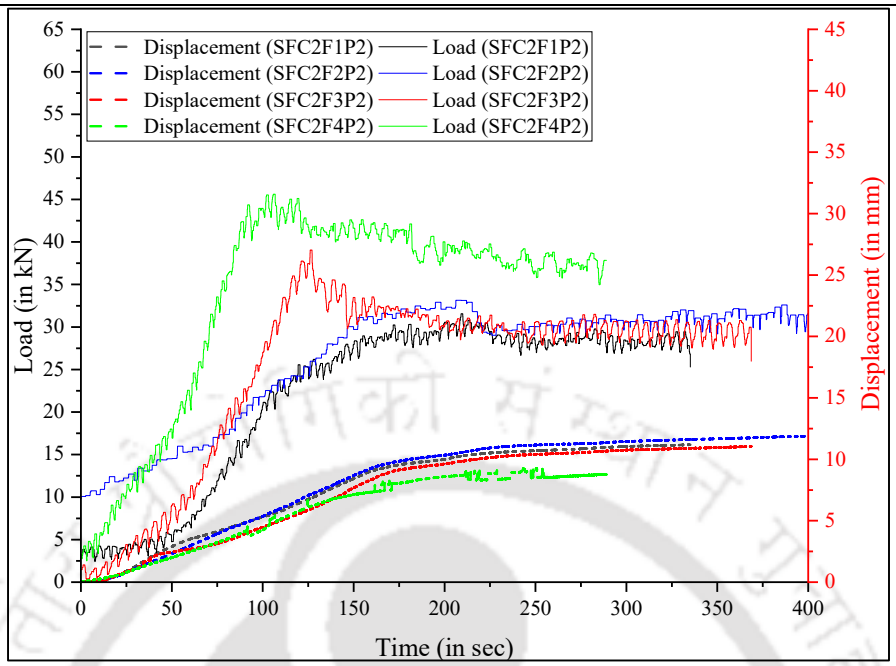

Figure 6.7: (J) Load vs. time and displacement vs. time curves of shear resistance between FCIB triplets (perpendicular to stretcher face) at the testing age of 56 days.

Note: In figures 6.7E, 6.7F, description of adopted various legends is provided below.

A: Comparison of all the mixes with SFC2F1P2 at 28 days, B: Comparison of all the mixes with SFC2F1P2 at 56 days, C: Comparison between 28 days and 56 days shear resistance of all mixes.

The comparative analysis of FCIB triplets under shear resistance (both perpendicular to header face and stretcher face) with respect to the corresponding compressive strength of FCIB triplets are presented in figures 6.8A, 6.8B. From, the results of comparative analysis, it is further evident that the lower particle size of FA and its early pozzolanic reaction are enhancing the early age shear resistance of FCIB by presenting an incremental trend in the comparative analysis at 28 days in figures 6.8A, 6.8B [Ramamurthy et al., 2009, Feng et al., 2018]. Further, at later ages the comparative analysis of shear resistance perpendicular to header face is presenting a decremental but less significant trend, where as in the case of shear resistance perpendicular to the stretcher face these variations are very minimal and insignificant owing to the synergistic effect of already high shear resistance at early age, limited pozzolanic activity at later age and the geometric effect of lower load bearing cross-sections (as described in later part of this section) [Xu and Sarkar, 1994, Ramamurthy et al., 2009, Feng et al., 2018, Sevim and Sengul, 2021]. Moreover, these FCIB triplets under shear forces are presenting a prolonged load bearing capacity even after the primary failure of sample in consistent with the compressive strength of FCIB and FCIB triplets. This can be attributed to the

synergistic effect of the high fibre and FA contents, which improve the microstructure of fiber-matrix interface thereby resulting in enhancement of the ductility behaviour of FC [Huang, 2001, Pan et al., 2007, Ramamurthy et al., 2009, Ganesan et al., 2015, Feng et al., 2018, Vishavkarma and Harish, 2024, Ahmad et al., 2022, Khan et al., 2022]. Further, a close observation of the mechanical interactions of the FCIB triplets under shear as presented in figures 6.7A, 6.7B, reveals that only few keys are participating in the shear resistance. In the case of loading condition perpendicular to header face, it is to be noted that only the keys 2, 3, 4, 6, 7 and 8 are participating as loadbearing components. On the other hand, in the case of loading condition perpendicular to stretcher face, the keys/locks 1, 4, 5 and 8 on one side of FCIB and keys 2, 3, 6 and 7 on the other side are participating as loadbearing components. This is further evident from the failure patterns presented in figures 6.8C, 6.8D, where only the keys/locks previously mentioned as loadbearing components are experiencing failure. Furthermore, only the loadbearing components with least cross-sectional area are experiencing failure. For instance, in the case of loading condition perpendicular to header face, keys 2 and 3 and keys 7 and 6 are acting together as single component and hence the keys 4 and 8 are experiencing failure due to their lower cross-sectional area when compared to the above-mentioned combined component. On the other hand, in the case of loading condition perpendicular to stretcher face, though the keys 2 and 3 and keys 7 and 6 are acting together as single component they are interacting with each other on one side of the FCIB, whereas on the other side keys 1, 4 are interacting with 5, 8. Hence, the effective areas are counter balancing each other, contributing to geometric effects leading to higher shear resistance for the case of loading condition perpendicular to stretcher face. Here it is to be noted, that though the load bearing capacity (figures 6.7G, 6.7H, 6.7I and 6.7J) in both the cases i.e., in the direction of perpendicular to the header face as well as stretcher face is equivalent, however due to the variations in the load bearing interlocking keys their respective shear resistances are varying. This equivalent load bearing capacity can be attributed to the equivalent failure sections (weakest sections) in both the cases. On the other hand, the effective load bearing cross-section is lower in the case of loading direction perpendicular to stretcher face resulting in higher shear resistance.

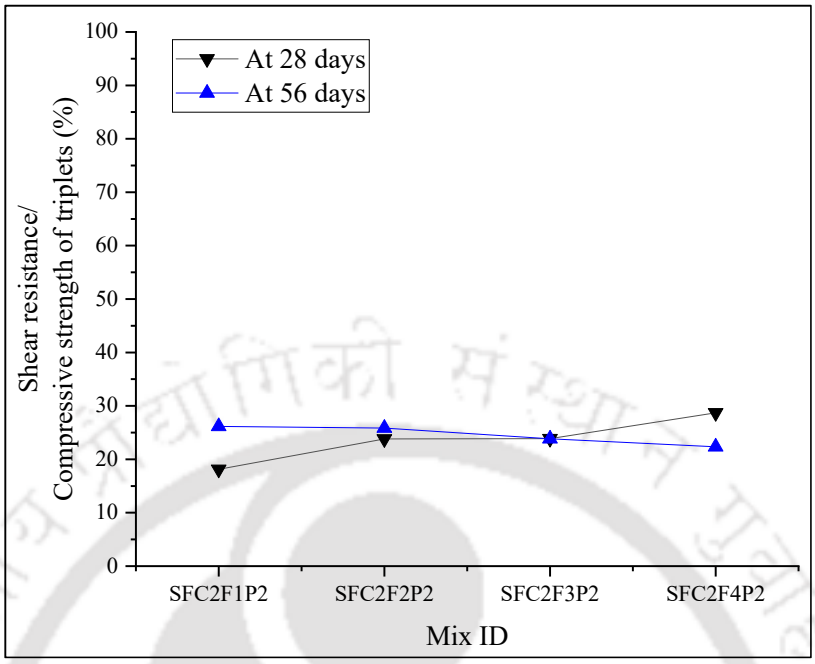

Figure 6.8: (A) Comparative analysis between shear resistance of FCIB triplets (perpendicular to header face) and the corresponding compressive strength of FCIB triplets at various testing ages.

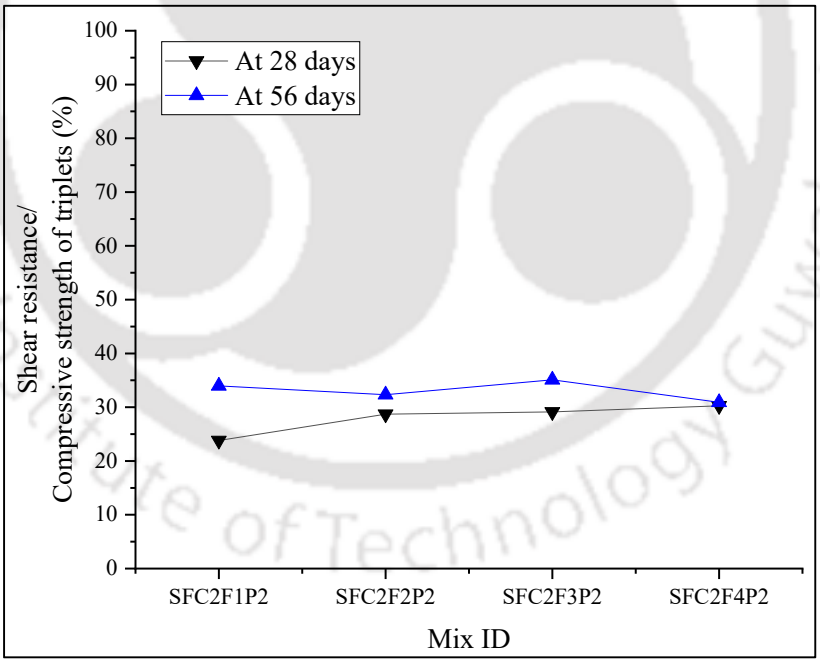

Figure 6.8: (B) Comparative analysis between shear resistance of FCIB triplets (perpendicular to Stretcher face) and the corresponding compressive strength of FCIB triplets at various testing ages.

Figure 6.8: (C) Typical failure pattern of FCIB prisms (triplets) under shear forces perpendicular to header face.

Figure 6.8: (D) Typical failure pattern of FCIB prisms (triplets) under shear forces perpendicular to stretcher face.

6.3.3 PERMEATION CHARACTERISTICS OF FCIB

In addition to their mechanical properties, masonry units' permeation characteristics have a significant impact on the performance and safety of masonry structures. The crucial permeation characteristics that determine whether a particular type of IB is suitable for a given application are the water absorption capacity of masonry units and the water permeability of the material used to create such masonry units. Having studied the mechanical properties of the FCIBs prepared using the selected mixes viz. SFC2F1P2,

SFC2F2P2, SFC2F3P2 and SFC2F4P2, as a next step, permeation characteristics of above concrete mixes is discussed in this section.

6.3.3.1 WATER ABSORPTION AND PERMEABILITY OF FCIB MADE WITH SELECTED MIXES

The water absorption of the proposed FCIB and the permeability of the corresponding FC mix are carried out in accordance with IS 3495-2: 2019 and IS 3085: 2021 (using the proposed sealing mechanism). Further, the results of these experiments are presented in figures 6.9A, 6.9B. Furthermore, various comparative analysis as described in the previous section are presented in figures 6.9C, 6.9D. The water absorption of the FCIB made with selected mixes, at the age of 28 days is found to be 11% ± 1%, indicating a very minimal variation with increase in FA and SP content which is also evident from scatter A of figure 6.9C. On a similar note, the permeability of these mixes at the age of 28 days is in the order of 10^{-4} cm/s and exhibits minimum variation with FA and SP content. (observed in figure 6.9B and scatter A of figure 6.9D). Comparative analysis of permeability of selected mixes in this section with the permeability of similar FC mixes as reported in chapter 4 of this thesis but without SP and with reduced fiber content (with a design density of 1500 kg/m^3 (FC2) consisting of cement: sand: FA = 1:1:1, W/S = 0.3, and 0.05% replacement of total solids with PP fiber) indicate that the permeability of selected mixes discussed in this section is relatively lesser. The reduction in permeation characteristics of FC2 mixes with SP can be attributed to the reduction in pore connectivity due to the enhanced packing efficiency of the matrix as a result of the dispersion effect by SP (figure 4.11A and 6.9E) [Huang, 2001].

Further, at the later age, the mixes with lower FA content viz. SFC2F1P2 and SFC2F2P2 mixes are exhibiting an increase in the water absorption with increase in age from 28 to 56 days (observed in figure 6.9A and scatter B, C of figure 6.9C). Contrary to above, minor reduction in the permeability of SFC2F1P2 mix at the age of 56 days in comparison with the same at the age of 28 days (observed in figure 6.9B and scatter B, C of figure 6.9D), is noted which indicates rise in its tortuosity. Further, the mixes with high FA and SP content viz. SFC2F3P2 and SFC2F4P2 mixes are exhibiting a minor reduction in the water absorption as well as permeability at the age of 56 days (observed in figure 6.9A and scatter B, C of figure 6.9C). The above reduction in permeation mechanism can

be attributed to the densification of microstructure due to adoption of appropriate SP dosage and pozzolanic activity as discussed in the earlier sections. Hence, it is rational to say that though PP fiber content increase the permeability of FC, the effect of FA and SP on densification of matrix and subsequent reduction in permeation is more predominant.

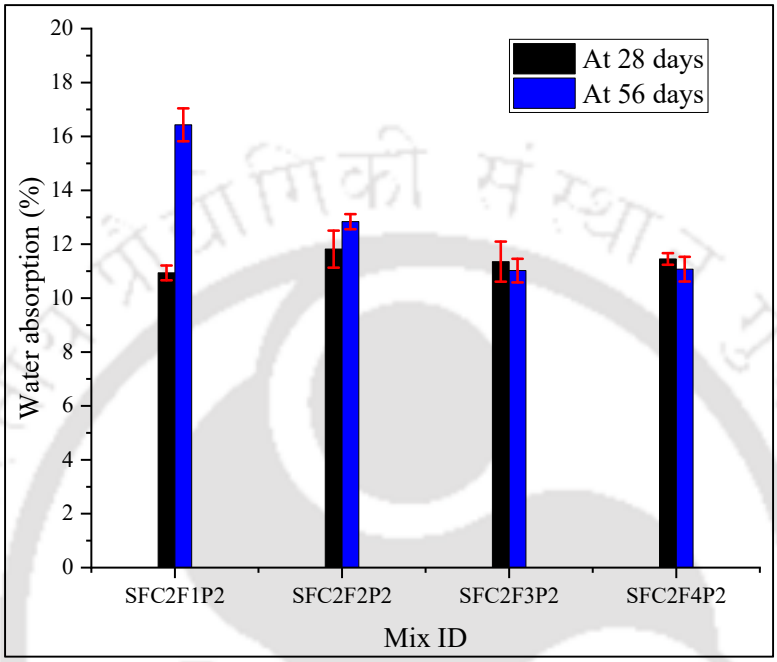

Figure 6.9: (A) Effect of variation in SP dosage and FA level on the water absorption capacity of FCIB prepared using the selected mixes.

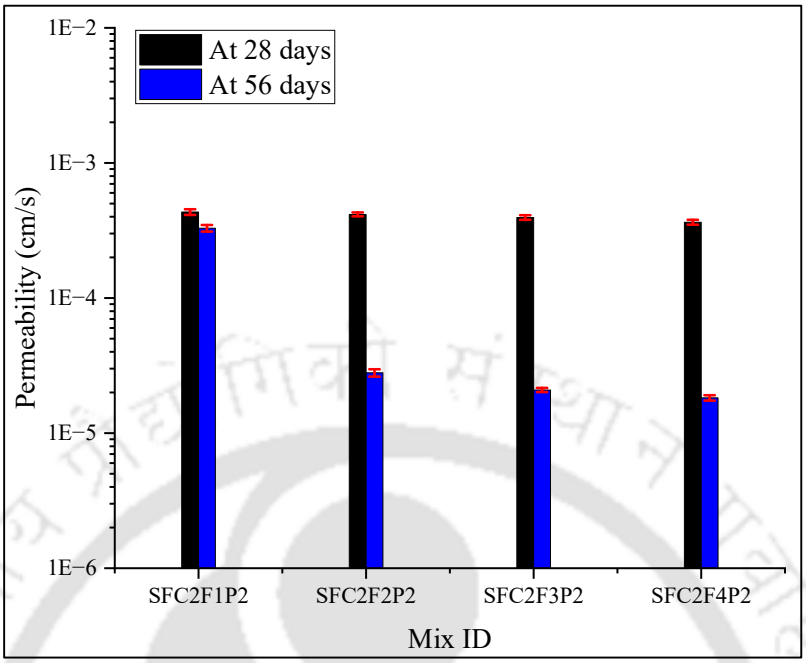

Figure 6.9: (B) Effect of variation in SP dosage and FA level on the permeability of FC samples prepared using the selected mixes.

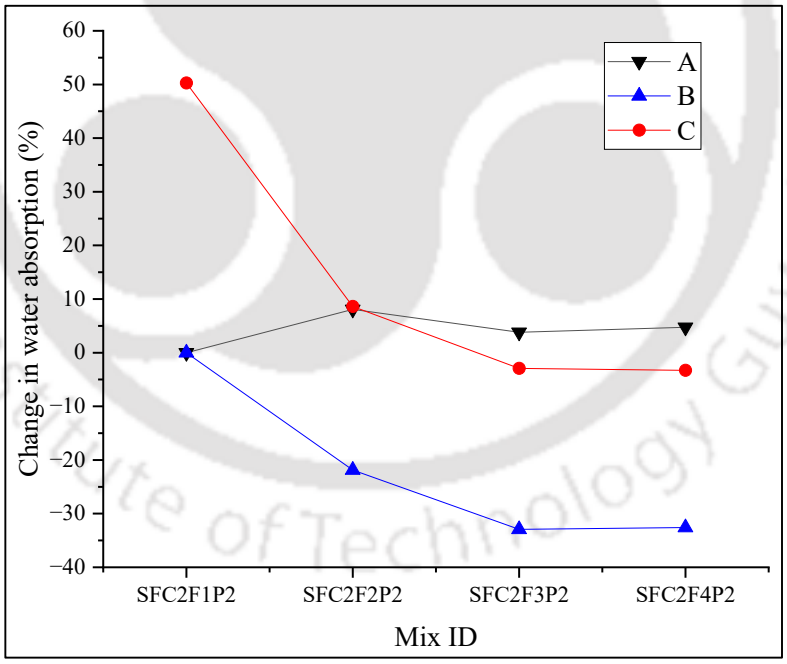

Figure 6.9: (C) Comparative analysis of water absorption capacity of FCIB prepared using the selected mixes.

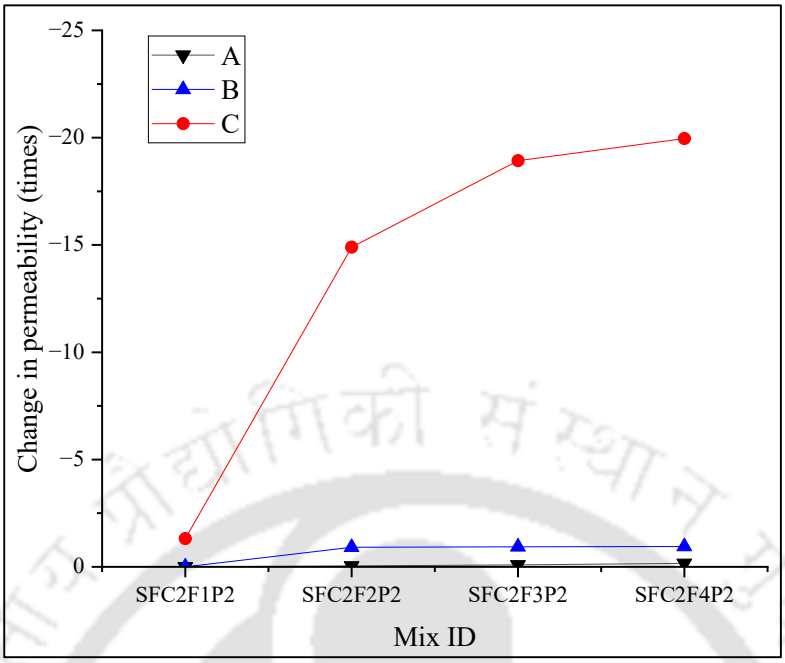

Figure 6.9: (D) Comparative analysis of permeability of FC samples prepared using the selected mixes.

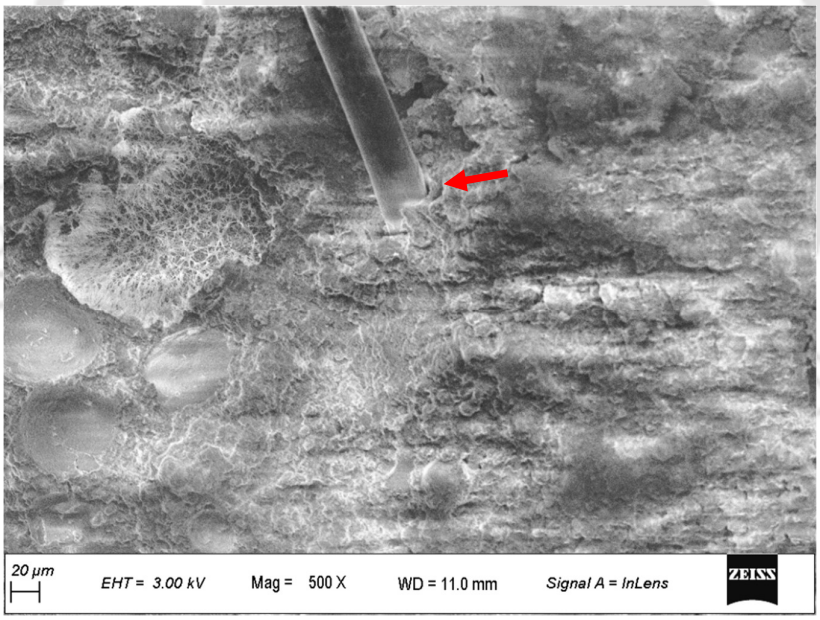

Figure 6.9: (E) SEM image of the fiber-matrix interface at 0.50 KX magnification.

Note: In figures 6.9C, 6.9D, description of adopted various legends is provided below.

A: Comparison of all the mixes with SFC2F1P2 at 28 days, B: Comparison of all the mixes with SFC2F1P2 at 56 days, C: Comparison between 28 days and 56 days water absorption/ permeability of all mixes.

6.4 SUMMARY

The various mechanical properties and permeation characteristics of the proposed IB produced using the selected mixes from the chapter 5 are being studied in his chapter. Firstly, the compressive strength of the proposed FCIB using the selected mixes is studied at the curing age of 28 days and 56 days. Due to the variation in IB pattern, shape and size, the compressive strength of FCIB is found to be 57% to 74% of FC cubes of size 50 mm which is in line with the existing literature. However, out of all the mixes, only the SFC2F4P2 mix (at 56 days of curing) meets the minimum compressive strength requirement of 20.7 N/mm^2 as recommended by ASTM C1372-23, for its intended use as dry-cast segmental retaining wall units. As a next step, the mechanical properties i.e. compressive strength and shear resistance of the masonry triplets prepared using the proposed FCIB is examined. It is discovered that the compressive strength of FCIB triplets ranges from 30% to 51% of FCIB, which is in line with research results reported by Jaafar et al., 2006. Further, these FCIB triplets have a shear resistance that ranges from 18% to 36% of their compressive strength when loading is in a direction perpendicular to the header or stretcher face. Here it is to be noted that, when the loading direction is perpendicular to the stretcher face, the effective load bearing cross-section is lower, which results in the higher shear resistance. Additionally, due to the improved ductility behaviour derived from PP fibre, both FCIB and triplets (under compressive or shear forces) exhibit a prolonged load bearing capacity. Furthermore, the water absorption by these FCIB's is in the range of 10% to 17% at various curing ages, which is within the limits recommended by ASTM C1372-23. On the other hand, these FC2 mixes are exhibiting a water permeability in the order of 10^{-5} cm/s which is higher than that of the conventional concrete. Hence, the proposed FCIB produced with SFC2F4P2 mix (at 56 days of curing) has the potential to be used in dry cast segmental retaining walls to facilitate dissipation of pore water pressure behind retaining walls. However, further studies are needed to verify the pore water pressure dissipation effect when used in retaining walls.

CHAPTER 7

CONCLUSIONS AND SCOPE FOR FUTURE WORK

7.1 CONCLUSIONS

The key findings from this research work are summarized in this section. The research on FCIB that are presented here can be divided into three main phases viz. (I) Influence of variation in foam content on properties of FC mixes with FA and PP fiber (II) Combined effect of different levels of FA (as replacement for sand) and fiber on spreadability and mechanical properties of FC (III) Development of FCIBs produced with FA and PP fiber-based mixes for dry-cast segmental retaining walls.

These three sections, which relate to the properties of the materials employed and the range of parameters evaluated, provide the results drawn from the experimental research.

7.2 INFLUENCE OF VARIATION IN FOAM CONTENT ON PROPERTIES OF FC MIXES WITH FA AND PP FIBER

Spreadability, strength, and water permeability of FC are tested using a total of 24 mix proportions that included FA, PP fiber, and pre-formed foam as binary and ternary replacements of solids.

The succeeding conclusions are drawn:

- In general, the replacement of solids with foam, FA and PP fiber individually have reduced the spread of FC mixes due to the higher cohesiveness of FC mixes, finer size particles and high-water demand of FA, and reduction in water content due to water adsorption by fiber and restriction in movement of particles by fiber. Further, the combined effect replacement of solids with foam, FA, and PP fiber (e.g., CFaPs and FCFaPs) showed an aggravated reduction in spread percentage of FC mixes as a consequence of the synergistic effect.

- The mechanical properties of all the mixes studied (at 56 days of testing) have significantly increased, when FA replaces 50% of the fine aggregate (300 μm) attributing to its pozzolanic effect, whereas replacement of the 0.05% of total solids (by weight) with PP fiber has shown minor reduction. Further, combination

mixes with both FA and PP fiber (i.e., FCFaPs) have shown a significant improvement in mechanical behaviour indicating the dominant role of FA from strength perspective.

- Replacement of solids with foam and PP fiber individually have increased the permeation of FC mixes due to modifications in the pore structure of concrete. On the other hand, replacement of 50% of sand with Class F FA in FC mixes has negative effect on permeation due to creation of denser microstructure. However, in combined mixes say FC1FaPs, the enhancement of permeation due to fiber addition outperforms the decrement in permeation due to FA addition and subsequently results in overall increment of permeation.
- A novel sealing mechanism to measure the water permeability of FC at higher pressures has been attempted with an iron clamp and spiral cylindrical casing system to compress the rubber tube onto the sidewalls of the sample and this is found to be effective up to a pressure head of 7 kg/cm^2. Hence, further studies are necessitated in this direction to enhance the sealing technique for highly impermeable FC samples which may require still higher-pressure head for conducting permeability test.

7.3 COMBINED EFFECT OF DIFFERENT LEVELS OF FA (AS REPLACEMENT FOR SAND) AND FIBER ON SPREADABILITY AND MECHANICAL PROPERTIES OF FC

Fresh state and mechanical properties viz. spreadability, density, compressive strength, split tensile strength and flexural strength are tested for the proposed 59 FC2 mix proportions that included FA, PP fiber, pre-formed foam and SP as ternary and quaternary replacements of solids.

The succeeding conclusions are drawn:

- The experimental results show that a constant SP dosage of 0.25% (% by weight of cement) is needed for every 25% replacement of sand with FA in order to achieve the desired consistency in terms of spreadability (minimum 40%). On a similar note, W/S (without SP addition) in the range of 0.3 to 0.425 for FC2 is needed for 0% to 100% replacement of sand with FA in order to achieve the aforementioned desired consistency. Moreover, it has been found that in order to

achieve the desired consistency in terms of spreadability for FC2 mixes, an additional W/S of 0.005 or 0.05% of SP dosage (% by weight of cement) is always required for every 0.2% replacement of total solids with PP fiber.

- The compressive strength and split tensile strength of mixes constantly increased with increase in FA level, whereas an inverted 'U' trend with maximum strength at 0.4% PP fiber level have been observed. This can be attributed to the pozzolanic reaction by FA, the fiber matrix interactions and restriction of crack propagation by PP fiber. On the other hand, both the matrix modifications have presented a consistent increase in the flexural strength of FC2 mixes. This can be attributed to the enhanced shear behaviour of FC due to the use of chopped 12 mm PP fiber. Furthermore, the mixes with SP instead of additional W/S have aggravated the synergistic effect in the enhancement of the mechanical properties of all the mixes studied. This can be attributed to the improvement in microstructure of fiber-matrix zone resulting from enhanced packing due to usage of SP.
- The quaternary replacement of solids has resulted in significant enhancements in the compressive strength, split tensile and flexural strength of FC2 mixes up to 29 N/mm^2, 3.43 N/mm^2 and 9.38 N/mm^2 respectively. Further, the f_t/f_c and f_{mor}/f_c of these mixes have significantly increased up to 0.26 and 1.2 respectively.
- As a result of their highest compressive strength (meeting ASTM C1372-23 guidelines), highest split tensile strength, satisfactory flexural strength, and greatest improvement in the f_t/f_c and f_{mor}/f_c, among all of the proposed FC2 mixes, the mixes SFC2F1P2, SFC2F2P2, SFC2F3P2 and SFC2F4P2 have been chosen for further research.

The aforementioned FC mixes have been selected as the potential FC candidate for its intended use in the production of IB for dry cast segmental retaining wall application. It is to be noted that, these mixes are satisfying the ASTM C1372-23 guidelines, based on cube strength results. Hence, further research is carried out to study the potential of these selected mixes as FCIB for retaining wall application.

7.4 DEVELOPMENT OF FCIB WITH FA AND PP FIBER BASED MIXES FOR DRY-CAST SEGMENTAL RETAINING WALLS

The compressive strength, shear resistance and permeation characteristics of FCIB produced using the selected mixes have been studied for samples at the age of 28 days and 56 days.

The succeeding conclusions are drawn:

- The compressive strength of FCIB is in the range of 57% to 74% of FC cubes of size 50 mm, as a result of the variation in IB pattern, shape and size, which is in line with the existing literature.
- Among the FCIB produced using the selected mixes, the mix SFC2F4P2 is satisfying the minimum compressive strength criteria of 20.7 N/mm^2 as dry cast segmental retaining wall units in accordance with ASTM C1372-23.
- The compressive strength of FCIB triplets is found to range from 30% to 51% of FCIB, due to the variation in IB pattern, shape and size.
- Under loads perpendicular to the header or stretcher face, the FCIB triplets exhibit a shear resistance varying between 18% and 36% of their compressive strength.
- Both FCIB and triplets demonstrate a prolonged load bearing capacity (under compressive or shear forces) because of the improved ductility behaviour derived from PP fiber.
- The water absorption capacity of these FCIBs falls between 10% to 17% at different curing ages, adhering to ASTM C1372-23 recommended limits.
- FC2 mixes are showing a water permeability of approximately 10^{-5} cm/s (higher than conventional concrete) and suitable for the intended application for dissipation of pore water pressure.

The above-mentioned conclusions drawn from this study are applicable to the characteristics of materials used and the range of parameters considered. To summarize, this thesis is an attempt to determine the mix composition of FC which could result in desired strength as well as permeability for its intended application in retaining walls to

facilitate dissipation of pore water pressure. Based on the comprehensive, experimental investigations carried out, it was found that FCIB made with SFC2F4P2 mix (at 56 days of curing) has the potential to be utilised in dry cast segmental retaining walls. Nevertheless, more research is required to verify the pore water pressure dissipation effect in retaining walls.

7.5 SCOPE FOR FUTURE WORK

The following areas can be the focus of future research to enhance the research output on FCIB in order to make it more useful to the construction industry:

i) Further research on matrix modification can be conducted using additional admixtures, fibers, and chemical techniques, such as FA (class C), rice husk ash, silica fume, ground granulated blast furnace slag, geopolymer concrete, etc., in order to enhance the mechanical properties of FC.

ii) Research on the FC's permeability and clogging potential along with the aforementioned matrix modifications can be carried out.

iii) Research on the microstructure of concrete and chemical analysis can be conducted along with experimental investigations on functional characteristics to examine the effects of adding different admixtures to FC.

iv) Investigations on the functional characteristics of masonry structures such as buildings, retaining walls, etc., constructed using the developed FCIB.

v) Durability studies to analyze the behaviour of FC in chemically hazardous environment can be conducted.

PUBLICATIONS/ PROJECTS/ AWARDS/ ACHIEVEMENTS BASED ON THE PRESENT RESEARCH WORK

Published in Refereed conferences: -

1. Wagh, C., Ranjani, I.S., Kamisetty, A. 2020. Thermal properties of foamed concrete; a review. 3rd International Conference on Innovative Technologies for Clean and Sustainable development (ITCSD2020), Chandigarh, India, Feb 2020, Springer-RILEM Bookseries, Proceedings. https://doi.org/10.1007/978-3-030-51485-3_9
2. Kamisetty, A., Ranjani, I.S., and Kumar, A. 2022. Exploring the Suitability of Using Foam Concrete as Pore Pressure Dissipation Measure for Slope Stability: A State of Art Review. Materials today Proceedings of International Conference on advances in Construction Materials and Structures (ICCMS 2021), December 15-17, 2021. https://doi.org/10.1016/j.matpr.2022.04.375
3. Kamisetty, A., Kumar, A. and Gandhi, I.S.R. 2023. Suitability of foam Concrete and Confined Masonry for Retaining Walls application in seismically active regions: A Review. 17th Symposium on Earthquake Engineering 2022, Springer nature.
4. Kamisetty, A., Gandhi, I.S.R., and Kumar, A., Pandit, A. A., Royal, B. N. Studies on the effect of replacement of sand with fly ash on foam concrete properties for use in Interlocking blocks. SEC 2024, (Accepted).

Published in Refereed journals: -

1. Kamisetty, A., Gandhi, I.S.R., and Kumar, A. 2023. Combined effect of fly ash and fiber on spreadability, strength and water permeability of foam concrete, Journal of building engineering, Journal of Building Engineering, Volume 78, 1 November 2023, 107607. https://doi.org/10.1016/j.jobe.2023.107607

Submitted/ Under Review Papers for Publication in Refereed journals: -

1. Kamisetty, A., Gandhi, I.S.R., and Kumar, A. Development of Foam Concrete Interlocking Blocks produced with fly ash and polypropylene fiber-based mixes

for dry-cast segmental retaining walls. Journal of Building Engineering (Submitted/Under Review).

Projects based on the present research work

1. NEWGEN IEDC project proposal titled "Low cost, energy efficient interlocking block confined masonry for seismic resistant structures in North East India". Team: Abhishek Kamisetty, Wagh Chandrashekar, Khwairakpam Selija, Principal Investigator: Dr. Indu Siva Ranjani Gandhi, Co-investigator: Dr. Abhishek Kumar, Funding Agency: National Science and Technology Entrepreneurship Development Board (NSTEDB), Department of Science & Technology (DST).

Awards/ Achievements based on the present research work

1. Won the 1st position in poster presentation competition at Indian urban housing conclave (IUHC 2022) under the theme of "Future of affordable housing in India" organised under Pradhan Mantri Awas Yojana by Ministry of Housing and Urban Affairs, Govt. of India.
2. Presented among the selected projects in December, 2022 at Namghar Samaroh, Auniati Satra, North Guwahati. On topic Low cost, energy efficient interlocking block confined masonry for affordable housing. Student team: Kamisetty, A., Wagh, C., Sahu, A. K., Investigators: Gandhi, I.S.R., and Kumar, A. Organised by Dean R&D affairs, IIT Guwahati.
3. Presented on behalf of IIT Guwahati in the event "Research work presentation (Structural engineering)" in Civil Conclave (Inter IIT), 2022. Title: Suitability of foam concrete, interlocking blocks and confined masonry for seismic resistance of buildings. Team: Abhishek Kamisetty. Organised by IIT Roorkee. (IIT Guwahati secured 3rd position in overall performance among all IIT's).
4. Presented among the selected projects at G20 summit in February, 2023. On topic Low cost, energy efficient interlocking block confined masonry for affordable housing. Student team: Kamisetty, A., Wagh, C., Sahu, A. K., Investigators: Gandhi, I.S.R., and Kumar, A. Organised by IIT Guwahati.

LIST OF REFERENCES

ACI Committee 523. (1993). “Guide for cellular concrete above 50 pcf and for aggregate concretes above 50 pcf with compressive strengths less than 2500 psi.” ACI 523.3R-93, American Concrete Institute, Farmington Hills, MI.

ACI Committee 523. (1996). “Guide for precast cellular concrete floor, roof and wall units.” ACI 523.2R–96, American Concrete Institute, Farmington Hills, MI,.

ACI Committee 523. (2006). “Guide for cast-in-place low-density cellular concrete.” ACI 523.1R-06, American Concrete Institute, Farmington Hills, MI.

ACI Committee 523. (2009). “Guide for design and construction with autoclaved aerated concrete panels.” ACI 523.4R-09, American Concrete Institute, Farmington Hills, MI.

Afraz, A., and Ali, M. (2021). “Effect of banana fiber on flexural properties of fiber reinforced concrete for sustainable construction.” Engineering Proceedings, Volume 12(1), 63.

Agrawal, Y., Gupta, T., Sharma, R.,Panwar, N. L., and Siddique, S. (2021). “A comprehensive review on the performance of structural lightweight aggregate concrete for sustainable construction.” Construction Materials, Volume 1, Pages 39-62. https://doi.org/10.3390/constrmater1010003

Agustini, N. K. A., Triwiyono, A., Sulistyo, D., and Suyitno, S. (2021). “Mechanical properties and thermal conductivity of fly ash-based geopolymer foams with polypropylene fibers.” Applied Science, Volume 11(11), 4886. https://doi.org/10.3390/app11114886

Ahmad, S., Azad, A. K., and Loughlin, K. F. (2012). “Effect of the key mixture parameters on tortuosity and permeability of concrete.” Journal of Advanced Concrete Technology, Volume 10, Pages 86-94.

Ahmad, S. (2014). “To study the behavior of interlocking of masonry units/blocks.” IOSR Journal of Engineering, Volume 4(3), Pages 39-47.

Ahmad, J., Burduhos-Nergis, D.D., Arbili,M.M., Alogla, S.M., Majdi, A., and Deifalla, A.F. (2022). “A Review on Failure Modes and Cracking Behaviors of Polypropylene Fibers Reinforced Concrete. Buildings 2022, 12, 1951. https://doi.org/10.3390/buildings12111951

Aldridge, D., Dhir, R. K., Newlands, M. D., and McCarthy, A. (2005). "Introduction to foamed concrete: What, why, how?" In Proceedings of the International Conference Held at the University of Dundee, Scotland, UK, Pages 1-14.

Ali, M., Gultom, R.J., and Chouw N. (2012). "Capacity of innovative interlocking blocks under monotonic loading." Construction and Building Materials, Volume 37, Pages 812-821.

Amran, Y. H. M., Farzadnia, N., and Ali, A. A. A. (2015). "Properties and applications of foamed concrete; a review." Construction and Building Materials, Volume 101, Part 1, Pages 990-1005.

Amran, Y. H. M., Alyousef, R., Alabduljabbar, H., Khudhair, M. H. R., Hejazi, F., Alaskar, A., Alrshoudi, F., and Siddika, A. (2020a). "Performance properties of structural fibred-foamed concrete." Results in Engineering, Volume 5, 100092.

Amran, M., Fediuk, R., Vatin, N., Huei Lee, Y., Murali, G., Ozbakkaloglu, T., Klyuev, S., and Alabduljabber, H. (2020b). "Fibre-reinforced foamed concretes: A review." Materials, Volume 13(19), 4323.

Anand, K.B., and Ramamurthy, K. (1999). "Techniques for accelerating masonry construction." International Journal for Housing Science and its Applications, Volume 23(4), Pages 233-241.

Anand, K.B., and Ramamurthy, K. (2000). "Development and performance evaluation of interlocking-block masonry." ASCE, Journal of Architectural Engineering, Volume 6(2).

Anand, K.B., Vasudevan, V., and Ramamurthy, K. (2003). "Water permeability assessment of alternative masonry systems." Building and Environment, Volume 38(7), Pages 947-957.

ASTM C109/C109M-21. (2021). "Standard test method for compressive strength of hydraulic cement mortars (using 2-in. or [50 mm] cube specimens)." American Society for Testing and Materials.

ASTM C230-17. (2020). "Standard specification for flow table for use in tests of hydraulic cement." American Society for Testing and Materials.

ASTM C348-21. (2021). "Standard test method for flexural strength of hydraulic-cement mortars." American Society for Testing and Materials.

ASTM C496-17. (2017). "Standard test method for splitting tensile strength of cylindrical concrete specimens." American Society for Testing and Materials.

ASTM C796-19. (2019). "Standard test method for foaming agents for use in producing cellular concrete using preformed foam." American Society for Testing and Materials.

ASTM C869-11. (2016). "Standard specification for foaming agents used in making preformed foam for cellular concrete." American Society for Testing and Materials.

ASTM C1372-23. (2023). "Standard specification for dry-cast segmental retaining wall units." American Society for Testing and Materials.

ASTM C1314-23b. (2023). "Standard test method for compressive strength of masonry prisms." American Society for Testing and Materials.

ASTM C1611-21. (2021). "Standard test method for slump flow of self-consolidating concrete." American Society for Testing and Materials.

Atoyebi, O. D., Odeyemi, S. O., Bello, S. A., and Ogbeifun, C. O. (2018). "Splitting tensile strength assessment of lightweight foamed concrete reinforced with waste tyre steel fibres." International Journal of Civil Engineering and Technology, Volume 9(9), Pages 1129-1137.

Awang, H., and Ahmad, M. H. (2012). "The effect of steel fiber inclusion on the mechanical properties and durability of lightweight foam concrete." Advanced Engineering Informatics, Volume 48, Pages 9348-9351.

Awang, H., Mydin, A.O., and Roslan, A.F. (2012). "Effect of additives on mechanical and thermal properties of lightweight foamed concrete." Advances in Applied Science Research, Volume 3(5), Pages 3326-3338.

Awang, H., and Ahmad, M. H. (2014). "Durability properties of foamed concrete with fiber inclusion." World Academy of Science, Engineering and Technology International Journal of Civil, Structural, Construction and Architectural Engineering, Volume 8(3), Pages 269-272.

Awang, H., Ahmad, M. H., and Al-Mulali, M. Z. (2015). "Influence of kenaf and polypropylene fibres on mechanical and durability properties of fibre reinforced lightweight foamed concrete." Journal of Engineering Science and Technology, Volume 10(4), Pages 496-508.

Bamforth, P. B. (1987). "The relationship between permeability coefficients for concrete obtained using liquid and gas." Magazine of Concrete Research, Volume 39(138), Pages 3-11.

Batra, S. S., Boddepalli, U., Gandhi, I. S. R., and Panda, B. (2023). "Influence of various admixtures on energy absorption characteristics of foam concrete measured using one dimensional strain analysis test." Materials Today: Proceedings.

Bertero, V.V., Popov, E.P., and Forzani, B. (1980). "Seismic behaviour of lightweight concrete beam column sub assemblages." ACI Journal Proceedings, Volume 77(1), Pages 44-52.

Beskopylny, A. N., Shcherban, E. M., Stel'makh, S. A., Mailyan, L. R., Meskhi, B., Varavka, V., Chernil'nik, A., and Pogrebnyak, A. (2023). "Improved fly ash based structural foam concrete with polypropylene fiber." Journal of Composites Science, Volume 7(2), 76.

Bhattacharyya, S.K., and Agarwal, A.K. (2014). "National labs: research highlights 2014." CSIR–Central Building Research Institute, Roorkee 247 667, India.

Bing, C., Zhen, W., and Ning, L. (2012). "Experimental research on properties of high-strength foamed concrete." Journal of Materials in Civil Engineering, Volume 24(1), Pages 113-118.

Brady, K. C., Watts, G. R. A., and Jones, M. R. (2001). "Specification for foamed concrete." TRL limited, PROJECT REPORT PR/IS/40/01.

BS EN 12390-8. (2019). "Testing hardened concrete, depth of penetration of water under pressure." London, UK: British Standards Institution.

Caggiano, A., Gambarelli, S., Martinelli, E., Nistico, N., and Pepe, M. (2016). "Experimental characterization of the post-cracking response in Hybrid Steel/Polypropylene Fiber-Reinforced Concrete." Construction and Building Materials, Volume 125, Pages 1035-1043.

Cao, T., Zhang, L., Sun, G., Wang, C., Zhang, Y., Yan, N., and Xu, A. (2019). "Model for predicting the tortuosity of Transport paths in cement-based materials." MDPI, Materials, Volume 12(21), 3623.

Castillo-Lara, J. F., Flores-Johnson, E. A., Valadez-Gonzalez, A., Herrera-Franco, P. J., Carrillo, J. G., Gonzalez-Chi, P. I., and Li, Q. M. (2020). "Mechanical properties of natural fiber reinforced foamed concrete." Materials, Volume 13(14), 3060.

Castro-Gomes, J. P. , Pereira de Oliveira, L. A., and Gonilho-Pereira, C. N. (2002). "Discussion of aggregate and concrete water absorption and permeability testing methodology." In: IAHS World Congress on Housing, Coimbra, Portugal, Oktay U, Abrantes V, Tadeu (Eds.).

Chandini, T. J., and Anand, K. B. (2018). "Utilization of recycled waste as filler in foam concrete." Journal of Building Engineering, Volume 19, Pages 154–160.

Chandrappa, A. K., and Biligiri, K. P. (2016). "Comprehensive investigation of permeability characteristics of pervious concrete: A hydrodynamic approach." Construction and Building Materials, Volume 123, Pages 627–637.

Chen, Y., Guan, L., Zhu, S., and Chen. W. (2021). "Foamed concrete containing fly ash: Properties and application to backfilling." Construction and Building Materials, Volume 273, 121685.

Chourasia, A., Singhal, and S., Parashar, J. (2020). "Seismic performance evaluation of full-scale confined masonry building using light weight cellular panels." Journal of Building Engineering, Volume 32, 101473.

CJJ/T 135-2009. "Chinese technical specifications for pervious concrete pavement."

Cox, L. and Dijk, S. V. (2002). "Foam concrete: A different kind of mix." Concrete, Volume 36(2), Pages 54–55.

Crofts, F. S. (1993). "State of the art of mortarless concrete masonry in south africa." Proceedings of the Sixth North American Masonry Conference, June, Philadelphia, Pennsylvania, Pages 875-884.

Dhasindrakrishna, K., Ramakrishnan, S., Pasupathy, K., and Sanjayan, J. (2021). "Collapse of fresh foam concrete: Mechanisms and influencing parameters." Cement and Concrete Composites, Volume 122, 104151.

DIN 1048-5: 1991. "Testing concrete; Testing of hardened concrete (specimens prepared in mould)." Berlin, Germany: German national standard.

Falliano, D., Domenico, D. D., Ricciardi, G., and Gugliandolo, E. (2018). "Experimental investigation on the compressive strength of foamed concrete: Effect of curing conditions, cement type, foaming agent and dry density." Construction and Building Materials, Volume 165, Pages 735-749.

Falliano, D., Domenico, D. D., Ricciardi, G., and Gugliandolo, E. (2019). "Compressive and flexural strength of fiber-reinforced foamed concrete: Effect of fiber content, curing conditions and dry density." Construction and Building Materials, Volume 198, Pages 479-493.

Fedorov, V., and Mestnikov, A. (2018). "Influence of cellulose fibers on structure and properties of fiber reinforced foam concrete." MATEC Web of Conferences, Volume 143, 02008. https://doi.org/10.1051/matecconf/201814302008

Feng, J., Sun, J., and Yan, P. (2018). "The influence of ground fly ash on cement hydration and mechanical property of mortar." Hindawi, Advances in Civil Engineering, Volume 2018, 4023178. https://doi.org/10.1155/2018/4023178

Forghani, R., Totoev, Y., Kanjanabootra, S., and Davison, A. (2016). "Experimental investigation of water penetration through semi-interlocking masonry walls." Journal of Architectural Engineering, Volume 23(1).

Fu, Y., Wang, X., Wang, L., and Li, Y. (2020). "Foam concrete: A state-of-the-art and state-of-the-practice review." Hindawi, Advances in Materials Science and Engineering, Volume 2020, 6153602.

Gandhi, I. S. R., Boddepalli, U., Bisht, R., and Wagh, C. (2023). "Impact of addition of fly ash (as sand replacement) and polypropylene fibers on energy absorption characteristics of foam concrete." Advances in Civil Engineering Materials, ASTM, Volume 12(1).

Ganesan, S., Mydin, M. A. O., Yunos, M. Y. M., and Nawi, M. N. M. (2015). "Thermal properties of foamed concrete with various densities and additives at ambient temperature." Applied Mechanics and Materials, Volume 747, Pages 230-233.

Gencel, O., Kazmi, S. M. S., Munir, M. J., Kaplan, G., Bayraktar, O. Y., Yarar, D. O., Karimipour, A., and Ahmad, M. R. (2021). "Influence of bottom ash and polypropylene fibers on the physico-mechanical, durability and thermal performance of foam concrete: An experimental investigation." Construction and Building Materials, Volume 306, 124887.

Ghosh, P. (2009). "Colloid and interface science." (PHI Learning Pvt. Ltd., New Delhi, 2009)

Gokce, H. S., Hatungimana, D., and Ramyar, K. (2019). "Effect of fly ash and silica fume on hardened properties of foam concrete." Constrction and Building Materials, Volume 194, Pages 1-11.

Gopalakrishnan, R., Sounthararajan, V. M., Mohan, A., and Tholkapiyan, M. (2020). "The strength and durability of fly ash and quarry dust light weight foam concrete." Materials Today: Proceedings, Volume 22, Part 3, Pages 1117-1124.

Grubesa, I. N., Markovic, B., Gojevic, A., and Brdaric, J. (2018). "Effect of hemp fibers on fire resistance of concrete." Construction and Building Materials, Volume 184, Pages 473-484.

Guntakal, S. N., and Selvan, S. (2017). "Application of pervious concrete for pavements: a review." Rasayan Journal of Chemistry, Volume 10(1), Pages 32-36.

Hadipramana, J., Samad, A. A. A., Zaidi, A. M. A., Mohammad, N., and Ali, N. (2013). "Contribution of polypropylene fibre in improving strength of foamed concrete." Advanced Materials Research, Volume 626, Pages 762-768.

Halse, Y., Pratt, P. L., Dalziel, J. A., and Gutteridge, W. A. (1984). "Development of microstructure and other properties in flyash OPC systems." Cement and Concrete Research, Volume 14, Pages 491-498.

Hao, Y., Yang, G., and Liang, K. (2022). "Development of fly ash and slag based high-strength alkali activated foam concrete." Cement and Concrete Composites, Volume 128, 104447.

Hazlin, A. R., Iman, A., Mohamad, N., Goh, W. I., Sia, L. M., Samad, A. A. A., and Ali, N. (2017). "Microstructure and tensile strength of foamed concrete with added polypropylene fibers." MATEC Web of Conferences, Volume 103, 01013.

He, Y., Gao, M., Zhao, H., and Zhao, Y. (2019). "Behaviour of foam concrete under impact loading based on SHPB experiments." Shock and Vibration, Volume 2019, 2065845.

Hilal, A. A., Thom, N. H., and Dawson, A. R. (2014). "Pore structure and permeation characteristics of foamed concrete." Journal of Advanced Concrete Technology, Volume 12, Pages 535-544.

Hilal, A. A., Thom, N. H., and Dawson, A. R. (2016). "Failure mechanism of foamed concrete made with/without additives and lightweight aggregate." Journal of Advanced Concrete Technology, Volume 14, Pages 511-520.

Hu, C., Li, H., Liu, Z., and Wang, Q. (2016). "Research on properties of foamed concrete reinforced with small sized glazed hollow beads." Advances in Building Technologies and Construction Materials, Volume 2016, 5820870. https://doi.org/10.1155/2016/5820870

Huang, W. H. (2001). "Improving the properties of cement–fly ash grout using fiber and superplasticizer." Cement and Concrete Research, Volume 31(7), Pages 1033-1041.

IS 269: 2020. "Ordinary Portland Cement -specification." Bureau of Indian Standards.

IS 2185-4: 2019. "Concrete masonry units -specification part 4 preformed foam cellular concrete blocks." Bureau of Indian Standards.

IS 3085: 2021. "Method of test for permeability of cement mortar and concrete." Bureau of Indian Standards.

IS 3495-1: 2019. "Burnt clay building bricks - Methods of Tests, Part 1 Determination of compressive strength." Bureau of Indian Standards.

IS 3495-2: 2019. "Burnt clay building bricks - Methods of tests, Part 2 Determination of water absorption." Bureau of Indian Standards.

IS 7597: 2019. "Surface active agents - Glossary of terms." Bureau of Indian Standards.

Jaafar, M. S., Thanoon, W. A., Najm, A. M. S., Abdulkadir, M. R. and Ali, A. B. A. (2006). "Strength correlation between individual block, prism, and basic wall panel for load bearing interlocking mortarless hollow block masonry." Construction and Building Materials, Volume 20, Pages 492-498.

Jessie, D. P. J., and Kotteeswaran, S. (2018). "Study on properties of foam concrete using fibers." International Journal of Research & Review, Volume 5(5).

Jones, M., and McCarthy, A. (2005a). "Utilising unprocessed low-lime coal fly ash in foamed concrete." Fuel, Volume 84(11), Pages 1398-1409.

Jones, M. R., and McCarthy, A. (2005b). "Preliminary views on the potential of foamed concrete as a structural material." Magazine of Concrete Research, Volume 57(1).

Jones, M. R., and Zheng, L. (2013). "Energy absorption of foamed concrete from low-velocity impacts." Magazine of Concrete Research, Volume 65(4), Pages 209-219.

Jose, S. K., Soman, M., and Evangeline, S. Y. (2020). "Foamcrete construction blocks using industrial wastes- A sustainable approach." Journal of Physics: Conference Series Volume 1706, 012128.

Kadela, M., Kozlowski, M., and Kukielka, A. (2017). "Application of foamed concrete in road pavement - weak soil system." Procedia Engineering, Volume 193, Pages 439-446.

Karahan, O., and Atis, C. D. (2011). "The durability properties of polypropylene fiber reinforced fly ash concrete." Materials and Design, Volume 32, Pages 1044-1049.

Katz, A., and Thompson, A. (1986). "Quantitative prediction of permeability in porous rock." Physical Review B, Volume 34(11), Pages 8179-8181.

Kavitha, S., and Kala, T. (2016). "Effectiveness of bamboo fiber as a strength enhancer in concrete." International Journal of Earth Sciences and Engineering, Volume 9, Pages 192–196.

Kearsley, E. P., and Booyens, P. (1998). "Reinforced foamed concrete, can it be durable." Concrete Beton, Volume 91, Pages 5-9.

Kearsley, E. P., and Mostert, H. F. (1999). "The use of foamcrete in southern africa." American Concrete Institute, Symposium Paper, SP 172-48, Pages 919-934.

Kearsley, E.P., and Wainwright, P.J. (2000). "The effect of high fly ash content on the compressive strength of foamed concrete." Cement and Concrete Research, Volume 31 (1), Pages 105-112

Kearsley, E.P., and Wainwright, P.J. (2001). "Porosity and permeability of foamed concrete." Cement and Concrete Research, Volume 31(5), Pages 805-812.

Khan, M., Shakeel, M., Khan, K., Akbar, S., and Khan, A. (2022). "A Review on fiber-reinforced foam concrete." MDPI, Engineering Proceedings, Volume 22(1), 13. https://doi.org/10.3390/engproc2022022013

Khwairakpam, S., and Gandhi, I. S. R. (2022). "Comprehensive investigation into the effect of the newly developed natural foaming agents and water to solids ratio on foam concrete behaviour." Journal of Building Engineering, Volume 58, 105042.

Kia, A., Wong, H. S., and Cheeseman, C. R. (2017). "Clogging in permeable concrete: A review." Journal of Environmental Management, Volume 193, Pages 221-233.

Kilic, A., Atis, C.D., Yasar, E., and Ozcan. F. (2003). "High-strength lightweight concrete made with scoria aggregate containing mineral admixtures." Cement and Concrete Research, Volume 33(10), Pages 1595–1599.

Kintingu, S. H. (2009). "Design of interlocking bricks for enhanced wall construction flexibility, alignment accuracy and load bearing." (PhD Thesis, The University of Warwick, School of Engineering).

Klinkenberg, L. J. (1941). "The permeability of porous media to liquids and gases." Drilling and Production Practice, Volume 2(2), Pages 200-213.

Kolias, S., and Georgiou, C. (2005). "The effect of paste volume and of water content on the strength and water absorption of concrete." Cement and Concrete Composites, Volume 27(2).

Kondraivendhan, B., Divsholi, B. S., and Teng, S. (2013). "Estimation of strength, permeability and hydraulic diffusivity of pozzolana blended concrete through pore size distribution." Journal of Advanced Concrete Technology, Volume 11, Pages 230-237.

Kou, S. C., Poon, C. S., and Chan, D. (2008). "Influence of fly ash as a cement addition on the hardened properties of recycled aggregate concrete." Materials and Structures, Volume 41, Pages1191–1201.

Kou, R., Guo, M. Z., Shi, Y., Mei, M., Jiang, L., Chu, H., Zhang, Y., Shen, H., and Xue, L. (2022). "Sound-insulation and photocatalytic foamed concrete prepared with dredged sediment." Journal of Cleaner Production, Volume 356, 131902.

Krishna, A. S., Siempu, R., and Kumar, G. A. V. S. S. (2021). "Study on the fresh and hardened properties of foam concrete incorporating fly ash." Materials Today: Proceedings, Volume 46, Part 17, Pages 8639-8644.

Kudyakov, A. I., and Steshenko, A. B. (2015). "Shrinkage deformation of cement foam concrete." IOP Conference Series: Materials Science and Engineering, Volume 71, 012019.

Laukaitis, A., Zurauskas, R., and Kerien, J. (2005). "The effect of foam polystyrene granules on cement composite properties." Cement and Concrete Composites, Volume 27(1), Pages 41-47.

Lecci, F., Mazzoli, C., Bartolomei, C., and Gulli, R. (2021). "Design of flat vaults with topological interlocking solids." Nexus Network Journal, Volume 23, Pages 607-627.

Lee, H. S., Ismail, M. A., Woo, Y. J., Min, T. B., and Choi, H. K. (2014). "Fundamental study on the development of structural lightweight concrete by using normal coarse aggregate and foaming agent." Materials, Volume 7(6), Pages 4536-4554. doi:10.3390/ma7064536, ISSN 1996-1944

Li, J., Chen, Z., Chen, W., and Xu, Z. (2020). "Seismic performance of precast self-insulation shear walls made by a new type of foam concrete with high strength and low thermal conductivity." Structures, Volume 24, Pages 124-136.

Li, S., Li, H., Yan, C., Ding, Y., Zhang, X., and Zhao, J. (2022). "Investigating the mechanical and durability characteristics of fly ash foam concrete." Materials, Volume 15(17), 6077. https://doi.org/10.3390/ma15176077

Lin, L. C. Q. (2020). "Preliminary study on lightweight interlocking block design." (Bachelor's report, Lee Kong Chian Faculty of Engineering and Science, Universiti Tunku Abdul Rahman).

Liu, X., Chia, K.S., and Zhang, M.-H. (2011). "Water absorption, permeability, and resistance to chloride-ion penetration of lightweight aggregate concrete." Construction and Building Materials, Volume 25, Pages 335–343.

Liu, Y., Wang, Z., Fan, Z., and Gu, J. (2020). "Study on properties of sisal fiber modified foamed concrete." In IOP Conference Series: Materials Science and Engineering,

Kuala Lumpur, Malaysia, 9–11 July 2020; IOP Publishing: Bristol, UK, Volume 744, 012042.

Liu, Y., Wang, L., Cao, K., and Sun, L. (2021). "Review on the durability of polypropylene fibre-reinforced concrete." Advances in Civil Engineering, Volume 2021, 6652077. https://doi.org/10.1155/2021/6652077.

Loosveldt, H., Lafhaj, Z., and Skoczylas, F. (2002). "Experimental study of gas and liquid permeability of a mortar." Cement and Concrete Research, Volume 32(9), Pages 1357-1363.

Lu, J., Jiang, J., Lu, Z., Li, J., Niu, Y., and Yang, Y. (2020). "Pore structure and hardened properties of aerogel/cement composites based on nanosilica and surface modification." Construction and Building Materials, Volume 245, 118434

Mahajan, L., and Bhagat, S. (2021). "Effect of fly ash and bottom ash on the ratio of splitting tensile strength to compressive strength of concrete." IOP Conf. Series: Materials Science and Engineering, Volume 1070, 012032.

Makul, N., and Sua-iam, G. (2016). "Characteristics and utilization of sugarcane filter cake waste in the production of lightweight foamed concrete." Journal of Cleaner Production, Volume 126, Pages 118-133.

Markin, V., Nerella, V. N., Schröfl, C., Guseynova, G., and Mechtcherine, V. (2019). "Material design and performance evaluation of foam concrete for digital fabrication." Materials, Volume 12(15), 2433.

Marthong, C., and Agarwal, T. P. (2012). "Effect of fly ash additive on concrete properties." International Journal of Engineering Research and Applications, Volume 2(4).

McGovern, G. (2000). "Manufacture and supply of ready-mix foamed concrete." One Day Awareness Seminar on Foamed Concrete Properties, Applications and Potential, Volume 294, University of Dundee, Scotland.

Mhedi, N. M., Hilal, A. A., and Al-Hadithi, A. (2018). "Re-use of waste plastic as fibers production of modified foamed concrete." In Proceedings of the 2018 11th International Conference on Developments in Systems Engineering (DeSE), Cambridge, UK, Pages 295–299.

Milla, J., Cavalline, T. L., Rupnow, T. D., Melugiri-Shankaramurthy, B., Lomboy, G., and Wang, K. (2021). "Methods of test for concrete permeability: A critical review." Advances in Civil Engineering Materials, Volume 10(1), Pages 172-209.

Mohrenholtz, O., Reddy, D. V., and Bobby, W. (1982). "Limit analysis of internally pressurised cut-and-cover type underground reactor containments." ACI Journal Proceedings, Volume 79(3), Pages 220-225.

Mydin, M.A.O., and Soleimanzadeh, S. (2012) "Effect of polypropylene fiber content on flexural strength of Lightweight foamed concrete at ambient and elevated temperatures." Advances in Applied Science Research, 3, 2837–2846.

Mydin, M. A. O., Rozlan, N. A., and Ganesan, S. (2015). "Experimental study on the mechanical properties of coconut fibre reinforced lightweight foamed concrete." Journal of Materials and Environmental Science, Volume 6, Pages 407–411.

Mydin, M. A. O., Md. Noordin, N., Utaberta, N., Mohd Yunos, M. Y., and Segeranazan, S. (2016). "Physical properties of foamed concrete incorporating coconut fibre." Jurnal Teknologi, Volume 78, 8250.

Nadeem, M., Gul, A., Bahrami, A., Azab, M., Khan, S. W., and Shahzada, K. (2023). "Evaluation of mechanical properties of cored interlocking blocks – A step toward affordable masonry material." Results in Engineering, Volume 18, 101128. https://doi.org/10.1016/j.rineng.2023.101128

Nambiar, E. K. K., and Ramamurthy, K. (2006). "Influence of filler type on the properties of foam concrete." Cement and Concrete Composites, Volume 28(5), Pages 475-480.

Nambiar, E. K. K., and Ramamurthy, K. (2007a). "Air - void characterisation of foam concrete." Cement and Concrete Research, Volume 37, Pages 221–230.

Nambiar, E. K. K., and Ramamurthy, K. (2007b). "Sorption characteristics of foam concrete." Cement and Concrete Research, Volume 37, Pages 1341–1347.

Nambiar, E. K. K., and Ramamurthy, K. (2008). "Fresh state characteristics of foam concrete." Journal of Materials in Civil Engineering, ASCE, Volume 20(2).

Narayanan, N., and Ramamurthy, K. (2000). "Structure and properties of aerated concrete : A review." Cement and Concrete Composites, Volume 22, Pages 321–329.

Noushini, A., Samali, B., and Vessalas, K. (2013). "Effect of polyvinyl alcohol (PVA) fibre on dynamic and material properties of fibre reinforced concrete." Construction and Building Materials, 49 (2013), pp. 374-383. https://doi:10.1016/j.conbuildmat.2013.08.035

Noushini, A., Vessalas, K., and Samali, B. (2014) "Static mechanical properties of polyvinyl alcohol fibre reinforced concrete (PVA-FRC)." Magazine of Concrete Research, 66(9) (2014) 465-483, https:// doi:10.1680/macr.13.00320

Nyame, B. K., and Buenfeld, N. (1986). "Permeability of normal and lightweight mortars." Magazine of Concrete Research, Volume 38(134).

Oginni, F. A. (2015). "Continental application of foamed concrete technology: lessons for infrastructural development in africa." British Journal of Applied Science & Technology, Volume 5(4), Pages 417-424.

Othman, R., Jaya, R. P., Muthusamy, K., Sulaiman, M., Duraisamy, Y., Abdullah, M. M. A. B., Przyby, A., Sochacki, W., Skrzypczak, T., Vizureanu, P., and Sandu, A. V. (2021). "Relation between density and compressive strength of foamed concrete." Materials, Volume 14(11), 2967.

Pan, Z., Hiromi, F., and Tionghuan, W. (2007). "Preparation of high-performance foamed concrete from cement, sand and mineral admixtures." Journal of Wuhan University of Technology- Materials Science Edition, Volume 22(2), Pages 295–298.

Panesar, D. K. (2013). "Cellular concrete properties and the effect of synthetic and protein foaming agents." Construction and Building Materials, Volume 44, Pages 575-584.

Park, S., Ju, S., Kim, H. K., Seo, Y. S., and Pyo, S. (2022). "Effect of the rheological properties of fresh binder on the compressive strength of pervious concrete." Journal of Materials Research and Technology, Volume 17, Pages 636-648.

Pereira-de-Oliveira, L. A., Nepomuceno, M. C. S., Castro-Gomes, J. P., Vila, M. F. C. (2014). "Permeability properties of self-compacting concrete with coarse recycled aggregates." Construction and Building Materials, Volume 51, Pages 113-120.

Porter, M. R. (1994). "Handbook of surfactants." 2nd edn. (Chapman & Hall, London).

Raj, A., Sathyan, D., and Mini, K.M. (2019). "Physical and functional characteristics of foam concrete: A review." Construction and Building Materials, Volume 221, 787-799.

Raj, B., Sathyan, D., Madhavan, M. K., and Raj, A. (2020). "Mechanical and durability properties of hybrid fiber reinforced foam concrete." Construction and Building Materials, Volume 245, 118373.

Ramamurthy, K., Nambiar, E. K. K., and Ranjani, G. I. S. (2009). "A classification of studies on properties of foam concrete." Cement and Concrete Composites, Volume 31(6), Pages 388–396.

Rasheed, M. A., and Prakash, S. S. (2015). "Mechanical behavior of sustainable hybrid-synthetic fiber reinforced cellular light weight concrete for structural applications of masonry." Construction and Building Materials, Volume 98, Pages 631-640

Raupit, F., Saggaff, A., Tan, C. S., Lee, Y. L., and Tahir, M. M. (2017). "Splitting tensile strength of lightweight foamed concrete with polypropylene fiber." International Journal on Advanced Science Engineering Information Technology, Volume 7(2).

Raut, M. V., and Deo, S. V. (2017). "A parametric study on effect of fly ash together with fiber for sustainable concrete." International Journal of Civil Engineering and Technology (IJCIET), Volume 8(3), Pages 100–110, IJCIET_08_03_010.

Richard, T. G., Dogobai, J., Gerhardt, T. D., and Young, W. C. (1975). "Cellular concrete - a potential load bearing insulation for cryogenic application." IEEE Transactions on Magnetics, Volume 11(2), Pages 500-503.

Richard, A. (2013). "Experimental production of sustainable lightweight foamed concrete." British Journal of Applied Science and Technology, Volume 12, Pages 994–1005.

RILEM TC 116-PCD. (1999). "Permeability of concrete as a criterion of its durability." Materials and Structures, Volume 32, Pages 174-179.

RILEM TC 127-MS, (1996). "Tests for masonry materials and structures." Materials and Structures, Volume 29, Pages 459-475.

Rosen, M. J. (2004). "Surfactants and interfacial phenomena." 3rd edn. (Wiley, Hoboken).

Sahu, S. S., Gandhi, I. S. R., and Khwairakpam, S. (2018). "State-of-the-art review on the characteristics of surfactants and foam from foam concrete perspective." Journal of the Institution of Engineers (India): Series A, Volume 99, Pages 391–405.

Sahu, S. S., and Gandhi, I. S. R. (2021). "Studies on influence of characteristics of surfactant and foam on foam concrete behaviour." Journal of Building Engineering, Volume 40, 102333.

Sahu, S. S., Gandhi, I. S. R., Kumar, A., and Garg, S. (2021). "Evaluation of suitability of carboxymethyl cellulose in performance improvement of sodium lauryl sulfate foam and compressive strength of foam concrete." Advances in Civil Engineering Materials, ASTM, Volume 10(1).

Sevim, O., and Sengul, C. G. (2021). "Comparison of the influence of silica-rich supplementary cementitious materials on cement mortar composites: mechanical and microstructural assessment." Silicon, Volume 13, Pages 1675–1690.

She, W., Zhao, G., Cai, D., Jiang, J., and Cao, X. (2017). "Numerical study on the effect of pore shapes on the thermal behaviors of cellular concrete." Construction and Building Materials, Volume 163, Pages 113-121.

She, W., Du, Y., Miao, C., Liu, J., Zhao, G., Jiang, J., and Zhang, Y. (2018). "Application of organic- and nanoparticle-modified foams in foamed concrete: Reinforcement and stabilization mechanisms." Cement and Concrete Research, Volume 106, Pages 12-22.

She, W., Zheng, Z., Zhang, Q., Zuo, W., Yang, J., Zhang, Y., Zheng, L., Hong, J., and Miao, C. (2020). "Predesigning matrix-directed super-hydrophobization and hierarchical strengthening of cement foam." Cement and Concrete Research, Volume 131, 106029.

Shi, T., Zhang, X., Hao, H., and Chen, C. (2021). "Experimental and numerical investigation on the compressive properties of interlocking blocks." Engineering Structures, Volume 228, 111561.

Siddique, R. (2003). "Effect of fine aggregate replacement with Class F fly ash on the mechanical properties of concrete." Cement and Concrete Research, Volume 33(4), Pages 539-547.

Siva, M., Ramamurthy, K., and Dhamodharan, R. (2015). "Sodium salt admixtures for enhancing the foaming characteristics of sodium lauryl sulphate." Cement and Concrete Composites, Volume 57, Pages 133–141.

Soongswang, P., Tia, M., Bloomquist, C., and Sessions, L. M. (1988). "Efficient test setup for determining the water-permeability of concrete." Transportation Research Record, Volume 1204, Pages 77-82.

Sun, J., Zhang, J., Gu, Y., Huang, Y., Sun, Y., and Ma, G. (2019). "Prediction of permeability and unconfined compressive strength of pervious concrete using evolved support vector regression" Construction and Building Materials, Volume 207, Pages 440-449.

Singh, G. B. (2005). "Site produced cellular lightweight concrete - A boon for housing" [Online]. Available: https://eco-web.com/edi/050113.html.

Svennberg, K., and Segerholm, I. (2006). "Performance of edge sealing systems used in moisture transport experiments." Research in Building Physics and Building Engineering.

Talukdar, P., Bora, R., and Dey, A. (2017). "Finite element based identification of the triggering mechanism of a failed hill slope." IACMAG, China.

Thamboo, J.A., Zahra, T., and Dhanasekar, R. (2020). "Development of design methodology for mortarless masonry system: Case study - A resettlement housing colony." Journal of Building Engineering, Volume 27, 100973.

Tikalsky, P. J., Pospisil, J., and MacDonald, W. (2004). "A method for assessment of the freeze-thaw resistance of preformed foam cellular concrete." Cement and Concrete Research, Volume 34, Pages 889–893.

Tosun, Y. I. (2014). "Foam concrete landfill use in landslide hazardous area in West Sirnak road." Construction Materials and Structures, IOS Press.

Uddin, N., Fouad, F., Vaidya, U. K., Khotpal, A., and Serrano-Perez, J. C. (2006). "Structural characterization of hybrid fiber reinforced polymer (FRP)-autoclave aerated concrete (AAC) panels." Journal of Reinforced Plastics and Composites, Volume 25 (9), Pages 981–999.

Valore, R. C. J. (1954). "Cellular concretes Part 2 physical properties." ACI Journal Proceedings, Volume 50(6), Pages 817-836.

Vishavkarma, A., and Harish, K. V. (2024). "Tension and bond characteristics of foam concrete for repair applications." Case Studies in Construction Materials, Volume 20, July 2024, e02767. https://doi.org/10.1016/j.cscm.2023.e02767

Wagh, C.D., Gandhi, I. S. R., and Kamisetty, A., (2021). "Thermal properties of foamed concrete: A review." D. K. Ashish et al. (eds.), 3rd International Conference on Innovative Technologies for Clean and Sustainable Development, (ITCSD 2020), RILEM Book Series, Volume 29.

Wang, C., Kong, F., and Pan, L. (2021). "Effects of polycarboxylate superplasticizers with different side-chain lengths on the resistance of concrete to chloride penetration and sulfate attack." Journal of Building Engineering, Volume 43, 102817. https://doi.org/10.1016/j.jobe.2021.102817

Wang, Z., Song, P., Isvoranu, F., and Pauly, M. (2019). "Design and structural optimization of topological interlocking assemblies." ACM Transactions on Graphics, Volume 38(6), 193.

Welker, C. D., Welker, M. A., Welker, M. F., Justman, M. A., and Hendricksen, R. S. (2000). "Foamed concrete compositional process." U.S. Patent 6,153,005, 28 November 2000.

Whelan, L. (1985). "Hollow concrete masonry unit shape modification to improve productivity of placement: Results of the preliminary research effort." Proceedings of the 3rd North American Masonry Conference, Arlington, Texas, 9.1-9.8.

Xie, G., Zhang, X., Hao, H., Bi, K., and Lin, Y. (2022). "Response of reinforced mortar-less interlocking brick wall under seismic loading." Bulletin of Earthquake Engineering, Volume 20, Pages 6129–6165, https://doi.org/10.1007/s10518-022-01436-6

Xu, A., and Sarkar, S. L. (1994). "Microstructural development in high-volume fly-ash cement system." Journal of Materials in Civil Engineering, Volume 6(1). https://doi.org/10.1061/(ASCE)0899-1561(1994)6:1(117)

Xu, H., Shao, Z., Wang, Z., Cai, L., Li, Z., Jin, H., and Chen, T. (2020) "Experimental study on mechanical properties of fiber reinforced concrete: Effect of cellulose fiber, polyvinyl alcohol fiber and polyolefin fiber." Construction and Building Materials, Volume 261, , 20 November 2020, 120610. https://doi.org/10.1016/j.conbuildmat.2020.120610

Xu, R., He, T., Da, Y., Liu, Y., Li, J., and Chen, C. (2019). "Utilizing wood fiber produced with wood waste to reinforce autoclaved aerated concrete." Construction and Building Materials, Volume 208, Pages 242–249.

Yan, L., Chouw, N., and Jayaraman, K. (2014). "Flax fibre and its composites—A review." Composites Part B Engineering, Volume 56, Pages 296–317.

Yang, J., Su, Y., He, X., Tan, H., Jiang, Y., Zeng, L., and Strnadel, B. (2018). "Pore structure evaluation of cementing composites blended with coal by-products: Calcined coal gangue and coal fly ash." Fuel Processing Technology, Volume 181, Pages 75-90.

Yoosuk, P., Suksiripattanapong, C., Sukontasukkul, P., and Chindaprasirt, P. (2021). "Properties of polypropylene fiber reinforced cellular lightweight high calcium fly ash geopolymer mortar." Case Studies in Construction Materials, Volume 15, e00730. https://doi.org/10.1016/j.cscm.2021.e00730

Yu, Z., Ni, C., Tang, M., and Shen, X. (2018). "Relationship between water permeability and pore structure of Portland cement paste blended with fly ash." Construction

and Building Material, Volume 175, Pages 458-466. https://doi.org/10.1016/j.conbuildmat.2018.04.147

Yuan, J., Chen, W., Tan, X., Yang, W., Yang, D., Yu, H., Zhou, B., and Yang, B. (2021). "Study on the permeability characteristics of foamed concrete using a pore-scale model from X-ray microcomputed tomography image reconstruction and numerical simulation." Journal of Materials in Civil Engineering, ASCE, Volume 33(6), 04021117.

Yuan, Z., and Jia, Y. (2021) "Mechanical properties and microstructure of glass fiber and polypropylene fiber reinforced concrete: An experimental study." Construction and Building Materials, Volume 266, Part A, 10 January 2021, 121048. https://doi.org/10.1016/j.conbuildmat.2020.121048

Zawawi, M. N. A. A., Muthusamy, K., Majeed, A. P. P. A., Musa, R. M., and Budiea, A. M. A. (2020). "Mechanical properties of oil palm waste lightweight aggregate concrete with fly ash as fine aggregate replacement." Journal of Building Engineering, Volume 27, 100924.

Zhang, P., and Li, Q. (2013). "Effect of polypropylene fiber on durability of concrete composite containing fly ash and silica fume." Composites Part B Engineering, Volume 45, Pages 1587-1594.

Zhang, R., Jin, L., Tian, Y., Dou, G., and Du, X. (2019). "Static and dynamic mechanical properties of eco-friendly polyvinyl alcohol fiber-reinforced ultra-high-strength concrete" Structural Concrete, https://doi:10.1002/suco.201800247

Zhao, W. S., Chen, W. Z., Ta, X. J., and Huang, S. (2013). "Study on foamed concrete used as seismic isolation material for tunnels in rock." Materials Research Innovations, Taylor & Francis group, ISSN: 1432-8917.

Zhihua, P., Hiromi, F., and Tionghuan, W. (2007). "Preparation of high performance foamed concrete from cement, sand and mineral admixtures." Journal of Wuhan University of Technology- Materials Science Edition, Volume 22, Pages 295–298.

Zhu, Z., Wang, Z., Zhou, Y., Wei, Y., and She, A. (2021). "Synthesis and structure of calcium silicate hydrate (C-S-H) modified by hydroxyl-terminated polydimethylsiloxane (PDMS)." Construction and Building Materials, Volume 267, 120731.

Appendix -A

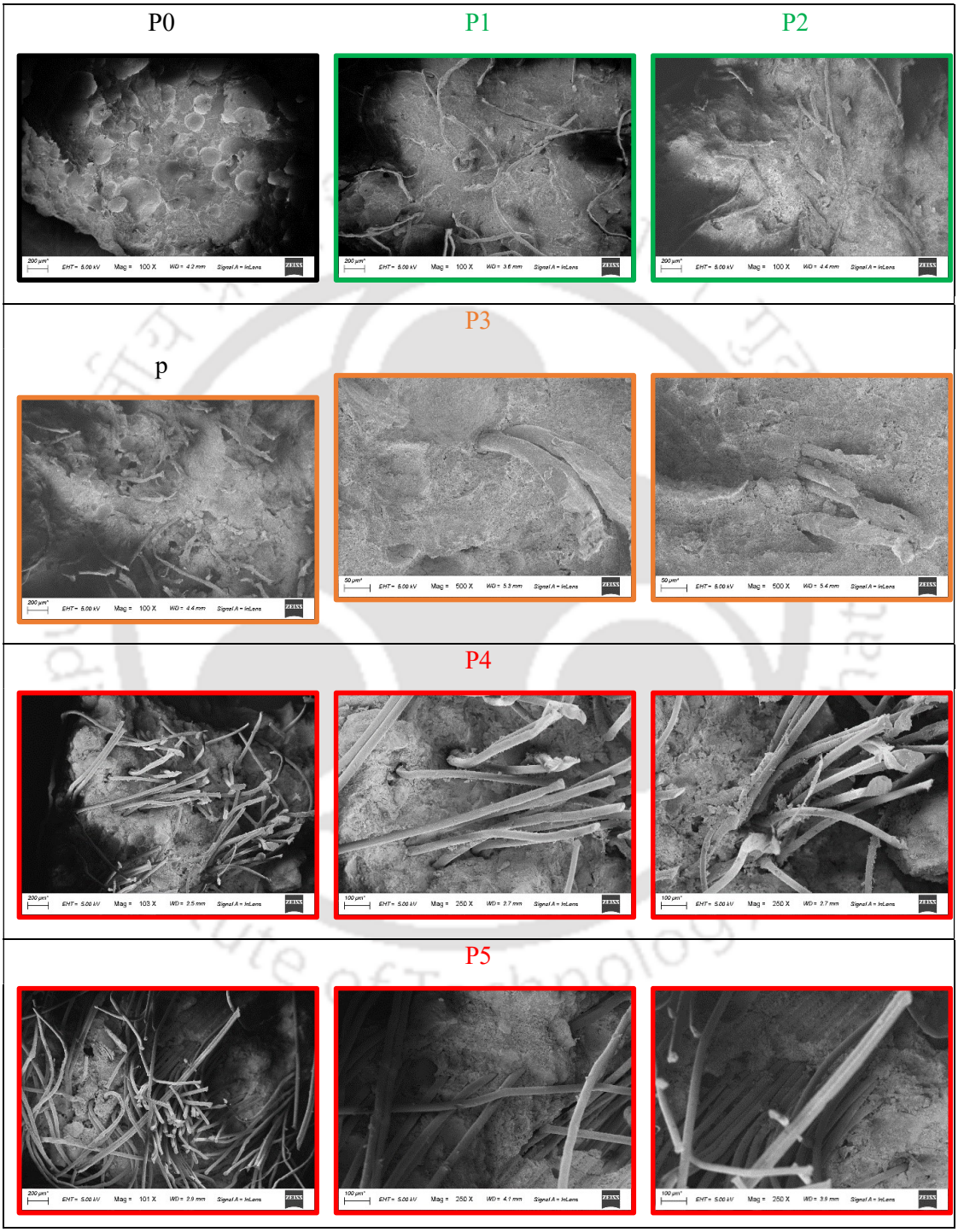

Figure A. 1: FESEM images of typical cross-sectional of FC2 mixes with PF content varying from 0% to 1% at 100X and 250X magnifications.